AWARD NUMBER: **W81XWH-12-1-0467**

TITLE: **Targeting Nuclear EGFR: Strategies for Improving Cetuximab Therapy in Lung Cancer**

PRINCIPAL INVESTIGATOR: **Deric L Wheeler**

CONTRACTING ORGANIZATION:

University of Wisconsin, Madison
Madison, WI 53715-1218

REPORT DATE: **December 2015**

TYPE OF REPORT: **Final Report**

PREPARED FOR: **U.S. Army Medical Research and Materiel Command**
Fort Detrick, Maryland 21702-5012

REPORT DOCUMENTATION PAGE			*Form Approved* *OMB No. 0704-0188*

1. REPORT DATE December 2015	**2. REPORT TYPE** Final Report	**3. DATES COVERED** 09/01/2012-08/31/2015

4. TITLE AND SUBTITLE

Targeting Nuclear EGFR: Strategies for Improving Cetuximab Therapy in Lung Cancer

5a. CONTRACT NUMBER

5b. GRANT NUMBER
W81XWH-12-1-0467

5c. PROGRAM ELEMENT NUMBER

6. AUTHOR(S)
Deric L Wheeler and Mari Iida

E-Mail: dlwheeler@wisc.edu

5d. PROJECT NUMBER

5e. TASK NUMBER

5f. WORK UNIT NUMBER

7. PERFORMING ORGANIZATION NAME(S) AND ADDRESS(ES)

University of Wisconsin, Madison
21 N Park St Suite 6401
Madison, WI 53715-1218

8. PERFORMING ORGANIZATION REPORT

9. SPONSORING / MONITORING AGENCY NAME(S) AND ADDRESS(ES)

U.S. Army Medical Research and Materiel Command
Fort Detrick, Maryland 21702-5012

10. SPONSOR/MONITOR'S ACRONYM(S)

11. SPONSOR/MONITOR'S REPORT NUMBER(S)

12. DISTRIBUTION / AVAILABILITY STATEMENT
Approved for Public Release; Distribution Unlimited

13. SUPPLEMENTARY NOTES

14. ABSTRACT
Non-Small Cell Lung Cancer (NSCLC) is a deadly disease that is driven by a multitude of factors. One of these factors is the epidermal growth factor receptor (EGFR). One of the most prominent molecular targeting agents to the EGFR is the antibody cetuximab. However, most patients develop resistance to this antibody. We have found in models of cetuximab resistance that the EGFR changes its location, to the nucleus, where it is not accessible to the large antibody and can lead to resistance to cetuximab. Over the life of this grant we have found that 1) SFK, but not AKT, inhibition can block nuclear translocation, increase EGFR on the plasma membrane, 2) that blocking nuclear translocation of the EGFR via SFK blockade can overcome acquired resistance to cetuximab and 3) nEGFR is expressed in NSCLC, with a prevalence in SCC and that it is a predictive factor for PFS and OS.

15. SUBJECT TERMS
cetuximab resistance, nuclear EGFR, dasatinib, non-small cell lung cancer

16. SECURITY CLASSIFICATION OF:			**17. LIMITATION**	**18. NUMBER OF PAGES**	**19a. NAME OF RESPONSIBLE PERSON** USAMRMC
a. REPORT U	**b. ABSTRACT** U	**c. THIS PAGE** U	UU	106	**19b. TELEPHONE NUMBER** *(include area code)*

TABLE OF CONTENTS

Page

INTRODUCTION:

The **goals** of this proposal are to **1)** determine if targeting the nuclear EGFR (nEGFR) signaling pathway can increase the efficacy of anti-EGFR antibody based therapies in non-small cell lung cancer (NSCLC) and **2)** determine if nEGFR can serve as a prognostic factor in NSCLC.

The EGFR is a ubiquitously expressed receptor tyrosine kinase (RTK) involved in the etiology of NSCLC. With this, intense efforts have been undertaken to stop EGFR function. These efforts have been highly fruitful as four drugs, including two small tyrosine kinase inhibitors (TKIs, gefitinib and erlotinib) and two antibodies (cetuximab and panitumumab), have moved to the clinic to target EGFR in NSCLC patients. In 2004, the identification of specific genetic mutations within the EGFR kinase domain of adenocarcinomas of the lung that predict response to EGFR-TKIs represented a landmark development in the EGFR field. Unfortunately, no such mutations that predict response to cetuximab have yet been identified. Clinical trials (FLEX trial[1]) investigating cetuximab in NSCLC showed clinical benefit. However, not all patients respond to cetuximab therapy and most acquire resistance to cetuximab.

It is well established that the EGFR can rely on two distinct compartments of signaling: **1)** Classical membrane bound signaling (classical EGFR pathway)[2] and **2)** nuclear signaling (nEGFR pathway)[3]. In the nEGFR pathway, recent data suggests that **the EGFR is phosphorylated by Src family kinases (SFKs)[4,5] and AKT[6], which are necessary, early, events for trafficking EGFR from the membrane to the nucleus**. In the nucleus EGFR is able to promote the transcription of genes essential for cell proliferation and cell cycle regulation[6-12].

To explore molecular mechanisms of resistance to cetuximab in NSCLC our lab developed a series of cetuximab-resistant models using NSCLC cancer lines[13]. During investigations into potential molecular mechanisms of resistance we found that NSCLC tumor cells that acquired resistance to cetuximab had increased SFK activity [14] and increased nEGFR[5]. Further investigation revealed that SFKs regulate EGFR translocation to the nucleus[5] and the nuclear activity of EGFR contributes to resistance to cetuximab therapy[5]. However, this preliminary work has led to several questions that form the **focus** of this application: **1)** Can blocking SFK and AKT activity decrease nuclear translocation of the EGFR *in vivo*, **2)** will this lead to increased expression of EGFR on the cell membrane, **3)** will this increase sensitivity to cetuximab therapy and **4)** what is the prevalence of nEGFR in NSCLC patient biopsies and can it serve as a prognostic factor? In this proposal we ***hypothesize*** that nEGFR contributes to NSCLC resistance to cetuximab and that targeting nEGFR, by abrogating its translocation to the nucleus via SFK or AKT inhibition, followed by targeting membrane bound EGFR with cetuximab will increase therapeutic response of NSCLC tumors to cetuximab. To test this hypothesis we propose the following specific aims:

Specific Aim 1: To determine if SFK or AKT inhibition can 1) block EGFR translocation to the nucleus 2) decrease nEGFR function and 3) increase EGFR expression on the cell membrane.

Specific Aim 2: Determine if targeting nEGFR, via SFK or AKT inhibition, can increase therapeutic response of nEGFR positive, cetuximab-resistant NSCLC tumors to cetuximab.

Specific Aim 3: Determine the prevalence of nEGFR protein expression in NSCLC using IHC and AQUA/Vectra analyses and determine if it serves as a prognostic factor in NSCLC.

KEYWORDS: cetuximab, epidermal growth factor receptor, src family kinases, non-small cell lung cancer, resistance, therapy, dasatinib, nuclear, Axl, receptor tyrosine kinase

OVERALL PROJECT SUMMARY:

A) What were the major goals of the project? The major goals of the project are highlighted in terms of each individual specific aim. The accomplishments will be discussed for each aim in B below.

Specific Aim 1: To determine if SFK or AKT inhibition can 1) block EGFR translocation to the nucleus 2) decrease nEGFR function and 3) increase EGFR expression on the cell membrane. *To accomplish the goals of this aim we will:* **1)** Treat nEGFR expressing, cetuximab-resistant NSCLC lines with SFK or AKT inhibitors (dasatinib or MK2206, respectively) and measure **i)** membrane and nEGFR levels (biochemical fractionation, flow cytometry and automated quantitative IHC analysis (AQUA/Vectra)) and **ii)** nEGFR function (ChIP and qPCR analysis of known EGFR target genes and PCNA activation, and 2) Utilize mouse xenograft models to determine if, *in vivo*, SFK or AKT inhibition can block EGFR translocation to the nucleus leading to increased membrane expression of the EGFR. Mice bearing human NSCLC tumors (with high nEGFR) will be treated with dasatinib or MK2206 and tumors analyzed for nuclear and non-nEGFR levels (AQUA/Vectra) in control versus experimental groups.

Specific Aim 2: Determine if targeting nEGFR, via SFK or AKT inhibition, can increase therapeutic response of nEGFR positive, cetuximab-resistant NSCLC tumors to cetuximab. To accomplish the goals of this aim we will grow cetuximab-resistant NSCLC tumors using mouse xenografts. Mice bearing resistant tumors will be treated with **1)** vehicle, **2)** cetuximab, **3)** dasatinib, **4)** MK2206, **5)** cetuximab plus dasatinib and **6)** cetuximab plus MK2206. We will measure the effects on tumor growth as well as nEGFR expression temporally throughout the experiment (AQUA/Vectra).

Specific Aim 3: **Determine the prevalence of nEGFR protein expression in NSCLC using IHC and AQUA/Vectra analyses and determine if it serves as a prognostic factor in NSCLC.** To accomplish this goal we will measure nEGFR protein expression in two human NSCLC tissue microarrays (TMAs). The first TMA is comprised of 88 stage I and II NSCLC patients from the University of Wisconsin Carbone Cancer Center (UW), and the second comprised of 300 stage I and II NSCLC patients from the University of Chicago Cancer Center (UC). In addition to early stage patients, we will measure nEGFR expression in 2700 tumors of advanced stage NSCLC from the UC TMA.

B) What was accomplished under these goals?

Specific Aim 1: To determine if SFK or AKT inhibition can 1) block EGFR translocation to the nucleus 2) decrease nEGFR function and 3) increase EGFR expression on the cell membrane. During the period of this award we completed to goals of aim 1. The key research accomplishments are bulleted below with details of work following.

Specific Aim 1: To determine if SFK or AKT inhibition can 1) block EGFR translocation to the nucleus and if this leads to decreased nEGFR function and 2) increase EGFR expression on the cell membrane. Over the last year we have made several findings in molecular signaling that leads to nuclear translocation of the EGFR. These are highlighted briefly below.

<u>*SFK blockade, but not AKT, results in robust blockade of EGFR nuclear translocation:*</u> It has been reported that targeting SFK and/or AKT may be able to block EGFR nuclear translocation. In vitro or in vivo studies suggested that SFK blockade could robustly block EGFR translocation whereas AKT inhibition could not. *This suggests that targeting Src Family Kinases, rather than AKT, may be the best opportunity to therapeutically intervene.*

<u>*De Novo derived, cetuximab resistant tumors have increased nEGFR:*</u> One criticism we often receive is that our model of cetuximab resistance was developed *in vitro* and it is not clear whether nuclear EGFR would be present in resistant tumors developed *in vivo*. To mimic the development of acquired resistance to cetuximab in the clinical setting we have previously developed numerous *de novo* acquired resistant models *in vivo* by treating established cetuximab sensitive tumors with continued cetuximab therapy until resistant tumor

emerge[15]. As depicted in **Figure 1**, tumors treated with IgG grew rapidly, while tumors treated with cetuximab displayed initial growth control. Acquired resistance was observed at approximately 30-60 days in 65% of tumors, where there was marked tumor growth in the presence of continued cetuximab therapy. IHC Analysis of these tumors indicated that 7/9 had increased nEGFR expression as compared to IgG treated tumors. This work has been replicated in other SCC models including *de novo* tumors established from the cetuximab sensitive cell lines H292 and SCC1.

Chemically induced lung tumors have increased nEGFR: To make more robust models of lung cancers harboring nuclear EGFR we created chemically derived tumors using NTCU as previously described. This tumor model will be used in Aim 2 for functional targeting studies of EGFR. Briefly, we started a collaboration with Dr. Ming You (MCW Cancer Center Director and consultant) who was the first to use NTCU to generate SCC in the mouse lung[16]. He determined that FVB/N mice gave approximately four SCC lesions/mouse eight months after treatment with NTCU. Further, the histopathology of the mouse lung SCC is similar to that seen in humans with well-defined pathological development from bronchial hyperplasia to SCC. To determine if chemically derived LSCC tumors in mice harbor nEGFR we stained 20 independent tumors and analyzed for nEGFR expression (**Figure 2**). Strikingly, the results showed that like human (**Figure 2A**), mouse LSCC harbored nEGFR whereas normal tissue had no nEGFR expression. Finally, of note, cetuximab does not react with the mouse EGFR. To overcome this experimental problem, we have obtained an MTA from ImClone that has generated a murine anti-EGFR antibody, termed ME1. This antibody binds the murine EGFR and inhibits its activity[17].

Other findings not written in the grant but found during investigations (work not yet published):

Cetuximab resistance is mediated by kinase independent functions of the EGFR: In 2009 we published data that indicated that overexpression of EGFR-WT-NLS resulted in increased cetuximab resistance in *in vitro* and *in vivo* models, however, what functions of nEGFR that mediate this resistance could not be determined via the use of this fusion protein. To elucidate what functions of nEGFR mediate this resistant phenotype we have taken several approaches (. Firstly, we transiently expressed **1)** EGFR-WT-NLS and **2)** EGFR-KD-NLS in the LSCC and HNSCC **cetuximab-sensitive** parental control cells HP and SP, where we found that both fusion proteins were effectively nuclear localized to similar degrees (**Figure 3A**). Next, cells expressing each construct were plated and challenged with cetuximab for 72 hours (**Figure 3B**). The results indicated that, relative to vector controls, both EGFR-WT-NLS and EGFR-KD-NLS expressing cells became resistant to cetuximab therapy (**Figure 3B**).

In a second, independent approach, we cloned a C-terminal domain (CTD) truncation variant of the EGFR, where the N-terminus, transmembrane domain, and kinase domain were deleted (**Figure 3C**). We **hypothesized** that this EGFR variant (EGFR-CTD-NLS), lacking its ability to be localized on the plasma membrane and function as a kinase, could still translocate to the nucleus and function as a co-transcription factor. This approach was based off our previous success investigating HER3 co-transcriptional activities through the use of a HER3-CTD construct that was transcriptionally viable [18,19]. The results from this experimentation indicated that, relative to vector controls, EGFR-CTD-NLS could also lead to increased cetuximab resistance, similar to the findings for the full length EGFR-WT-NLS (**Figure 3D**). *Collectively these data strongly indicate that nEGFR, independent of its kinase activities, can drive resistance to cetuximab therapy providing further rationale for the investigation of nEGFR kinase independent functions in cetuximab resistance.*

Nuclear translocation of EGFR is linked to the Axl Tyrosine Kinase Receptor: One of the major goals of our laboratory is to modulate EGFR trafficking to the nucleus to increase therapeutic response to cetuximab. In studies over the last 24 months we have learned that the receptor tyrosine kinase Axl is critical for nuclear EGFR translocation. In a paper recently submitted to *Cancer Research* we reported that Axl and EGFR bind, Axl phosphorylates EGFR resulting in binding of Src Family Kinases, which in turn phosphorylate tyrosine 1101, the site necessary for nuclear translocation of the EGFR. By targeting Axl with siRNA or degrading antibodies we could completely prevent nuclear translocation of the EGFR. *This suggests that targeting Axl, rather than the Src Family Kinases, may represent a novel approach to blocking EGFR nuclear translocation; the major goal of this grant. This data is novel and stems from the funding from the DoD*

Specific Aim 2: Determine if targeting nEGFR, via SFK or AKT inhibition, can increase therapeutic response of nEGFR positive, cetuximab-resistant NSCLC tumors to cetuximab. During the period of this award we completed to goals of aim 2. The key research accomplishments are bulleted below with details of work following.

Targeting the nEGFR signaling network with dasatinib in cetuximab resistant tumors sensitizes to cetuximab: Although we published this working in lung, we found that this mechanism was true in cetuximab resistant TNBC. We published in both settings that targeting both the nEGFR and classical signaling pathways simultaneously was efficacious. These works lead to an R01 being funded in TNBC and is currently a clinical trial based directly on the results funded by this DOD grant.

Specific Aim 3: **Determine the prevalence of nEGFR protein expression in NSCLC using IHC and AQUA/Vectra analyses and determine if it serves as a prognostic factor in NSCLC.** During the period of this award we completed to goals of aim 3. The key research accomplishments are bulleted below with details of work following.

Specific Aim 3: *Determine the prevalence of nEGFR protein expression in NSCLC using IHC and AQUA analyses and determine if it serves as a prognostic factor in NSCLC.* The focus of this aim was to use two NSCLC TMAs with various stages of NSCLC. In a first effort we focused our time on the 88 patient TMA that contained only stage I and II patients. Briefly, the findings are summarized below:

Introduction: Nuclear EGFR (nEGFR) has been identified in various human tumor tissues, including cancers of the breast, ovary, oropharynx, and esophagus, and has predicted poor patient outcomes. We sought to determine if protein expression of nEGFR is prognostic in early stage non-small cell lung cancer (NSCLC). Methods: Resected stages I and II NSCLC specimens were evaluated for nEGFR protein expression using immunohistochemistry (IHC). Cases with at least one replicate core containing ≥5% of tumor cells demonstrating strong dot-like nucleolar EGFR expression were scored as nEGFR positive.

Results: Twenty-three (26.1% of the population) of 88 resected specimens stained positively for nEGFR. Nuclear EGFR protein expression was associated with higher disease stage (45.5% of stage II vs. 14.5% of stage I; $p = 0.023$), histology (41.7% in squamous cell carcinoma vs. 17.1% in adenocarcinoma; $p = 0.028$), shorter progression-free survival (PFS) (median PFS 8.7 months [95% CI 5.1–10.7 mo] for nEGFR positive vs. 14.5 months [95% CI 9.5–17.4 mo] for nEGFR negative; hazard ratio (HR) of 1.89 [95% CI 1.15–3.10]; $p = 0.011$), and shorter overall survival (OS) (median OS 14.1 months [95% CI 10.3–22.7 mo] for nEGFR positive vs. 23.4 months [95% CI 20.1–29.4 mo] for nEGFR negative; HR of 1.83 [95% CI 1.12–2.99]; $p = 0.014$).

Conclusions: Expression of nEGFR protein was associated with higher stage and squamous cell histology, and predicted shorter PFS and OS, in this patient cohort. Nuclear EGFR serves as a useful independent prognostic variable and as a potential therapeutic target in NSCLC.

Current work: This paper was published in the journal of Lung Cancer[20] is attached in the appendix. We are now currently focusing on the development of a larger TMA with stages I-IV patients to determine if nEGFR can serve as a predictive biomarker in lung cancer. A description of the current work is provided.

Determine if nEGFR expression is a predictive biomarker for cetuximab resistance in advanced LSCC. To accomplish this aim we will determine nEGFR levels in human LSCC tumor specimens and test for a correlation with cetuximab clinical benefit. We will examine nEGFR expression in human tumor specimens (tissue microarray) obtained from the University of Chicago iBridge Network.

Hypothesis – We hypothesize that the clinical benefit of cetuximab in advanced LSCC patients will be predicted by nEGFR expression.

Rationale – Randomized trials have documented that the addition of cetuximab to conventional chemotherapy in advanced NSCLC results in minimal improvements in clinical outcome[21]. We and others have hypothesized that the marginal benefit observed is a consequence of inadequate patient selection; a robust predictive biomarker for cetuximab efficacy in NSCLC has not been identified[22,23]. Total EGFR expression has been correlated with cetuximab survival benefit, however, the predictive power is quite modest[24]. We have recently shown that nEGFR is a prognostic factor in early stage NSCLC[20]. Further, in experimental model systems, we have shown that elevated nEGFR leads to cetuximab resistance in a variety of cancers[5,14,25-27]. Therefore, it is biologically plausible that nEGFR may be a predictive biomarker of cetuximab efficacy and permit optimal patient selection for cetuximab use in advanced NSCLC.

Clinical Sample Set – We will confirm the prognostic significance of nEGFR in advanced LSCC (stage IV) and determine if nEGFR is a predictive biomarker for cetuximab efficacy. In order to do so, we will employ the thoracic oncology research program standard operating procedure (SOP) within the iBridge network (http://www.ibridgenetwork.org) directed by Dr. Salgia (collaborator) at the University of Chicago. The iBridge network SOP is a large research bioinformatics platform representing more than 4000 total lung cancer samples and tissue microarrays. Specimens are linked to comprehensive clinical information including outcomes (RR, OS, PFS) as well as characteristics such as age, sex, race, stage at initial diagnosis, and therapeutic history. The dataset has contributed to several large-scale lung cancer analyses similar to the analysis proposed herein[28,29]. Among regional utilizers/contributors to the iBridge network, cetuximab was frequently employed in the advanced NSCLC population prior to the availability of phase III trial evidence of minimal clinical benefit. Consequently, we have identified 200 advanced LSCC patients treated with carboplatin/paclitaxel/cetuximab. An additional 300-advanced LSCC patients treated with carboplatin/paclitaxel have been identified. To extrapolate from the Lynch trial, there was no difference in overall survival between chemotherapy with or without cetuximab[30]. However, our hypothesis is that the predictive value of cetuximab response would be dependent on nuclear or non-nuclear localization of EGFR. As can be appreciated, the iBridge network has the SOP of our database as well as the tumor tissue repository. This was initially created by Dr. Salgia and his colleagues with ARRA funding and has been made available to anyone for free. Since establishment, the initial SOP has been licensed by over 80 institutions (including Harvard, Hopkins, Yale, Boston University, Columbia, etc). The SOP is available in Microsoft Access, Oracle based system, as well as RedCap. In the metropolitan Chicago area, we have a combined effort with Rush, UIC, North Shore, Ingalls Hospital, and our phase II consortium (containing 13 affiliates).

Correlation of EGFR localization and clinical outcome **–** Tissue microarrays will be prepared from this patient cohort through the University of Chicago Pathology Core. We will then stain, using several EGFR antibodies that have been used in analysis of nEGFR[20]. In particular, we will determine the expression of cytoplasmic/membranous versus nEGFR and correlate with clinical benefit rate. **Expected results –** We expect that nEGFR expression will be prognostic in advanced LSCC patients with lower clinical benefit rates with both chemotherapy and the combination of chemotherapy and cetuximab in nEGFR expressors compared to nEGFR non-expressors. Critically, we expect that nEGFR expression will be associated with no improvement in clinical benefit rate with the addition of cetuximab. In contrast, we anticipate that advanced LSCC patients without nEGFR expression will significantly benefit from the addition of cetuximab.

Statistical analysis – Power analysis is based on clinical benefit rate, defined by the rate of response plus stable disease at 12 weeks. The four groups for comparison are (1) nEGFR negative treated with chemotherapy (CT), (2) nEGFR negative treated with cetuximab and chemotherapy (CTX+CT), (3) nEGFR positive treated with CT and (4) nEGFR positive treated with CTX + CT. Based on our preliminary work, we expect 40% or more samples to be nEGFR negative in this advanced stage population. The clinical benefit rates of both CT and CTX+CT are expected to be about 30% for nEGFR positive groups (i.e. there will be no benefit to the addition of CTX). The clinical benefit rate from CT is estimated to be higher in the nEGFR negative group by about 5%-10% (prognostic). We hypothesize the clinical benefit rate will be higher with the addition of CTX in the nEGFR negative cohort (predictive). For statistical analysis, we estimate the absolute magnitude of the CTX benefit in the nEGFR negative cohort to be approximately 20%. We perform our power analysis based on detecting this predictive effect of nEGFR status using an interaction logistic regression model, which is to detect statistically significant interaction between nEGFR status and cetuximab. The type I error is set at 10%

level and the resulting powers range from 0.78 or 0.92 depending on the possible values for the proportion of nEGFR negative, clinical benefit rates of CT in nEGFR negative and positive groups (see Tables XX and XX in the appendix). The calculation is based on 200 samples of CT+CTX and 300 samples of CT alone. We will conduct our analysis based on logistic regression models.

Potential Pitfalls and Alternative Approaches – Our laboratory reported that nEGFR leads to resistance to cetuximab therapy. However, which nuclear function of EGFR that plays a role in this process is not yet known. To investigate this, we developed a nEGFR mutant that lacks the ability to mediate transcription. This results in a potential pitfall in Aim 2A, since tumors lacking nEGFR transcriptional functions may grow differently from tumors overexpressing EGFRWT. In order to determine cetuximab response we will do both time-matched and size-matched cetuximab response experiments and measure the tumor growth delay as compared to the EGFRWT control. Due to the heterogeneity of the studied patient population, clinical outcomes (RR, OS, PFS) will vary. This potential pitfall is limited by design with inclusion of only metastatic patients. If statistical significance is compromised by patient heterogeneity in Aim 2B, a number of approaches may be taken to increase power and elucidate the predictive value of nEGFR expression including time-to-event analysis. Additional tissue samples are available from the University of Wisconsin if analyses are underpowered (see Traynor letter). Moreover, analysis of nEGFR expression as a continuous variable and/or examination of the cytoplasmic-to-nEGFR ratio may provide opportunities to enhance statistical power of correlations between EGFR expression and localization with clinical outcomes.

KEY RESEARCH ACCOMPLISHMENTS

Key Research Accomplishments for Aim 1:

- Modulation of Src Family Kinase Activity impairs nuclear translocation of EGFR
- AKT inhibition is not robust in preventing nuclear EGFR trafficking
- Tyrosine 1101 of the EGFR is a critical determinant necessary for nuclear translocation of the EGFR
- Src Family Kinases show functional redundancy in phosphorylating Y1101 leading to nuclear translocation
- Genetic variants of SFKs can prevent or enhance nuclear translocation of the EGFR.
- Src Family Kinase blockade using dasatinib increases EGFR on the membrane of the cell making it accessible to cetuximab therapy.
- Chemically derived tumors harbor nuclear EGFR
- *De novo* derived cetuximab resistant tumors harbor nuclear EGFR
- EGFR can mediate cetuximab resistance independent of its kinase activity
- Axl receptor tyrosine kinase is implicated in EGFR nuclear trafficking
- Axl expression in NSCLC increases expressions of SFKs and the HER3 ligand neuregulin
- These factors lead to phosphorylation of Y1101 and EGFR dimerization with HER3 leading to nuclear translocation.

Key Research Accomplishments for Aim 2:

- *In vivo* xenograft tumors treated with dasatinib results in decreased nuclear EGFR and increased plasma membrane EGFR.
- Cetuximab resistant tumors treated with the dasatinib plus cetuximab has increased tumor response than either drug alone.

Key Research Accomplishments for Aim 3:

- Identified that nEGFR is expressed in approximately 26% of NSCLC patients.
- Identified that nEGFR was more prevalent in SCC versus adenocarcinoma.
- Identified that nEGFR expressing patients had a shorter progression free survival.
- Identified that nEGFR expression patients had shorter overall survival.
- Identified that nEGFR was associated with a higher disease stage.

REPORTABLE OUTCOMES

Publications During the Period of Support of the DOD Grant:

Lay Press, Highlight features

FY14 LCRP publicity materials; LC110082 - Targeting Nuclear EGFR: Strategies for Improving Cetuximab Therapy in Lung Cancer) was highlighted in our upcoming FY14 LCRP publicity materials.

1. Stegeman H, Kaanders JH, **Wheeler DL**, van der Kogel AJ, Verheijen MM, Waaijer SJ, Iida M, Grénman R, Span PN, Bussink J. Activation of AKT by hypoxia: a potential target for hypoxic tumors of the head and neck. BMC Cancer. 2012 Oct 10;12:463. PMID: 23046567, PMCID: PMC3517352

2. Stegeman H, Kaanders JH, van der Kogel AJ, Iida M, **Wheeler DL**, Span PN, Bussink J. Predictive value of hypoxia, proliferation and tyrosine kinase receptors for EGFR-inhibition and radiotherapy sensitivity in head and neck cancer models. Radiother Oncol. 2013 Feb 27. PMID: 23453541

3. Iida M, Brand TM, Campbell DA, Li C, **Wheeler DL**. Yes and Lyn play a role in nuclear translocation of the epidermal growth factor receptor. Oncogene. 2013 Feb 7;32(6):759-67. PMID: 22430206, PMCID: PMC3381861

4. Iida, M, Brand, TM, Campbell, D, Starr, M, Luthar, N, Traynor, AM, **Wheeler, DL**. Targeting AKT With The Allosteric AKT Inhibitor MK-2206 in Non-Small Cell Lung Cancer cells with Acquired Resistance to Cetuximab. Cancer Biol Ther. 2013 Jun;14(6):481-91. PMID: 23760490, PMCID: PMC3813564

5. Traynor, AM, Weigel, TL, Oettel, KR, Yang, DT, Zhang, C, KyungMann, K, Salgia, R, Iida, M, Brand, TM, Hoang, T, Campbell, TC, Hernan, HR, **Wheeler, DL**. Nuclear EGFR protein expression predicts poor survival in early stage non-small cell lung cancer. Lung Cancer 2013 July 81(1)134-41. PMID: 23628526, PMCID: PMC3679338

6. Stegeman, Span, PN, Rijken, SC, **Wheeler, DL**, Iida, M, van der Kogel, AJ, Kaanders, JHAM, H, Kaanders, Bussink, J. Dasatinib inhibits DNA repair specifically in pSFK expressing tumor areas in head and neck xenograft tumors. Transl Oncol. 013 Aug 1;6(4):413-9. PMID:23908684, PMCID:PMC3730016

7. Brand, TM, Iida, M, Luthar, N, Wleklinski, MJ, Starr, MM, **Wheeler, DL**. Full-length nuclear HER3 regulates the cyclin D1 promoter through a bi-partite C-terminal transactivation domain. PLoS One. 2013 Aug 8;8(8):e71518. PMID23951180, PMCID:PMC373852

8. Kawada, I, Hasina, R, Lennon, FE, Bindokas, V, Usatyuk, P, Tan, C, S. Krishnaswamy, S E. Smithberger, E, Q Arif, Q, M Tretiakova, Brand, TM, Iida M, **Wheeler, DL**, Husain, AN, Natarajan, V, Vokes, EE, Singleton PA, and Salgia, R. Paxillin mutations affect focal adhesions and lead to altered mitochondrial dynamics: relevance to lung cancer. Cancer Biol Ther. 2013 Jul 1;14(7):679-91. PMID:23792636, PMCID:PMC3742497

9. Li, C, Brand, TM Iida, M, Huang, S, Armstrong, EA, Van Der Kogel, B, **Wheeler, DL**. Human epidermal growth factor receptor 3 (HER3) blockade with U3-1287/AMG888 enhances the efficacy of radiation therapy in lung and head and neck carcinomas, Discov. Med. 2013 Sep;16(87):79-92. PMID: 23998444, PMCID: PMC3901945

10. Brand, TM, Iida, M, Luthar, N, Starr, MM, Huppert, EJ, **Wheeler, DL.** Nuclear EGFR as a molecular target in cancer. Radiother Oncol. 2013 Sep;108(3):370-7. PMID: 23830194, PMCID: PMC3818450

11. Iida, M, Brand TM, Starr, M, **Wheeler, DL**, The EGFR blocking antibodies, SYM004, can overcome acquired resistance to cetuximab, Neoplasia 2013 Oct;15(10):1196-206. PMID:24204198, PMCID:PMC3819635

12. Rolle, CE, Surati, M, Nandi, S, Kanteti, R, Yala, S, Tretiakova, M, Arif, Q, Hembrough, T, Brandon, TM, **Wheeler, DL**, Husain, AN, Vokes, EE, Bharati, A, Salgia, R. MET inhibition and Topoisomerase I inhibition synergize to block cell growth of small cell lung cancer. Mol Cancer Ther. 2013 Dec 10. PMID:24327519, PMCID: PMC4286701

13. Stegeman, Span, Kaanders, JHAM, H, Kaanders, Verhheijen, MM, Peeters, WJ, **Wheeler**, DL, Iida, M, Grenman, R, Van der Kogel, AJ, Span, PN, and Bussink, J. Combining radiotherapy with MEK1/2, STAT5 or STAT6 inhibition reduces survival of head and neck cancer lines, Mol. Cancer, 2013 Nov 5;12(1):133. PMID:24192080, PMCID:PMC3842630

14. Brand, TM, Iida, M, Dunn, E, Luthar, N, Kostopoulus, KT, Corrigan, KL, Yang, Wleklinski, D, Wisinski, KB, Salgia, R, **Wheeler, DL**. Nuclear EGFR serves as a functional molecular target in Triple-negative breast cancer Mol Cancer Ther. 2014 May;13(5):1356-68. PMID: 24634415, PMCID: PMC4013210

15. Brand, TM, Iida, M, Stein, AP, Corrigan, KL, Braverman, CM, Luthar, N, Toulany, M, Gill, PS, Salgia, R, Kimple, RJ, **Wheeler, DL.** AXL Mediates Resistance to Cetuximab Therapy, Cancer Res. 2014 Sep 15;74(18):5152-64 *Cancer research* (2014). PMID: 25136066, PMCID: PMC4167493

16. Iida, M, Brand TM, Starr, M, Huppert, E, Corrigan, K, Salgia, R, **Wheeler, DL**, Overcoming acquired resistance to cetuximab by blockade of HER3 using U3-1287. Mol Cancer. 2014 Oct 24;13(1):242. PMID: 25344208

17. Brand TM, Iida M, Stein AP, Corrigan KL, Braverman CM, Coan JP, Pearson HE, Bahrar H, Fowler TL, Bednarz BP, Saha S, Yang D, Gill PS, Lingen MW, Saloura V, Villaflor VM, Salgia R, Kimple RJ, **Wheeler DL**. AXL is a logical molecular target in head and neck squamous cell carcinoma, Clin Cancer Res. 2015 Mar 12. [Epub ahead of print]

18. Ashok, S, Singh, A, Bauer, SJ, **Wheeler, DL**, Havighurst, TC, Kim, KM, and Verma, AKGenetic deletion of TNFα inhibits ultraviolet radiation-induced development of cutaneous squamous cell carcinomas in PKCε transgenic mice via inhibition of cell survival signals, Carcinogenesis, 2015. [Epub ahead of print]

19. Brand, TM, Iida, T, Corrigan, KL, Braverman, CM, Coan, J, Flanigan, B, Stein, AP, Salgia, R, Kimple, RJ and **Wheeler, DL**, AXL mediates the nuclear translocation of the epidermal growth factor receptor, Science Signaling, Submitted

20. Flanigan, B, Brand, TM, Iida, T Black, NK, Salgia, R, Kimple, RJ and **Wheeler, DL,** Tyrosine 1101 of the EGFR is a critical determinant or nuclear translocation of the EGFR, Oncogene, in preparation

Abstracts During the Period of Support of the DOD Grant:

1. Li, C, Iida, M, Huang, S, Armstrong, EA, Brand, TM, Peet, CR, **Wheeler, DL**, Human epidermal growth factor 3 (HER3) blockade with U3-1287/AMG888 modulates radiosensitivity in the lung and head and neck carcinomas cetuximab, Am. Assoc. Cancer Res. Chicago, IL, April 2012

2. Brand, TM, Iida, M, Wlenski, M, Luthar, N, Li, C, **Wheeler, DL**, Full length nuclear HER3 regulates the cyclin D1 promoter via a bipartite C-terminal transactivation domain. 1st annual Michael N. Hart Pathology Research Day, Madison, WI, August 2012**. Poster Award Winner**

3. Brand, TM, Iida, M, Luthar, N, Li, C, **Wheeler, DL**, Full-length nuclear HER3 regulates the cyclin D1

promoter through a bi-partite C-terminal transactivation domain, 37th Symposium on Hormones and Cell Regulation: Receptor Tyrosine Kinases (RTKs): from Structural Biology to Systems Biology, Mont Ste Odile, Ascale, France, October 2012, October 11-14, 2012 **Travel Grant Award Winner**

4. Brand, TM, Iida, M, Luthar, N, **Wheeler, DL**, Mapping the transcriptional activation domains of the HER family of receptor tyrosine kinases. Am. Assoc. Cancer Res. Washington, DC, 2013

5. Iida, M, Brand, TM, Starr, MM, Luthar, N, **Wheeler, DL**, Overcoming Acquired Resistance to Cetuximab by Dual Targeting of HER Family Members Using Antibody Based Therapy, Am. Assoc. Cancer Res. Washington, DC, April 2013

6. Brand, TM, Iida, M, Luthar, N, Li, C, **Wheeler, DL**, and Nuclear EGFR serves as functional molecular target in triple-negative breast cancer. Am. Assoc. Cancer Res. Washington, DC, 2013 **Late-breaking abstract**

7. Stegeman, Span, PN, Rijken, SC, **Wheeler, DL**, Iida, M, van der Kogel, AJ, Kaanders, JHAM, H, Kaanders, Bussink, J, Dasatinib inhibits DNA repair specifically in pSFK expressing tumor areas in head and neck xenograft tumors, ESTRO, Geneva, Switzerland, April, 2013

8. Brand, TM, Iida, M, Luthar, N, Li, C, and **Wheeler, DL**, Nuclear EGFR serves as functional molecular target in triple-negative breast cancer. Wolfsberg Meeting on Molecular Radiation Biology/Oncology, Switzerland, June 2013

9. Singh, A, Singh, A, Bauer, S, **Wheeler, DL**, and Verma, AK, Tumor necrosis factor-alpha is linked to Protein Kinase C-epsilon mediated sensitivity to the development of cutaneous squamous cell carcinomas. SID meeting, 2014

10. Villaflor, VM, Wheeler, DL, Iida, M, Vidwans, S, Turski, M, Brand TM, Won, B, Ferguson, M, Patti, M, Posner, M, Waxman, I, Vokes, EE, Salgia, R, Genetic alterations in Esophageal Cancers—Detection by next generation sequencing and potential for therapeutic targets. ASCO, 2014

11. Brand, TM, Iida, M, Corrigan, KL, Luthar, N, Hornung, M, Toulany, Gill, P, Salgia, R, **Wheeler, DL**, The receptor tyrosine kinase Axl plays a role in acquired resistance to cetuximab. Am. Assoc. Cancer Res. San Diego, CA, April 2014. **Late-Breaking Abstract**

12. Toulany, M, Iida, M, **Wheeler, DL**, Rodemann, Double targeting of PI3K and MAPK is an effective strategy to enhance radiation response of K-RAS mutated non-small cell lung cancer cell. Wolfsberg Meeting on Molecular Radiation Biology/Oncology, Switzerland, June 2013

Invited Reviews During the Period of Support of the DOD Grant:

1. Brand TM, **Wheeler DL**. KRAS mutant colorectal tumors: past and present. Small GTPases. 2012 Jan-Mar;3(1):34-9. PMID: 22714415, PMCID: PMC3398915

2. Brand, TM, Iida, M, Luthar, N, Starr, MM, Huppert, EJ, **Wheeler, DL.** Nuclear EGFR as a molecular target in cancer. Radiother Oncol. 2013 Sep;108(3):370-7. PMID: 23830194, PMCID: PMC3818450

Books Reviews During the Period of Support of the DOD Grant:

1. **The Receptor Tyrosine Kinases: Structure, Function, Biology and Human Disease**–Lead Editor: **DL Wheeler**, Springer Science; I initiated this book with Springer Science Publishing to summarize the major aspects of our field in regards to basic structural and functional biology of receptor tyrosine kinases in in human disease. It is 13 chapters in length with contributions from world-leaders in receptor tyrosine kinase

biology. http://www.springer.com/br/book/9781493920525

2. **Receptor Tyrosine Kinase: The Families** Lead Editor: **DL Wheeler**, Springer Science; I initiated this book with Springer Science Publishing to summarize all of the 58-receptor tyrosine kinases broken down into 20 families. There is 20 chapters, one for each family, summarizing the discovery, gene and protein structure, role in cell signaling and human disease. Contributions are from the world leaders on each respective family of receptor tyrosine kinases. http://www.springer.com/br/book/9783319118871

Presentations Given During the Period of Support of the DOD Grant:

2012 Speaker, Northwestern University, Comprehensive Cancer Center, Chicago, Illinois. *Strategies To Improve Cetuximab Therapy In HNSCC And NSCLC*

Speaker, Symphogen, Copenhagen, Denmark. *Sym004 And Overcoming Acquired Resistance To Cetuximab*

Speaker, Radboud University, Department of Radiation Oncology, Nijmegen Medical Center, Nijmegen, Netherlands. *Src Family Kinases, Nuclear EGFR And Resistance To Cetuximab Therapy: Strategies For Improving Cetuximab Therapy In NSCLC*

Speaker, University of Tubingen, Division of Radiobiology and Molecular Environmental Research, Tubingen, Germany. *Understanding The Role Of Nuclear EGFR In Resistance To Cancer Therapeutics*

2013 Speaker, Cancer Therapy Discovery and Development, Madison, Wisconsin, *Targeting Nuclear EGFR In Triple Negative Breast Cancer*

Speaker, University of Tubingen, Division of Radiobiology and Molecular Environmental Research, Tubingen, Germany. *Targeting Nuclear EGFR In Triple Negative Breast Cancer*

Speaker (**Keynote speaker)**, Wolfsberg Meeting Series on Molecular Radiation Biology and Oncology, Switzerland. *Targeting Nuclear EGFR In Triple Negative Breast Cancer*

2014 Speaker, University of Iowa, Department of Pathology, Iowa City, IA, *Nuclear EGFR As A Logical Therapeutic Target In Triple-Negative Breast Cancer*, February 2014 **(Grand Rounds, Invited)**

2015 Speaker, City of Hope, Beckman Research Center, Duarte, CA, *Nuclear EGFR As A Logical Therapeutic Target In Triple-Negative Breast Cancer and the implications of Axl*, November 2015 **(Grand Rounds)**

Patents and licenses applied for and/or issued; **N/A**
Degrees obtained that are supported by this award; **PhD in Cell and Molecular Biology for Toni M. Brand**
Development of cell lines, tissue, or serum repositories; **N/A**
Informatics such as databases and animal models, etc.; **N/A**
Funding applied for based on work supported by this award;

- Submitted an R01 expanding nuclear EGFR and cetuximab resistance; R01 grant scored a 23rd percentile on the A0 and 18th percentile on the A1. We are in preparation to resubmit in June 2016.
- Submitted an R01 expanding nuclear EGFR and cetuximab resistance in Triple Negative Breast Cancer (a direct result of dollars from the DOD grant); R01 grant scored a 16th percentile on the A0 and 5th percentile on the A1. We are working with the NCI to submit our IRB approval to gain the NoA.
- Submitted an institutional SPORE application to the NCI on the role of Axl in resistance to cetuximab therapy in NSCLC and HNSCC in October of 2015.

- Submitted an R01 application to the NCI on the role of Axl in resistance to cetuximab therapy in NSCLC and HNSCC in October of 2015.

Employment or research opportunities applied for and/or received based on experience/training supported by this award;

- Toni M. Brand, Postdoctoral position in Jennifer Grandis Lab at the University California, San Francisco
- Deric L Wheeler, University of Wisconsin Institute of Clinical and Translational Scholar
-

CONCLUSIONS:

NSCLC is a deadly disease that is driven by a multitude of factors. One of these factors is the epidermal growth factor receptor (EGFR). One of the most prominent molecular targeting agents to the EGFR is the antibody cetuximab. However, most patients develop resistance to this antibody. We have found in models of cetuximab resistance that the EGFR changes its location, to the nucleus, where it is not accessible to the large antibody. Our work over the last several years has discovered how to target the nEGFR, by blocking its translocation to the nucleus through Src Family Kinase blockade.

Specific Aim 1

We have determined, using, genetic and pharmacological approaches, that SFK inhibition but not AKT inhibition can block nuclear translocation of the EGFR**. Further using systematically designed EGFR mutants we** developed a new avenue by creating a novel EGFR mutant that lacks its transcriptional potential. This has allowed us to directly test the role of nEGFR in biology and cetuximab resistance. Results indicate that nEGFR can modulate its resistance to cetuximab independent of its kinase activity. Finally a new a novel avenue stemming from this grant is that first is that Axl receptor tyrosine kinase is a critical mediator of nuclear translocation of the EGFR. This novel finding may indicate that target Axl may serve as a secondary approach to block the nuclear functions of EGFR.

Specific Aim 2

We have determined that we can target nEGFR *in vivo* and redistribute to the membrane *in vivo* and increase nEGFR expressing, cetuximab resistant tumors to cetuximab by blocking nuclear translocation with dasatinib.

Specific Aim 3

We have determined that nEGFR can serve as a prognostic factor in early stage NSCLC patients. We are building on this finding to see if nEGFR can serve as a predictive biomarker for cetuximab response in lung SCC.

REFERENCES

1. Pirker, R.*, et al.* Cetuximab plus chemotherapy in patients with advanced non-small-cell lung cancer (FLEX): an open-label randomised phase III trial. *Lancet* **373**, 1525-1531 (2009).
2. Yarden, Y. & Sliwkowski, M.X. Untangling the ErbB signalling network. *Nat Rev Mol Cell Biol* **2**, 127-137 (2001).
3. Wang, S.C. & Hung, M.C. Nuclear translocation of the epidermal growth factor receptor family membrane tyrosine kinase receptors. *Clinical cancer research : an official journal of the American Association for Cancer Research* **15**, 6484-6489 (2009).
4. Li, C., Iida, M., Dunn, E.F. & Wheeler, D.L. Dasatinib blocks cetuximab- and radiation-induced nuclear translocation of the epidermal growth factor receptor in head and neck squamous cell carcinoma. *Radiother Oncol* (2010).
5. Li, C., Iida, M., Dunn, E.F., Ghia, A.J. & Wheeler, D.L. Nuclear EGFR contributes to acquired resistance to cetuximab. *Oncogene* **28**, 3801-3813 (2009).
6. Huang, W.C.*, et al.* Nuclear Translocation of Epidermal Growth Factor Receptor by Akt-dependent Phosphorylation Enhances Breast Cancer-resistant Protein Expression in Gefitinib-resistant Cells. *The Journal of biological chemistry* **286**, 20558-20568 (2011).
7. Lin, S.Y.*, et al.* Nuclear localization of EGF receptor and its potential new role as a transcription factor. *Nat Cell Biol* **3**, 802-808 (2001).
8. Lo, H.W.*, et al.* Nuclear interaction of EGFR and STAT3 in the activation of the iNOS/NO pathway. *Cancer Cell* **7**, 575-589 (2005).
9. Hanada, N.*, et al.* Co-regulation of B-Myb expression by E2F1 and EGF receptor. *Mol Carcinog* **45**, 10-17 (2006).
10. Jaganathan, S.*, et al.* A functional nuclear epidermal growth factor receptor, SRC and stat3 heteromeric complex in pancreatic cancer cells. *PloS one* **6**, e19605 (2011).
11. Hung, L.Y.*, et al.* Nuclear epidermal growth factor receptor (EGFR) interacts with signal transducer and activator of transcription 5 (STAT5) in activating Aurora-A gene expression. *Nucleic Acids Res* **36**, 4337-4351 (2008).
12. Lo, H.W., Cao, X., Zhu, H. & Ali-Osman, F. Cyclooxygenase-2 is a novel transcriptional target of the nuclear EGFR-STAT3 and EGFRvIII-STAT3 signaling axes. *Molecular cancer research : MCR* **8**, 232-245 (2010).
13. Wheeler, D.L.*, et al.* Mechanisms of acquired resistance to cetuximab: role of HER (ErbB) family members. *Oncogene* **27**, 3944-3956 (2008).
14. Wheeler, D.L.*, et al.* Epidermal growth factor receptor cooperates with Src family kinases in acquired resistance to cetuximab. *Cancer biology & therapy* **8**, 696-703 (2009).
15. Iida, M.*, et al.* Sym004, a novel EGFR antibody mixture, can overcome acquired resistance to cetuximab. *Neoplasia* **15**, 1196-1206 (2013).
16. Wang, Y.*, et al.* A chemically induced model for squamous cell carcinoma of the lung in mice: histopathology and strain susceptibility. *Cancer research* **64**, 1647-1654 (2004).
17. Surguladze, D.*, et al.* Tumor necrosis factor-alpha and interleukin-1 antagonists alleviate inflammatory skin changes associated with epidermal growth factor receptor antibody therapy in mice. *Cancer research* **69**, 5643-5647 (2009).
18. Brand, T.M.*, et al.* Mapping C-terminal transactivation domains of the nuclear HER family receptor tyrosine kinase HER3. *PloS one* **8**, e71518 (2013).
19. Brand, T.M., Iida, M., Luthar, N. & Wheeler, D.L. Mapping the transcriptional activation domains of the HER family of receptor tyrosine kinases. in *American Association of Cancer Research* (Washington, DC, 2013).
20. Traynor, A.M.*, et al.* Nuclear EGFR protein expression predicts poor survival in early stage non-small cell lung cancer. *Lung cancer* **81**, 138-141 (2013).
21. Pujol, J.L.*, et al.* Meta-analysis of individual patient data from randomized trials of chemotherapy plus cetuximab as first-line treatment for advanced non-small cell lung cancer. *Lung cancer* **83**, 211-218 (2014).
22. Di Maio, M. Is there still room for large registrative trials in unselected cancer patients? The case of anti-epidermal growth factor receptor antibodies in advanced non-small-cell lung cancer. *Expert Opin. Biol. Ther.* **11**, 1131-1133 (2011).
23. Khambata-Ford, S.*, et al.* Analysis of potential predictive markers of cetuximab benefit in BMS099, a phase III study of cetuximab and first-line taxane/carboplatin in advanced non-small-cell lung cancer. *Journal of clinical oncology : official journal of the American Society of Clinical Oncology* **28**, 918-927 (2010).
24. Pirker, R.*, et al.* EGFR expression as a predictor of survival for first-line chemotherapy plus cetuximab in patients with advanced non-small-cell lung cancer: analysis of data from the phase 3 FLEX study. *The lancet oncology* **13**, 33-42 (2012).
25. Brand, T.M.*, et al.* Nuclear Epidermal Growth Factor Receptor Is a Functional Molecular Target in Triple-Negative Breast Cancer. *Molecular cancer therapeutics* (2014).
26. Iida, M., Brand, T.M., Campbell, D.A., Li, C. & Wheeler, D.L. Yes and Lyn play a role in nuclear translocation of the epidermal growth factor receptor. *Oncogene* **32**, 759-767 (2013).
27. Li, C., Iida, M., Dunn, E.F. & Wheeler, D.L. Dasatinib blocks cetuximab- and radiation-induced nuclear translocation of the epidermal growth factor receptor in head and neck squamous cell carcinoma. *Radiotherapy and oncology : journal of the European Society for Therapeutic Radiology and Oncology* **97**, 330-337 (2010).
28. Carey, G.B.*, et al.* Utilisation of a thoracic oncology database to capture radiological and pathological images for evaluation of response to chemotherapy in patients with malignant pleural mesothelioma. *BMJ open* **2**(2012).
29. Surati, M.*, et al.* Proteomic characterization of non-small cell lung cancer in a comprehensive translational thoracic oncology database. *Journal of clinical bioinformatics* **1**, 1-11 (2011).

30. Lynch, T.J*., et al.* Cetuximab and first-line taxane/carboplatin chemotherapy in advanced non-small-cell lung cancer: results of the randomized multicenter phase III trial BMS099. *Journal of clinical oncology : official journal of the American Society of Clinical Oncology* **28**, 911-917 (2010).

APPENDICES: Papers directly related to the aims of the project

1. Brand TM, Iida M, Stein AP, Corrigan KL, Braverman CM, Coan JP, Pearson HE, Bahrar H, Fowler TL, Bednarz BP, Saha S, Yang D, Gill PS, Lingen MW, Saloura V, Villaflor VM, Salgia R, Kimple RJ, **Wheeler DL**. AXL is a logical molecular target in head and neck squamous cell carcinoma, Clin Cancer Res. 2015 Mar 12. [Epub ahead of print]

2. Brand, TM, Iida, M, Stein, AP, Corrigan, KL, Braverman, CM, Luthar, N, Toulany, M, Gill, PS, Salgia, R, Kimple, RJ, **Wheeler, DL.** AXL Mediates Resistance to Cetuximab Therapy, Cancer Res. 2014 Sep 15;74(18):5152-64 *Cancer research* (2014). PMID: 25136066, PMCID: PMC4167493

3. Brand, TM, Iida, M, Dunn, E, Luthar, N, Kostopoulus, KT, Corrigan, KL, Yang, Wleklinski, D, Wisinski, KB, Salgia, R, **Wheeler, DL**. Nuclear EGFR serves as a functional molecular target in Triple-negative breast cancer Mol Cancer Ther. 2014 May;13(5):1356-68. PMID: 24634415, PMCID: PMC4013210

4. Iida, M, Brand TM, Starr, M, **Wheeler, DL**, The EGFR blocking antibodies, SYM004, can overcome acquired resistance to cetuximab, Neoplasia 2013 Oct;15(10):1196-206. PMID:24204198, PMCID:PMC3819635

5. Iida M, Brand TM, Campbell DA, Li C, **Wheeler DL**. Yes and Lyn play a role in nuclear translocation of the epidermal growth factor receptor. Oncogene. 2013 Feb 7;32(6):759-67. PMID: 22430206, PMCID: PMC3381861

6. Brand, TM, Iida, M, Luthar, N, Starr, MM, Huppert, EJ, **Wheeler, DL.** Nuclear EGFR as a molecular target in cancer. Radiother Oncol. 2013 Sep;108(3):370-7. PMID: 23830194, PMCID: PMC3818450

7. Traynor, AM, Weigel, TL, Oettel, KR, Yang, DT, Zhang, C, KyungMann, K, Salgia, R, Iida, M, Brand, TM, Hoang, T, Campbell, TC, Hernan, HR, **Wheeler, DL**. Nuclear EGFR protein expression predicts poor survival in early stage non-small cell lung cancer. Lung Cancer 2013 July 81(1)134-41. PMID: 23628526, PMCID: PMC3679338

8. Iida, M, Brand, TM, Campbell, D, Starr, M, Luthar, N, Traynor, AM, **Wheeler, DL**. Targeting AKT With The Allosteric AKT Inhibitor MK-2206 in Non-Small Cell Lung Cancer cells with Acquired Resistance to Cetuximab. Cancer Biol Ther. 2013 Jun;14(6):481-91. PMID: 23760490, PMCID: PMC3813564

SUPPORTING DATA:

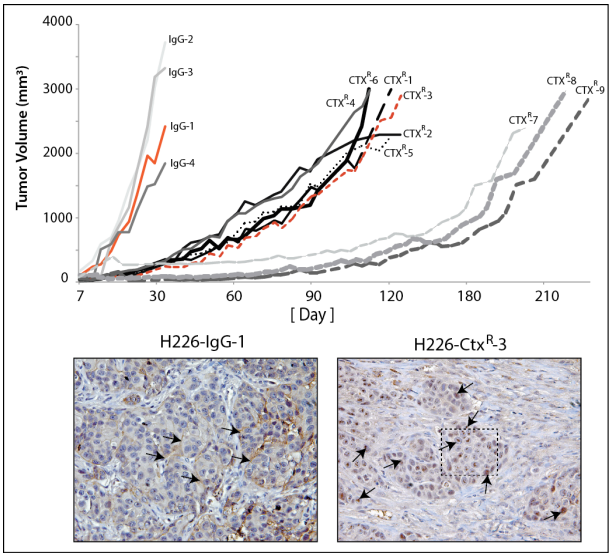

Figure 1: **Cetuximab resistant tumors derived *in vivo* harbor increased nEGFR as compared to IgG control tumors**. Arrows depict LSCC nuclear foci. H226 was used with similar results seen in HNSCC1 and 6 (data not shown).

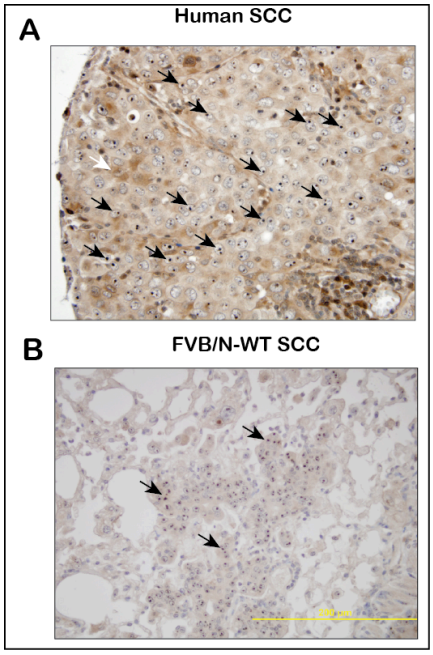

Figure 3: NTCU derived LSCC tumors harbor nEGFR. A) Human LSCC stained for nEGFR. B) Mouse NTCU treated LSCC tumor harbor nEGFR**.**

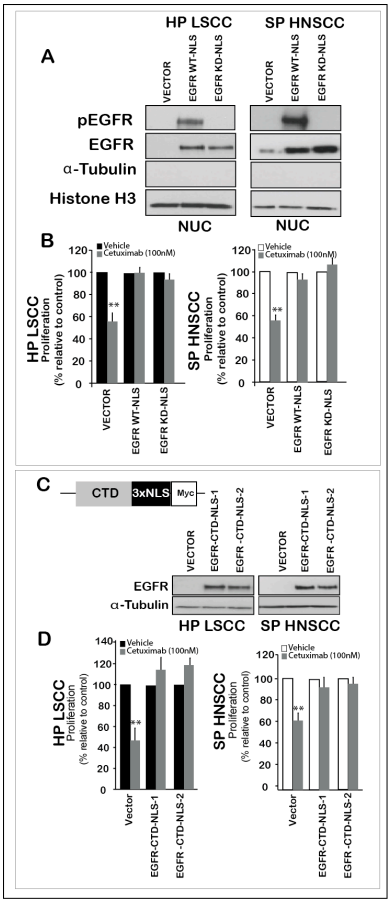

Figure 3: Nuclear EGFR, independent of its kinase activity, can drive cetuximab resistance. A) LSCC (HP) and HNSCC (SP) parental lines were transfected with EGFRWT-NLS or EGFR-KD-NLS. **B)** Both EGFRWT-NLS or EGFRKD-NLS could confer resistance to cetuximab upon cetuximab challenge. **C&D)** Isolation of the C-terminal of the EGFR could confer resistance to cetuximab therapy. ** P<0.005

Published OnlineFirst March 12, 2015; DOI: 10.1158/1078-0432.CCR-14-2648

Clinical Cancer Research

AXL Is a Logical Molecular Target in Head and Neck Squamous Cell Carcinoma

Toni M. Brand[1], Mari Iida[1], Andrew P. Stein[1], Kelsey L. Corrigan[1], Cara M. Braverman[1], John P. Coan[1], Hannah E. Pearson[1], Harsh Bahrar[1], Tyler L. Fowler[1,2], Bryan P. Bednarz[2], Sandeep Saha[3], David Yang[4], Parkash S. Gill[5], Mark W. Lingen[6], Vassiliki Saloura[7], Victoria M. Villaflor[7], Ravi Salgia[7], Randall J. Kimple[1], and Deric L. Wheeler[1]

Abstract

Purpose: Head and neck squamous cell carcinoma (HNSCC) represents the eighth most common malignancy worldwide. Standard-of-care treatments for patients with HNSCC include surgery, radiation, and chemotherapy. In addition, the anti-EGFR monoclonal antibody cetuximab is often used in combination with these treatment modalities. Despite clinical success with these therapeutics, HNSCC remains a difficult malignancy to treat. Thus, identification of new molecular targets is critical.

Experimental Design: In the current study, the receptor tyrosine kinase AXL was investigated as a molecular target in HNSCC using established cell lines, HNSCC patient-derived xenografts (PDX), and human tumors. HNSCC dependency on AXL was evaluated with both anti-AXL siRNAs and the small-molecule AXL inhibitor R428. Furthermore, AXL inhibition was evaluated with standard-of-care treatment regimens used in HNSCC.

Results: AXL was found to be highly overexpressed in several models of HNSCC, where AXL was significantly associated with higher pathologic grade, presence of distant metastases, and shorter relapse-free survival in patients with HNSCC. Further investigations indicated that HNSCC cells were reliant on AXL for cellular proliferation, migration, and invasion. In addition, targeting AXL increased HNSCC cell line sensitivity to chemotherapy, cetuximab, and radiation. Moreover, radiation-resistant HNSCC cell line xenografts and PDXs expressed elevated levels of both total and activated AXL, indicating a role for AXL in radiation resistance.

Conclusion: This study provides evidence for the role of AXL in HNSCC pathogenesis and supports further preclinical and clinical evaluation of anti-AXL therapeutics for the treatment of patients with HNSCC. *Clin Cancer Res; 1–12. ©2015 AACR.*

Introduction

With more than 600,000 new cases diagnosed worldwide each year, head and neck squamous cell carcinoma (HNSCC) represents the eighth most common malignancy (1). HNSCC arises from epithelial cells that comprise the mucosal surfaces of the lips, oral cavity, larynx, pharynx, and nasal passages. Classically, these malignancies were highly associated with alcohol and tobacco abuse, but over the past decade, it has been determined that human papillomavirus (HPV) is causally associated with a subset of HNSCCs (2).

Approximately 60% of patients with HNSCC present with locoregionally advanced disease at the time of diagnosis. To achieve the greatest chance for cure, these patients are typically treated with a multimodality approach of systemic chemotherapy, radiation, and surgery (3–5). Advances in molecular targeting of HNSCC have found that cetuximab, an anti-EGFR monoclonal antibody, can benefit patients when combined with platinum chemotherapy or radiation (6–8). Although advances in these treatment modalities have improved patient outcomes, many patients still develop recurrent tumors and distant metastases. Upon relapse, patient survival remains poor. In this manner, the identification of new therapeutic targets is critical.

The receptor tyrosine kinase AXL has now been implicated in the development and progression of many malignancies, including lung (9–14), breast (12, 15–19), ovarian (20), colon (21), head and neck (22), thyroid (23), prostate (24), pancreatic (25), osteosarcoma (26), and Kaposi sarcoma (27). These studies indicate a role for AXL in cancer cell proliferation, migration, angiogenesis, and metastasis (reviewed in refs. 28, 29). Moreover, AXL mRNA expression has been correlated with poor disease outcome in HNSCC (22), indicating a putative role for AXL in the formation and/or progression of this disease. Recent studies have also found that AXL can mediate resistance to anti-EGFR inhibitors, further unveiling a role for AXL in cancer progression (9, 11, 13, 22, 30, 31). In the current study,

[1]Department of Human Oncology, University of Wisconsin School of Medicine and Public Health, Madison, Wisconsin. [2]Department of Medical Physics, University of Wisconsin, Madison, Wisconsin. [3]Department of Biostatistics and Medical Informatics, University of Wisconsin, Madison, Wisconsin. [4]Department of Pathology and Laboratory Medicine, University of Wisconsin, Madison, Wisconsin. [5]Departments of Medicine and Pathology, University of Southern California, Los Angeles, California. [6]Department of Pathology, University of Chicago Medical Center, Chicago, Illinois. [7]Division of Hematology/Oncology, Department of Medicine, University of Chicago, Chicago, Illinois.

Note: Supplementary data for this article are available at Clinical Cancer Research Online (http://clincancerres.aacrjournals.org/).

Corresponding Author: Deric L. Wheeler, Department of Human Oncology, University of Wisconsin Comprehensive Cancer Center, 1111 Highland Avenue, WIMR 3159, Madison, WI 53705. Phone: 608-262-7837; Fax: 608-263-9947; E-mail: dlwheeler@wisc.edu

doi: 10.1158/1078-0432.CCR-14-2648

Published OnlineFirst March 12, 2015; DOI: 10.1158/1078-0432.CCR-14-2648

Translational Relevance

Head and neck squamous cell carcinoma (HNSCC) represents the eighth most common malignancy worldwide. Standard-of-care treatments include surgery, radiation, and chemotherapy. In addition, the anti-EGFR monoclonal antibody cetuximab is commonly used. Despite clinical success with these therapies, HNSCC remains a difficult malignancy to treat. Thus, identification of molecular targets is critical. In the current study, the receptor tyrosine kinase AXL was overexpressed and significantly associated with higher pathologic grade, distant metastases, and shorter relapse free-survival in patients with HNSCC. On the basis of these findings, AXL was evaluated as a molecular target in HNSCC models using the clinically relevant tyrosine kinase inhibitor R428, where AXL targeting enhanced the efficacy of platinum chemotherapy, cetuximab, and radiation. Importantly, AXL was overexpressed and hyperactivated in radiation-resistant *in vivo* HNSCC models. Collectively, these studies provide rationale for the clinical evaluation of anti-AXL therapeutics for the treatment of patients with HNSCC.

we sought to determine whether AXL is a functional molecular target in HNSCC, and whether targeting AXL could enhance the efficacy of standard treatments used to treat patients with this disease.

Materials and Methods

Cell lines

All cell lines were obtained from the indicated sources (Supplementary Materials and Methods). The identity of all cell lines was confirmed via short tandem repeat testing.

Antibodies and compounds

All antibodies used are as follows: R&D Systems: AXL (for immunoblotting) and pAXL (Y779). Cell Signaling Technology: Phospho-SFK (Y419), pDNA-PK (S216), DNA-PK, pAKT (S473), AKT, p-γ-H2AX (S139), GAPDH, and pan-tyrosine (pan-Tyr). Santa Cruz Biotechnology Inc.: AXL (for immunoprecipitation; IP), E-Cadherin, vimentin, and horseradish peroxidase (HRP)–conjugated goat–anti-rabbit IgG, goat–anti-mouse IgG, and donkey–anti-goat IgG. Abcam: EGFR and pEGFR (Y1101). Calbiochem: α-tubulin. R428 was purchased from Selleckchem. Cetuximab (ICM-225; Erbitux) was purchased from University of Wisconsin Pharmacy (Madison, WI). Cisplatin, carboplatin, and camptothecin were purchased from LC Laboratories.

Plasmids, transfection, and siRNA technology

Plasmid construction and stable selection of AXL overexpressing cells were described previously (30). Cells were transiently transfected with AXL siRNA (siAXL-1; ON-TARGETplus, SMARTpool #L-003104; GE Dharmacon, Lafayette, CO, USA or siAXL-2; Cell Signaling AXL siRNA I #6263) or nontargeting siRNA (siNT; ON-TARGETplus Non-targeting Pool, #D-001810; Dharmacon) using Lipofectamine RNAiMAX according to the manufacturer's instructions (Life Technologies). siAXL-1 was used for cisplatin, cetuximab, and radiation studies.

Cell proliferation assay and clonogenic survival assay

Crystal violet assay and Cell Counting Kit-8 (Dojindo Molecular Technologies) were performed as previously described and in the Supplementary Materials and Methods (30, 32). Crystal violet assays were performed to identify the combinatorial effect of siAXL and radiation.

Apoptosis assay

HNSCC cell lines were treated with 0.5 or 1.0 μmol/L of R428 for 24 hours before staining with YO-PRO-1 and propidium iodide according to the manufacturer's instructions (Vybrant Apoptosis Assay Kit #4, YO-PRO-1/propidium iodide, Invitrogen). Uptake of YO-PRO-1 and PI was measured using a FACSCalibur flow cytometer (BD Biosciences) and FlowJo analysis software (TreeStar Inc).

Immunoblot analysis

Whole-cell lysis, immunoprecipitation, and Western blot analysis were performed as previously described (30). Enhanced chemiluminescence (ECL) detection system was used to visualize proteins.

Wound-healing assay

Cells were plated in 6-well culture plates. Upon 80% to 90% confluence, the cell layer was scratched with a p-200 pipette tip (3 scratches per well, 2–3 wells per treatment). The cells were then cultivated in complete medium with/without indicated doses of R428. Alternatively, cells were transfected with siAXL or siNT for 24 hours before wound exposure. Photographs of the wound adjacent to reference lines were taken using an Olympus IX51 microscope (×20) at indicated time points. CellSens Standard 1.9 software (Olympus) was used to digitally measure wound closure; wound closure at each time point was normalized to the averaged scratch width measured at time 0.

Cell invasion assay

CultreCoat Low BME Cell Invasion Assay was purchased from R&D Systems. Cells were plated in 96-well CultreCoat plates with either vehicle or R428. Twenty-four hours post therapy, cell invasion was measured as per manufacturer's instructions.

γ-H2AX fluorescent assay

Cells were plated in 96-well dishes and pretreated with vehicle or R428 (1 μmol/L). A novel high-throughput irradiator utilizing a 50 kVp X-ray beam spectrum was used to deliver 4 gray (Gy) as previously described (33, 34). Cells were fixed in 4% paraformaldehyde 4 hours later, permeabilized in 90% methanol, blocked, and incubated with γ-H2AX primary antibody (1:500) overnight. Cells were washed and incubated with FITC-conjugated secondary antibody (1:1,000; Santa Cruz Biotechnology). γ-H2AX fluorescence per cell was evaluated via a SpectraMax i3 plate reader with MiniMax 300 imaging cytometer using SoftMax Pro v6.4 software (Molecular Devices). All γ-H2AX fluorescent values were averaged and then normalized to averaged values from vehicle-treated cells.

Cell line xenografts, patient-derived xenografts (PDX), and radiation response

Cell line xenografts and patient-derived xenografts (PDX) were established as previously described (30, 35, 36). Radiation response was evaluated as described in the Supplementary Materials and Methods.

Published OnlineFirst March 12, 2015; DOI: 10.1158/1078-0432.CCR-14-2648

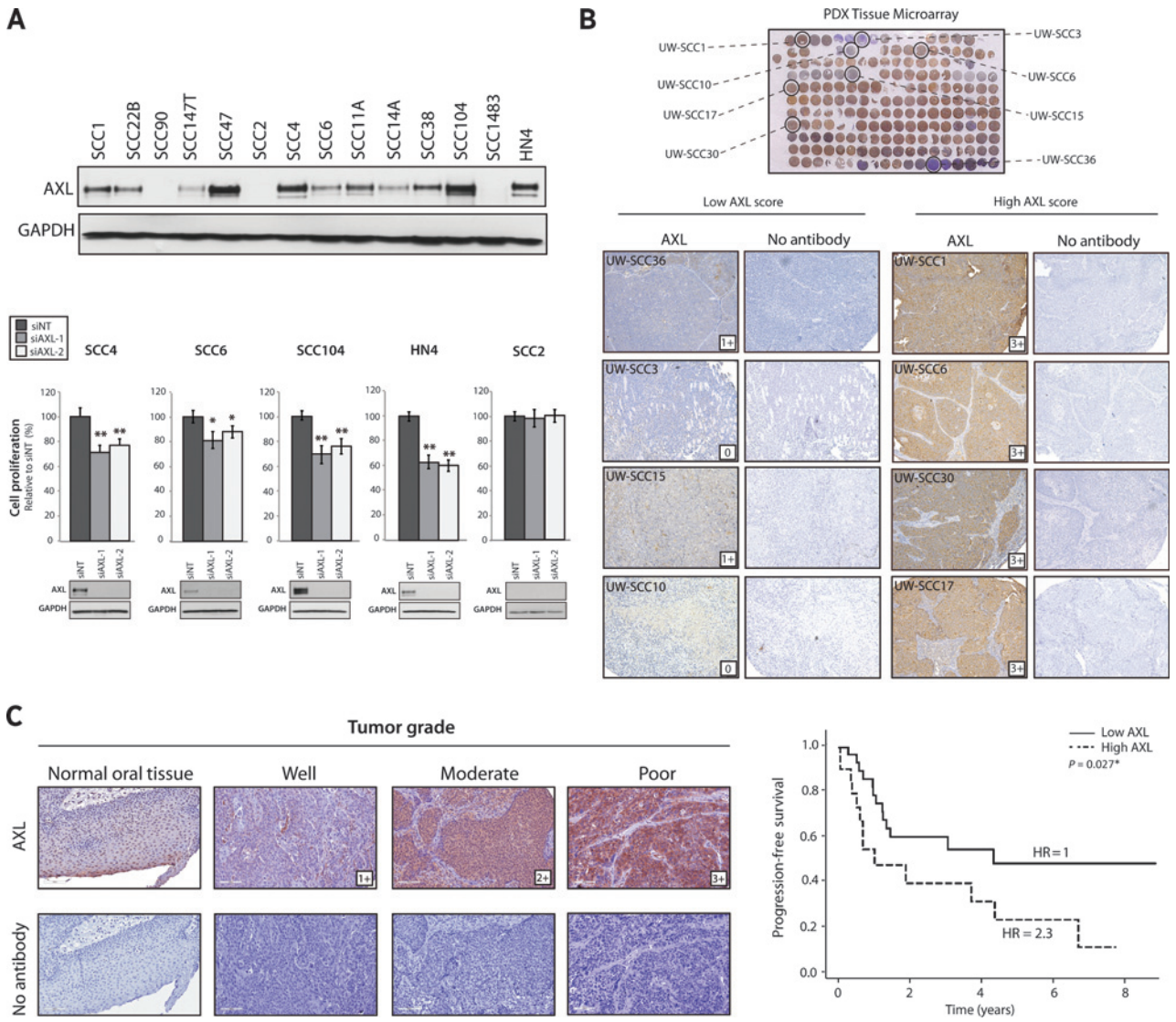

Figure 1.

HNSCC cell lines, PDXs, and human tumors express AXL. A, whole-cell lysate was harvested from 14 HNSCC cell lines and evaluated for AXL expression. GAPDH was used as a loading control. AXL-expressing cell lines were transfected with siAXL-1 (50 nmol/L), siAXL-2 (100 nmol/L), or nontargeting (NT) siRNA for 72 hours before performing proliferation assays ($n = 4$–6 replicates in three independent experiments). Whole-cell lysate was harvested at the same time to confirm AXL knockdown. Data points are represented as mean ± SEM. *, $P < 0.05$; **, $P < 0.01$. B, AXL is differentially expressed in a 22 HNSCC PDX TMA consisting of several early passaged tumors per PDX. Representative images of low and high AXL expressing PDXs are shown (×10). Pathologic IHC quantitation (by D. Yang) was determined via a categorical scale from 0 to 4+. C, high AXL expression is associated with increased tumor grade in a 63 HNSCC patient cohort. Representative images of low and high AXL expressing patient tumors corresponding to pathologic tumor grade are shown (×20). Pathologic IHC quantitation (by M.W. Lingen) was determined via a categorical scale from 0 to 3+. High AXL expression was significantly associated with shorter median PFS in patients with HNSCC as analyzed by the Kaplan–Meier method. *, $P < 0.05$. HR; hazard ratio.

HNSCC patient cohort and tissue microarray construction

Patients with HNSCC completed written consent in accordance with Institutional Review Board approval from the University of Chicago (Chicago, IL; protocol number 10-343-A). See Supplementary Materials and Methods for details.

Statistical analysis

HNSCC patient demographics and clinical characteristics were summarized using descriptive statistics in the Supplementary Materials and Methods. Student *t* test was used to evaluate differences in cell proliferation, migration, and invasion. Differences were considered statistically significant if *, $P < 0.05$; **, $P < 0.01$.

Results

AXL is expressed in HNSCC cell lines, PDXs, and human tumors

To determine whether AXL could represent a molecular target in HNSCC, AXL expression was evaluated in a panel of 14 HSNCC cell lines (Fig. 1A, top). These results indicated that 11 of the 14 cell lines expressed AXL, whereas three cell lines (SCC90, SCC2,

Published OnlineFirst March 12, 2015; DOI: 10.1158/1078-0432.CCR-14-2648

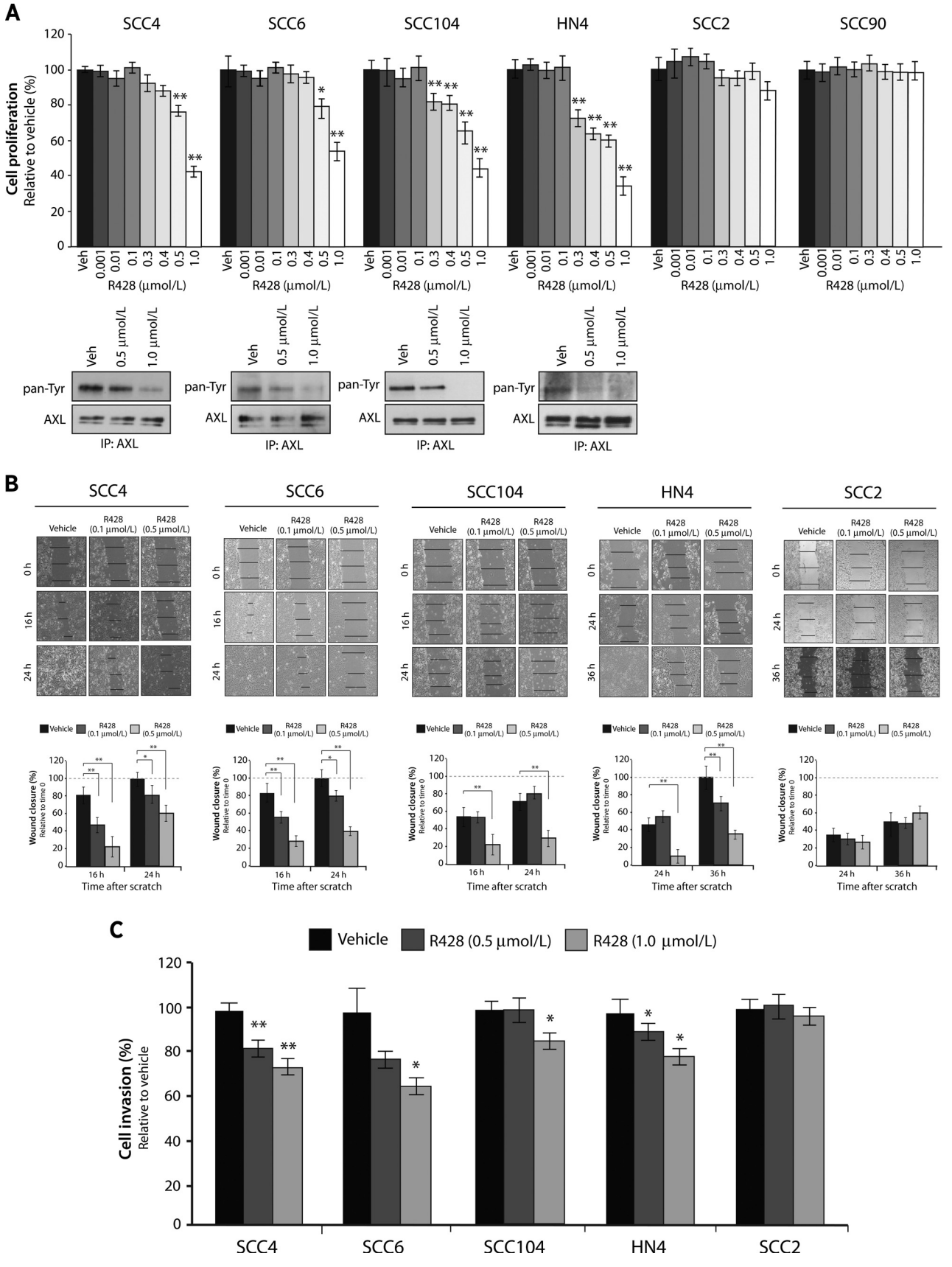

Published OnlineFirst March 12, 2015; DOI: 10.1158/1078-0432.CCR-14-2648

and SCC1483) had either low or undetectable AXL protein levels. Because AXL was differentially expressed, the dependency of these cell lines on AXL for proliferation was evaluated with AXL siRNAs. Four AXL-positive cell lines were transfected with a pooled AXL-siRNA (siAXL-1), a second individual AXL siRNA (siAXL-2) or a nontargeting siRNA control (siNT; Fig. 1A, bottom), and cellular proliferation was measured 72 hours posttransfection. Genetic ablation of AXL with either siAXL-1 or siAXL-2 resulted in statistically significant inhibition of cellular proliferation in the AXL-expressing cell lines SCC4, SCC6, SCC104, and HN4, whereas the AXL-negative cell line, SCC2, was unaffected. Collectively, these data indicated that HNSCC cell lines expressed AXL and were dependent on this receptor for proliferation.

To expand these findings, a 22 PDX tissue microarray (TMA) was stained for AXL via IHC using a previously validated anti-AXL antibody (30). This TMA contained several early passaged tumors from each PDX to evaluate consistency of protein expression across passages. Each TMA core was scored for AXL expression on a categorical scale from 0 to 4+, where 0 represented no staining and 4+ was the most intense staining. Pathologic analysis (by D. Yang) of AXL staining patterns indicated that 82% of the PDXs expressed AXL, where AXL expression remained relatively consistent across early passaged tumors (Fig. 1B). Four percent of the PDXs were negative for AXL expression. Collectively, these data indicate that AXL is commonly expressed in a clinically relevant model of HNSCC.

To further define the expression status of AXL in HNSCC, 63 HNSCC patient tumors were evaluated for AXL expression by IHC on a categorical scale of 0–3+, where 0–1+ was considered a low AXL score, and 2–3+ was considered a high AXL score (see Supplementary Table S1 for clinical information of the patient cohort). Pathologic analysis (by M.W. Lingen) of this cohort indicated that 38% expressed high levels of AXL, whereas 62% expressed either low or no AXL (Fig. 1C). Normal oral tissue from six different patients was stained for AXL, where AXL staining was low or undetectable, indicating increased expression of AXL specifically in tumor cells (Fig. 1C). Using a logistic regression model, the multivariate predictors of elevated AXL expression included: male versus female gender [OR, 6.38 (95% confidence interval (CI), 1.18–34.5)], poorly differentiated versus moderate/well differentiated tumor grade (OR, 4.03; 95% CI, 1.05–15.48) and presence of distant metastasis (OR, 3.58; 95% CI, 1.03–12.53; Supplementary Table S2A). The expression of p16, indicative of HPV-associated cancers (37), was not associated with AXL expression. Progression-free survival (PFS) in this cohort was determined by evaluating the number of patients in the low and high AXL groups who experienced a recurrence of their disease or passed away. There was a significant association between PFS and AXL score ($P = 0.027$), where median PFS was shorter in patients with high AXL (1.0 years; 95% CI, 0.6–∞) as compared with patients with low AXL (4.3 years; 95% CI, 1.4–∞; Fig. 1C and Supplementary Table S2B). The hazard ratio (HR) for PFS among patients with high versus low AXL score was 2.3 (95% CI, 1.1–5.1), indicating a higher probability of death or recurrence in patients with high AXL expression. Collectively, these results indicate that AXL is overexpressed in more aggressive HNSCCs and is related to poor clinical outcome.

AXL inhibition effectively reduces HNSCC cell growth, migration, and invasion

Because several HNSCC cell lines were sensitive to AXL knockdown by siRNA, we hypothesized that these cells would also be sensitive to the AXL tyrosine kinase inhibitor R428. R428 specificity for AXL has been previously evaluated (15), and this agent has now undergone successful phase Ia clinical evaluation (38). HNSCC cells were treated with increasing doses of R428 (0.001–1.0 μmol/L) for 72 to 96 hours before performing proliferation assays. All AXL-expressing HNSCC cell lines were significantly growth inhibited with increasing doses of R428 (Fig. 2A). The AXL-negative cell lines, SCC2 and SCC90, were used as controls, and their proliferation was not significantly altered with increasing doses of R428. Furthermore, via evaluation of pan phosphotyrosine post-immunoprecipitation with an anti-AXL antibody, R428 inhibited AXL activation at several doses that also resulted in the most robust antiproliferative responses (0.5 and 1.0 μmol/L).

In addition to influencing cellular proliferation pathways, AXL has been shown to mediate the metastatic potential of cancer cells (26, 27). To determine whether AXL regulates the migratory potential of HNSCC cells, wound-healing assays were performed using SCC4, SCC6, SCC104, HN4, and SCC2 cells post AXL inhibition. In this assay, cells were subjected to injury directly after treatment with either 0.1 or 0.5 μmol/L R428. Wound length was measured after the wound was first made (0 hour) and at the indicated time points post wound exposure (Fig. 2B). SCC4 and SCC6 cells treated with either dose of R428 displayed less wound closure at both time points as compared with vehicle-treated cells (where the wound was completely closed at 24 hours). SCC104 and HN4 cells displayed less wound closure when treated with 0.5 μmol/L of R428 at both displayed time points. The AXL-negative cell line, SCC2, was the least migratory of all HNSCC cell lines tested, and R428 did not have an impact on its migratory capacity. To further validate the specificity of R428 for AXL, cells were transfected with siNT or siAXL for 24 hours before performing wound-healing assays (Supplementary Fig. S1). AXL knockdown significantly impacted wound closure in all AXL-expressing cell lines tested as compared with cells transfected with siNT.

Next, the invasive potential of the HNSCC cells was measured via Boyden chamber invasion assays 24 hours after R428 treatment (Fig. 2C). All AXL-expressing cell lines examined were significantly inhibited in their invasive potential when pretreated with 1.0 μmol/L of R428, whereas HN4 and SCC4 cells were inhibited at lower doses (0.5 μmol/L). In addition, R428 did not impede the invasive potential of SCC2 cells.

Figure 2.

AXL mediates HNSCC cell proliferation, migration, and invasion. A, cells were treated with R428 at indicated doses for 72 to 96 hours before performing proliferation assays. Proliferation is plotted as a percentage of growth relative to vehicle-treated cells ($n = 6$ in three independent experiments). R428 inhibition of AXL activity was evaluated via IP analysis for pan-tyrosine 24 hours posttreatment. B, cells were treated with R428 or vehicle and subsequently subjected to wound exposure. Wound length was imaged and measured after the wound was first made (0 hour) and at the indicated time points post wound exposure (×20; $n = 3$–6 replicates in three independent experiments). C, cells were plated in a 96-well Boyden chamber and subsequently treated with R428 (indicated doses) or vehicle. Twenty-four hours later, invading cells that had penetrated the bottom side of the chamber were quantified by calcein-AM. Cell invasion was calculated by normalizing fluorescent values of R428-treated invading cells to vehicle controls ($n = 9$ in three independent experiments). All data points are represented as mean ± SEM. *, $P < 0.05$; **, $P < 0.01$.

Published OnlineFirst March 12, 2015; DOI: 10.1158/1078-0432.CCR-14-2648

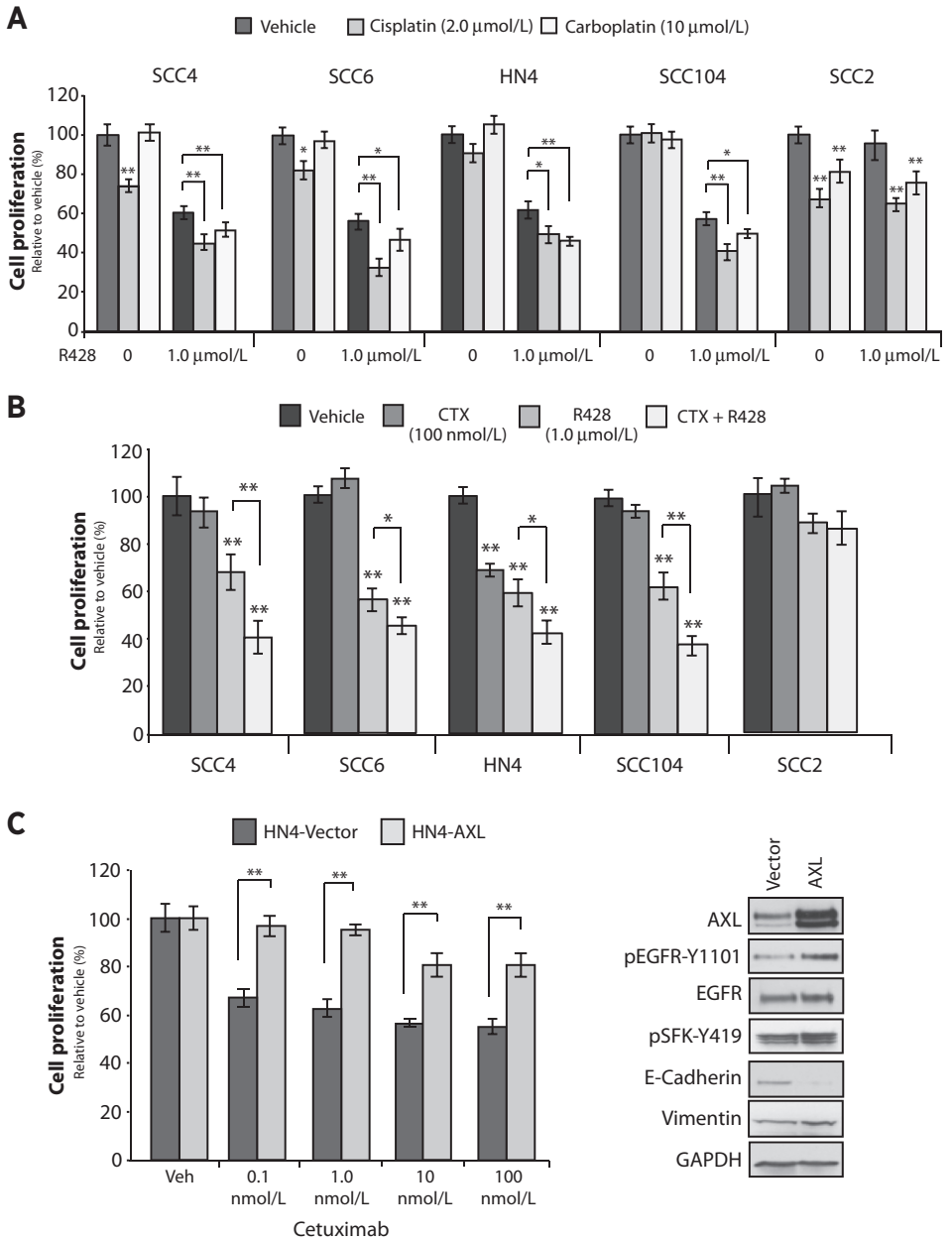

Figure 3.
AXL inhibition increases the sensitivity of HNSCC cells to chemotherapy and cetuximab. A, cells were treated with cisplatin (2.0 μmol/L), carboplatin (10 μmol/L), R428 (1.0 μmol/L), or the combination of R428 and each chemotherapy for 72 to 96 hours before performing proliferation assays. B, cells were treated with vehicle, cetuximab (100 nmol/L), R428 (1.0 μmol/L), or the combination for 72 hours before performing proliferation assays. C, HN4 cells stably overexpressing AXL (HN4-AXL) or pcDNA6.0 Vector (HN4-Vector) were treated with increasing doses of cetuximab (0.1–100 nmol/L) for 72 hours before performing proliferation assays. Whole-cell lysate was harvested and subjected to immunoblot analysis. GAPDH was used as a loading control. All proliferation assays are plotted as a percentage of growth relative to vehicle-treated cells ($n = 6$ in three independent experiments). Data points are represented as mean ± SEM. *, $P < 0.05$; **, $P < 0.01$.

To ensure R428's effects on migration and invasion were not due to changes in cell death or proliferation, cellular proliferation and apoptosis were measured 24 hours posttreatment with 0.5 and 1.0 μmol/L R428 (Supplementary Fig. S2). This analysis indicated that HNSCC cell proliferation and apoptosis were not significantly altered by increasing doses of R428 at this time point, supporting R428's specific effects on the migratory and invasive capacity of HNSCC cells. Overall, AXL inhibition effectively reduced proliferation, migration, and invasion of HNSCC cell lines suggesting that AXL may represent a potent molecular target in HNSCC.

AXL inhibition increases the sensitivity of HNSCC cells to chemotherapy and cetuximab

To evaluate whether AXL inhibition could augment the sensitivity of HNSCC cells to standard of care treatments, we first tested whether AXL inhibition enhanced HNSCC cell line sensitivity to the platinum-based chemotherapies cisplatin and carboplatin (Fig. 3A). Evaluation of cellular proliferation 72 to 96 hours posttreatment indicated differential responses to cisplatin and carboplatin monotherapy. However, addition of R428 to either cytotoxic agent led to statistically significant reductions in cell proliferation as compared to cells treated with R428 only. The AXL-negative cell line, SCC2, was the most sensitive to chemotherapy, and R428 did not augment response. Using the fractional product method (described by Chou and Talalay; refs. 39–41), the nature of the interaction between R428 and each chemotherapy was evaluated for synergy as described in the Supplementary Materials and Methods. AXL inhibition synergized with both cisplatin and carboplatin in all AXL-expressing cell lines, where the ratio of the observed

Published OnlineFirst March 12, 2015; DOI: 10.1158/1078-0432.CCR-14-2648

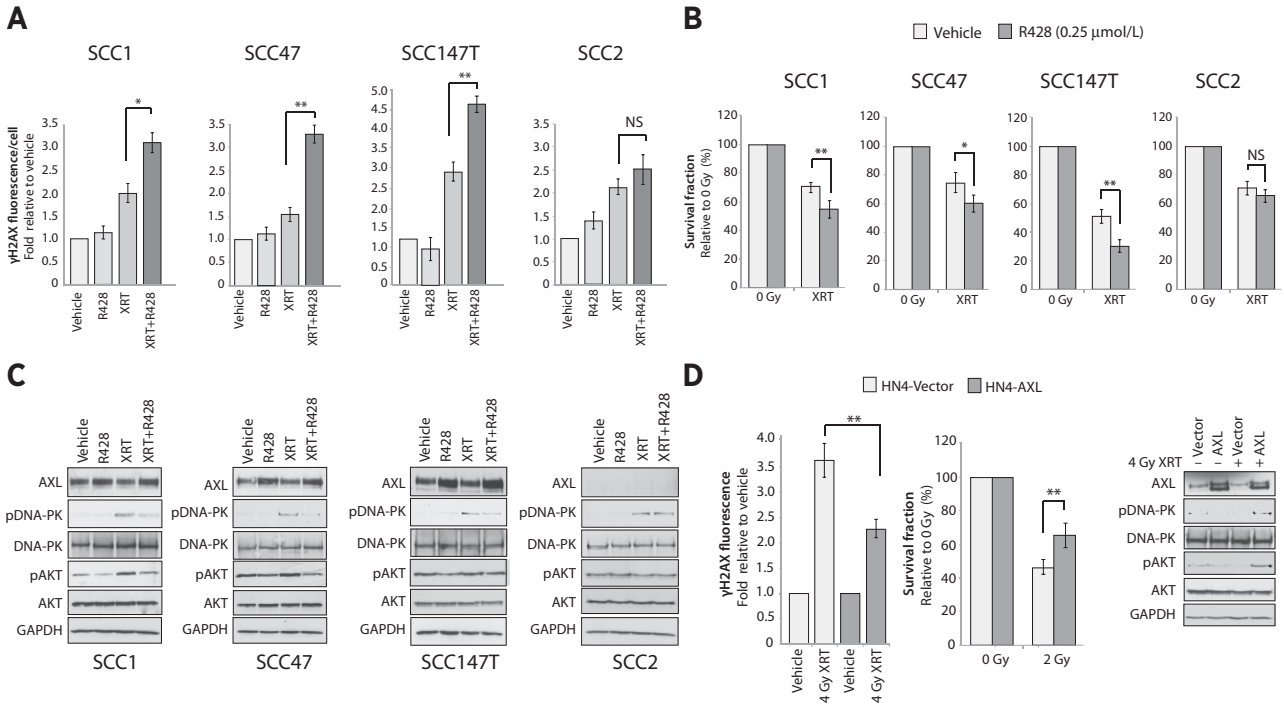

Figure 4.

Targeting AXL can enhance the efficacy of radiation therapy in HNSCC. A, cells were pretreated with vehicle or R428 (1.0 μmol/L) for 24 hours and then subjected to 4 Gy radiation (XRT). γ-H2AX fluorescence per cell was evaluated via a SpectraMax i3 plate reader with MiniMax 300 imaging cytometer four hours post XRT. All γ-H2AX fluorescent values were averaged and normalized to averaged values from vehicle-treated cells ($n = 12$ in three independent experiments). B, cells were pretreated with vehicle or R428 and then subjected to indicated doses of radiation: 4 Gy (SCC1, SCC47, and SCC2) or 2 Gy (SCC147T). Clonogenic survival was determined 10 to 14 days postradiotherapy ($n = 6$ in three independent experiments). C, cells were pretreated with R428 (1.0 μmol/L) for 24 hours before receiving 4 Gy XRT. Fifteen minutes after radiotherapy, cells were lysed and processed for immunoblot analysis for indicated proteins. GAPDH was used as a loading control. D, HN4-Vector and HN4-AXL stable cells were subjected to 4 Gy radiation before fixation and γ-H2AX evaluation as in A. Clonogenic survival analysis and immunoblot analysis were performed as in B and C. Data points are represented as mean ± SEM. *, $P < 0.05$; **, $P < 0.01$.

(O) to expected (E) effect was less than 1 (Supplementary Table S3A and S3B). In addition, siRNA-targeting AXL synergized with cisplatin, providing further evidence for the specificity of R428 for AXL inhibition (Supplementary Fig. S3A). Collectively, these results demonstrate that AXL inhibition enhances chemotherapy sensitivity in HNSCC cells.

Because AXL expression has been shown to mediate cetuximab resistance (30), we hypothesized that AXL inhibition may improve the efficacy of cetuximab therapy in HNSCC. Therefore, five HNSCC cell lines were treated with vehicle, R428 (1.0 μmol/L), cetuximab (100 nmol/L), or the combination, and cellular proliferation was measured 72 hours later (Fig. 3B). Three cell lines (SCC4, SCC6, and SCC104) were resistant to cetuximab, whereas HN4 cells were sensitive to cetuximab monotherapy. Importantly, when treated with both R428 and cetuximab, all cell lines demonstrated significant reduction in cellular proliferation as compared with cells treated with R428 only. The resulting effect of both drugs was determined to be synergistic in all cell lines except for HN4, where an additive effect was observed (Supplementary Table S3C). Additional siRNA studies confirmed specificity of R428 for AXL inhibition, as AXL knockdown synergized with cetuximab in all cell lines tested (Supplementary Fig. S3B). To further evaluate whether AXL mediates cetuximab response in HNSCC cells, the cetuximab-sensitive cell line HN4 was manipulated to highly overexpress AXL via stable transfection. Cetuximab dose–response proliferation assays demonstrated HN4-AXL cells were statistically more resistant to increasing doses of cetuximab as compared with HN4-Vector cells (Fig. 3C). Immunoblot analysis of HN4-AXL cells indicated increased activation of proteins previously reported to play a role in cetuximab resistance, including increased phosphorylation of EGFR on tyrosine 1101 and src family kinases (SFK; refs. 42–44). In addition, HN4-AXL cells had decreased levels of E-cadherin and increased levels of vimentin, two hallmarks of cells that have undergone epithelial-to-mesenchymal transition (EMT). Taken together, these studies support a role for AXL in cetuximab resistance, and suggest that AXL inhibition can enhance cetuximab sensitivity in HNSCC cells.

Targeting AXL can enhance the efficacy of radiation therapy in HNSCC

It is well established that several RTKs play a role in modulating DNA repair pathways and response to radiation therapy (45, 46). However, the role of AXL in radiation response has never been investigated. A previous report has indicated differential radiation responses for several HNSCC cell lines that express AXL (Fig. 1A), including SCC1, SCC47, and SCC147T (35). Therefore, we examined if AXL inhibition could augment the sensitivity of these cell lines to radiotherapy. Using a high-throughput X-ray radiation system that delivers the same absorbed dose of ionizing radiation

Published OnlineFirst March 12, 2015; DOI: 10.1158/1078-0432.CCR-14-2648

to cells plated in a 96-well format (development and characterization; ref. 33), SCC1, SCC47, SCC147T, and SCC2 were irradiated with 4 Gy after 24 hour pretreatment with either vehicle or R428 (1 μmol/L). Then, the induction of DNA double-strand breaks (DSB) were examined via γ-H2AX, which is phosphorylated and recruited to sites of DNA damage in response to radiation (Fig. 4A). At 4 hours postirradiation, total γ-H2AX fluorescent intensity per cell was determined via a fluorescent plate reader with image cytometer. This system allowed for the quantitation of multiple replicates at the same time ($n = 12$ wells per treatment group) while simultaneously eliminating human error in counting γ-H2AX foci. A significant increase in γ-H2AX fluorescent foci was observed in cells treated with R428 and radiation as compared with cells treated with radiation only. The AXL-negative cell line, SCC2, was used as a control, and there was not a significant difference in γ-H2AX between either radiation treatment group.

To further assess the impact of AXL inhibition on radiation response, clonogenic survival assays were performed after exposure to R428 and radiation (Fig. 4B). In this experiment, an equal number of cells were plated per well and subsequently pretreated with 0.25 μmol/L R428 for 24 hours before XRT exposure. Nonirradiated cells treated with vehicle or R428 demonstrated similar plating efficiency (data not shown). However, all AXL-expressing cell lines pretreated with R428 demonstrated significantly reduced survival following radiation exposure as compared with cells treated with radiation only. The effect of R428 and radiation was determined to be synergistic in all AXL-expressing cell lines tested (Supplementary Table S3C). R428 pretreated SCC2 cells did not demonstrate a reduction in survival as compared with cells treated with radiation only. Finally, AXL knockdown with siRNA before radiation exposure resulted in reduced cellular viability, further supporting the AXL-specific radiosensitizing effects of R428 (Supplementary Fig. S3C).

To investigate the potential molecular mechanisms underlying this enhanced radiation response, the activation of DNA-protein kinase (DNA-PK) and AKT was examined post R428 and radiation therapy (Fig. 4C). DNA-PK is largely responsible for mediating DNA DSB repair through nonhomologous end joining, and thus, when activated can lead to radiation resistance (47). AKT is an intracellular serine/threonine kinase that directly interacts with DNA-PK to promote DNA DSB repair and cell survival (48). AXL-expressing HNSCC cells treated with R428 and radiation expressed considerably less activated DNA-PK and AKT levels as compared with cells treated with radiation alone. R428 did not augment radiation-induced DNA-PK or AKT activation in the AXL-negative cell line SCC2. Collectively, these data suggest that AXL signaling mediates DNA DSB repair and therefore targeting AXL may enhance the efficacy of radiation therapy.

To further define AXL's role in radiation response and DNA DSB repair, HN4-Vector and HN4-AXL stable cells were irradiated and γ-H2AX fluorescence was measured 4 hours later (Fig. 4D, left). HN4-AXL cells had less γ-H2AX foci indicating that these cells had more repaired DNA DSBs as compared with HN4-Vector cells. Clonogenic survival analyses indicated that HN4-AXL cells had significantly more surviving cells postirradiation as compared with HN4-Vector cells (Fig. 4D, middle). In addition, HN4-AXL cells expressed increased levels of phosphorylated DNA-PK and AKT postirradiation (Fig. 4D, right). Collectively, these studies support a putative role for AXL in the regulation of DNA repair and resistance to radiation.

AXL is overexpressed in radiation-resistant cell lines and patient-derived xenografts

To expand these findings, the HNSCC cell lines SCC2, SCC22B, SCC90, SCC1, SCC47, and SCC147T were injected into both dorsal flanks of athymic nude mice ($n = 24$ mice per cell line). Once tumors reached approximately 200 mm^3, mice were stratified into two treatment groups: control or radiation ($n = 12$ mice/24 tumors per group). The radiation group was subjected to four 2 Gy fractions over a period of 2 weeks. After completing the treatment regimen, tumor growth was monitored on a weekly basis to evaluate response to radiation. The results of this experimentation indicated that SCC2, SCC22B, and SCC90 cell line xenografts were sensitive to radiation, whereas SCC1, SCC47, and SCC147T were resistant (Fig. 5). Tumors harvested from mice in the control groups were evaluated for AXL expression and activation by IHC and staining intensity was scored as described in Fig. 1B. On average, the radiosensitive tumors expressed low levels of both AXL and pAXL-Y779 (1+ to 2+), with SCC2 and SCC90 having the lowest levels of staining (consistent with AXL expression levels detected in Fig. 1A). The radioresistant tumors, SCC1, SCC47, and SCC147T, expressed considerably more AXL and pAXL-Y779 (2+ to 4+ staining), especially SCC147T tumors. AXL expression was not associated with the HPV status of the HNSCC cell lines used (see Supplementary Materials and Methods for HPV status of cell lines used).

Next, the radiation responses of five HNSCC PDXs were evaluated for AXL and pAXL-Y779 expression levels (see Supplementary Table S4 for clinical parameters of patients before PDX establishment). For each PDX, dual flank tumors were established in 16 athymic nude mice. When tumors reached approximately 200 mm^3, mice were stratified into two treatment groups: control or radiation ($n = 8$ mice/16 tumors per group). After completing the treatment regimen, tumor growth was monitored to evaluate response to radiation. The results of this experimentation indicated that two PDXs were sensitive to radiation (UW-SCC36 and UW-SCC22), whereas three were resistant (UW-SCC1, UW-SCC30, and UW-SCC6; Fig. 6). PDXs harvested from early passaged tumors before treatment were stained for both AXL and pAXL-Y779 by IHC and staining intensity was scored as described in Fig. 1B. Consistent with Fig. 5, radiosensitive PDXs expressed low levels of both AXL and pAXL-Y779. In comparison, radiation-resistant PDXs had intense AXL and pAXL-Y779 staining (3+ staining for both markers). In this small PDX cohort ($n = 5$), HPV status was not associated with AXL expression or radiation response. Taken together, these data demonstrate that AXL is overexpressed and activated in PDXs that are intrinsically resistant to radiation therapy.

Discussion

The current study identifies AXL to be highly expressed and associated with worse clinical outcome in HNSCC. Elevated AXL expression has been identified as a poor prognostic factor for shorter relapse-free survival or overall survival in colon cancer (21), pancreatic cancer (25), and osteosarcoma (26). In addition, AXL expression was prognostic for increased lymph node involvement and/or clinical stage in lung adenocarcinoma (14), ovarian cancer (20), and breast cancer (19). Interestingly, male gender was

Published OnlineFirst March 12, 2015; DOI: 10.1158/1078-0432.CCR-14-2648

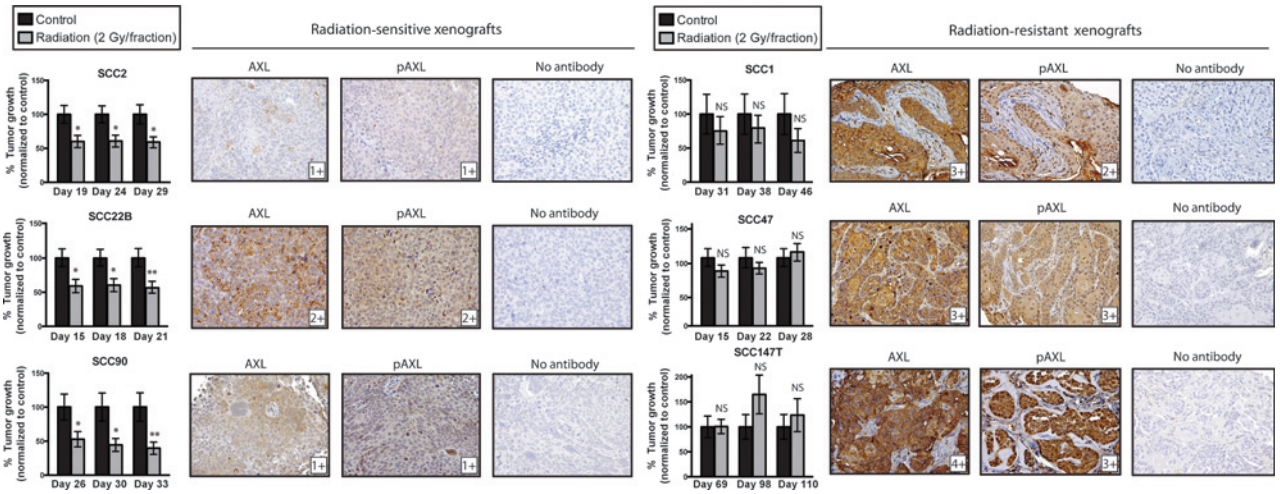

Figure 5.

AXL is overexpressed and activated in radiation-resistant HNSCC cell line xenografts. Cell line xenografts were established and evaluated for radiation response as described in the Supplementary Materials and Methods. Tumor growth was plotted as a percentage of averaged vehicle-treated tumor volumes at the last three time points of the study; *, $P < 0.05$; **, $P < 0.01$. Representative IHC images of AXL and pAXL-Y779 staining from control group tumors are depicted (×20). Pathologic IHC quantitation (by D. Yang) was determined via a categorical scale from 0 to 4+. NS, not significant.

associated with high AXL expression in the current study, which is an association that has not been reported in other cancers. Several preclinical studies have highlighted the importance of AXL in regulating the metastatic potential of cancer cells (12, 14, 15, 17–19, 23, 24, 27), which is in agreement with the current findings (Figs. 2B and C). HNSCC cell proliferation was also decreased upon AXL knockdown or kinase inhibition (Figs. 1A and 2A), which is contrary to studies in ovarian cancer where only metastatic spread was abrogated after AXL knockdown (20). In models of breast and lung cancer, cell proliferation was decreased upon AXL inhibition as well, which corresponded to increased chemosensitivity (10, 18, 49). Taken together, targeting AXL may inhibit both proliferation and motility pathways in HNSCC.

AXL has been reported to play a role in resistance to chemotherapy and anti-EGFR therapies in non–small cell lung cancer (NSCLC; refs. 9–11, 49), triple-negative breast cancer (TNBC; refs. 13, 16, 49), and HNSCC (22). In this study, several HNSCC cell lines that were intrinsically resistant to cetuximab were sensitized upon transfection with siAXL or treatment with R428 (Fig. 3B and Supplementary Fig. S3B). In addition, AXL inhibition enhanced the antiproliferative effect of cetuximab in a cetuximab sensitive cell line (HN4; Fig. 3B). These data indicate that dual targeting both AXL and EGFR may provide beneficial antitumor responses irrespective of initial sensitivity to monotherapy. The enhanced efficacy of cetuximab may be due to the suppression of both EMT and SFK activity after AXL inhibition. EMT has been previously implicated in cetuximab-resistant HNSCCs, where resistant cells had increased vimentin and decreased E-cadherin levels (50). In addition, SFK activation of EGFR-Y1101 has been implicated in mediating the nuclear translocation of EGFR, a reported mechanism of cetuximab resistance (42, 44). In the current study, HN4 cells stably overexpressing AXL had an increased EMT signature, SFK activity and pEGFR-Y1101, all of which corresponded to increased cetuximab resistance (Fig. 3C). These data are supported by studies identifying a similar AXL regulated EMT signature in erlotinib-resistant HNSCC (22), TNBC (16), and NSCLC cell models (9, 49).

One of the most profound findings of the current study was the identification of AXL overexpression and hyperactivation in radiation-resistant HNSCC cell line xenografts and PDXs (Figs. 5 and 6). The correlation between AXL expression and activity in the radiation-resistant tumors implies an inherent role for AXL in radiation resistance. This is supported in Fig. 4, where AXL inhibition increased γ-H2AX foci and enhanced the sensitivity of HNSCC cells to radiation (Fig. 4A and B). AXL was further found to regulate the DNA repair pathway via AKT and DNA-PK activity (Fig. 4C and D). Because AKT and DNA-PK mediate DNA repair, their increased activity has been indicative of radioresistant cancer cells (47, 48); thus, targeting AXL may have radiosensitizing effects in HNSCC. Collectively, these studies are the first to identify AXL as a mediator of radiation response in HNSCC.

HPV infection has been shown to play a causal role in the development of a subset of HNSCCs (2). Importantly, patients with HPV-positive HNSCC demonstrate significantly improved survival outcomes with standard-of-care treatments (37, 51). One mechanism underlying the improved outcome of the HPV-positive population has been attributed to their increased sensitivity to radiation therapy (37, 52). However, there are several important molecular differences driving oncogenesis in HPV-positive versus HPV-negative HNSCCs that likely underlie the differential treatment response observed (53, 54). In the current study, among the 63 patient cohort, AXL expression was not associated with HPV positivity (as determined by p16 IHC). Although no correlation was determined, it is important to note that approximately 27% of the patients in this cohort had oropharyngeal cancer (anatomic area including the tonsils, base of tongue, soft palate, and lateral/posterior pharyngeal walls). Considering the oropharynx represents the site with the greatest proportion of HPV-associated cancers that are accurately defined by p16 expression (55), it would be important in the future to specifically evaluate the relationship between HPV status and AXL staining in patients with oropharyngeal cancers and compare the results

Published OnlineFirst March 12, 2015; DOI: 10.1158/1078-0432.CCR-14-2648

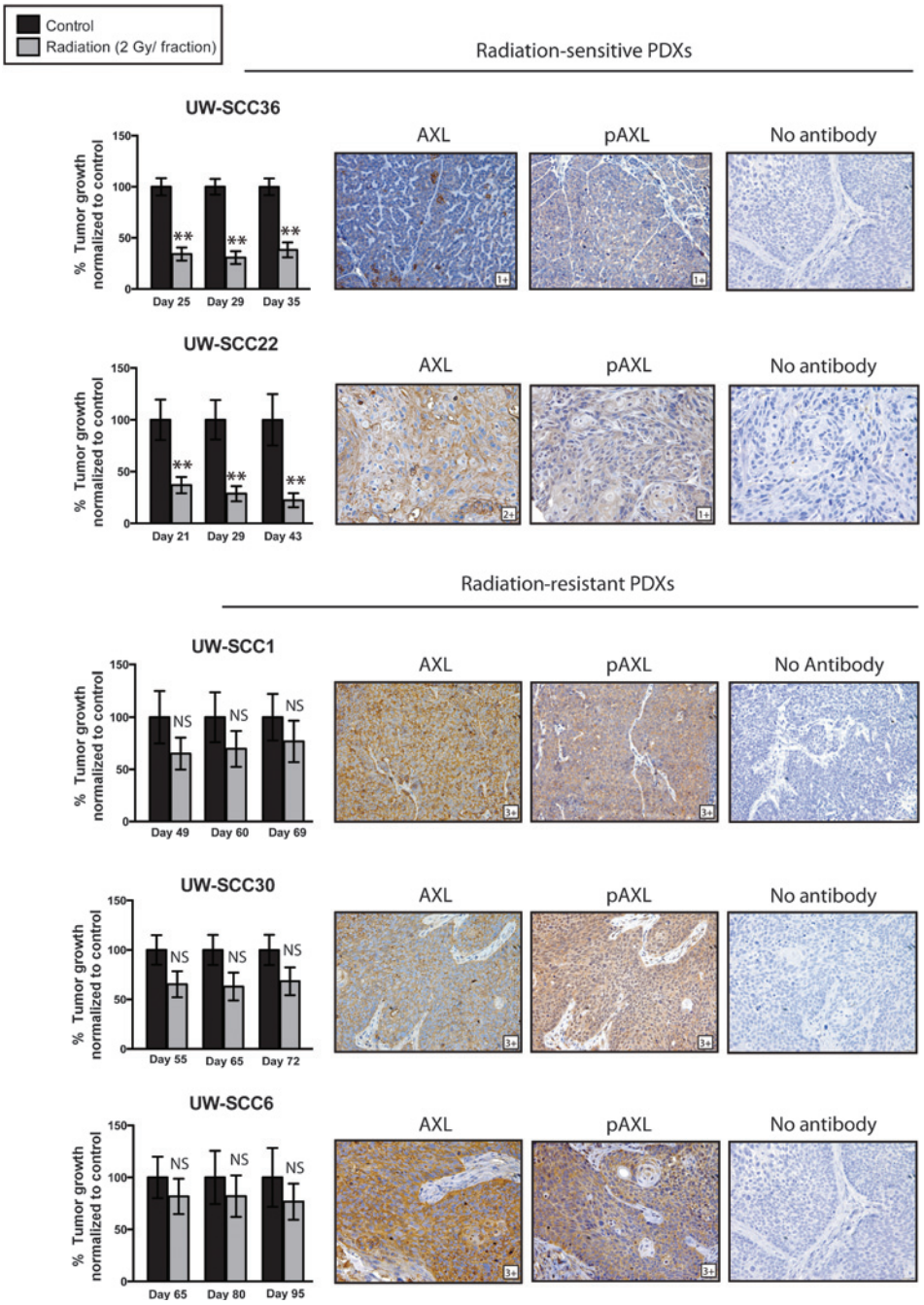

Figure 6.
AXL is overexpressed and activated in radiation-resistant HNSCC PDXs. PDXs were evaluated for radiation response as described in the Supplementary Materials and Methods. Tumor growth was plotted as a percentage of averaged vehicle-treated tumor volumes at the last three time points of the study; **, $P < 0.01$. Representative IHC images of AXL and pAXL-Y779 staining in early passaged PDXs are shown (×20). Pathologic IHC quantitation (by D. Yang) was determined via a categorical scale from 0 to 4+. NS, not significant.

to patients with nonoropharyngeal malignancies. In this manner, further research is required to determine whether there is a significant relationship between HPV status and AXL expression/function in HNSCC.

Several anti-AXL therapeutics are currently being evaluated for movement into clinical trials. R428, licensed as BGB324, has now undergone successful phase Ia clinical evaluation in healthy volunteers, where it was deemed safe and well tolerated (38). Although R428 is greater than 100 times more selective for AXL than several other tyrosine kinases (such as the insulin receptor, EGFR, and HER2), we cannot rule out the possibility that the antitumor responses observed in the current study were solely due to AXL inhibition (15). However, the use of both AXL siRNAs and the AXL-negative cell line, SCC2, throughout this study supports the specificity for AXL inhibition by R428. Several neutralizing anti-AXL monoclonal antibodies have also been designed, including YW327.6S2 and MAb173 (13, 27, 30); however, these therapies are still undergoing preclinical evaluation. To date, R428 is the most clinically advanced anti-AXL therapeutic, and thus, further evaluation of its benefit in HNSCC is warranted.

Disclosure of Potential Conflicts of Interest

No potential conflicts of interest were disclosed.

Authors' Contributions

Conception and design: T.M. Brand, D.L. Wheeler, A.P. Stein, R. Salgia, R.J. Kimple

Development of methodology: T.M. Brand, D.L. Wheeler, M. Iida, A.P. Stein, T.L. Fowler, P.S. Gill, R.J. Kimple

Acquisition of data (provided animals, acquired and managed patients, provided facilities, etc.): T.M. Brand, M. Iida, A.P. Stein, K.L. Corrigan, C. Braverman, J.P. Coan, T.L. Fowler, D. Yang, M.W. Lingen, V. Saloura, V.M. Villaflor, R. Salgia, R.J. Kimple

Analysis and interpretation of data (e.g., statistical analysis, biostatistics, computational analysis): T.M. Brand, D.L. Wheeler, A.P. Stein, K.L. Corrigan, J.P. Coan, S. Saha, D. Yang, M.W. Lingen, R. Salgia, R.J. Kimple

Writing, review, and/or revision of the manuscript: T.M. Brand, D.L. Wheeler, M. Iida, A.P. Stein, T.L. Fowler, P.S. Gill, M.W. Lingen, V.M. Villaflor, R. Salgia, R.J. Kimple

Administrative, technical, or material support (i.e., reporting or organizing data, constructing databases): T.M. Brand, D.L. Wheeler, H. Bahrar, P.S. Gill

Study supervision: T.M. Brand, D.L. Wheeler, B.P. Bednarz

Other (data acquisition): H.E. Pearson

Acknowledgments

The authors acknowledge the University of Wisconsin Medical Radiation Research Center for their assistance during this project.

Grant Support

This work was supported by the Clinical and Translational Science Award (CTSA) program, through the NIH National Center for Advancing Translational Sciences (NCATS) grant UL1TR000427 (KL2TR000428), grant RSG-10-193-01-TBG from the American Cancer Society (to D.L. Wheeler), and grant W81XWH-12-1-0467 from United States Army Medical Research and Materiel Command (to D.L. Wheeler), CA160639 (to R.J. Kimple), and the NIH/NCI P30 CA014520 (UW Comprehensive Cancer Center Grant). T.L. Fowler was supported in part by the University of Wisconsin Science and Medicine Graduate Research Scholars program.

The costs of publication of this article were defrayed in part by the payment of page charges. This article must therefore be hereby marked *advertisement* in accordance with 18 U.S.C. Section 1734 solely to indicate this fact.

Received October 13, 2014; revised February 5, 2015; accepted February 27, 2015; published OnlineFirst March 12, 2015.

References

1. Ferlay J, Shin HR, Bray F, Forman D, Mathers C, Parkin DM. Estimates of worldwide burden of cancer in 2008: GLOBOCAN 2008. Int J Cancer 2010;127:2893–917.
2. Gillison ML, Koch WM, Capone RB, Spafford M, Westra WH, Wu L, et al. Evidence for a causal association between human papillomavirus and a subset of head and neck cancers. J Natl Cancer Inst 2000;92:709–20.
3. Vermorken JB, Specenier P. Optimal treatment for recurrent/metastatic head and neck cancer. Ann Oncol 2010;21 (Suppl 7):vii252–61.
4. Posner MR, Haddad RI, Wirth L, Norris CM, Goguen LA, Mahadevan A, et al. Induction chemotherapy in locally advanced squamous cell cancer of the head and neck: evolution of the sequential treatment approach. Semin Oncol 2004;31:778–85.
5. Vermorken JB. Medical treatment in head and neck cancer. Ann Oncol 2005;16 Suppl 2:ii258–64.
6. Bonner JA, Harari PM, Giralt J, Azarnia N, Shin DM, Cohen RB, et al. Radiotherapy plus cetuximab for squamous-cell carcinoma of the head and neck. N Engl J Med 2006;354:567–78.
7. Egloff AM, Lee JW, Langer CJ, Quon H, Vaezi A, Grandis JR, et al. Phase II study of cetuximab in combination with cisplatin and radiation in unresectable, locally advanced head and neck squamous cell carcinoma: eastern cooperative oncology group trial E3303. Clin Cancer Res 2014;20:5041–51.
8. Vermorken JB, Mesia R, Rivera F, Remenar E, Kawecki A, Rottey S, et al. Platinum-based chemotherapy plus cetuximab in head and neck cancer. N Engl J Med 2008;359:1116–27.
9. Zhang Z, Lee JC, Lin L, Olivas V, Au V, LaFramboise T, et al. Activation of the AXL kinase causes resistance to EGFR-targeted therapy in lung cancer. Nat Genet 2012;44:852–60.
10. Linger RM, Cohen RA, Cummings CT, Sather S, Migdall-Wilson J, Middleton DH, et al. Mer or Axl receptor tyrosine kinase inhibition promotes apoptosis, blocks growth and enhances chemosensitivity of human non-small cell lung cancer. Oncogene 2013;32:3420–31.
11. Byers LA, Diao L, Wang J, Saintigny P, Girard L, Peyton M, et al. An epithelial-mesenchymal transition gene signature predicts resistance to EGFR and PI3K inhibitors and identifies Axl as a therapeutic target for overcoming EGFR inhibitor resistance. Clin Cancer Res 2013;19:279–90.
12. Li Y, Ye X, Tan C, Hongo JA, Zha J, Liu J, et al. Axl as a potential therapeutic target in cancer: role of Axl in tumor growth, metastasis and angiogenesis. Oncogene 2009;28:3442–55.
13. Ye X, Li Y, Stawicki S, Couto S, Eastham-Anderson J, Kallop D, et al. An anti-Axl monoclonal antibody attenuates xenograft tumor growth and enhances the effect of multiple anticancer therapies. Oncogene 2010;29:5254–64.
14. Shieh YS, Lai CY, Kao YR, Shiah SG, Chu YW, Lee HS, et al. Expression of axl in lung adenocarcinoma and correlation with tumor progression. Neoplasia 2005;7:1058–64.
15. Holland SJ, Pan A, Franci C, Hu Y, Chang B, Li W, et al. R428, a selective small molecule inhibitor of Axl kinase, blocks tumor spread and prolongs survival in models of metastatic breast cancer. Cancer Res 2010;70:1544–54.
16. Meyer AS, Miller MA, Gertler FB, Lauffenburger DA. The receptor AXL diversifies EGFR signaling and limits the response to EGFR-targeted inhibitors in triple-negative breast cancer cells. Sci Signal 2013;6:ra66.
17. Zhang YX, Knyazev PG, Cheburkin YV, Sharma K, Knyazev YP, Orfi L, et al. AXL is a potential target for therapeutic intervention in breast cancer progression. Cancer Res 2008;68:1905–15.
18. Asiedu MK, Beauchamp-Perez FD, Ingle JN, Behrens MD, Radisky DC, Knutson KL. AXL induces epithelial-to-mesenchymal transition and regulates the function of breast cancer stem cells. Oncogene 2014;33:1316–24.
19. D'Alfonso TM, Hannah J, Chen Z, Liu Y, Zhou P, Shin SJ. Axl receptor tyrosine kinase expression in breast cancer. J Clin Pathol 2014;67:690–6.
20. Rankin EB, Fuh KC, Taylor TE, Krieg AJ, Musser M, Yuan J, et al. AXL is an essential factor and therapeutic target for metastatic ovarian cancer. Cancer Res 2010;70:7570–9.
21. Dunne PD, McArt DG, Blayney JK, Kalimutho M, Greer S, Wang T, et al. AXL is a key regulator of inherent and chemotherapy-induced invasion and predicts a poor clinical outcome in early-stage colon cancer. Clin Cancer Res 2014;20:164–75.
22. Giles KM, Kalinowski FC, Candy PA, Epis MR, Zhang PM, Redfern AD, et al. Axl mediates acquired resistance of head and neck cancer cells to the epidermal growth factor receptor inhibitor erlotinib. Mol Cancer Ther 2013;12:2541–58.
23. Avilla E, Guarino V, Visciano C, Liotti F, Svelto M, Krishnamoorthy G, et al. Activation of TYRO3/AXL tyrosine kinase receptors in thyroid cancer. Cancer Res 2011;71:1792–804.
24. Paccez JD, Vasques GJ, Correa RG, Vasconcellos JF, Duncan K, Gu X, et al. The receptor tyrosine kinase Axl is an essential regulator of prostate cancer proliferation and tumor growth and represents a new therapeutic target. Oncogene 2013;32:689–98.
25. Song X, Wang H, Logsdon CD, Rashid A, Fleming JB, Abbruzzese JL, et al. Overexpression of receptor tyrosine kinase Axl promotes tumor cell invasion and survival in pancreatic ductal adenocarcinoma. Cancer 2011;117:734–43.
26. Han J, Tian R, Yong B, Luo C, Tan P, Shen J, et al. Gas6/Axl mediates tumor cell apoptosis, migration and invasion and predicts the clinical outcome of

osteosarcoma patients. Biochem Biophys Res Commun 2013;435:493–500.
27. Liu R, Gong M, Li X, Zhou Y, Gao W, Tulpule A, et al. Induction, regulation, and biologic function of Axl receptor tyrosine kinase in Kaposi sarcoma. Blood 2010;116:297–305.
28. Linger RM, Keating AK, Earp HS, Graham DK. TAM receptor tyrosine kinases: biologic functions, signaling, and potential therapeutic targeting in human cancer. Adv Cancer Res 2008;100:35–83.
29. Feneyrolles C, Spenlinhauer A, Guiet L, Fauvel B, Dayde-Cazals B, Warnault P, et al. Axl kinase as a key target for oncology: focus on small molecule inhibitors. Mol Cancer Ther 2014;13:2141–8.
30. Brand TM, Iida M, Stein AP, Corrigan KL, Braverman CM, Luthar N, et al. AXL mediates resistance to cetuximab therapy. Cancer Res 2014;74:5152–64.
31. Rho JK, Choi YJ, Kim SY, Kim TW, Choi EK, Yoon SJ, et al. MET and AXL inhibitor NPS-1034 exerts efficacy against lung cancer cells resistant to EGFR kinase inhibitors because of MET or AXL activation. Cancer Res 2014;74:253–62.
32. Li C, Brand TM, Iida M, Huang S, Armstrong EA, van der Kogel A, et al. Human epidermal growth factor receptor 3 (HER3) blockade with U3-1287/AMG888 enhances the efficacy of radiation therapy in lung and head and neck carcinoma. Discov Med 2013;16:79–92.
33. Fowler TL, Fulkerson RK, Micka JA, Kimple RJ, Bednarz BP. A novel high-throughput irradiator for *in vitro* radiation sensitivity bioassays. Phys Med Biol 2014;59:1459–70.
34. Fowler TL, Bailey AM, Bednarz BP, Kimple RJ. High-throughput detection of DNA double-strand breaks using image cytometry. BioTechniques 2014;58:37–9.
35. Kimple RJ, Smith MA, Blitzer GC, Torres AD, Martin JA, Yang RZ, et al. Enhanced radiation sensitivity in HPV-positive head and neck cancer. Cancer Res 2013;73:4791–800.
36. Kimple RJ, Harari PM, Torres AD, Yang RZ, Soriano BJ, Yu M, et al. Development and characterization of HPV-positive and HPV-negative head and neck squamous cell carcinoma tumorgrafts. Clin Cancer Res 2013;19:855–64.
37. Rischin D, Young RJ, Fisher R, Fox SB, Le QT, Peters LJ, et al. Prognostic significance of p16INK4A and human papillomavirus in patients with oropharyngeal cancer treated on TROG 02.02 phase III trial. J Clin Oncol 2010;28:4142–8.
38. Wnuk-Lipinska K, Tiron C, Gausdal G, Sandal T, Frink R, Hinz S, et al. BGB324, a selective small molecule Axl kinase inhibitor to overcome EMT-associated drug resistance in carcinomas: therapeutic rationale and early clinical studies [abstract]. In: Proceedings of the 105th Annual Meeting of the American Association for Cancer Research; 2014 Apr 5–9; San Diego, CA. Philadelphia (PA): AACR; 2014. Abstract nr 1747.
39. Chou TC. Theoretical basis, experimental design, and computerized simulation of synergism and antagonism in drug combination studies. Pharmacol Rev 2006;58:621–81.
40. Chou TC. Drug combination studies and their synergy quantification using the chou-talalay method. Cancer Res 2010;70:440–6.
41. Chou TC, Talalay P. Quantitative analysis of dose-effect relationships: the combined effects of multiple drugs or enzyme inhibitors. Adv Enzyme Regul 1984;22:27–55.
42. Wheeler DL, Iida M, Kruser TJ, Nechrebecki MM, Dunn EF, Armstrong EA, et al. Epidermal growth factor receptor cooperates with Src family kinases in acquired resistance to cetuximab. Cancer Biol Ther 2009;8:696–703.
43. Iida M, Brand TM, Campbell DA, Li C, Wheeler DL. Yes and Lyn play a role in nuclear translocation of the epidermal growth factor receptor. Oncogene 2013;32:759–67.
44. Li C, Iida M, Dunn EF, Ghia AJ, Wheeler DL. Nuclear EGFR contributes to acquired resistance to cetuximab. Oncogene 2009;28:3801–13.
45. Schmidt-Ullrich RK, Contessa JN, Lammering G, Amorino G, Lin PS. ERBB receptor tyrosine kinases and cellular radiation responses. Oncogene 2003;22:5855–65.
46. Meyn RE, Munshi A, Haymach JV, Milas L, Ang KK. Receptor signaling as a regulatory mechanism of DNA repair. Radiother Oncol 2009;92:316–22.
47. Peng Y, Zhang Q, Nagasawa H, Okayasu R, Liber HL, Bedford JS. Silencing expression of the catalytic subunit of DNA-dependent protein kinase by small interfering RNA sensitizes human cells for radiation-induced chromosome damage, cell killing, and mutation. Cancer Res 2002;62:6400–4.
48. Toulany M, Kehlbach R, Florczak U, Sak A, Wang S, Chen J, et al. Targeting of AKT1 enhances radiation toxicity of human tumor cells by inhibiting DNA-PKcs-dependent DNA double-strand break repair. Mol Cancer Ther 2008;7:1772–81.
49. Wilson C, Ye X, Pham T, Lin E, Chan S, McNamara E, et al. AXL inhibition sensitizes mesenchymal cancer cells to antimitotic drugs. Cancer Res 2014;74:5878–90.
50. Basu D, Nguyen TTK, Montone KT, Zhang G, Wang LP, Diehl JA, et al. Evidence for mesenchymal-like sub-populations within squamous cell carcinomas possessing chemoresistance and phenotypic plasticity. Oncogene 2010;29:4170–82.
51. Hong AM, Dobbins TA, Lee CS, Jones D, Harnett GB, Armstrong BK, et al. Human papillomavirus predicts outcome in oropharyngeal cancer in patients treated primarily with surgery or radiation therapy. Br J Cancer 2010;103:1510–7.
52. Fakhry C, Westra WH, Li S, Cmelak A, Ridge JA, Pinto H, et al. Improved survival of patients with human papillomavirus-positive head and neck squamous cell carcinoma in a prospective clinical trial. J Natl Cancer Inst 2008;100:261–9.
53. Weinberger PM, Yu Z, Kountourakis P, Sasaki C, Haffty BG, Kowalski D, et al. Defining molecular phenotypes of human papillomavirus-associated oropharyngeal squamous cell carcinoma: validation of three-class hypothesis. Otolaryngol Head Neck Surg 2009;141:382–9.
54. Strati K, Pitot HC, Lambert PF. Identification of biomarkers that distinguish human papillomavirus (HPV)-positive versus HPV-negative head and neck cancers in a mouse model. Proc Natl Acad Sci U S A 2006;103:14152–7.
55. Ndiaye C, Mena M, Alemany L, Arbyn M, Castellsague X, Laporte L, et al. HPV DNA, E6/E7 mRNA, and p16(INK4a) detection in head and neck cancers: a systematic review and meta-analysis. Lancet Oncol 2014;15:1319–31.

Published OnlineFirst March 12, 2015; DOI: 10.1158/1078-0432.CCR-14-2648

Clinical Cancer Research

AXL Is a Logical Molecular Target in Head and Neck Squamous Cell Carcinoma

Toni M. Brand, Mari Iida, Andrew P. Stein, et al.

Clin Cancer Res Published OnlineFirst March 12, 2015.

Molecular Cancer Therapeutics

Nuclear Epidermal Growth Factor Receptor Is a Functional Molecular Target in Triple-Negative Breast Cancer

Toni M. Brand[1], Mari Iida[1], Emily F. Dunn[1], Neha Luthar[1], Kellie T. Kostopoulos[1], Kelsey L. Corrigan[1], Matthew J. Wleklinski[1], David Yang[2], Kari B. Wisinski[3], Ravi Salgia[4], and Deric L. Wheeler[1]

Abstract

Triple-negative breast cancer (TNBC) is a subclass of breast cancers (i.e., estrogen receptor–negative, progesterone receptor–negative, and HER2-negative) that have poor prognosis and very few identified molecular targets. Strikingly, a high percentage of TNBCs overexpresses the EGF receptor (EGFR), yet EGFR inhibition has yielded little clinical benefit. Over the last decade, advances in EGFR biology have established that EGFR functions in two distinct signaling pathways: (i) classical membrane-bound signaling and (ii) nuclear signaling. Previous studies have demonstrated that nuclear EGFR (nEGFR) can enhance resistance to anti-EGFR therapies and is correlated with poor overall survival in breast cancer. On the basis of these findings, we hypothesized that nEGFR may promote intrinsic resistance to cetuximab in TNBC. To examine this question, a battery of TNBC cell lines and human tumors were screened and found to express nEGFR. Knockdown of EGFR expression demonstrated that TNBC cell lines retained dependency on EGFR for proliferation, yet all cell lines were resistant to cetuximab. Furthermore, Src Family Kinases (SFKs) influenced nEGFR translocation in TNBC cell lines and *in vivo* tumor models, where inhibition of SFK activity led to potent reductions in nEGFR expression. Inhibition of nEGFR translocation led to a subsequent accumulation of EGFR on the plasma membrane, which greatly enhanced sensitivity of TNBC cells to cetuximab. Collectively, these data suggest that targeting both the nEGFR signaling pathway, through the inhibition of its nuclear transport, and the classical EGFR signaling pathway with cetuximab may be a viable approach for the treatment of patients with TNBC. *Mol Cancer Ther; 13(5); 1356–68. ©2014 AACR.*

Introduction

Approximately 15% to 20% of all breast cancers lack expression of the estrogen receptor, progesterone receptor, and HER2, and are thus considered to be triple-negative breast cancers (TNBC; refs. 1, 2). Although a high percentage of patients with TNBC initially respond to conventional chemotherapy, they tend to have a higher rate of relapse and worse prognosis as compared with other breast cancer subtypes (1, 2). In efforts to identify new molecular targets in TNBC, various groups have performed gene expression profiling studies and identified that the EGF receptor (EGFR) is commonly overexpressed (3–6). Although inhibition of EGFR activity has yielded modest clinical success in TNBC, substantial gains in clinical response rates have not been achieved (7, 8). Thus, improving the efficacy of anti-EGFR therapy in TNBC is imperative.

Classically, EGFR functions as a plasma membrane-bound receptor tyrosine kinase that initiates growth and survival signals (9). However, studies over the last 15 years have identified that EGFR can be localized and function from intracellular organelles, one of which includes the nucleus (10, 11). Within the nucleus, EGFR can function as a cotranscription factor to regulate genes involved in tumor progression (10, 11), in addition to functioning as a nuclear kinase to enhance DNA replication and repair (12–14). These nuclear functions have been linked to three parameters of tumor biology: (i) inverse correlation with overall survival in numerous cancers (15–20), (ii) resistance to therapeutic agents including radiation (12, 21–24), chemotherapy (12, 13, 24), and anti-EGFR therapies gefitinib (25) and cetuximab (26), and (iii) enhanced tumor growth (27, 28). These findings suggest that tumors rely on two distinct compartments of EGFR signaling to sustain their oncogenic phenotype: (i) classical membrane-bound EGFR signaling, and (ii) nuclear EGFR (nEGFR) signaling.

Previous work from our laboratory has identified that non–small cell lung cancer (NSCLC) cells that have acquired resistance to cetuximab express increased nEGFR and Src Family Kinase (SFK) activity (26, 29). SFK inhibition blocked nEGFR translocation in cetuximab-resistant

Authors' Affiliations: Departments of [1]Human Oncology and [2]Pathology and Laboratory Medicine, University of Wisconsin School of Medicine and Public Health, [3]Department of Medicine, University of Wisconsin Carbone Cancer Center, Madison, Wisconsin; and [4]Division of Hematology/Oncology, Department of Medicine, University of Chicago, Chicago, Illinois

Note: Supplementary data for this article are available at Molecular Cancer Therapeutics Online (http://mct.aacrjournals.org/).

Corresponding Author: Deric L. Wheeler, University of Wisconsin, 1111 Highland Ave, WIMR 3159, Madison, WI 53705. Phone: 608-262-7837; Fax: 608-263-9947; E-mail: dlwheeler@wisc.edu

doi: 10.1158/1535-7163.MCT-13-1021

cells, and led to an increase in plasma membrane EGFR expression and enhanced sensitivity to cetuximab (26, 30). Furthermore, the SFK-dependent phosphorylation site on EGFR, tyrosine 1101 (Y1101), was identified to play a critical role in initiating EGFR's nuclear transport (30). These studies suggest that nEGFR is a critical molecular determinant for cetuximab resistance and that SFKs play an important role in regulating nEGFR translocation.

On the basis of these previous studies, we hypothesized that nEGFR may promote intrinsic resistance to cetuximab in TNBC. To examine this question, a battery of TNBC cell lines and human tumors were screened and found to express nEGFR. Although TNBC cell lines were notably resistant to cetuximab therapy, all lines retained dependency on EGFR for proliferation. Furthermore, SFKs influenced nEGFR transport in TNBC, where the overexpression of a negative regulator of Src decreased EGFR activity at tyrosine 1101 and inhibited nEGFR translocation. Interestingly, the creation of stable cell lines overexpressing each SFK demonstrated that all SFKs could promote nEGFR translocation. Treatment of TNBC cell lines and xenograft tumors with the anti-SFK therapeutic dasatinib inhibited nEGFR translocation, and enhanced surface level EGFR accumulation. Importantly, pretreatment of TNBC cell lines with dasatinib greatly enhanced the sensitivity of cetuximab-resistant TNBC cell lines to cetuximab. Collectively, our data suggest that abrogating nEGFR translocation with SFK inhibitors may greatly enhance the efficacy of cetuximab in TNBC.

Materials and Methods

Cell lines

The human breast cancer cell lines SKBr3, BT474, BT549, MDAMB231 and MDAMB468, MCF-7, and the Chinese hamster ovary cell line CHOK1 were purchased from American Type Culture Collection in November 2010. SUM149, SUM229, and SUM159 were purchased from Asterand in November 2010. All cell lines were authenticated by the indicated source and not by our laboratory. All cell lines were maintained in their respective media (Mediatech Inc.) with 1% penicillin and streptomycin; SKBr3, BT549, and MDAMB231, Dulbecco's Modified Eagle's Medium with 10% FBS; BT474, RPMI-1640 with 10% FBS; SUM149, SUM229, and SUM159, F12K medium with 5% FBS, 1 μg/mL hydrocortisone and 5 μg/mL insulin; MDAMB468 and MCF-7, DMEM/F12K medium with 10% FBS; CHOK1 F12K medium with 10% FBS.

Antibodies, compounds, and TMAs

All antibodies were obtained from the following sources: EGFR (SC-03), pEGFR-1173 (SC-10168), HER2 (SC-284), SLAP (SC-1215), Histone H3 (SC-8654), horseradish peroxidase-conjugated goat-anti-rabbit immunoglobulin G (IgG), goat-anti-mouse IgG, donkey-anti-goat IgG, EGFR blocking peptide (SC-03 P) purchased from Santa Cruz Biotechnology Inc. SFK (CS2123), pSFK-Y419 (CS2101), pEGFR-Y1045 (CS2237), pEGFR-Y1068 (CS3777), pHER2-Y1221/1222 (CS2243), c-Cbl (CS2747), glyceraldehyde-3-phosphate dehydrogenase (GAPDH; CS2118), calnexin (CS2679), and anti-Flag (CS8146) purchased from Cell Signaling Technology. pEGFR-Y1101 (ab76195) and EGFR (ab52894) purchased from Abcam. α-Tubulin purchased from Calbiochem. Dasatinib (BMS-354825, Sprycel) was purchased from LC Laboratories and cetuximab (C225, Erbitux) was purchased from University of Wisconsin Pharmacy (Madison, WI). EGF was purchased from Millipore. Two human TNBC tissue microarrays (TMA; #695711112B and #69572306) were purchased from TriStar Technology Group.

Cellular fractionation and immunoblotting analysis

Cellular fractionation and whole-cell lysis were performed and quantitated as previously described (26, 31). ECL chemiluminescence detection system was used to visualize proteins. α-Tubulin, calnexin, and Histone H3 were used as loading and purity controls, respectively.

Immunoprecipitation

Cells were processed for immunoprecipitation as previously described (31). Of note, 250 μg of protein and 2 μg of Src-like adaptor protein (SLAP) primary antibody were used for immunoprecipitation.

Plasmids constructs, transfection, and siRNA technology

The following vectors were kindly supplied: pcDNA3.0-caSrc, -wtSRC and –EGFR wild-type (WT) and –EGFRY1101F, Dr. J.Boerner (Wayne State University School of Medicine, Karmanos Cancer Institute, Detroit, MI); pcDNA3-SLAP, Dr. S. Roche (Centre de Recherche de Biochimie Macromoléculaire, Montpellier, France); pTRE2pur-HA-Fyn, -Hck, and -Lck, Dr. P.S. Mischel (University of California, San Diego, La Jolla, CA). WT human pDONR223-FGR (Plasmid 23877) and pDONR223-Blk (Plasmid 23940) were purchased from Addgene. pQCXIP-YES and –LYN as previously described (30). All SFKs were subcloned into the PAC1/AGEI restriction sites of the pQCXIP expression vector (Clontech). Both transient and stable transfections were performed using Lipofectamine LTX and Opti-MEM I (Life Technology). Stable transfection was commenced 48 hours posttransfection via addition of 500 ng/mL puromycin to the growth media. Single cell clones were chosen for expansion and validation for specific SFK expression.

For siRNAs, cells were transfected with 30 nmol/L siEGFR (ON-TARGETplus, SMART pool #L-003114-00, Dharmacon) or siNon-targeting (NT; ON-TARGETplus Non-targeting Pool, D-001810, Dharmacon) using Lipofectamine RNAiMAX (Life Technology) according to the manufacturer's instructions. Vehicle (Veh)-treated cells were treated with RNAiMAX only.

Cell proliferation assay

Crystal violet assay and Cell Counting Kit-8 (Dojindo Molecular Technologies) were performed as previously

described (26, 32). Cellular proliferation was measured 72 to 96 hours post siRNA and 96 hours post drug treatment.

Transmission electron microscopy

Cells were plated on glass cover slips at approximately 90% confluency. The pre-embedding labeling method was used for processing as previously described (33). Specifically, 0.8% Triton X-100 was used for permeabilization and 7 μg/mL of EGFR primary antibody was used (SC-03, Santa Cruz Biotechnology). Cells were silver enhanced for 1.5 hour. Cells were sectioned onto copper grids at approximately 90 nm slices.

Immunofluorescence

Cells were processed for immunofluorescence staining of EGFR as previously described (31). Primary antibody: EGFR (SC-03), 1:100. Secondary antibody (Life technologies): Alex Fluor 546 at 1:600 for 30 minutes to 1 hour. All cells were mounted with ProLong Gold Antifade Reagent with 4′, 6-diamidino-2-phenylindole (DAPI; Life Technologies). Confocal immunofluorescence microscopy was performed using an A1 Nikon confocal microscope (×600). Z-slices were taken at 150 nm slices.

Nuance imaging analysis

For image analysis, EGFR (ab52894, 1:50) and anti-E Cadherin antibody (NCH-38, Dako at 1:100 dilution) were used for immunofluorescence staining. Images were acquired on the Nuance Multispectral Imaging System (Caliper Life Sciences, ×200). A spectral library composed of the fluorescent spectrum of each fluorophore was constructed from vehicle treated cells stained with each fluorophore individually. Images were analyzed on the inForm Image Analysis Software (Caliper Life Sciences) as previously described (34) by pathologist D. Yang. Relative expression of EGFR in each compartment was expressed as a ratio of proportion of counts in the high intensity bins (bins 6–10) divided by the proportion of counts in the low intensity bins (bins 1–5).

Immunohistochemistry

Cells were processed for immunohistochemistry (IHC) as previously described (32). EGFR antibody (SC-03) was used at a 1:100 dilution. The nEGFR staining pattern was scored by pathologist (D. Yang) analysis at 5% increments by visual estimation at ×20 magnification. Cases with at least one replicate core containing at least 5% of tumor cells demonstrating strong nEGFR IHC protein expression were scored as nEGFR positive.

Flow cytometry

Cells were processed as previously described (26). Cells were analyzed using a FACSCalibur flow cytometer (BD Biosciences). Propidium iodide was added to each sample at a final concentration of 5 mg/mL. Histogram analysis was performed using FlowJo software (Tree Star Inc.).

Mouse xenograft model and tumor collection

Athymic nude mice (4–6-week-old females) were obtained from Harlan Laboratories. All animal procedures and maintenance were conducted in accordance with the institutional guidelines of the University of Wisconsin. Twelve mice were injected in the dorsal flank with 2×10^6 MDAMB468 cells. Once tumors reached 100 mm^3, mice were randomized into treatment groups: vehicle (sodium citrate monobasic buffer) or dasatinib (50 mg/kg/d). Mice were treated once daily for 4 days via oral gavage. Tumor volume measurements were evaluated by digital calipers and calculated by the formula $(p)/6 \times (\text{large diameter}) \times (\text{small diameter})^2$. Tumors were collected, processed, and stained as previously described (32, 35).

Statistical analysis

Student *t* tests were used to evaluate the significance in proliferation rate between vehicle and siEGFR or drug-treated cells. Student *t* tests were also used to evaluate significance in nEGFR expression levels by Nuance imaging analysis between vehicle- and dasatinib-treated cells. Differences were considered statistically significant if *, $P < 0.05$. Pearson correlation coefficient and Manders' overlap coefficient for colocalization were calculated using Nikon NIS-Elements software. Significance of strong interaction is considered for values ≥ 0.5 (36).

Results

TNBC cell lines and human tumors express nuclear localized EGFR

Six established TNBC cell lines were evaluated for EGFR expression (Fig. 1A). All cell lines expressed total and activated forms of EGFR, in which the autophosphorylation status of EGFR at tyrosine 1068, 1173, and 1045, as well as the SFK-specific phosphorylation site, tyrosine 1101, were evaluated. All TNBC cell lines expressed activated SFKs, as observed in previous studies (refs. 37, 38; Fig. 1A). Total and activated HER2 expression levels were low in all TNBC cell lines compared with HER2-positive cell lines SKBr3 and BT474.

Because TNBC cell lines expressed EGFR, we hypothesized that some cell lines may also express nEGFR. Variant levels of nEGFR expression were observed in TNBC cell lines by nuclear fractionation analysis (Fig. 1B). The harvested nuclear lysate was free from contaminating cytoplasmic and ER-associated proteins, as indicated by lack of α-tubulin and calnexin. The nuclear protein Histone H3 was used as a loading and nuclear protein purity control. In addition, confocal immunofluorescent microscopy indicated strong nEGFR immunofluorescent staining in MDAMB468, SUM229, and SUM149 cells (Fig. 1B) by merging DAPI and Alexa Fluor 546-labeled EGFR (white arrows, magnified image). Statistical significance of colocalization was analyzed by Pearson and Manders' correlation coefficients (significance of a strong interaction is

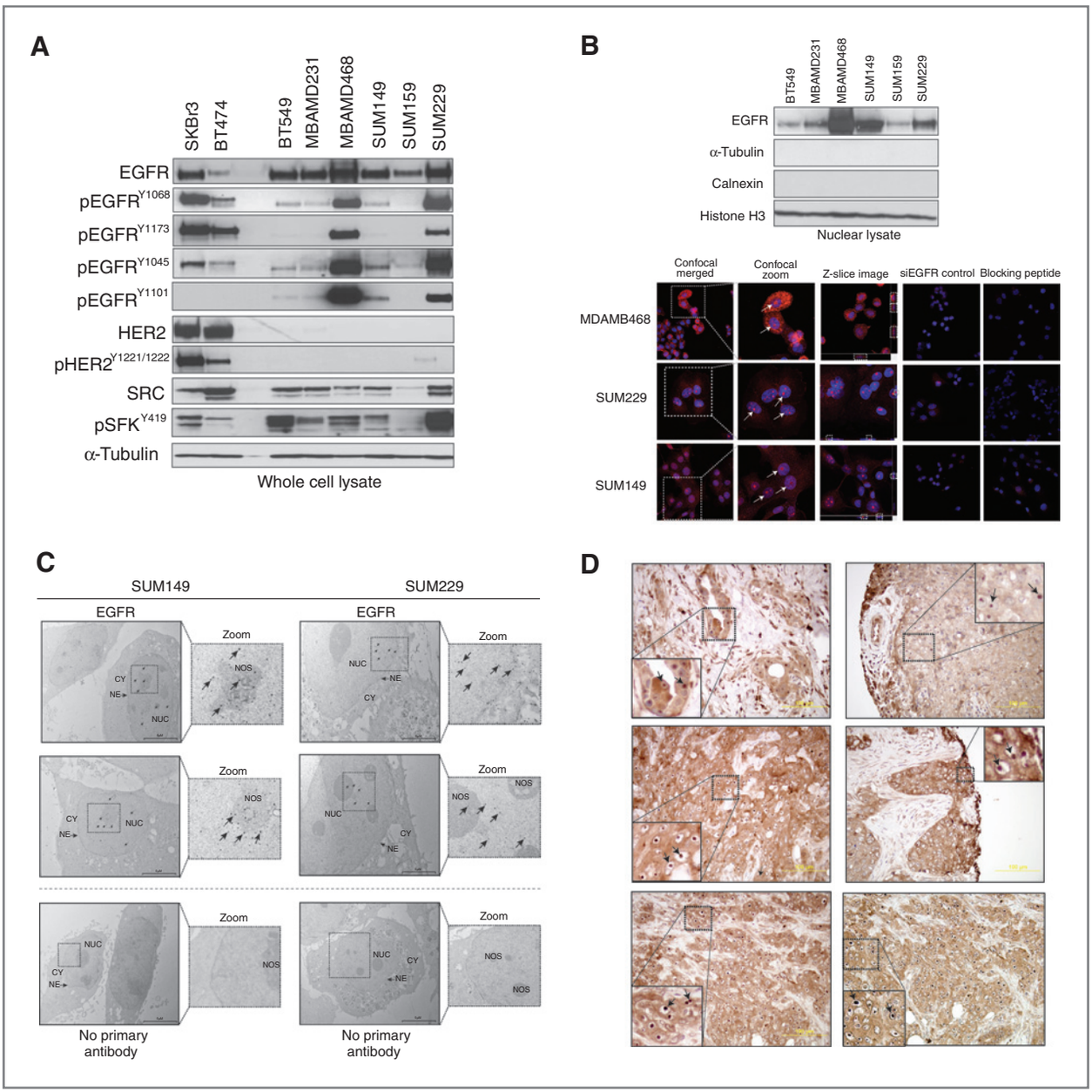

Figure 1. TNBC cell lines and human tumors express nuclear localized EGFR. A, TNBC cells express total and activated forms of EGFR. Whole-cell lysate was harvested from six TNBC cell lines and two HER2-positive cell lines. α-Tubulin was used as a loading control. B, TNBC cells express nEGFR. Cell lines were harvested for nuclear proteins. α-Tubulin, calnexin, and Histone H3 were used as loading and purity controls, respectively. Confocal immunofluorescence (IF) microscopy depicts nEGFR expression. Merged images were magnified to depict nEGFR (confocal zoom, white arrows). A single Z-Slice image depicts overlap between blue and red signal (white dashed-line boxes). ×600 magnification. EGFR primary antibody specificity was validated with siEGFR and blocking peptides. C, immunogold labeling of nEGFR. TNBC cells were fixed and processed for transmission EM. CY, cytoplasm; NE, nuclear envelope; NUC, nucleus; NOS, nucleolus. Images were digitally zoomed to highlight gold particles in the nucleus (black arrows). D, human TNBC tumors express nEGFR. Immunohistochemical staining for EGFR was performed on a total of 74 TNBC patient tumor sections. Representative cases demonstrating nEGFR expression are depicted (black arrows).

≥0.5; ref. 36). For MDAMB468, SUM229, and SUM149, the Pearson coefficients were 0.52 ± 0.04, 0.58 ± 0.01, and 0.65 ± 0.02, and the Manders' overlap coefficients were 0.70 ± 0.02, 0.78 ± 0.03, and 0.84 ± 0.01 ($n = 50$ cells). Although homogenous nEGFR staining was observed in SUM149 and SUM229 cells by immunofluorescence, nEGFR staining in MDAMB468 cells was more heterogeneous. Knockdown of EGFR using siRNA or preincubation of primary antibody with blocking peptides led to dramatic decreases in EGFR signal. There was no signal detected from cells

incubated with secondary antibody only (data not shown). We further validated nEGFR expression using transmission electron microscopy (Fig. 1C). EGFR labeled with immunogold conjugated secondary antibodies indicated that EGFR was indeed localized in the nucleus, with localization in the nucleolus and around the nuclear envelope.

Given that nEGFR was expressed in established TNBC cell lines, we probed a human TMA containing 74 TNBC patient tumors for EGFR expression and localization. Pathologist analysis of tumors stained for EGFR via IHC indicated that 19% of the tumors expressed nEGFR (Fig. 1D). Interestingly, nEGFR was highly localized to the nucleolus in more than 5% of nEGFR-positive tumors. In addition, some tumor sections contained concentrated nEGFR, whereas other areas of the same tumor lacked nEGFR expression. There was no signal detected from cores stained with secondary antibody only (data not shown). Collectively, these data demonstrate that TNBC cell lines and human tumors express nEGFR.

TNBC cells are resistant to cetuximab therapy, but dependent on EGFR for proliferation

To determine the role of EGFR in TNBC proliferation, studies were performed to knock down EGFR expression in various TNBC cell lines using an EGFR-directed siRNA pool. Loss of EGFR expression led to a 23% to 50% reduction in cell proliferation as compared to cells treated with vehicle or NT siRNA (Fig. 2). Each cell line challenged with increasing doses of cetuximab (from 0.01 nmol/L to 100 nmol/L) demonstrated only minor reductions in proliferation. The cell lines MDAMB231 (Fig. 2B) and MDAMB468 (Fig. 2D) demonstrated a 15% reduction in proliferation upon treatment with 100 nmol/L of cetuximab, whereas the SUM159 (Fig. 2A), SUM229 (Fig. 2C), and SUM149 (Fig. 2E) were unaffected at this dose. In addition, TNBC cell lines treated with increasing doses of dasatinib (0.01–100 nmol/L) were relatively resistant to growth inhibition. These results indicate that TNBC cell lines depend on EGFR for proliferation but are relatively resistant to cetuximab.

SFKs mediate the nuclear translocation of EGFR in TNBC

Previous studies from our laboratory indicate that SFKs influence nEGFR translocation in lung cancer (26, 30). To investigate whether SFKs influence EGFR translocation from the plasma membrane to the nucleus in TNBC, constitutively active Src (caSrc) was overexpressed in SUM159, BT549, and MDAMB231 cells. The overexpression of caSrc, indicated by enhanced pSFK-Y419, led to increases in nEGFR expression (Fig. 3A). Next, a negative regulator of Src, SLAP (39), was overexpressed in SUM149, SUM229, and MDAMB468 cells. The overexpression of SLAP, indicated by the expression of the Flag tag, led to decreases in nEGFR levels (Fig. 3B). These studies indicate that modulation of SFK activity can influence nEGFR expression in TNBC cell lines.

Previous studies elucidating the functions of SLAP have identified that SLAP functions as an antagonist for Src-induced mitogenesis partly through the binding of Src substrates and effector molecules (39). Overexpression of SLAP resulted in its association with EGFR in three TNBC cell lines by coimmunoprecipitation analysis (Fig. 3C). Immunoprecipitation with an IgG control yielded no signal (data not shown). Because EGFR deficient in tyrosine 1101 (Y1101) phosphorylation is hindered in nuclear translocation (Fig. 3C, Inset 1; ref. 30), we probed for phosphorylated EGFR at Y1101 post SLAP transfection. Indeed, TNBC cell lines overexpressing SLAP had decreased phosphorylation of EGFR at Y1101 (Fig. 3C), which correlated with decreased nEGFR (Fig. 3B). These data demonstrate that SFK phosphorylation of EGFR at Y1101 can influence nEGFR translocation in TNBC.

SFKs exhibit functional redundancy in their ability to influence nEGFR translocation

Previous reports suggest that the SFKs Yes and Lyn play a role in the nuclear translocation of EGFR (30). However, experiments in Fig. 3 indicated that caSrc and SLAP could influence nEGFR translocation in TNBC cells, suggesting that global increased activity of SFKs may influence nEGFR expression. To test this hypothesis, stable clones of individual SFKs (Src, Yes, Lyn, Lck, Hck, Fyn, Blk, and Fgr) were engineered in the breast cancer cell line MCF-7. One or two stable clones were chosen for each SFK for comparison with an empty vector stable cell line (Fig. 4A). The overexpression of each SFK led to the enhanced expression and nuclear translocation of EGFR. All cell lines were stimulated with 5 nmol/L EGF to promote the nuclear translocation of EGFR; however, a basal level of nEGFR was detected in nonstimulated SFK stable cells (data not shown). In addition, the stable overexpression of each SFK led to their increased activation, corresponding to a downregulation of the E3 ubiquitin ligase, c-Cbl (Fig. 4B). This result may explain why an increase in total EGFR was observed in Fig. 4A. Collectively, these data suggest that SFKs play functional redundant roles in promoting nEGFR translocation.

Therapeutic inhibition of SFKs can block nEGFR translocation in *in vitro* and *in vivo* TNBC tumor models

Because the modulation of SFK activity influenced nEGFR, the SFK inhibitor dasatinib was utilized to determine whether it could abrogate EGFR translocation from the membrane to nucleus. Treatment of TNBC cells with dasatinib led to potent decreases in nEGFR levels (at 24 and 72 hours in SUM149 and SUM229, and at 72 hours in MDAMB468 cells; Fig. 5A). Analysis of whole-cell lysate indicated that EGFR activity on Y1101 was inhibited by dasatinib at both time points. In addition, dasatinib treatment led to subsequent increases in non-nEGFR levels (Fig. 5A). Nuance imaging and Inform software was further used to analyze nEGFR levels post-dasatinib treatment (Fig. 5B). Cells were stained for EGFR, E-Cadherin, and DAPI; E-Cadherin and DAPI were used to create a spectral

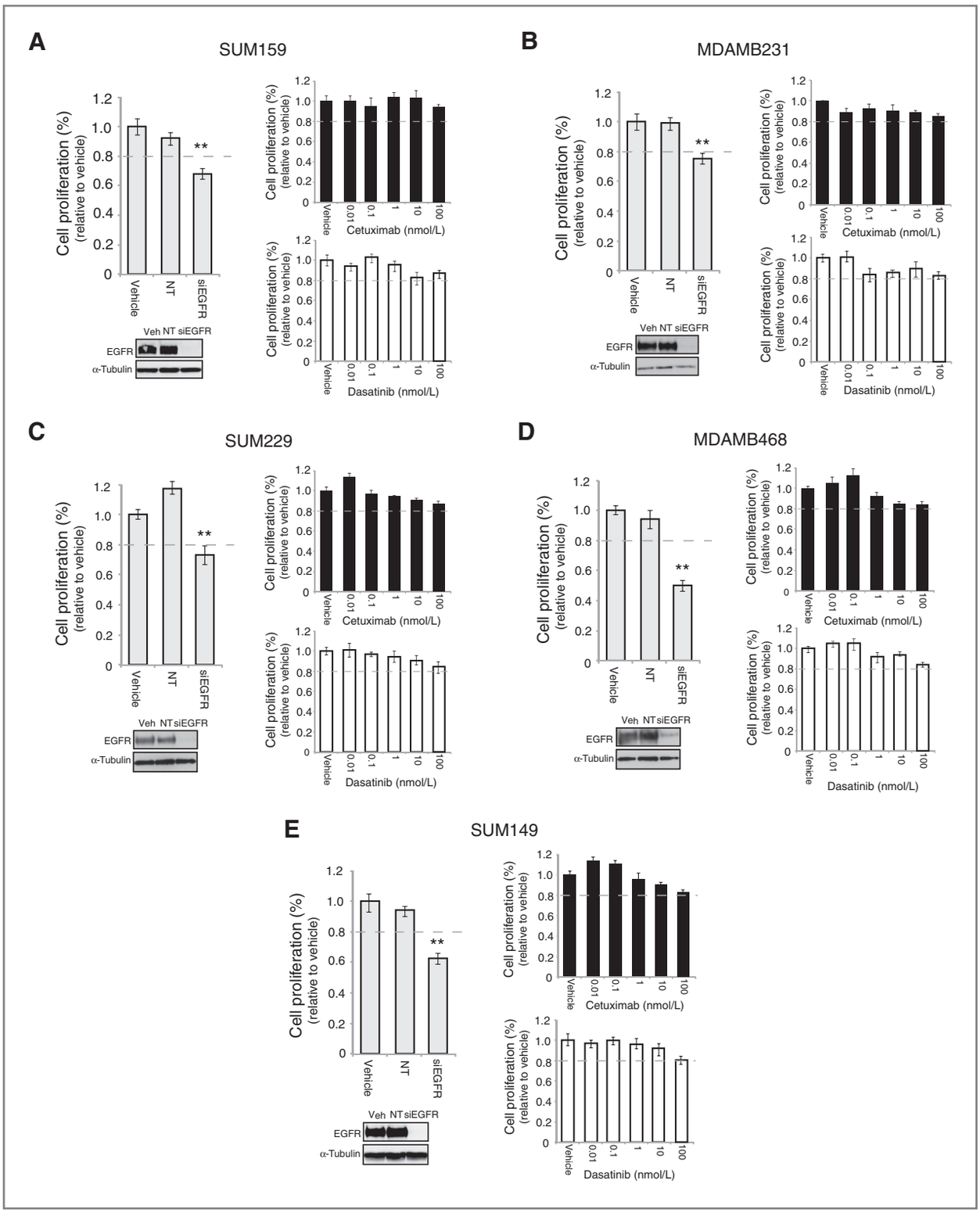

Figure 2. TNBC cell lines are dependent on EGFR for proliferation, but are intrinsically resistant to cetuximab and dasatinib. Cell lines were incubated with siEGFR, nontargeting (NT) siRNA, or vehicle for 72 to 96 hours before performing proliferation assays (A–E). Cells were treated with cetuximab or dasatinib at indicated doses for the same time course. Proliferation is plotted as a percentage of growth relative to vehicle-treated cells ($n = 3$). Whole-cell lysate was harvested from all cell lines at the same time point to confirm knockdown of EGFR. Data, mean ± SEM. **, $P < 0.01$.

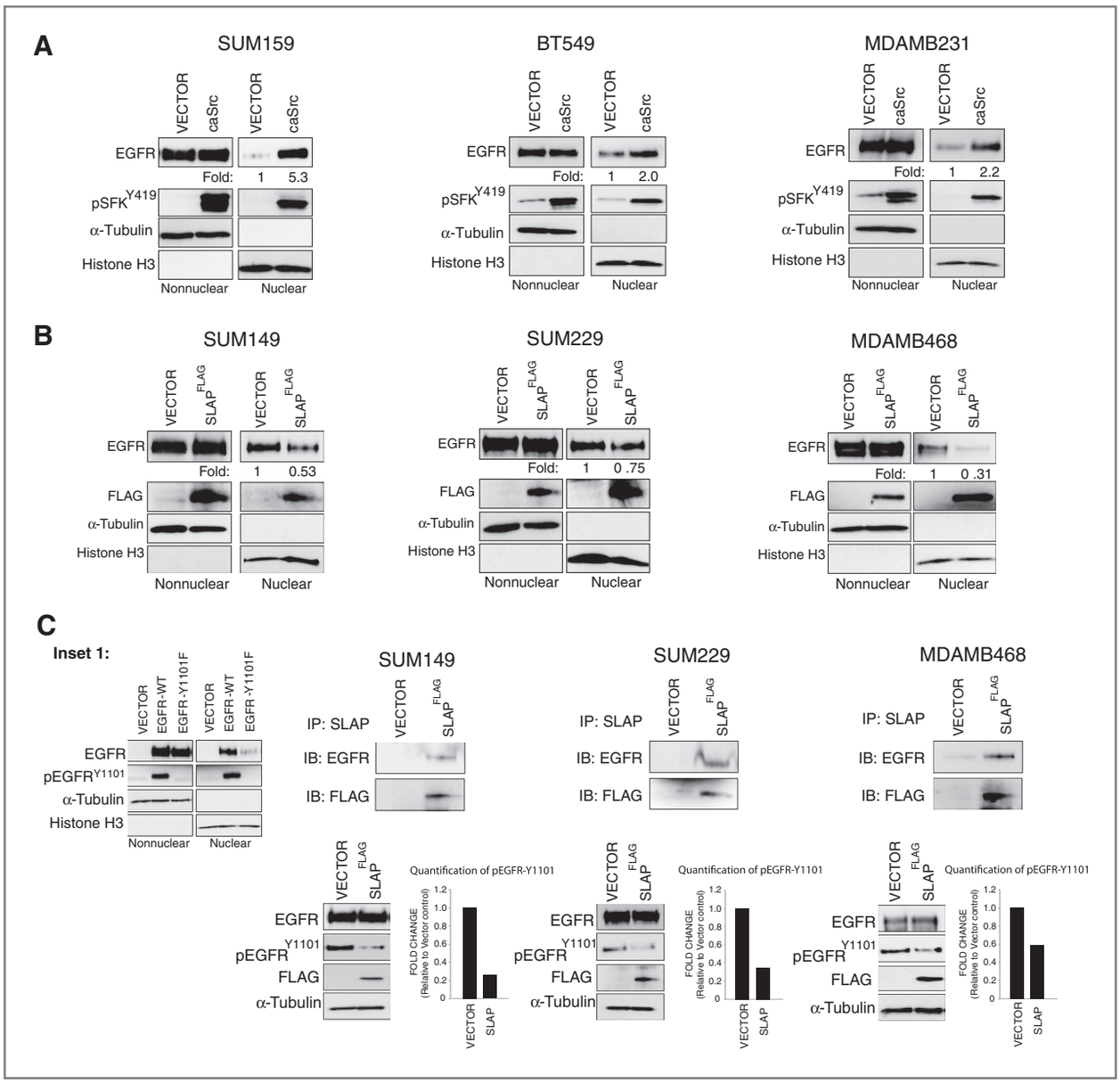

Figure 3. SFKs mediate nEGFR translocation in TNBC. A, constitutively active Src (caSrc) enhances nEGFR translocation in TNBC cell lines. Cells were transfected with caSrc or an empty vector control for 48 hours before stimulation with EGF (5 nmol/L, 45 minutes) to induce nEGFR translocation. Nonnuclear and nuclear proteins were harvested. nEGFR expression was quantitated using ImageJ software. B, a negative regulator of Src, SLAP, blocks nEGFR translocation in TNBC cell lines. Cells were transfected with SLAP-FLAG or an empty vector control for 48 hours before harvesting nonnuclear and nuclear proteins. nEGFR expression was analyzed. C, SLAP can interact with EGFR and decrease EGFR activation at tyrosine 1101. Cells were transfected with SLAP-FLAG or an empty vector control for 48 hours before harvesting whole-cell lysate. 250 μg of cell lysate was immunoprecipitated with an anti-SLAP antibody. The same lysate was subjected to immunoblot analysis for activation of EGFR at tyrosine 1101. pEGFR-Y1101 activity was quantitated using ImageJ software. Inset 1, EGFR mutated at tyrosine 1101 is deficient in nuclear localization. Vector, EGFR-WT, and EGFR-Y1101F were transfected into CHOK1 cells for 48 hours before stimulation with EGF (5 nmol/L, 45 minutes). Nonnuclear and nuclear proteins were harvested, and nEGFR expression was analyzed.

library that segmented each cell into cytoplasm and nucleus as previously described (34). InForm software analysis of each cell line ($n = 2$) demonstrated that dasatinib-treated cells trended toward less nEGFR staining as compared with vehicle-treated cells ($P = 0.08$ at 48 hours).

To further characterize the effect of dasatinib on non-nEGFR expression, surface level EGFR was analyzed by flow cytometry. TNBC cells treated with dasatinib for 24 hours contained 30% to 42% more plasma membrane-bound EGFR as compared with vehicle-treated cells (Fig. 5C). There was no additional increase in EGFR surface expression 72 hours posttreatment (data not shown). Together, these data suggest that EGFR accumulates on the plasma membrane when nEGFR translocation is blocked by dasatinib.

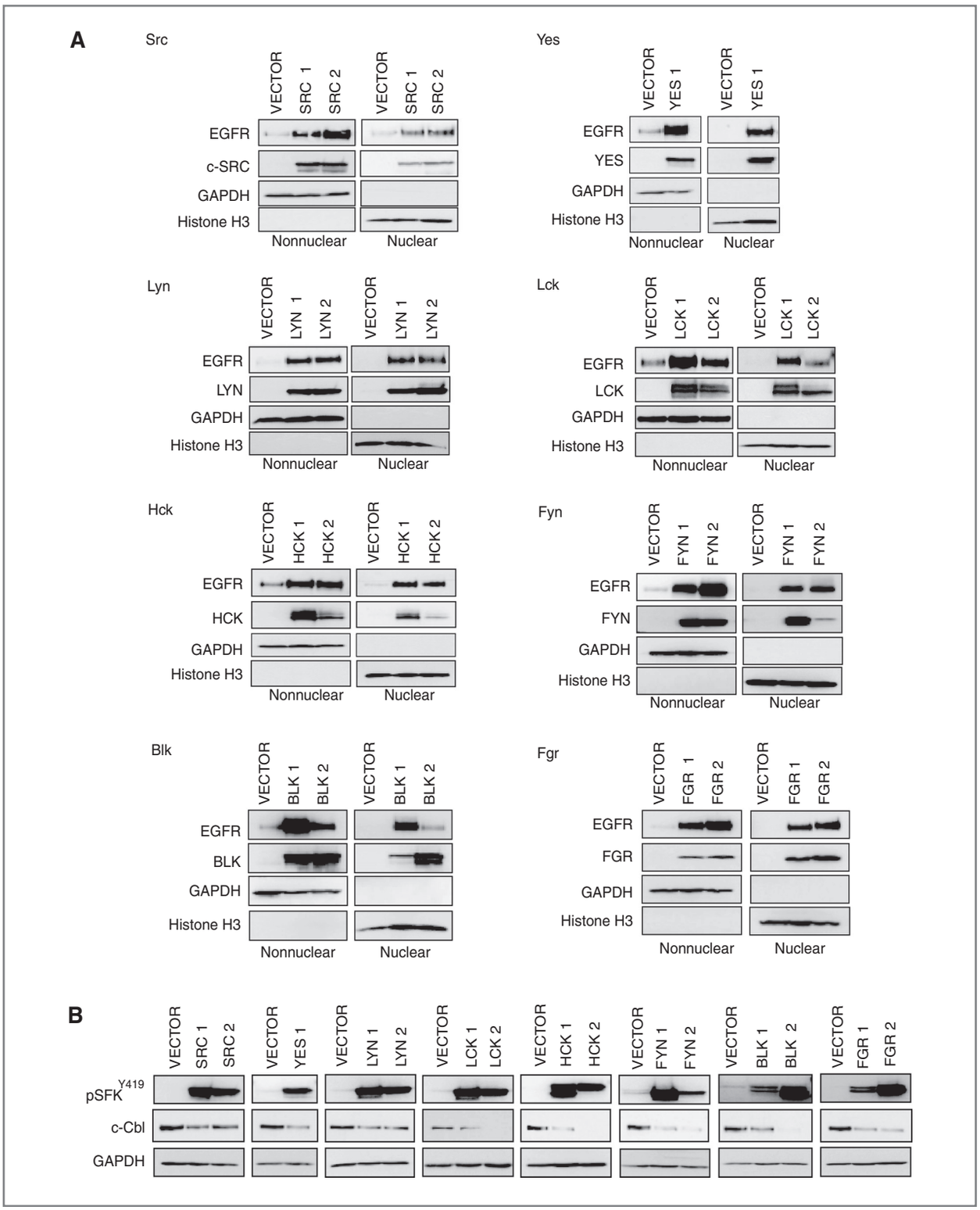

Figure 4. SFKs exhibit functional redundancy in their ability to influence nEGFR translocation. A, the stable overexpression of SFKs increase nEGFR expression. Eight different SFKs were stably overexpressed in the breast cancer cell line MCF-7. SFK stable clones or an empty vector stable cell line were stimulated with EGF (5 nmol/L, 45 minutes) to induce nEGFR translocation, before harvesting nonnuclear and nuclear proteins. GAPDH and Histone H3 were used as loading and purity controls, respectively. B, the stable overexpression of SFKs downregulate c-Cbl. Whole-cell lysate was harvested from SFK stable clones or an empty vector stable cell line. GAPDH was used as loading control.

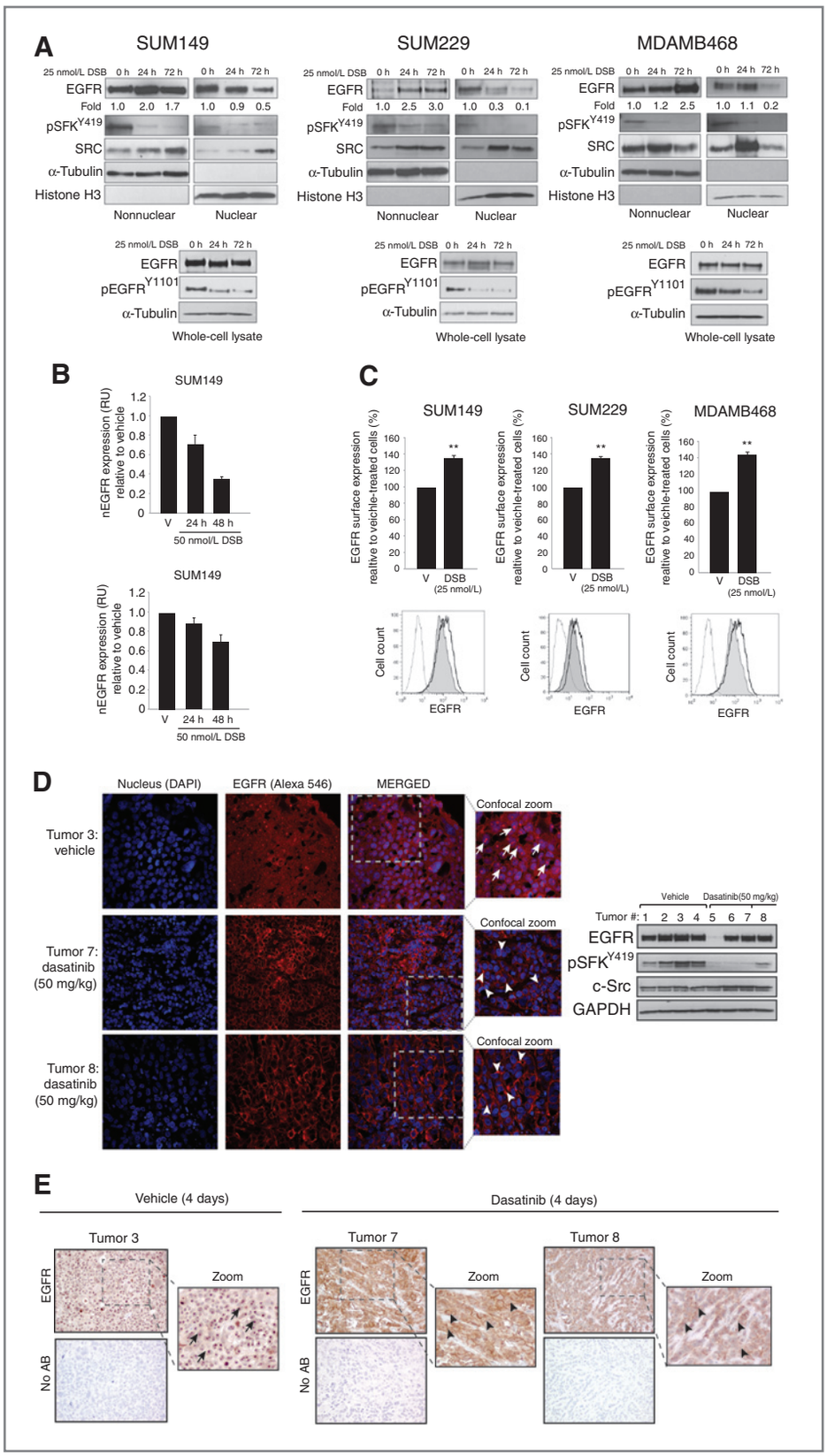

Figure 5. Therapeutic inhibition of SFKs can block nEGFR translocation in TNBC cell lines and tumor models. A, dasatinib can inhibit nEGFR translocation and enhance nonnuclear EGFR levels. Cells were treated with vehicle or dasatinib (25 nmol/L) for 24 and 72 hours before harvesting whole cell, nonnuclear, and nuclear proteins. B, dasatinib can block nEGFR translocation measured by Nuance imaging analysis. Cells were treated with vehicle or dasatinib (50 nmol/L) for 24 and 48 hours before staining for EGFR, E-Cadherin, and DAPI. nEGFR fluorescence detected from dasatinib-treated cells was normalized to nEGFR fluorescence detected from vehicle-treated cells using InForm software ($n = 2$). C, dasatinib can enhance plasma membrane-bound EGFR levels measured by flow cytometry. Cells were treated with dasatinib (25 nmol/L) for 24 hours before EGFR surface level analysis. Surface level EGFR expression of dasatinib-treated cells was normalized to vehicle-treated cells ($n = 3$). Shaded histogram, vehicle-treated cells; nonshaded histograms, dasatinib-treated cells. IgG-treated cells are used as a control (dotted line). D and E, dasatinib can block nEGFR translocation in MDAMB468 xenograft tumors. Mice with established MDAMB468 tumors were treated with 50 mg/kg of dasatinib or vehicle once a day for 4 days. Tumors were analyzed by confocal immunofluorescence (IF; D) and IHC (E) for EGFR expression. IF, merged images were magnified to depict nEGFR (arrows) and non-nEGFR (triangle). ×600 magnification for IF and ×400 for IHC. Four tumors from vehicle (tumor # 1–4) or dasatinib-treated mice (tumor # 5–8) were harvested for protein and analyzed for the indicated proteins. Data, mean±SEM. **, $P < 0.01$.

To investigate whether therapeutic inhibition of SFKs can abrogate nEGFR translocation *in vivo*, MDAMB468 cells were established as xenograft tumors in female athymic nude mice. Mice were randomized into two groups receiving 50 mg/kg of dasatinib or vehicle once daily for 4 days. Figure 5D represents confocal immunofluorescence analyses of representative tumor sections harvested from either vehicle- or dasatinib-treated mice stained for EGFR. EGFR was highly nuclear localized in tumors from vehicle-treated mice. However, tumors harvested from dasatinib-treated mice harbored much less nEGFR, with a noticeable increase in plasma membrane localized EGFR expression. Immunoblot analysis of harvested tumors validated that dasatinib inhibited SFK activity; one dasatinib-treated tumor (#5) contained less total EGFR expression. The inhibition of nEGFR translocation was also visualized by immunohistochemical staining of tumors harvested from dasatinib-treated mice (Fig. 5E). Interestingly, we found that dasatinib treatment of mice harboring colorectal tumors also contained less nEGFR expression within the tumor (Supplementary Fig. S1), suggesting that SFKs may influence nEGFR translocation in different tumor types. Collectively, these data indicate that SFK inhibition prevents nEGFR translocation and enhances membrane accumulation of EGFR *in vivo*.

SFK inhibition can sensitize TNBC cells to cetuximab growth inhibition

Because SFK inhibition enhanced plasma membrane-bound EGFR expression, we hypothesized that TNBC cells may become more sensitive to cetuximab upon pretreatment with dasatinib. To investigate this, we performed proliferation assays after pretreating TNBC cells with dasatinib or vehicle for 24 hours, the time point at which an increase in surface level EGFR was detected, and subsequently treating cells with increasing doses of cetuximab for an additional 72 hours (Fig. 6). All cell lines pretreated with vehicle and subsequently treated

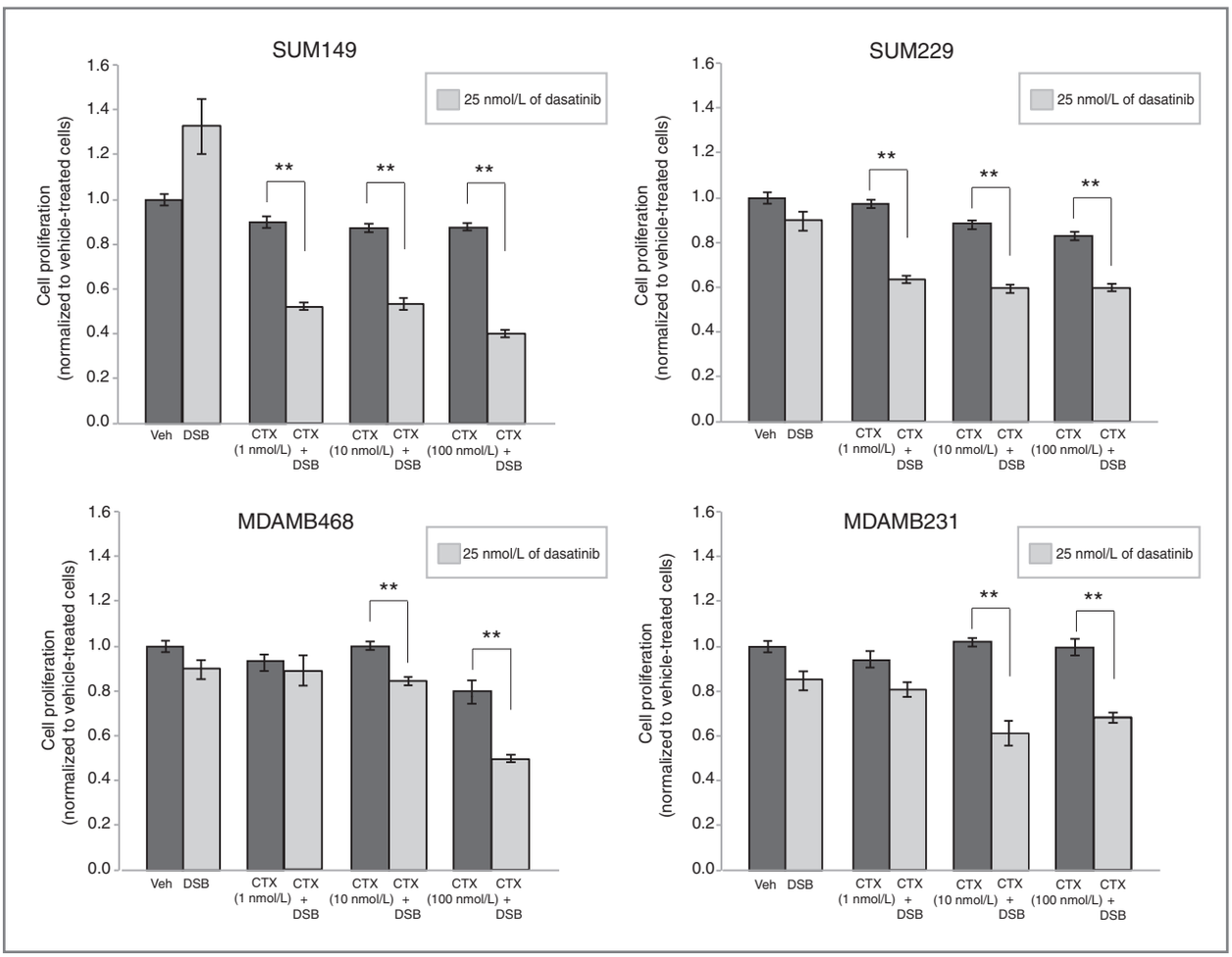

Figure 6. Therapeutic inhibition of SFK activity can sensitize TNBC cells to cetuximab. Cells were pretreated with vehicle or dasatinib (25 nmol/L) for 24 hours before adding cetuximab to the growth medium at the indicated doses (1, 10, and 100 nmol/L) for an additional 72 hours. Proliferation assays were performed and plotted as a percentage of growth relative to vehicle-treated cells ($n = 3$). Data, mean ± SEM. **, $P < 0.01$.

with increasing doses of cetuximab demonstrated minor reductions in proliferation, consistent with data in Fig. 2. In addition, cells treated with 25 nmol/L dasatinib monotherapy did not exhibit significant inhibition of proliferation. However, TNBC cell lines that received dasatinib for 24 hours before cetuximab treatment demonstrated significant reductions in proliferation over a wide range of cetuximab doses (1–100 nmol/L). SUM149 and SUM229 cells demonstrated significant reductions in proliferation at low doses of cetuximab (1 nmol/L), whereas MDAMB468 and MDAMB231 cells exhibited proliferation inhibition at higher doses of cetuximab (10 and 100 nmol/L). Collectively, these data suggest that the blockade of nEGFR translocation via SFK inhibition can increase TNBC cell sensitivity to cetuximab.

Discussion

TNBC is a subset of breast cancers that commonly overexpress the EGFR (3–6). Unfortunately, clinical trials targeting EGFR with cetuximab have yielded minimal benefit in TNBC (7, 8), even with the addition of platinum-based chemotherapies (1, 5, 36). Thus, understanding why TNBCs are intrinsically resistant to cetuximab has become an important clinical question. Over the last decade, numerous studies have identified a role for nEGFR in resistance to anti-EGFR agents (25, 26). Previous studies from our laboratory demonstrated that NSCLC cell lines that had acquired resistance to cetuximab relied on nEGFR signaling to maintain their resistant phenotype (26). On the basis of these studies, we hypothesized that nEGFR may be a critical molecular determinant for cetuximab resistance in TNBC.

In the current study, nEGFR was detected in a panel of established TNBC cell lines and human tumors (Fig. 1). In prior studies, 38% of a 130 breast cancer patient cohort (15) and 40% of a 113 breast cancer patient cohort (19) stained positive for nEGFR, which was further correlated with worse overall survival. The heterogeneity observed in nEGFR expression in the current study of TNBC tumors highlights the importance of simultaneously targeting both nEGFR and non-nEGFR cell populations. Another interesting observation lies in the localization of EGFR in the nucleolus, functions that have yet to be investigated and may be playing important roles in TNBC pathogenesis. Collectively, the preclinical data presented in the current study suggest that nEGFR may be indicative of cetuximab-resistant tumors warranting further investigation for its role as a predictive marker for cetuximab response in TNBC.

Recent work from our laboratory has found that SFK-dependent phosphorylation of EGFR on Y1101 is a necessary and early event for EGFR translocation from the plasma membrane to the nucleus (30). The current study aimed to identify whether this mechanism of nuclear translocation was present in TNBC. We found that three TNBC cell lines (MDAMB468, SUM149, and SUM229) with the highest levels of phosphorylated Y1101 also expressed the highest levels of nEGFR (Fig. 1A and B). In addition, inhibition of SFK activity led to decreased phosphorylation of EGFR on Y1101 and reduced nEGFR levels (Figs. 3C and 5A and B). Interestingly, Fig. 5C indicates that surface level EGFR was enhanced within 24 hours of dasatinib treatment, even though a decrease in nEGFR expression was more prominent at later time points posttreatment (Fig. 5A and B); this suggests that the rate of nEGFR export, via its nuclear export sequence (28), varies between cell lines. Collectively, these data suggest that SFK phosphorylation of EGFR on Y1101 may be a critical step for EGFR nuclear translocation in TNBC.

SFKs consist of 11 intracellular tyrosine kinases that are differentially expressed in a variety of cancers (40). In the current study, eight individual SFKs were stably overexpressed, and found to function similarly in their ability to influence (i) the steady state expression of total EGFR, (ii) nEGFR translocation, and (iii) degradation of c-Cbl (Fig. 4). These data suggest that SFKs exhibit functional redundancy in their ability to influence nEGFR translocation, and thus the use of broad-spectrum SFK inhibitors, such as dasatinib, may be highly beneficial in nEGFR-positive cancers.

In the current study, SFK inhibition of nEGFR translocation led to an accumulation of plasma membrane-bound EGFR and sensitization to cetuximab therapy (Figs. 5 and 6). Recent studies support our findings, where antitumorigenic effects of both cetuximab and dasatinib dual treatment with chemotherapy (41) and the use of noncompetitive monoclonal antibodies degrading the EGFR (42) have been documented in TNBC. In addition, a recent report demonstrated that targeting PCNA, a nEGFR substrate, could delay TNBC tumor growth (43). In the current study, sensitization to cetuximab was observed after pretreatment of TNBC cells with dasatinib for 24 hours, the time point at which EGFR accumulation was detected on the plasma membrane due to the inhibition of nEGFR translocation. We speculate that the inhibition of nEGFR translocation drives TNBC cells to rely solely on classical membrane-bound EGFR signaling for sustained proliferation and survival signals; thus, TNBC cells become sensitized to cetuximab because cetuximab can abrogate classical EGFR signaling pathways. Previous studies in EGFR expressing NSCLC and HNSCC cell lines support this, where cell lines that lacked nEGFR expression were found to be more sensitive to cetuximab monotherapy (26, 30). Currently, the growth inhibitory effect of cetuximab and dasatinib therapy is being accessed *in vivo* TNBC models in our laboratory, a critical step for the movement of this proposed drug combination into clinical trials. Collectively, the data presented herein indicate that the dual targeting of both nEGFR and plasma membrane-bound EGFR is necessary for the complete inhibition of EGFR's oncogenic functions, a therapeutic strategy that can be readily translated for the treatment of nEGFR expressing TNBC patients.

Disclosure of Potential Conflicts of Interest

No potential conflicts of interest were disclosed.

Authors' Contributions

Conception and design: T.M. Brand, R. Salgia, D.L. Wheeler
Development of methodology: T.M. Brand, M. Iida, R. Salgia, D.L. Wheeler
Acquisition of data (provided animals, acquired and managed patients, provided facilities, etc.): T.M. Brand, M. Iida, E.F. Dunn, N. Luthar, K.T. Kostopoulos, K.L. Corrigan, D. Yang, K.B. Wisinski, R. Salgia, D.L. Wheeler
Analysis and interpretation of data (e.g., statistical analysis, biostatistics, computational analysis): T.M. Brand, M. Iida, K.T. Kostopoulos, R. Salgia, D.L. Wheeler
Writing, review, and/or revision of the manuscript: T.M. Brand, M. Iida, E.F. Dunn, N. Luthar, R. Salgia, D.L. Wheeler
Administrative, technical, or material support (i.e., reporting or organizing data, constructing databases): T.M. Brand, M. Iida, M.J. Wleklinski, D. Yang, D.L. Wheeler

Acknowledgments

The authors thank Drs. Roche, Mischel, and Boerner for kindly sharing their expression vectors, Lance Rodenkirch and the Keck Laboratory for Biological Imaging for their expertise in confocal microscopy, and Ben August and Amanda Thoma for their training and expertise in electron microscopy.

Grant Support

This work was supported by Grant UL1TR000427 from the Clinical and Translational Science Award program, through the NIH National Center for Advancing Translational Sciences (to D.L. Wheeler), grant RSG-10-193-01-TBG from the American Cancer Society (to D.L.Wheeler), grant W81XWH-12-1-0467 from United States Army Medical Research and Materiel Command (to D.L.Wheeler), Mary Kay Foundation grant MSN152261 (to D.L. Wheeler), and NIH grant Q3 T32 GM08.1061-01A2 from Graduate Training in Cellular and Molecular Pathogenesis of Human Diseases (to T.M. Brand).

The costs of publication of this article were defrayed in part by the payment of page charges. This article must therefore be hereby marked *advertisement* in accordance with 18 U.S.C. Section 1734 solely to indicate this fact.

Received December 2, 2013; revised January 31, 2014; accepted February 16, 2014; published OnlineFirst March 14, 2014.

References

1. Schneider BP, Winer EP, Foulkes WD, Garber J, Perou CM, Richardson A, et al. Triple-negative breast cancer: risk factors to potential targets. Clin Cancer Res 2008;14:8010–8.
2. Stevens KN, Vachon CM, Couch FJ. Genetic susceptibility to triple-negative breast cancer. Cancer Res 2013;73:2025–30.
3. Corkery B, Crown J, Clynes M, O'Donovan N. Epidermal growth factor receptor as a potential therapeutic target in triple-negative breast cancer. Ann Oncol 2009;20:862–7.
4. Sorlie T, Tibshirani R, Parker J, Hastie T, Marron JS, Nobel A, et al. Repeated observation of breast tumor subtypes in independent gene expression data sets. Proc Natl Acad Sci U S A 2003;100:8418–23.
5. Nielsen TO, Hsu FD, Jensen K, Cheang M, Karaca G, Hu Z, et al. Immunohistochemical and clinical characterization of the basal-like subtype of invasive breast carcinoma. Clin Cancer Res 2004;10:5367–74.
6. Lehmann BD, Bauer JA, Chen X, Sanders ME, Chakravarthy AB, Shyr Y, et al. Identification of human triple-negative breast cancer subtypes and preclinical models for selection of targeted therapies. J Clin Invest 2011;121:2750–67.
7. Masuda H, Zhang D, Bartholomeusz C, Doihara H, Hortobagyi GN, Ueno NT. Role of epidermal growth factor receptor in breast cancer. Breast Cancer Res Treat 2012;136:331–45.
8. Gelmon K, Dent R, Mackey JR, Laing K, McLeod D, Verma S. Targeting triple-negative breast cancer: optimising therapeutic outcomes. Ann Oncol 2012;23:2223–34.
9. Yarden Y, Pines G. The ERBB network: at last, cancer therapy meets systems biology. Nat Rev Cancer 2012;12:553–63.
10. Brand TM, Iida M, Li C, Wheeler DL. The nuclear epidermal growth factor receptor signaling network and its role in cancer. Discov Med 2011;12:419–32.
11. Han W, Lo HW. Landscape of EGFR signaling network in human cancers: biology and therapeutic response in relation to receptor subcellular locations. Cancer Lett 2012;318:124–34.
12. Dittmann K, Mayer C, Fehrenbacher B, Schaller M, Raju U, Milas L, et al. Radiation-induced epidermal growth factor receptor nuclear import is linked to activation of DNA-dependent protein kinase. J Biol Chem 2005;280:31182–9.
13. Hsu SC, Miller SA, Wang Y, Hung MC. Nuclear EGFR is required for cisplatin resistance and DNA repair. Am J Transl Res 2009;1:249–58.
14. Wang SC, Nakajima Y, Yu YL, Xia W, Chen CT, Yang CC, et al. Tyrosine phosphorylation controls PCNA function through protein stability. Nat Cell Biol 2006;8:1359–68.
15. Lo HW, Xia W, Wei Y, Ali-Seyed M, Huang SF, Hung MC. Novel prognostic value of nuclear epidermal growth factor receptor in breast cancer. Cancer Res 2005;65:338–48.
16. Psyrri A, Yu Z, Weinberger PM, Sasaki C, Haffty B, Camp R, et al. Quantitative determination of nuclear and cytoplasmic epidermal growth factor receptor expression in oropharyngeal squamous cell cancer by using automated quantitative analysis. Clin Cancer Res 2005;11:5856–62.
17. Li CF, Fang FM, Wang JM, Tzeng CC, Tai HC, Wei YC, et al. EGFR nuclear import in gallbladder carcinoma: nuclear phosphorylated EGFR upregulates iNOS expression and confers independent prognostic impact. Ann Surg Oncol 2012;19:443–54.
18. Xia WY, Wei YK, Du Y, Liu JS, Chang B, Yu YL, et al. Nuclear expression of epidermal growth factor receptor is a novel prognostic value in patients eith Ovarian cancer. Mol Carcinog 2009;48:610–7.
19. Hadzisejdic I, Mustac E, Jonjic N, Petkovic M, Grahovac B. Nuclear EGFR in ductal invasive breast cancer: correlation with cyclin-D1 and prognosis. Mod Pathol 2010;23:392–403.
20. Traynor AM, Weigel TL, Oettel KR, Yang DT, Zhang C, Kim K, et al. Nuclear EGFR protein expression predicts poor survival in early stage non-small cell lung cancer. Lung Cancer 2013;81:138–41.
21. Dittmann K, Mayer C, Fehrenbacher B, Schaller M, Kehlbach R, Rodemann HP. Nuclear EGFR shuttling induced by ionizing radiation is regulated by phosphorylation at residue Thr654. FEBS Lett 2010;584:3878–84.
22. Dittmann K, Mayer C, Fehrenbacher B, Schaller M, Kehlbach R, Rodemann HP. Nuclear epidermal growth factor receptor modulates cellular radio-sensitivity by regulation of chromatin access. Radiother Oncol 2011;99:317–22.
23. Dittmann K, Mayer C, Rodemann HP. Inhibition of radiation-induced EGFR nuclear import by C225 (Cetuximab) suppresses DNA-PK activity. Radiother Oncol 2005;76:157–61.
24. Liccardi G, Hartley JA, Hochhauser D. EGFR nuclear translocation modulates DNA repair following cisplatin and ionizing radiation treatment. Cancer Res 2011;71:1103–14.
25. Huang WC, Chen YJ, Li LY, Wei YL, Hsu SC, Tsai SL, et al. Nuclear translocation of epidermal growth factor receptor by Akt-dependent phosphorylation enhances breast cancer-resistant protein expression in gefitinib-resistant cells. J Biol Chem 2011;286:20558–68.
26. Li C, Iida M, Dunn EF, Ghia AJ, Wheeler DL. Nuclear EGFR contributes to acquired resistance to cetuximab. Oncogene 2009;28:3801–13.
27. Lo HW, Cao X, Zhu H, Ali-Osman F. Cyclooxygenase-2 is a novel transcriptional target of the nuclear EGFR-STAT3 and EGFRvIII-STAT3 signaling axes. Mol Cancer Res 2010;8:232–45.
28. Gururaj AE, Gibson L, Panchabhai S, Bai M, Manyam G, Lu Y, et al. Access to the nucleus and functional association with c-Myc is required for the full oncogenic potential of DeltaEGFR/EGFRvIII. J Biol Chem 2013;288:3428–38.
29. Wheeler DL, Iida M, Kruser TJ, Nechrebecki MM, Dunn EF, Armstrong EA, et al. Epidermal growth factor receptor cooperates with Src family

kinases in acquired resistance to cetuximab. Cancer Biol Ther 2009; 8:696–703.
30. Iida M, Brand TM, Campbell DA, Li C, Wheeler DL. Yes and Lyn play a role in nuclear translocation of the epidermal growth factor receptor. Oncogene 2012;32:759–67.
31. Brand TM, Iida M, Luthar N, Wleklinski MJ, Starr MM, Wheeler DL. Mapping C-terminal transactivation domains of the nuclear HER family receptor tyrosine kinase HER3. PLoS ONE 2013;8: e71518.
32. Li C, Brand TM, Iida M, Huang S, Armstrong EA, van der Kogel A, et al. Human epidermal growth factor receptor 3 (HER3) blockade with U3-1287/AMG888 enhances the efficacy of radiation therapy in lung and head and neck carcinoma. Discov Med 2013; 16:79–92.
33. Yi H, Leunissen JLM, Shi GM, Gutekunst CA, Hersch SM. A novel procedure for pre-embedding double immunogold-silver labeling at the ultrastructural level. J Histochem Cytochem 2001; 49:279–83.
34. Huang W, Hennrick K, Drew S. A colorful future of quantitative pathology: validation of Vectra technology using chromogenic multiplexed immunohistochemistry and prostate tissue microarrays. Hum Pathol 2013;44:29–38.
35. Iida M, Brand TM, Starr MM, Li C, Huppert EJ, Luthar N, et al. Sym004, a novel EGFR antibody mixture, can overcome acquired resistance to cetuximab. Neoplasia 2013;15:1196–206.
36. Dunn KW, Kamocka MM, McDonald JH. A practical guide to evaluating colocalization in biological microscopy. Am J Physiol Cell Physiol 2011;300:C723–42.
37. Tryfonopoulos D, Walsh S, Collins DM, Flanagan L, Quinn C, Corkery B, et al. Src: a potential target for the treatment of triple-negative breast cancer. Ann Oncol 2011;22:2234–40.
38. Elsberger B, Tan BA, Mitchell TJ, Brown SB, Mallon EA, Tovey SM, et al. Is expression or activation of Src kinase associated with cancer-specific survival in ER-, PR- and HER2-negative breast cancer patients? Am J Pathol 2009;175:1389–97.
39. Manes G, Bello P, Roche S. Slap negatively regulates Src mitogenic function but does not revert Src-induced cell morphology changes. Mol Cell Biol 2000;20:3396–406.
40. Sen B, Johnson FM. Regulation of SRC family kinases in human cancers. J Signal transduct 2011;2011:865819.
41. Kim EM, Mueller K, Gartner E, Boerner J. Dasatinib is synergistic with cetuximab and cisplatin in triple-negative breast cancer cells. J Surg Res 2013;185:231–9.
42. Ferraro DA, Gaborit N, Maron R, Cohen-Dvashi H, Porat Z, Pareja F, et al. Inhibition of triple-negative breast cancer models by combinations of antibodies to EGFR. Proc Natl Acad Sci U S A 2013;110:1815–20.
43. Yu YL, Chou RH, Liang JH, Chang WJ, Su KJ, Tseng YJ, et al. Targeting the EGFR/PCNA signaling suppresses tumor growth of triple-negative breast cancer cells with cell-penetrating PCNA peptides. PLoS ONE 2013;8:e61362.

Published OnlineFirst August 18, 2014; DOI: 10.1158/0008-5472.CAN-14-0294

Cancer Research

AXL Mediates Resistance to Cetuximab Therapy

Toni M. Brand, Mari Iida, Andrew P. Stein, et al.

Cancer Res Published OnlineFirst August 18, 2014.

Published OnlineFirst August 18, 2014; DOI: 10.1158/0008-5472.CAN-14-0294

Cancer Research

AXL Mediates Resistance to Cetuximab Therapy

Toni M. Brand[1], Mari Iida[1], Andrew P. Stein[1], Kelsey L. Corrigan[1], Cara M. Braverman[1], Neha Luthar[1], Mahmoud Toulany[2], Parkash S. Gill[3], Ravi Salgia[4], Randall J. Kimple[1], and Deric L. Wheeler[1]

Abstract

The EGFR antibody cetuximab is used to treat numerous cancers, but intrinsic and acquired resistance to this agent is a common clinical outcome. In this study, we show that overexpression of the oncogenic receptor tyrosine kinase AXL is sufficient to mediate acquired resistance to cetuximab in models of non–small cell lung cancer (NSCLC) and head and neck squamous cell carcinoma (HNSCC), where AXL was overexpressed, activated, and tightly associated with EGFR expression in cells resistant to cetuximab (Ctx^R cells). Using RNAi methods and novel AXL-targeting agents, we found that AXL activation stimulated cell proliferation, EGFR activation, and MAPK signaling in Ctx^R cells. Notably, EGFR directly regulated the expression of AXL mRNA through MAPK signaling and the transcription factor c-Jun in Ctx^R cells, creating a positive feedback loop that maintained EGFR activation by AXL. Cetuximab-sensitive parental cells were rendered resistant to cetuximab by stable overexpression of AXL or stimulation with EGFR ligands, the latter of which increased AXL activity and association with the EGFR. In tumor xenograft models, the development of resistance following prolonged treatment with cetuximab was associated with AXL hyperactivation and EGFR association. Furthermore, in an examination of patient-derived xenografts established from surgically resected HNSCCs, AXL was overexpressed and activated in tumors that displayed intrinsic resistance to cetuximab. Collectively, our results identify AXL as a key mediator of cetuximab resistance, providing a rationale for clinical evaluation of AXL-targeting drugs to treat cetuximab-resistant cancers. *Cancer Res; 1–13. ©2014 AACR.*

Introduction

The TAM family of receptor tyrosine kinases (RTK) is composed of three family members: Tyro-3 (Sky), AXL (Ark or Ufo), and MerTK. Cognate ligand binding to TAM receptors on the cell surface leads to receptor dimerization, kinase domain activation, and auto/trans-phosphorylation of tyrosine residues located on each receptor's cytoplasmic tail (1). The activation of TAM receptors stimulate PI3K/AKT and Ras/Raf/Mek/Erk (MAPK) signaling cascades, leading to increased cell survival, proliferation, migration, invasion, and angiogenesis (1–4).

TAM family overexpression and activation have been observed in many human cancers (1–11). Recently, the AXL receptor has been implicated in cancer cell resistance to anti-EGFR tyrosine kinase inhibitors (TKI; refs. 12–17) and other chemotherapeutics (10, 15, 18). Collectively, these data indicate that AXL functions as a potent oncogene that can modulate resistance to conventional and targeted cancer therapies.

Cetuximab is an anti-EGFR monoclonal antibody that has shown efficacy in treating head and neck squamous cell carcinoma (HNSCC), metastatic colorectal cancer (mCRC), and non–small cell lung cancer (NSCLC; refs. 19–26). Unfortunately, clinical studies indicate that most patients who initially respond to cetuximab eventually acquire resistance (27–29). To understand the mechanisms of acquired resistance, we previously created a model in which the cetuximab-sensitive (Ctx^S) NSCLC cell line NCI-H226 was treated with increasing doses of cetuximab for a period of six months until resistant single cell clones emerged (30). Analysis of cetuximab-resistant (Ctx^R) clones demonstrated that the expression of EGFR and its activation was dramatically increased because of dysregulated EGFR internalization and degradation without mutation of the receptor (30). Overall, Ctx^R cells remained highly addicted to the EGFR signaling network (30–32).

On the basis of these previous findings, we investigated whether the AXL receptor played a role in cetuximab resistance. Examination of *in vitro* NSCLC and HNSCC models of acquired resistance indicated that AXL was highly overexpressed and activated in Ctx^R cells. Further analysis indicated that Ctx^R cells had increased dependency on AXL for cellular proliferation, EGFR activation, and MAPK signaling. AXL activity

[1]Department of Human Oncology, University of Wisconsin School of Medicine and Public Health, Madison, Wisconsin. [2]Division of Radiobiology and Molecular Environmental Research, Department of Radiation Oncology, Eberhard Karls University Tübingen, Tübingen, Germany. [3]Departments of Medicine and Pathology, University of Southern California, Los Angeles, California. [4]Department of Medicine, Division of Hematology/Oncology, University of Chicago, Chicago, Illinois.

Note: Supplementary data for this article are available at Cancer Research Online (http://cancerres.aacrjournals.org/).

Corresponding Author: Deric L. Wheeler, Department of Human Oncology, University of Wisconsin Comprehensive Cancer Center, 1111 Highland Avenue, WIMR 3159, Madison, WI 53705. Phone: 608-262-7837; Fax: 608-263-9947; E-mail: dlwheeler@wisc.edu

doi: 10.1158/0008-5472.CAN-14-0294

Published OnlineFirst August 18, 2014; DOI: 10.1158/0008-5472.CAN-14-0294

was also examined in tumors harvested from *de novo*–acquired Ctx^R NCI-H226 xenografts, where AXL was highly activated and associated with the EGFR. Finally, AXL was overexpressed and hyperactivated in HNSCC patient-derived xenografts (PDX) that were intrinsically resistant to cetuximab therapy. Collectively, this work indicates that AXL plays a role in cetuximab resistance and provides rationale for the clinical evaluation of anti-AXL therapeutics for the treatment of cetuximab resistant cancers.

Materials and Methods

Cell lines and development of acquired resistance

The human NSCLC cell line NCI-H226 was purchased from ATCC and maintained in 10% FBS in RPMI-1640 (Mediatech Inc.) with 1% penicillin and streptomycin. The HNSCC cell line UM-SCC1 was provided by Dr. Thomas E. Carey (University of Michigan, Ann Harbor, MI) and maintained in 10% FBS in Dulbecco's Modified Eagle Medium (DMEM) with 1% penicillin and streptomycin. The development of Ctx^R cells has been previously described (30–32). All Ctx^R cell lines were validated to express wild-type (WT) EGFR by sequencing.

Materials

R428 was purchased from Selleckchem and MAb173 was produced in the laboratory of Dr. Parkash Gill (Department of Medicine and Pathology, University of Southern California, Los Angeles, CA). Cetuximab (ICM-225; Erbitux) was purchased from University of Wisconsin Pharmacy. EGF was purchased from Millipore and TGFα was purchased from Sigma-Aldrich.

Antibodies

All antibodies were purchased from commercial sources as indicated below:

R&D Systems: AXL (for immunoblotting) and pAXL-Y779. Cell Signaling Technology: pAXL-Y702, pEGFR-Y1068, pMAPK (T202/Y204), MAPK, p-cRAF (S289/296/301), cRAF, p-AKT (S473), AKT, p-rpS6 (S240/244), rpS6, p-c-Jun (S73), c-Jun, and GAPDH. Santa Cruz Biotechnology Inc.: pEGFR-Y1173, AXL (for immunoprecipitation), and horseradish peroxidase (HRP)–conjugated goat–anti-rabbit IgG, goat–anti-mouse IgG, and donkey–anti-goat IgG. Life Technologies: AXL (for immunofluorescence). Abcam: EGFR. Calbiochem: α-tubulin.

siRNA and transfection

Ctx^R cells were transiently transfected with AXL siRNA (siAXL; ON-TARGETplus, SMARTpool #L-003104; Dharmacon), siEGFR (ON-TARGETplus, SMARTpool #L-003114; Dharmacon), siHER2 (ON-TARGETplus, SMARTpool #L-003126; Dharmacon), siHER3 (ON-TARGETplus, SMARTpool #L-003127; Dharmacon), p44/42 MAPK (ERK1/2) siRNA (Cell Signaling Technology; #6560), AKT1 siRNA (ON-TARGETplus, SMARTpool #L-003000; Dharmacon), c-Jun siRNA (ON-TARGETplus, SMARTpool #L-003268; Dharmacon), or nontargeting siRNA (siNT; ON-TARGETplus Non-targeting Pool, #D-001810; Dharmacon) using Lipofectamine RNAiMAX according to the manufacturer's instructions (Life Technologies).

Immunoblot analysis

Whole-cell lysis was performed as previously described (31, 33). Enhanced chemiluminescence (ECL) detection system was used to visualize proteins. For detection of phosphorylated AXL, cells were treated with pervanadate (0.12 mmol/L Na_3VO_4 in 0.002% H_2O_2) for 2 minutes before cell lysis, a method previously described (10). EGF and TGFα ligands were added to growth media 45 minutes before lysis.

Immunoprecipitation

Cells were processed for immunoprecipitation as previously described (34). Five-hundred micrograms of protein, 2 μg of anti-AXL (Santa Cruz Biotechnology), cetuximab, or IgG antibody (Santa Cruz Biotechnology) were used.

Cell proliferation assay

Crystal violet assay and Cell Counting Kit-8 (Dojindo Molecular Technologies) were performed as previously described (31, 35). Cellular proliferation was measured 72 hours after siRNA or drug treatment.

Flow cytometric analysis

Cells were processed as previously described (36) and analyzed using a FACSCalibur flow cytometer (BD Biosciences). Propidium iodide was added to each sample at a final concentration of 5 mg/mL. Histogram analysis was performed using FlowJo software (TreeStar Inc.).

Plasmids, transfection, and stable cell line construction

pDONR223-AXL (Plasmid 23945) was purchased from Addgene and subcloned into the *Bam*H1/*Eco*R1 restriction sites of the pcDNA6.0 expression vector (Life Technologies). Stable transfection was performed using Lipofectamine LTX and Opti-MEM I (Life Technology) commencing 48 hours after transfection via 6 μg/mL blasticidin to the growth media. Single-cell clones were chosen for expansion and validation for AXL expression.

cDNA synthesis and qPCR

Total RNA and cDNA synthesis were prepared as previously described (34). All reactions were performed in triplicate. To determine the normalized value, $2^{\Delta\Delta Ct}$ values were compared between AXL and 18S, where the change in crossing threshold $(\Delta C_t) = C_{t\ AXL} - C_{t\ 18S}$ and $\Delta\Delta C_t = \Delta C_{t(HC1,\ HC4,\ or\ HC8)} - \Delta C_{t(HP)}$ or $\Delta\Delta C_t = \Delta C_{t(NT)} - \Delta C_{t(siAXL)}$.

Cetuximab-resistant cell line xenografts and PDXs

Ctx^R cell line xenografts were established as previously described (31), and HNSCC PDXs were established and evaluated for cetuximab response as described in Supplementary Materials and Methods.

Statistical analysis

Student *t* tests were used to evaluate differences in proliferation, AXL mRNA expression, and pAXL-Y779 expression levels by IHC. Differences were considered statistically significant if *, $P < 0.05$.

Published OnlineFirst August 18, 2014; DOI: 10.1158/0008-5472.CAN-14-0294

Results

AXL is overexpressed and activated in a model of acquired resistance to cetuximab

The NSCLC Ctx^R clones HC1, HC4, and HC8 have been previously shown to be resistant to increasing doses of cetuximab as compared to the Ctx^S NCI-H226 parental cell line HP (30, 31). Analysis of Ctx^R clones HC1, HC4, and HC8 demonstrated that all clones expressed increased AXL mRNA and protein as compared to HP cells (Fig. 1A). Furthermore, AXL exhibited increased phosphorylation on tyrosine 702 and 779 in all Ctx^R clones. In addition, MAPK and AKT pathways were hyperactivated and there was increased expression and phosphorylation of the transcription factor c-Jun in Ctx^R clones. Moreover, plasma membrane levels of AXL were detected via flow cytometry, where Ctx^R cells had approximately 50% to 80% more surface AXL expression as compared to HP cells (Fig. 1B). Collectively, these data demonstrate that AXL is overexpressed and activated in established clones with acquired resistance to cetuximab.

AXL and EGFR cooperate in Ctx^R clones to sustain proliferation via MAPK and c-Jun

Ctx^R clones are known to be highly dependent on EGFR for proliferation (30–32). To determine whether AXL also plays a role in Ctx^R cell proliferation, proliferation assays were performed 72 hours after transfection with a pooled siAXL or siNT (Fig. 2A). Loss of AXL expression resulted in statistically significant inhibition of proliferation (25%–35%) in all three Ctx^R clones. As compared with parental HP cells, the Ctx^R clones demonstrated significantly greater decreases in proliferation after AXL knockdown ($P < 0.01$). Analysis of Ctx^R clones after AXL knockdown demonstrated that EGFR activation was severely diminished at both tyrosine 1068 and 1173, autophosphorylation sites responsible for recruiting Grb2 and Shc (Fig. 2B; ref. 37). In addition, the activation of c-Raf, p44/42 MAPK, AKT, and ribosomal protein S6 (rpS6) were diminished in all Ctx^R clones upon AXL knockdown, whereas the activation of these molecules were relatively unchanged or slightly increased in HP cells (Fig. 2B). Interestingly, ablation of HER2 or HER3 receptors, previously shown to be hyperactivated in Ctx^R cells (30), did not affect the phosphorylation of EGFR at either tyrosine site (Fig. 2B, inset). Collectively, these data demonstrate that Ctx^R clones are dependent on AXL for cellular proliferation via EGFR activation and downstream signaling.

To determine whether AXL and EGFR were physically associated in Ctx^R clones, coimmunoprecipitation experiments were performed and indicated that AXL was associated with EGFR in all Ctx^R clones but not parental cells (Fig. 2C). EGFR and AXL cooperation was further analyzed by reciprocally knocking down EGFR expression with siRNA (Fig. 2D). EGFR knockdown

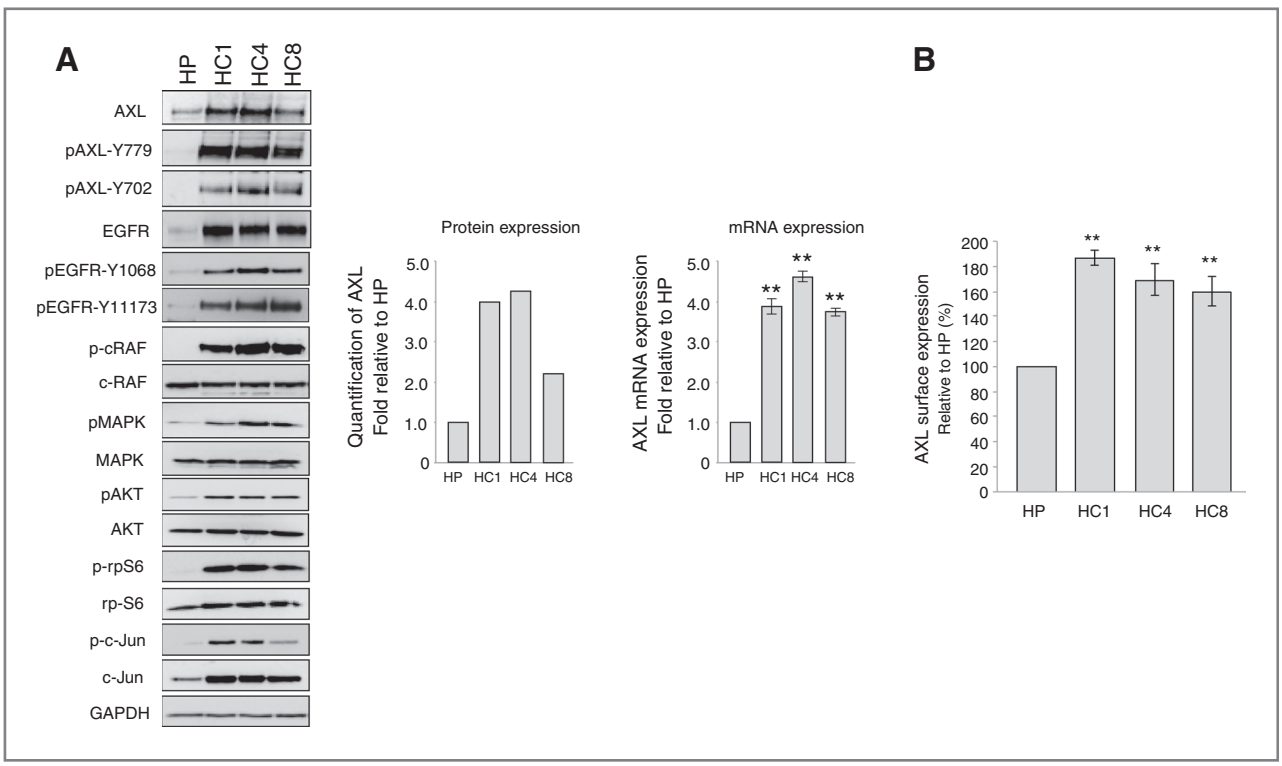

Figure 1. The RTK AXL and its downstream effector molecules are overexpressed in cetuximab resistant cells. A, whole-cell lysate was harvested from the Ctx^S parental cell line (HP) and three Ctx^R cell clones (HC1, HC4, and HC8) followed by immunoblotting for the indicated proteins. GAPDH was used as a loading control. Total AXL protein expression was quantitated using ImageJ software. AXL mRNA expression was detected by qPCR and normalized to AXL expression in HP cells ($n = 3$ in three independent experiments). 18S was used as an endogenous control. B, surface level AXL expression was detected by flow cytometry and normalized to HP. IgG-stained cells were used as a background control ($n = 3$ in two independent experiments). Data, mean ± SEM. **, $P < 0.01$.

Published OnlineFirst August 18, 2014; DOI: 10.1158/0008-5472.CAN-14-0294

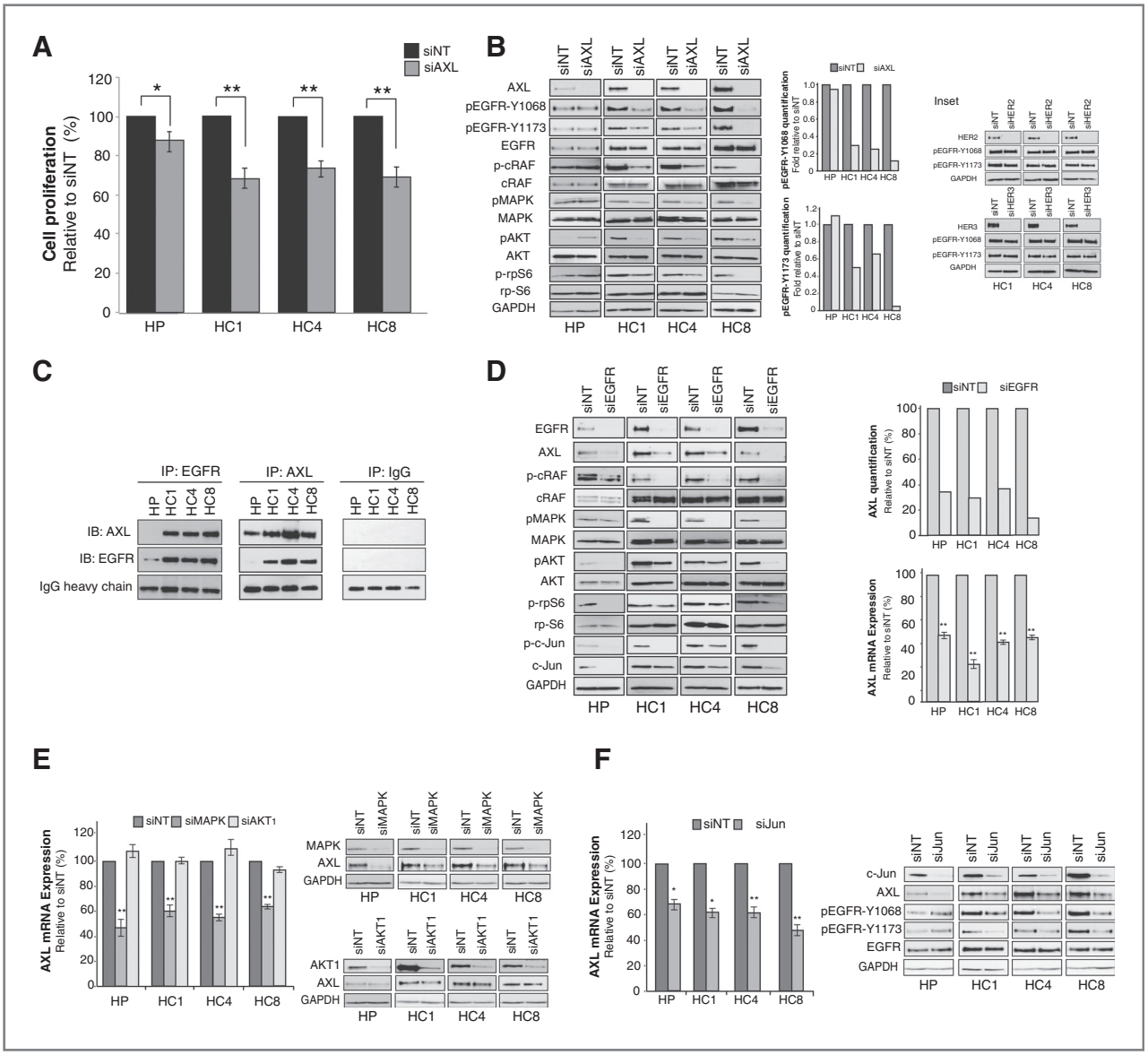

Figure 2. Cetuximab-resistant cells depend on AXL and its cooperation with EGFR. A, cells were transfected with siAXL or siNT for 72 hours before performing proliferation assays. Proliferation is plotted as percentage of growth relative to NT-transfected cells ($n = 6$ in three independent experiments). B, cells were incubated with siAXL or NT siRNA for 72 hours before harvesting whole-cell lysate and immunoblotting for the indicated proteins. GAPDH was used as a loading control. Phosphorylation of EGFR on tyrosine 1068 and 1173 were quantitated using ImageJ software. Inset, cells were transfected with siRNA against HER2, HER3, or NT siRNA for 72 hours before harvesting whole-cell lysate. GAPDH was used as a loading control. C, 500 μg of whole-cell lysate was subjected to immunoprecipitation (IP) analysis with cetuximab (IP:EGFR), anti-AXL (IP:AXL), or anti-IgG (IP:IgG) antibody followed by immunoblotting (IB) for either AXL or EGFR. IgG heavy chain staining from the IB:AXL blot was used as a loading control. D–F, whole-cell lysate and mRNA were harvested from Ctx^R clones 72 hours after transfection with EGFR siRNA (D), MAPK and AKT1 siRNAs (E), c-Jun siRNA (F), or NT siRNA. GAPDH was used as loading control for protein. In D, AXL protein expression was quantitated using ImageJ software. AXL mRNA expression was detected by qPCR and normalized to AXL expression in siNT-transfected cells ($n = 3$ in three independent experiments). 18S was used as an endogenous control. Data, mean ± SEM. *, $P < 0.05$; **, $P < 0.01$.

led to a loss of total AXL protein and mRNA expression in Ctx^R clones and parental HP cells, as well as diminished activation of c-Raf, p44/42 MAPK, AKT, rpS6, and c-Jun. To examine whether EGFR regulation of AXL was contingent on MAPK or AKT signaling directly, we alternatively knocked down p44/42 MAPK or AKT1 with siRNA (Fig. 2E). This experiment indicated that knockdown of p44/42 MAPK led to a loss of AXL mRNA and protein expression, whereas AKT1 did not regulate AXL expression. These results suggest that EGFR regulates AXL expression specifically through MAPK signaling.

Previous studies indicated that the AXL promoter contains binding motifs for AP-1 family transcription factors, in which phorbol myristate acetate (PMA) stimulation of leukemia cells led to increased AXL expression through MAPK signaling to

Published OnlineFirst August 18, 2014; DOI: 10.1158/0008-5472.CAN-14-0294

the transcription factor c-Jun (38). Because Ctx^R clones were found to overexpress c-Jun (Fig. 1A), we hypothesized that c-Jun may function downstream of MAPK to regulate AXL mRNA expression. To investigate this, c-Jun was knocked down with siRNA (Fig. 2F), leading to an approximate 35% to 55% decrease in AXL mRNA levels. Moreover, there was a loss of AXL protein expression, which appeared similar to the levels detected after EGFR or MAPK knockdown (Fig. 2D and E). Importantly, this led to a loss of EGFR activation in Ctx^R clones, but not in parental HP cells, indicating that AXL is required for EGFR activation and subsequent signaling in the resistant setting. Collectively, these data indicate that AXL expression and subsequent EGFR activation are regulated through the MAPK/c-Jun signaling pathway in Ctx^R clones.

Ctx^R cells are sensitive to anti-AXL monoclonal antibody and TKI therapies

Because Ctx^R clones were sensitive to AXL knockdown by siRNA, we hypothesized that these cells would also be sensitive to anti-AXL therapeutics. First, we tested the ability for the anti-AXL monoclonal antibody MAb173 to inhibit Ctx^R cell proliferation (Fig. 3A). Ctx^R clones were significantly growth inhibited upon treatment with increasing doses of MAb173, whereas Ctx^S HP cells were less sensitive. In addition, the growth-inhibitory effects of Ctx^R clones were statistically decreased from the effect on HP cells when treated with 50 and 100 μg/mL of MAb173 ($P < 0.01$). Consistent with previous studies (9), MAb173 induced AXL degradation (Fig. 3B). Interestingly, total EGFR protein levels were reduced upon MAb173 treatment of Ctx^R clones, in addition to loss of MAPK signaling. MAb173 did not affect the activation of EGFR or MAPK signaling in HP cells.

Next, the small-molecule TKI R428, which has greater than 100-fold selectivity for AXL as compared with EGFR or Tyro and 50-fold greater affinity than Mer (39), was tested for therapeutic benefit in Ctx^R clones (Fig. 4A). All Ctx^R clones demonstrated robust antiproliferative effects upon treatment with 0.8 and 1 μmol/L of R428, whereas HP cells were less

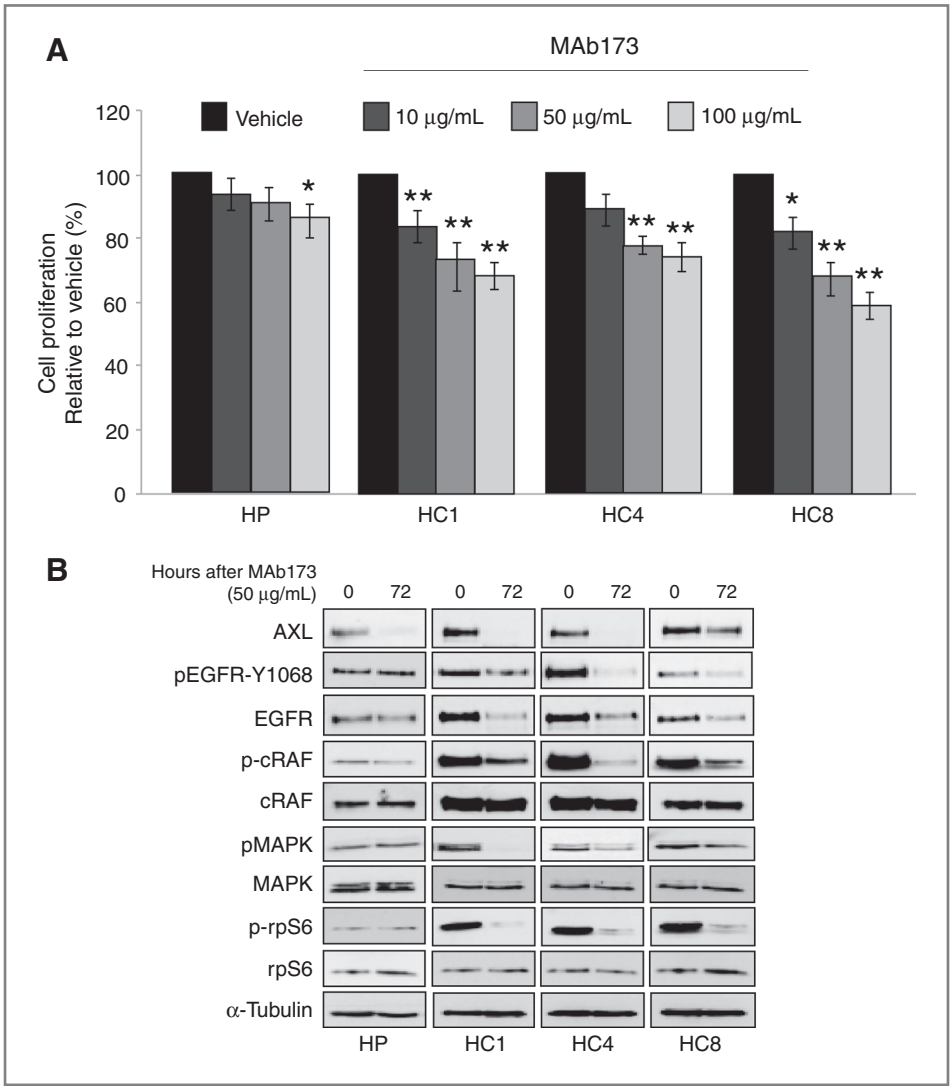

Figure 3. Cetuximab-resistant cells are sensitive to therapeutic degradation of AXL with the monoclonal antibody MAb173. A, cells were subjected to increasing doses of MAb173 (10, 50, and 100 μg/mL) for 72 hours before performing proliferation assays. Proliferation is plotted as a percentage of growth relative to vehicle treated cells ($n = 6$ in three independent experiments). Data, mean ± SEM. *, $P < 0.05$; **, $P < 0.01$. B, cells were subjected to 50 μg/mL of MAb173 for 72 hours before harvesting whole-cell lysate and immunoblotting for the indicated proteins. α-Tubulin was used as a loading control.

Published OnlineFirst August 18, 2014; DOI: 10.1158/0008-5472.CAN-14-0294

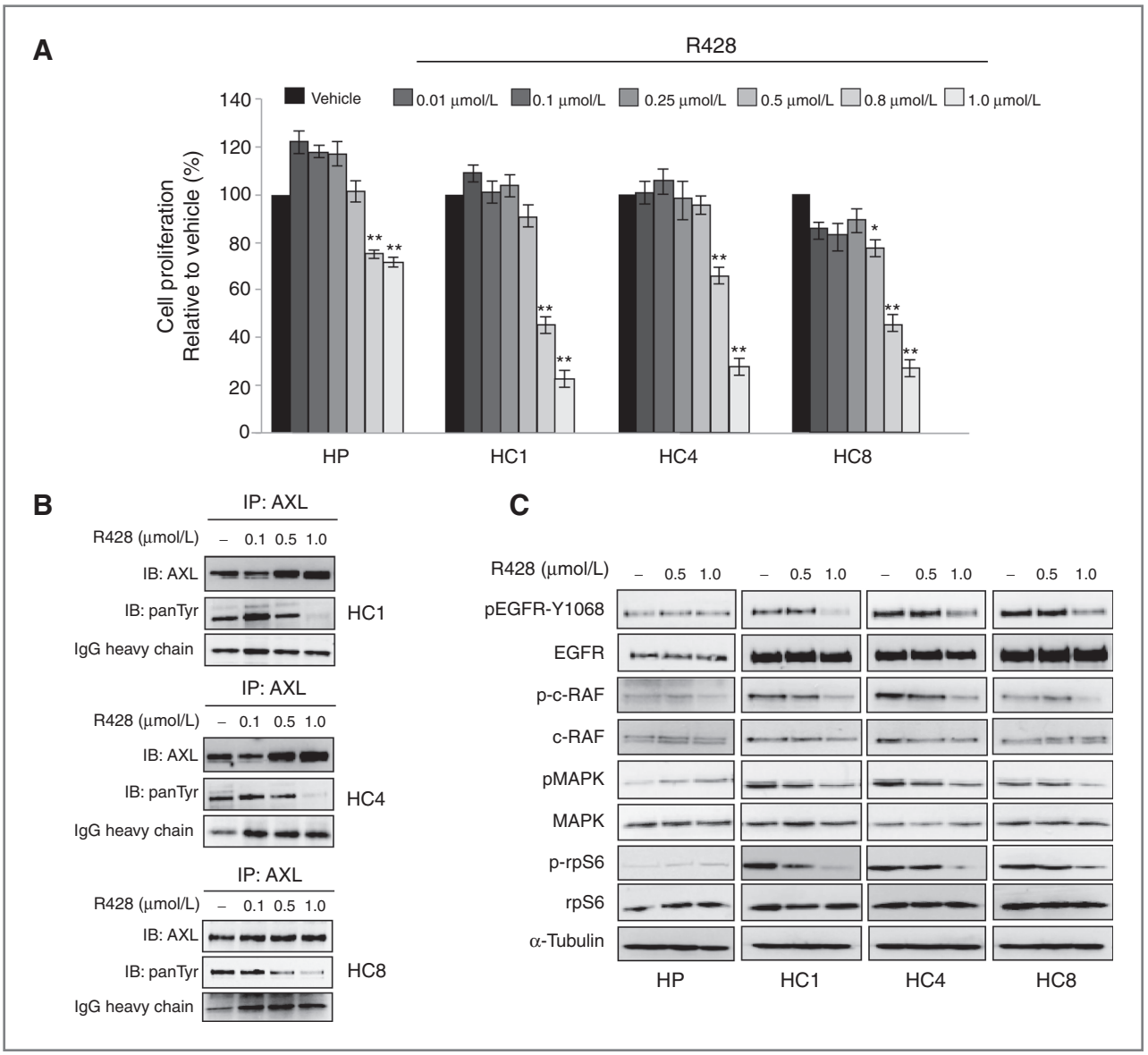

Figure 4. Cetuximab-resistant cells are sensitive to therapeutic blockade of AXL activity with the AXL TKI R428. A, cells were subjected to increasing doses of R428 (0.01–1 μmol/L) for 72 hours before performing proliferation assays. Proliferation is plotted as a percentage of growth relative to vehicle-treated cells ($n = 6$ in four independent experiments). Data, mean ± SEM. *, $P < 0.05$; **, $P < 0.01$. B, cells were treated with vehicle (–) or indicated doses of R428 for 24 hours. 500 μg of whole-cell lysate was subjected to immunoprecipitation analysis with an anti-AXL antibody followed by immunoblotting for either AXL or pan-tyrosine (panTyr). IgG heavy chain staining from the IB:AXL blot was used as a loading control. C, cells were treated with vehicle (–) or indicated doses of R428 for 24 hours before harvesting whole-cell lysate and immunoblotting for the indicated proteins. α-Tubulin was used as a loading control.

sensitive at these concentrations. In addition, the growth-inhibitory effects of Ctx^R clones were statistically decreased from the effect on HP cells when treated with 0.8 and 1 μmol/L of R428 ($P < 0.01$). Analysis of Ctx^R clones after treatment, via pan-tyrosine, demonstrated that AXL phosphorylation was inhibited with 1.0 μmol/L of R428, the same dose that elicited antiproliferative responses (Fig. 4B). In addition, R428 treatment led to a loss of EGFR phosphorylation on tyrosine 1068 and MAPK signaling, whereas these targets were relatively unaffected in HP cells (Fig. 4C). Interestingly, both MAb173 and R428 did not influence the apoptosis pathway in Ctx^R clones (data not shown), indicating that AXL more predominantly activates growth-promoting pathways in resistant cells.

AXL activation and overexpression confers cetuximab resistance *in vitro* and *in vivo* mouse xenograft models

To confirm the role of AXL in cetuximab resistance, AXL was stably overexpressed in the Ctx^S parental cell line HP (Fig. 5A). Immunoprecipitation analysis of HP-AXL stable cells indicated that AXL was phosphorylated on tyrosine 779, resulting in

Published OnlineFirst August 18, 2014; DOI: 10.1158/0008-5472.CAN-14-0294

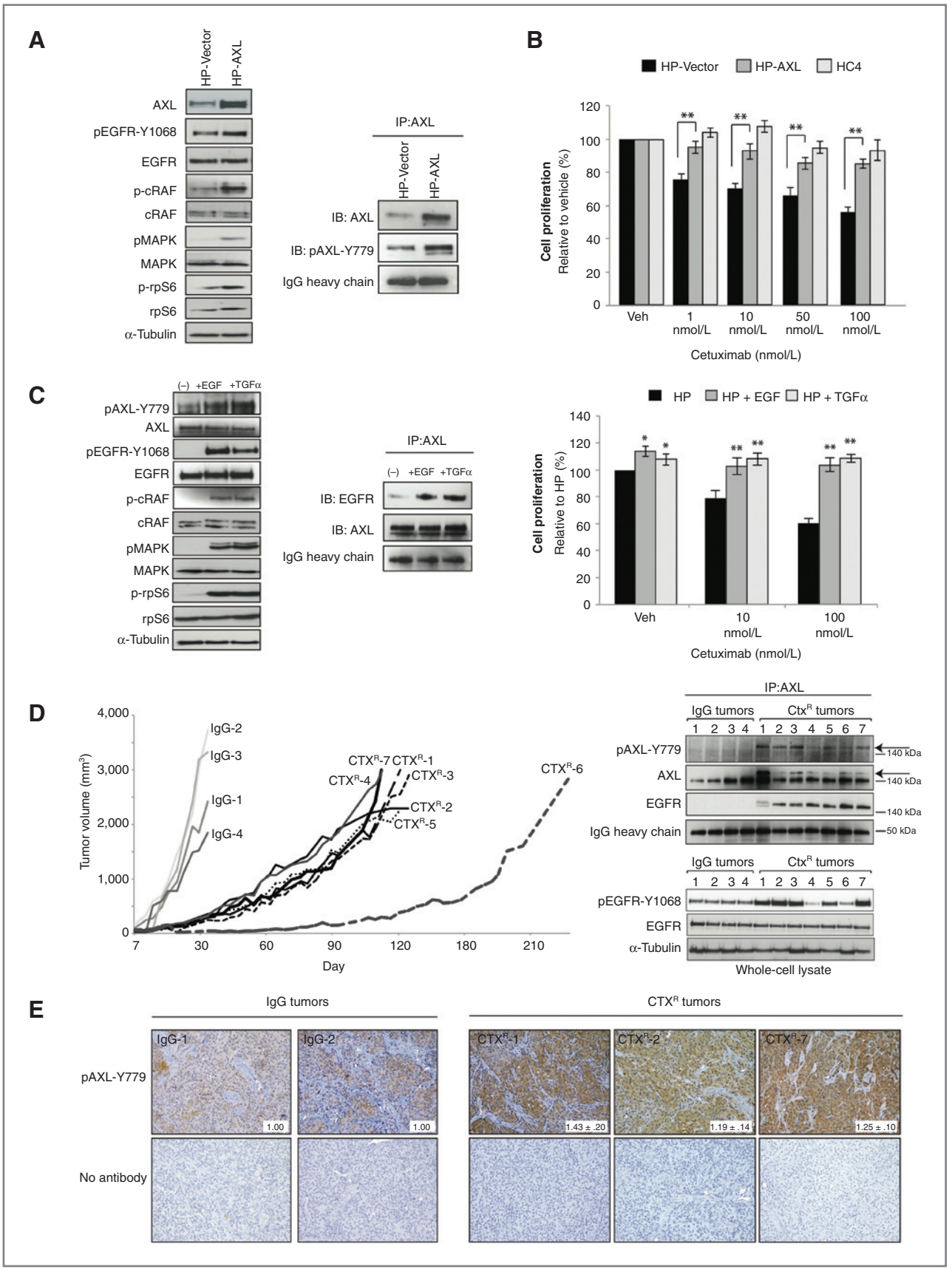

Published OnlineFirst August 18, 2014; DOI: 10.1158/0008-5472.CAN-14-0294

increased phosphorylation of EGFR and downstream MAPK signaling. Cetuximab dose–response proliferation assays demonstrated that HP-AXL cells were statistically more resistant to cetuximab as compared with HP-Vector cells ($P < 0.01$; Fig. 5B). HC4 cells served as a cetuximab-resistant control in these experiments. These data demonstrate that the stable overexpression of AXL can confer resistance to cetuximab in a Ctx^S cell line, supporting a putative role for AXL in the development of cetuximab resistance.

We previously reported that Ctx^R clones overexpressed EGFR ligands (36); however, whether EGFR ligands influenced cetuximab resistance through regulating AXL activity and/or association with the EGFR was not investigated. Therefore, HP cells were stimulated with two EGFR ligands, EGF or TGFα, and subsequently measured for AXL activation, association with the EGFR, and cetuximab response (Fig. 5C). Analysis of HP cells after ligand stimulation indicated that both ligands led to increased AXL activation and association with the EGFR (detected by immunoprecipitation analysis). In addition, incubation with either ligand resulted in increased resistance to cetuximab. Interestingly, the ligand for AXL, Gas6, was not overexpressed in Ctx^R clones and did not drive resistance in HP cells (data not shown). Collectively, these data suggest that EGFR ligands may influence cetuximab resistance through stimulating AXL activation and association with the EGFR.

To further analyze the role of AXL in cetuximab resistance, we developed *de novo* tumors with acquired resistance to cetuximab *in vivo* (31, 32). To develop *de novo*–acquired resistance, the Ctx^S cell line NCI-H226 was inoculated unilaterally into the dorsal flank of 11 athymic nude mice (Fig. 5D). Once tumors reached approximately 100 mm^3, 4 mice were treated with IgG control antibody (1 mg/mouse) and 7 mice were treated with cetuximab (1 mg/mouse) by intraperitoneal injection twice weekly. Tumors treated with IgG grew rapidly (tumors denoted as IgG-1 to IgG-4 in Fig. 5D), whereas all cetuximab-treated tumors displayed initial growth control. Acquired resistance was observed after approximately 30 days of cetuximab exposure in 6 of the cetuximab-treated mice (tumors denoted as Ctx^R-1 to Ctx^R-5, and Ctx^R-7), at which point there was marked tumor growth in the presence of continued cetuximab therapy (Fig. 5D). One mouse was continued on cetuximab for 90 days until a significant increase in tumor growth was observed (Ctx^R-6). Once tumors reached 2,000 mm^3, they were harvested and processed for immunoblot analysis (Fig. 5D) and IHC (Fig. 5E). To detect the levels of total and activated AXL (Y779), immunoprecipitation analysis was performed from tumor lysates. Strikingly, a double banding pattern for total AXL was observed in all Ctx^R tumors, whereas a single AXL band was observed in the IgG-treated tumors. The upper band corresponds to a shift in AXL molecular weight due to the presence of phosphorylated AXL, which was detected by the phospho AXL-Y779 antibody (Fig. 5D, arrows). In addition, AXL was associated with EGFR only in the Ctx^R tumors by immunoprecipitation (Fig. 5D). Analysis of whole-cell lysate indicated that EGFR was also highly activated (indicated by tyrosine 1068 phosphorylation) in the Ctx^R tumors that expressed the highest levels of pAXL-Y779. IHC analysis of IgG versus Ctx^R tumors revealed that Ctx^R tumors had statistically significant increases in pAXL-Y779 staining (Fig. 5E). Collectively, these data demonstrate that AXL overexpression and/or activation plays a role in acquired resistance to cetuximab *in vitro* and *in vivo*.

To expand these findings to a more clinically relevant model system, we determined whether there was a correlation between cetuximab response and AXL expression in PDXs established directly from surgically resected HNSCCs. Six PDXs were established from patients who had not received prior cetuximab therapy (see Supplementary Table S1 for clinical characteristics of patients before surgery). For each PDX, dual flank tumors were established in 16 athymic nude mice. When tumors reached approximately 200 mm^3, the mice were stratified into two treatment groups: control (vehicle-treated) and cetuximab ($n = 8$ mice/16 tumors per group). After completing the treatment regimen, tumor growth was monitored to evaluate response to therapy. Overall, there were three cetuximab-sensitive PDXs (UW-SCC36, UW-SCC22, and UW-SCC52) and three cetuximab-resistant PDXs (UW-SCC1, UW-SCC17, and UW-SCC25; Fig. 6).

PDXs harvested from early-passaged tumors before treatment were evaluated for AXL expression and activation by IHC analysis (Fig. 6). The cetuximab-sensitive PDXs had low levels of AXL and pAXL-Y779 staining, with UW-SCC36 having nearly absent expression of both markers. In comparison, the three cetuximab-resistant PDXs expressed 1.8- to 2.5-fold increases in pAXL-Y779 expression, and 2.5- to 4.3-fold increases in total AXL expression as compared with the staining intensity

Figure 5. AXL overexpression and activity results in cetuximab resistance in Ctx^S cells *in vitro* and in *de novo* models of Ctx^R *in vivo*. A, HP cells were made to stably express either pcDNA6.0-AXL (HP-AXL) or pcDNA6.0-Vector (HP-Vector). Whole-cell lysate was harvested and subjected to immunoblot analysis. α-Tubulin was used as a loading control. 500 μg of protein was subjected to immunoprecipitation with an anti-AXL antibody for analysis of pAXL-Y779. IgG heavy chain staining from the IB:AXL blot was used as a loading control. B, HP-AXL, HP-Vector, or HC4 cells were treated with increasing doses of cetuximab (1–100 nmol/L) for 72 hours before performing proliferation assays. Proliferation is plotted as a percentage of growth relative to vehicle treated cells ($n = 6$ for four independent experiments). Data, mean ± SEM. **, $P < 0.01$. C, HP cells were stimulated with 50 ng/mL of EGF or TGFα for 45 minutes before harvesting whole-cell lysate. Of note, 500 μg of protein was subjected to immunoprecipitation with an anti-AXL antibody for analysis of EGFR association. Proliferation assays were performed 72 hours after treatment with increasing doses of cetuximab and either 50 ng/mL EGF or TGFα. Proliferation is plotted as a percentage of growth relative to vehicle-treated HP cells ($n = 8$ for three independent experiments). Data, mean ± SEM. *, $P < 0.05$; **, $P < 0.01$. D and E, established Ctx^S NCI-H226 xenografts were treated with cetuximab (1 mg/mouse) or IgG twice weekly. IgG-treated tumors grew uninhibited (IgG-1–IgG-4), whereas acquired resistance to cetuximab was observed after day 30 in 6 of 7 treated mice (Ctx^R-1 to Ctx^R-5, and Ctx^R-7). Ctx^R-6 acquired resistance after 90 days of treatment. D, 500 μg of tumor cell lysate was subjected to immunoprecipitation with an anti-AXL antibody followed by immunoblotting for pAXL-Y779, AXL, or EGFR. IgG heavy chain staining from the IB:AXL blot was used as a loading control. pEGFR-Y1068 status was defined by Western blot analysis. α-Tubulin was used as a loading control. E, IHC analysis of pAXL-Y779 in tumor samples (20×). Quantitation of IHC was performed via ImageJ software (average of 5 independent fields of view per tumor); values were normalized to the average staining in IgG tumor sections.

Published OnlineFirst August 18, 2014; DOI: 10.1158/0008-5472.CAN-14-0294

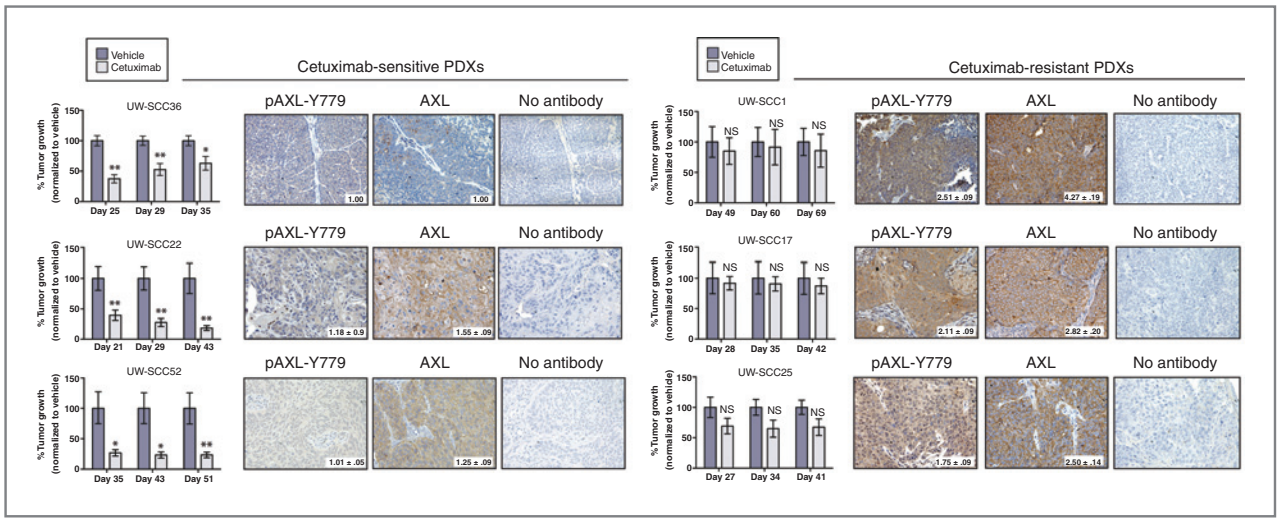

Figure 6. AXL is overexpressed and activated in cetuximab-resistant HNSCC PDXs. PDXs were evaluated for cetuximab response as described in Supplementary Materials and Methods. Tumor growth was plotted as a percentage of averaged vehicle treated tumor volumes at the last three time points of the study; *, $P < 0.05$; **, $P < 0.01$. Representative images of IHC analysis of AXL and pAXL-Y779 staining in early-passaged PDXs are shown (20×). Quantitation of IHC was performed via ImageJ software (average of 2–5 independent tumors were stained and imaged); values were normalized to the average staining of UW-SCC36. NS, not significant.

detected in UW-SCC36 tumors. Collectively, these data demonstrate that AXL is overexpressed and activated in PDXs that are intrinsically resistant to cetuximab therapy.

AXL plays a role in acquired resistance to cetuximab in HNSCC

To further investigate whether AXL plays a more global role in acquired resistance to cetuximab, we developed a model of acquired resistance to cetuximab using the Ctx^S parental cell line UM-SCC1 (30). This resulted in a parental SCC1 cell line (SP) and three cetuximab-resistant clones (SP7, SP8, and SP11). SP cell growth was inhibited upon treatment with increasing doses of cetuximab, while the three HNSCC Ctx^R clones remained resistant (Fig. 7A). Analysis of HNSCC Ctx^R clones indicated that all clones had increased steady-state expression of AXL as compared with SP (Fig. 7B). In addition, each clone demonstrated increased activation of c-Raf, p44/42 MAPK, AKT, rpS6, and c-Jun (Fig. 7B). To determine whether AXL influenced HNSCC Ctx^R cell proliferation, cells were transfected with siAXL or NT siRNA and proliferation assays were performed. Loss of AXL expression resulted in a significant inhibition in cellular proliferation (20%–25%) in HNSCC Ctx^R clones, while parental SP cells were nonresponsive (Fig. 7C). The growth-inhibitory effects of siAXL in HNSCC Ctx^R clones were statistically decreased compared with the effect on SP cells ($P < 0.01$). Furthermore, all HNSCC Ctx^R clones expressed diminished activation of EGFR (by tyrosine 1068 phosphorylation) as well as MAPK and AKT signaling pathways upon AXL knockdown, whereas the activation of these molecules was relatively unchanged or slightly increased in SP cells. Collectively, these data suggest that AXL plays a role in acquired resistance to cetuximab in HNSCC.

Discussion

Cetuximab is a commonly used anti-EGFR monoclonal antibody that has demonstrated efficacy in treating in HNSCC, mCRC, and NSCLC (19–26). Although cetuximab treatment has yielded clinical benefit, both intrinsic and acquired resistance are common outcomes. Recently, a novel mutation was identified in the EGFR (S492R) that mediates resistance to cetuximab (40); however, resistance also occurs in the WT setting. Multiple mechanisms of cetuximab resistance exist, including upregulation of EGFR ligands (41), nuclear translocation of EGFR (36), oncogenic shift to vascular endothelial growth factor receptor-1 (VEGFR-1; ref. 42), and constitutive activation of downstream signaling molecules such as KRAS (43) and c-Src (44). This study is the first to describe a role for AXL in mediating cetuximab resistance in the setting of wild type (WT) EGFR, and thus provides rationale for the development and use of anti-AXL therapeutics for treatment of Ctx^R tumors.

Cetuximab resistance is challenging to study due to the lack of access to patient tissue upon relapse. To model Ctx^R mechanisms that may occur in humans, several models of acquired resistance were established via prolonged exposure of Ctx^S cells to cetuximab (30–32). These models indicated that Ctx^R clones and tumors had increased expression and dependency on the EGFR (30–32). In this study, AXL was found to activate EGFR in Ctx^R clones, whereas HER2 and HER3 receptors did not, suggesting that AXL is a key mediator of EGFR activity in the resistant setting. Furthermore, EGFR and AXL were associated in Ctx^R clones and tumors (Figs. 2C and 5D), a finding previously reported in triple-negative breast cancers (TNBC; ref. 14), tumors that are intrinsically resistant to cetuximab. Interestingly, EGF mediated AXL-induced signaling pathways in TNBC, whereas Gas6 did not (14), similar to our findings in Fig. 5C. Another novel finding was that EGFR signaling led to increased AXL mRNA expression in Ctx^R

Published OnlineFirst August 18, 2014; DOI: 10.1158/0008-5472.CAN-14-0294

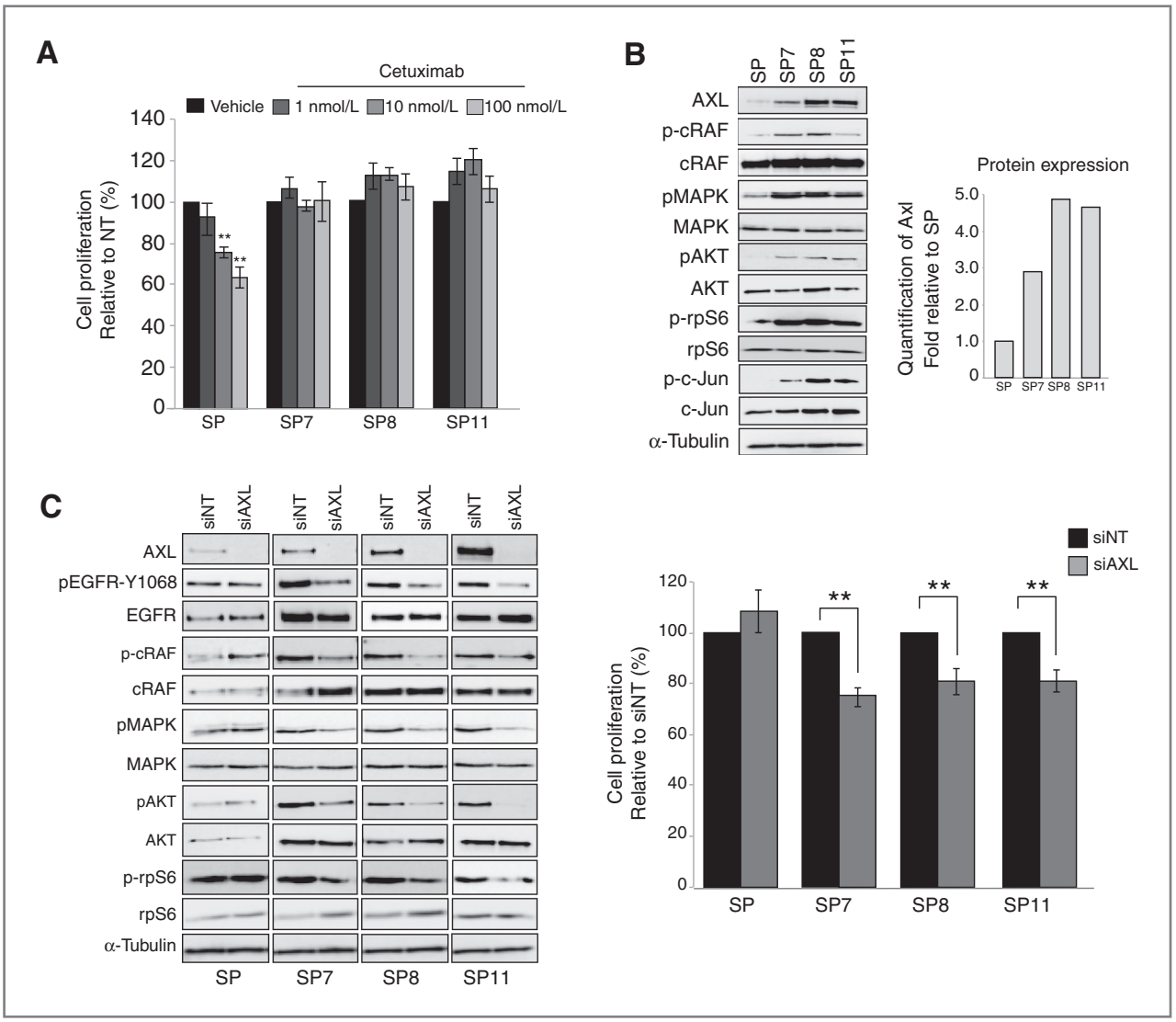

Figure 7. AXL mediates acquired resistance to cetuximab in HNSCC. A, Ctx^R cell clones (SP7, SP8, and SP11) and the Ctx^S parental cell line (SP) were treated with increasing doses of cetuximab (1, 10, and 100 nmol/L) for 72 hours before performing proliferation assays. Proliferation is plotted as a percentage of growth relative to vehicle-treated cells ($n = 5$ for three independent experiments). B, whole-cell lysate was harvested from cells followed by immunoblotting for the indicated proteins. α-Tubulin was used as a loading control. Total AXL protein expression was quantitated using ImageJ software. C, cells were incubated with siAXL or nontargeting (NT) siRNA for 72 hours before performing proliferation assays or isolation of whole-cell lysate and immunoblotting for indicated proteins. α-Tubulin was used as a loading control. Proliferation is plotted as a percentage of growth relative to NT-transfected cells ($n = 3$ for three independent experiments). Data, mean ± SEM. **, $P < 0.01$.

clones. The regulation of AXL mRNA was contingent on MAPK and c-Jun because knockdown of either decreased AXL expression (Fig. 2E and F).

These data support a positive-feedback loop that occurs in EGFR-dependent Ctx^R cells (Fig. 8). In this model, resistance is characterized by increased EGFR ligand production, dimerization, and transactivation of AXL and EGFR. This interaction results in hyperactivated MAPK/c-Jun signaling, upregulation of AXL mRNA expression, and maintenance of constitutive EGFR activation and cetuximab resistance. The *de novo* Ctx^R cell line xenografts support this model, as Ctx^R tumors expressed increased total and activated AXL (especially as compared with IgG-1 and IgG-2). Although c-Jun was capable of regulating AXL mRNA expression in Ctx^S parental cells, this regulation did not reduce EGFR activity (Fig. 2F), suggesting that EGFR and AXL are not coupled in Ctx^S cells.

Because of limited availability of patient tissue after cetuximab failure, the expression status of AXL and pAXL-Y779 was evaluated in intrinsically resistant HNSCC PDXs. PDXs are clinically relevant cancer models because they accurately maintain many aspects of the parental tumor, including its histology, gene expression profile, copy number variance, and metastatic patterns (45, 46). In this study, total and activated AXL were highly overexpressed in HNSCC PDXs that were resistant to cetuximab (Fig. 6). The strong correlation between AXL and cetuximab resistance observed in the PDXs supports

Published OnlineFirst August 18, 2014; DOI: 10.1158/0008-5472.CAN-14-0294

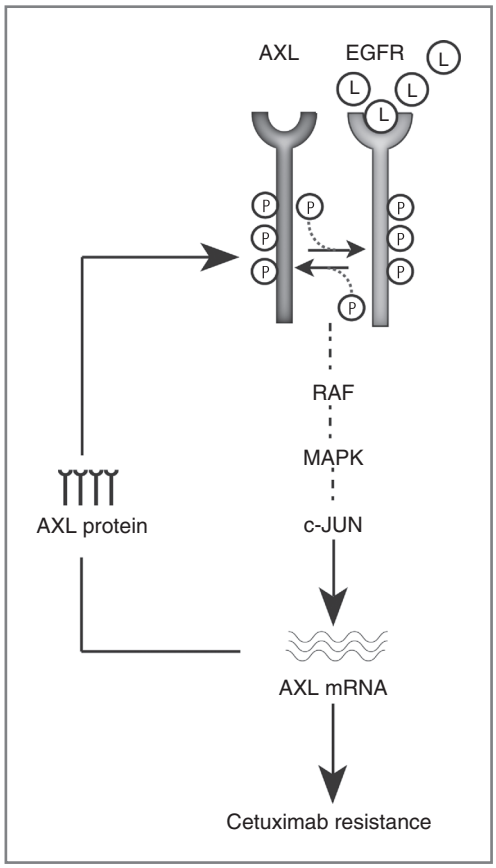

Figure 8. Model for AXL and EGFR cooperation in cetuximab resistance. Cetuximab resistance is characterized by increased AXL mRNA and protein expression, EGFR activation, and MAPK pathway signaling. In Ctx^R cells, increased EGFR ligand (L) production leads to AXL and EGFR association and transactivation. This results in MAPK and c-Jun signaling and subsequent increases in AXL transcription. Increases in AXL mRNA result in elevated AXL protein levels and maintenance of EGFR activation and signaling. This positive feedback loop results in the constitutive activation of both AXL and EGFR in Ctx^R cells and thereby mediates cetuximab resistance.

the mechanistic work performed in this study and suggests that AXL may mediate both intrinsic and acquired resistance to cetuximab.

To date, AXL has been identified to play a role in resistance to EGFR TKIs in NSCLC (16), HNSCC (13), and TNBC (14). In NSCLC, AXL was overexpressed and activated in EGFR-mutant erlotinib-resistant cells, where AXL inhibition resensitized tumor cells to erlotinib (13, 16). In this study, AXL inhibition was sufficient to inhibit the growth of Ctx^R clones, but did not resensitize Ctx^R clones to cetuximab (data not shown). This likely occurred because AXL inhibition robustly decreased EGFR activation; thus, adding cetuximab provided no further benefit. Although AXL inhibition led to robust antiproliferative effects in Ctx^R clones, cell growth was not completely arrested, suggesting that other RTKs may influence resistance. Previous work from our laboratory and others suggests that signaling emanating from HER2:HER3 heterodimers play a role in resistance to anti-EGFR agents (30, 47). Thus, targeting AXL and either HER2 or HER3 may result in even more robust antiproliferative responses because EGFR signaling could be abrogated through AXL inhibition and HER2:HER3 signaling could be blocked with anti-HER2 or HER3 agents. Ultimately, this approach may lead to a complete loss of HER family signaling capabilities and serve as a powerful strategy for the treatment of Ctx^R cancers.

With increasing evidence supporting the role of AXL in resistance to anti-EGFR agents, the development of anti-AXL therapeutics is essential. In this study, two novel anti-AXL therapeutics were tested: MAb173, an anti-AXL–neutralizing monoclonal antibody, and R428, a selective small-molecule AXL TKI. In previous studies, researchers demonstrated that AXL was hyperactivated in Kaposi sarcoma and that MAb173 induced AXL endocytosis and degradation (9). In addition to AXL, total EGFR expression was decreased upon MAb173 treatment of Ctx^R cells (Fig. 3B), supporting the existence of AXL and EGFR heterodimers and the utility of this antibody in the setting of cetuximab resistance. Furthermore, EGFR was not degraded in MAb173-treated HP cells, which lack AXL and EGFR association (Fig. 2C). The anti-AXL TKI R428 has also shown antitumorigenic effects in multiple cancer models, including breast cancer (14, 39) and HNSCC (13). The differences in growth inhibition observed between MAb173 and R428 may result from off-target effects of R428, leading to more robust antiproliferative responses. R428 has now entered phase I clinical trials, whereas MAb173 is still undergoing preclinical testing.

Overall, AXL plays a key role in tumor growth, metastasis, angiogenesis, and resistance to anti-EGFR agents (12–17). In addition, AXL inhibition has been shown to enhance the efficacy of standard chemotherapy regimens (10, 15, 18). With AXL at the forefront, Tyro and Mer receptors also influence parameters of tumor biology (1, 4). In fact, both Tyro and Mer receptors were differentially overexpressed in the current Ctx^R models (unpublished data), promoting further research on the global role of TAM receptors in cetuximab resistance. Collectively, the studies herein have strong potential for translation into future clinical trials and therapies for patients with cetuximab-resistant tumors.

Disclosure of Potential Conflicts of Interest

P.S. Gill is CSO of Vasgene Therapeutics and has ownership interest (including patents) in the same. No potential conflicts of interest were disclosed by the other authors.

Authors' Contributions

Conception and design: T.M. Brand, M. Toulany, P.S. Gill, R. Salgia, D.L. Wheeler

Development of methodology: T.M. Brand, M. Iida, A.P. Stein, P.S. Gill, R. Salgia, D.L. Wheeler

Acquisition of data (provided animals, acquired and managed patients, provided facilities, etc.): T.M. Brand, A.P. Stein, K.L. Corrigan, C. Braverman, N. Luthar, R. Salgia

Analysis and interpretation of data (e.g., statistical analysis, biostatistics, computational analysis): T.M. Brand, M. Iida, A.P. Stein, M. Toulany, K.L. Corrigan, R. Salgia, R.J. Kimple, D.L. Wheeler

Writing, review, and/or revision of the manuscript: T.M. Brand, M. Iida, A.P. Stein, K.L. Corrigan, M. Toulany, P.S. Gill, R. Salgia, R.J. Kimple, D.L. Wheeler

Administrative, technical, or material support (i.e., reporting or organizing data, constructing databases): T.M. Brand, M. Iida, D.L. Wheeler

Study supervision: T.M. Brand, R. Salgia, R.J. Kimple, D.L. Wheeler

Published OnlineFirst August 18, 2014; DOI: 10.1158/0008-5472.CAN-14-0294

Grant Support

This study was supported by grant UL1TR000427 from the Clinical and Translational Science Award program (to D.L. Wheeler), through the NIH National Center for Advancing Translational Sciences, grant RSG-10-193-01-TBG from the American Cancer Society (to D.L. Wheeler), grant W81XWH-12-1-0467 from United States Army Medical Research and Materiel Command (to D.L. Wheeler), University of Wisconsin Carbone Cancer Center Cancer Center Support Grant P30 CA014520 (to D.L. Wheeler) and Mary Kay Foundation grant MSN152261 (to D.L. Wheeler).

The costs of publication of this article were defrayed in part by the payment of page charges. This article must therefore be hereby marked *advertisement* in accordance with 18 U.S.C. Section 1734 solely to indicate this fact.

Received February 5, 2014; revised June 11, 2014; accepted June 30, 2014; published OnlineFirst August 18, 2014.

References

1. Linger RM, Keating AK, Earp HS, Graham DK. TAM receptor tyrosine kinases: biologic functions, signaling, and potential therapeutic targeting in human cancer. Adv Cancer Res 2008;100:35–83.
2. Verma A, Warner SL, Vankayalapati H, Bearss DJ, Sharma S. Targeting AXL and Mer kinases in cancer. Mol Cancer Ther 2011;10:1763–73.
3. Li Y, Ye X, Tan C, Hongo JA, Zha J, Liu J, et al. AXL as a potential therapeutic target in cancer: role of AXL in tumor growth, metastasis and angiogenesis. Oncogene 2009;28:3442–55.
4. Linger RM, Keating AK, Earp HS, Graham DK. Taking aim at Mer and AXL receptor tyrosine kinases as novel therapeutic targets in solid tumors. Expert Opin Ther Targets 2010;14:1073–90.
5. Paccez JD, Vogelsang M, Parker MI, Zerbini LF. The receptor tyrosine kinase AXL in cancer: biological functions and therapeutic implications. Int J Cancer 2014;134:1024–33.
6. Zhang YX, Knyazev PG, Cheburkin YV, Sharma K, Knyazev YP, Orfi L, et al. AXL is a potential target for therapeutic intervention in breast cancer progression. Cancer Res 2008;68:1905–15.
7. Rankin EB, Fuh KC, Taylor TE, Krieg AJ, Musser M, Yuan J, et al. AXL is an essential factor and therapeutic target for metastatic ovarian cancer. Cancer Res 2010;70:7570–9.
8. Paccez JD, Vasques GJ, Correa RG, Vasconcellos JF, Duncan K, Gu X, et al. The receptor tyrosine kinase AXL is an essential regulator of prostate cancer proliferation and tumor growth and represents a new therapeutic target. Oncogene 2013;32:689–98.
9. Liu R, Gong M, Li X, Zhou Y, Gao W, Tulpule A, et al. Induction, regulation, and biologic function of AXL receptor tyrosine kinase in Kaposi sarcoma. Blood 2010;116:297–305.
10. Linger RM, Cohen RA, Cummings CT, Sather S, Migdall-Wilson J, Middleton DH, et al. Mer or AXL receptor tyrosine kinase inhibition promotes apoptosis, blocks growth and enhances chemosensitivity of human non–small cell lung cancer. Oncogene 2013;32:3420–31.
11. Han J, Tian R, Yong B, Luo C, Tan P, Shen J, et al. Gas6/AXL mediates tumor cell apoptosis, migration and invasion and predicts the clinical outcome of osteosarcoma patients. Biochem Biophys Res Commun 2013;435:493–500.
12. Byers LA, Diao L, Wang J, Saintigny P, Girard L, Peyton M, et al. An epithelial–mesenchymal transition gene signature predicts resistance to EGFR and PI3K inhibitors and identifies AXL as a therapeutic target for overcoming EGFR inhibitor resistance. Clin Cancer Res 2013;19:279–90.
13. Giles KM, Kalinowski FC, Candy PA, Epis MR, Zhang PM, Redfern AD, et al. AXL mediates acquired resistance of head and neck cancer cells to the epidermal growth factor receptor inhibitor erlotinib. Mol Cancer Ther 2013;12:2541–58.
14. Meyer AS, Miller MA, Gertler FB, Lauffenburger DA. The receptor AXL diversifies EGFR signaling and limits the response to EGFR-targeted inhibitors in triple-negative breast cancer cells. Sci Signal 2013;6:ra66.
15. Ye X, Li Y, Stawicki S, Couto S, Eastham-Anderson J, Kallop D, et al. An anti-AXL monoclonal antibody attenuates xenograft tumor growth and enhances the effect of multiple anticancer therapies. Oncogene 2010;29:5254–64.
16. Zhang Z, Lee JC, Lin L, Olivas V, Au V, LaFramboise T, et al. Activation of the AXL kinase causes resistance to EGFR-targeted therapy in lung cancer. Nat Genet 2012;44:852–60.
17. Rho JK, Choi YJ, Kim SY, Kim TW, Choi EK, Yoon SJ, et al. MET and AXL inhibitor NPS-1034 exerts efficacy against lung cancer cells resistant to EGFR kinase inhibitors because of MET or AXL activation. Cancer Res 2014;74:253–62.
18. Dunne PD, McArt DG, Blayney JK, Kalimutho M, Greer S, Wang T, et al. AXL is a key regulator of inherent and chemotherapy-induced invasion and predicts a poor clinical outcome in early-stage colon cancer. Clin Cancer Res 2014;20:164–75.
19. Baselga J. The EGFR as a target for anticancer therapy—focus on cetuximab. Eur J Cancer 2001;37(Suppl 4):S16–22.
20. Bonner JA, Harari PM, Giralt J, Azarnia N, Shin DM, Cohen RB, et al. Radiotherapy plus cetuximab for squamous-cell carcinoma of the head and neck. N Engl J Med 2006;354:567–78.
21. Govindan R. Cetuximab in advanced non–small cell lung cancer. Clin Cancer Res 2004;10:4241S–4S.
22. Pirker R, Pereira JR, Szczesna A, von Pawel J, Krzakowski M, Ramlau R, et al. Cetuximab plus chemotherapy in patients with advanced non–small-cell lung cancer (FLEX): an open-label randomised phase III trial. Lancet 2009;373:1525–31.
23. Thienelt CD, Bunn PA, Hanna N, Rosenberg A, Needle MN, Long ME, et al. Multicenter phase I/II study of cetuximab with paclitaxel and carboplatin in untreated patients with stage IV non–small-cell lung cancer. J Clin Oncol 2005;23:8786–93.
24. Van Cutsem E, Kohne CH, Hitre E, Zaluski J, Chang Chien CR, Makhson A, et al. Cetuximab and chemotherapy as initial treatment for metastatic colorectal cancer. N Engl J Med 2009;360:1408–17.
25. Vermorken JB, Mesia R, Rivera F, Remenar E, Kawecki A, Rottey S, et al. Platinum-based chemotherapy plus cetuximab in head and neck cancer. N Engl J Med 2008;359:1116–27.
26. Lynch TJ, Patel T, Dreisbach L, McCleod M, Heim WJ, Hermann RC, et al. Cetuximab and first-line taxane/carboplatin chemotherapy in advanced non–small-cell lung cancer: results of the randomized multicenter phase III trial BMS099. J Clin Oncol 2010;28:911–7.
27. Bardelli A, Siena S. Molecular mechanisms of resistance to cetuximab and panitumumab in colorectal cancer. J Clin Oncol 2010;28:1254–61.
28. Brand TM, Iida M, Wheeler DL. Molecular mechanisms of resistance to the EGFR monoclonal antibody cetuximab. Cancer Biol Ther 2011;11:777–92.
29. Diaz LA Jr, Williams RT, Wu J, Kinde I, Hecht JR, Berlin J, et al. The molecular evolution of acquired resistance to targeted EGFR blockade in colorectal cancers. Nature 2012;486:537–40.
30. Wheeler DL, Huang S, Kruser TJ, Nechrebecki MM, Armstrong EA, Benavente S, et al. Mechanisms of acquired resistance to cetuximab: role of HER (ErbB) family members. Oncogene 2008;27:3944–56.
31. Iida M, Brand TM, Starr MM, Li C, Huppert EJ, Luthar N, et al. Sym004, a novel EGFR antibody mixture, can overcome acquired resistance to cetuximab. Neoplasia 2013;15:1196–206.
32. Brand TM, Dunn EF, Iida M, Myers RA, Kostopoulos KT, Li C, et al. Erlotinib is a viable treatment for tumors with acquired resistance to cetuximab. Cancer Biol Ther 2011;12:436–46.
33. Iida M, Brand TM, Campbell DA, Li C, Wheeler DL. Yes and Lyn play a role in nuclear translocation of the epidermal growth factor receptor. Oncogene 2013;32:759–67.
34. Brand TM, Iida M, Luthar N, Wleklinski MJ, Starr MM, Wheeler DL. Mapping C-terminal transactivation domains of the nuclear HER family receptor tyrosine kinase HER3. PLoS ONE 2013;8:e71518.
35. Li C, Brand TM, Iida M, Huang S, Armstrong EA, van der Kogel A, et al. Human epidermal growth factor receptor 3 (HER3) blockade with U3-1287/AMG888 enhances the efficacy of radiation therapy in lung and head and neck carcinoma. Discov Med 2013;16:79–92.
36. Li C, Iida M, Dunn EF, Ghia AJ, Wheeler DL. Nuclear EGFR contributes to acquired resistance to cetuximab. Oncogene 2009;28:3801–13.

Published OnlineFirst August 18, 2014; DOI: 10.1158/0008-5472.CAN-14-0294

37. Yarden Y, Pines G. The ERBB network: at last, cancer therapy meets systems biology. Nat Rev Cancer 2012;12:553–63.
38. Mudduluru G, Leupold JH, Stroebel P, Allgayer H. PMA up-regulates the transcription of AXL by AP-1 transcription factor binding to TRE sequences via the MAPK cascade in leukaemia cells. Biol Cell 2010;103:21–33.
39. Holland SJ, Pan A, Franci C, Hu Y, Chang B, Li W, et al. R428, a selective small molecule inhibitor of AXL kinase, blocks tumor spread and prolongs survival in models of metastatic breast cancer. Cancer Res 2010;70:1544–54.
40. Montagut C, Dalmases A, Bellosillo B, Crespo M, Pairet S, Iglesias M, et al. Identification of a mutation in the extracellular domain of the Epidermal Growth Factor Receptor conferring cetuximab resistance in colorectal cancer. Nat Med 2012;18:221–3.
41. Hatakeyama H, Cheng HX, Wirth P, Counsell A, Marcrom SR, Wood CB, et al. Regulation of heparin-binding EGF-like growth factor by miR-212 and acquired cetuximab-resistance in head and neck squamous cell carcinoma. PLoS ONE 2010;5:e12702.
42. Bianco R, Rosa R, Damiano V, Daniele G, Gelardi T, Garofalo S, et al. Vascular endothelial growth factor receptor-1 contributes to resistance to anti-epidermal growth factor receptor drugs in human cancer cells. Clin Cancer Res 2008;14:5069–80.
43. Normanno N, Tejpar S, Morgillo F, De Luca A, Van Cutsem E, Ciardiello F. Implications for KRAS status and EGFR-targeted therapies in metastatic CRC. Nat Rev Clin Oncol 2009;6:519–27.
44. Wheeler DL, Iida M, Kruser TJ, Nechrebecki MM, Dunn EF, Armstrong EA, et al. Epidermal growth factor receptor cooperates with Src family kinases in acquired resistance to cetuximab. Cancer Biol Ther 2009;8:696–703.
45. Siolas D, Hannon GJ. Patient-derived tumor xenografts: transforming clinical samples into mouse models. Cancer Res 2013;73:5315–9.
46. Kimple RJ, Harari PM, Torres AD, Yang RZ, Soriano BJ, Yu M, et al. Development and characterization of HPV-positive and HPV-negative head and neck squamous cell carcinoma tumorgrafts. Clin Cancer Res 2013;19:855–64.
47. Zhang L, Castanaro C, Luan B, Yang K, Fan L, Fairhurst JL, et al. ERBB3/HER2 signaling promotes resistance to EGFR blockade in head and neck and colorectal cancer models. Mol Cancer Ther 2014;13:1345–55.

Lung Cancer 81 (2013) 138–141

Contents lists available at SciVerse ScienceDirect

Lung Cancer

journal homepage: www.elsevier.com/locate/lungcan

Early report

Nuclear EGFR protein expression predicts poor survival in early stage non-small cell lung cancer

Anne M. Traynor[a], Tracey L. Weigel[b], Kurt R. Oettel[c], David T. Yang[d], Chong Zhang[e], KyungMann Kim[e], Ravi Salgia[f], Mari Iida[g], Toni M. Brand[g], Tien Hoang[a], Toby C. Campbell[a], Hilary R. Hernan[a], Deric L. Wheeler[g,*]

[a] Department of Medicine and Carbone Cancer Center, University of Wisconsin School of Medicine and Public Health, Madison, WI, USA
[b] Department of Surgery and Carbone Cancer Center, University of Wisconsin School of Medicine and Public Health, Madison, WI, USA
[c] Gundersen Lutheran Center for Cancer & Blood Disorders, Gundersen Lutheran Medical Center, LaCrosse, WI, USA
[d] Department of Pathology and Laboratory Medicine and Carbone Cancer Center, University of Wisconsin School of Medicine and Public Health, Madison, WI, USA
[e] Department of Biostatistics and Medical Informatics and Carbone Cancer Center, University of Wisconsin School of Medicine and Public Health, Madison, WI, USA
[f] Department of Medicine and Cancer Research Center, Pritzker School of Medicine, University of Chicago, Chicago, IL, USA
[g] Department of Human Oncology and Carbone Cancer Center, University of Wisconsin School of Medicine and Public Health, Madison, WI, USA

ARTICLE INFO

Article history:
Received 8 January 2013
Received in revised form 15 February 2013
Accepted 28 March 2013

Keywords:
Non-small cell lung cancer
Nuclear
Epidermal growth factor receptor
Prognosis
Biomarker
Survival analysis

ABSTRACT

Introduction: Nuclear EGFR (nEGFR) has been identified in various human tumor tissues, including cancers of the breast, ovary, oropharynx, and esophagus, and has predicted poor patient outcomes. We sought to determine if protein expression of nEGFR is prognostic in early stage non-small cell lung cancer (NSCLC).
Methods: Resected stages I and II NSCLC specimens were evaluated for nEGFR protein expression using immunohistochemistry (IHC). Cases with at least one replicate core containing ≥5% of tumor cells demonstrating strong dot-like nucleolar EGFR expression were scored as nEGFR positive.
Results: Twenty-three (26.1% of the population) of 88 resected specimens stained positively for nEGFR. Nuclear EGFR protein expression was associated with higher disease stage (45.5% of stage II vs. 14.5% of stage I; $p = 0.023$), histology (41.7% in squamous cell carcinoma vs. 17.1% in adenocarcinoma; $p = 0.028$), shorter progression-free survival (PFS) (median PFS 8.7 months [95% CI 5.1–10.7 mo] for nEGFR positive vs. 14.5 months [95% CI 9.5–17.4 mo] for nEGFR negative; hazard ratio (HR) of 1.89 [95% CI 1.15–3.10]; $p = 0.011$), and shorter overall survival (OS) (median OS 14.1 months [95% CI 10.3–22.7 mo] for nEGFR positive vs. 23.4 months [95% CI 20.1–29.4 mo] for nEGFR negative; HR of 1.83 [95% CI 1.12–2.99]; $p = 0.014$).
Conclusions: Expression of nEGFR protein was associated with higher stage and squamous cell histology, and predicted shorter PFS and OS, in this patient cohort. Nuclear EGFR serves as a useful independent prognostic variable and as a potential therapeutic target in NSCLC.

1. Introduction

Non-small cell lung cancer is a heterogeneous malignancy, comprised of multiple histologic subtypes. Predicting the course of disease based upon staging is suboptimal. The identification of biological markers of aggressive clinical behavior is needed in an effort to individualize treatment and develop novel therapeutic targets.

Protein expression of membrane bound EGFR was neither prognostic nor predictive of efficacy with the use of erlotinib, gefitinib, or cetuximab in NSCLC [1,2]. However, emerging preclinical and clinical evidence supports the role of nEGFR in enhancing tumor cell growth, survival, and resistance to systemic and radiation therapies [3–10]. Herein, we report identification of nEGFR protein expression as an independent prognostic variable in early stage NSCLC.

2. Materials and methods

2.1. Patients and specimen collection

For this retrospective analysis of patients who underwent curative intent resections, de-identified tumor specimens from 88 deceased patients with stages I and II NSCLC were collected from the University of Wisconsin Hospitals and Clinics (UWHC; Madison, WI) and from the Gundersen Lutheran Medical Center (GLMC;

* Corresponding author at: Department of Human Oncology and Carbone Cancer Center, University of Wisconsin School of Medicine and Public Health, 3159 WIMR, 1111 Highland Avenue, Madison, WI 53705, USA. Tel.: +1 608 262 7837; fax: +1 608 263-9947.
E-mail address: dlwheeler@wisc.edu (D.L. Wheeler).

0169-5002/$ – see front matter © 2013 Elsevier Ireland Ltd. All rights reserved.
http://dx.doi.org/10.1016/j.lungcan.2013.03.020

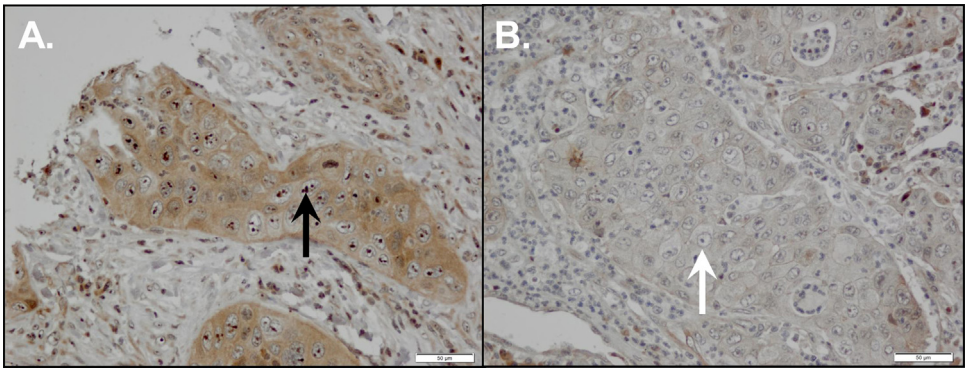

Fig. 1. Nuclear EGFR (nEGFR) is detected in early stage NSCLC specimens. We analyzed 88 primary NSCLC tumors for nEGFR protein expression using immunohistochemistry. (A) Representative case demonstrating nEGFR expression. All positive cases had a similar distinctive pattern of strong nucleolar staining (black arrow). (B) Representative case demonstrating a lack of nEGFR protein expression. Despite the presence of prominent nucleoli, no nEGFR protein is detected (white arrow).

LaCrosse, WI). Patients did not receive either pre- or post-operative anti-cancer therapy. We also collected: age, sex, histology, smoking history, pathologic stage (AJCC Staging 6th edition), type of resection, date of relapse, and date of death. Approval for this research was obtained from the IRBs of UW-Madison and the GLMC.

2.2. Tissue microarray construction and protein expression analyses

Tumor tissue quality and pathology were confirmed by the study pathologist (DTY). Tissues were harvested within 30 min of resection, fixed with 10% neutral buffered formalin and embedded in paraffin. Areas of tumor and adjacent benign tissue were marked on a representative H & E stained section. Duplicate 0.6 mm cores from the corresponding paraffin block were punched out and assembled with a Manual Tissue Arrayer (Beecher Instruments, Sun Prairie, WI).

For nEGFR protein expression analyses, tissue sections were deparaffinized and antigen retrieval was performed in citrate buffer (pH 6.0) with 0.05% Tween-20. Samples were incubated with EGFR polyclonal antibody (sc-03, Santa Cruz Biotechnology, Inc., Santa Cruz, CA, USA) overnight at 4C. Samples were washed and incubated in secondary antibody for 1 hour followed by incubation with Vectastain ABC Elite kit (Vector Laboratories, Burlingame, CA, USA). 3,3-Diaminobenzidine staining was used as the color-developing reagent. Slides were counterstained with Mayer hematoxylin, dehydrated through a graded series of ethanol washes to xylene, and coverslipped with Permount (Fisher, Springfield, NJ).

We initially hypothesized that assessment of nEGFR protein would require the quantitative and subcellular localization capacity of automated quantitative analysis (AQUA). When we observed that the nuclear staining of EGFR protein revealed a distinct, robust nucleolar pattern (Fig. 1A) that clearly contrasted with negative cases (Fig. 1B) using routine IHC staining, we switched to the IHC methodology due to its easier translation to clinical practice. The nEGFR staining pattern was scored by the study pathologist at 5% increments by visual estimation at 20× magnification. Accordingly, cases with at least one replicate core containing at least 5% of tumor cells demonstrating strong dot-like nucleolar EGFR IHC protein expression were scored as nEGFR positive.

2.3. Statistical analyses

Our endpoints were protein expression of nEGFR and PFS and OS. Originally this study had an approximate power of 0.902, 0.747 and 0.477 to detect a hazard ratio of 2, 1.75 and 1.5, respectively, using a two-sided log-rank test at a significance level 0.05, given the sample size of 88 when the AQUA score was dichotomized using its median. The prognostic impact of nEGFR was assessed using the log-rank test and Cox proportional hazards regression models for PFS and OS. Kaplan–Meier method was used to summarize PFS and OS for patients per nEGFR IHC. Association between nEGFR protein expression and sex, histology, smoking history and pathologic stage was assessed using Fisher's exact test.

3. Results

3.1. Patient characteristics

Table 1 summarizes the characteristics of the 88 patient samples studied. None of the patients received either pre- or post-operative anti-cancer therapy. The median PFS and OS for our population

Table 1
Patient characteristics.

	N
Number of patients	88
Median age (range)	73 (43–96 yrs)
Sex	
Male	55 (62.5%)
Female	33 (37.5%)
Histology	
Adenocarcinoma	41 (46.6%)
Squamous cell	36 (40.9%)
Bronchioloalveolar	4 (4.5%)
Large cell	3 (3.4%)
Non-small cell, NOS	2 (2.3%)
Adenosquamous carcinoma	2 (2.3%)
Smoking history	
Current or former	84 (95.5%)
Type of surgery	
Lobectomy	80 (90.9%)
Pneumonectomy	7 (8%)
Bilobectomy	1 (1.1%)
Disease stage	
IA	23 (26.1%)
IB	32 (36.4)
IIA	9 (10.2%)
IIB	24 (27.3%)
T stage	
T1	31 (35.2%)
T2	52 (59.1%)
T3	5 (5.7%)
N stage	
N0	60 (68.2%)
N1	28 (31.8%)
Nuclear EGFR protein expression	
Positive	23 (26.1%)

Table 2
Distribution of nuclear EGFR protein staining per IHC across all tumor specimens.

Patient number	Percent of cells with positive nuclear EGFR protein staining per IHC			
	Cores (all specimens run in duplicate when tissue available)			
	Tumor 1	Tumor 2	Adjacent normal lung 1	Adjacent normal lung 2
1	50	NC	0	0
2	80	60	0	0
3	80	20	0	0
4	50	75	0	0
5	95	50	0	0
6	25	25	0	0
7	0	5	0	0
8	60	20	NC	NC
9	10	5	0	0
10	60	50	NC	NC
11	20	30	0	0
12	30	80	0	0
13	5	10	0	0
14	80	90	0	0
15	15	5	0	0
16	30	100	0	0
17	20	NC	0	0
18	60	70	0	0
19	40	70	0	0
20	90	90	0	0
21	30	NC	NC	NC
22	40	60	0	0
23	30	5	0	0
Specimens from remaining 65 patients	0	0	0	0

NC, no core available.

were 11.3 months (95% CI 9.1–16.2 mo) and 22.0 months (95% CI 15.9–24.7 mo), respectively, shorter than expected. Fifty-nine patients experienced disease relapse. Since only four patients were non-smokers, and seven underwent a pneumonectomy, these two clinical characteristics were dropped from further analyses.

Twenty-three (26.1% of the population) of 88 patients had specimens that stained positively for nEGFR (Fig. 1A). When nEGFR expression was seen, greater than 40% of tumor cells were positive in most cases. Nuclear EGFR was seen in between 1% and 4% of tumor cells very rarely (4/165 tumor cores). Control cores comprised of EGFR positive ductal carcinoma of the breast and matched adjacent normal lung from each tumor were represented on the TMA as external and internal controls, respectively. Cytoplasmic and membrane EGFR staining were confirmed in the breast control, and no nEGFR expression was observed in any of the adjacent normal lung tissue. Table 2 depicts the distribution of nEGFR positivity per IHC staining across our tumor samples.

3.2. Nuclear EGFR protein expression and survival

According to the log-rank test, nEGFR protein positivity was associated with shorter PFS (median PFS 8.7 months [95% CI 5.1–10.7 mo] for nEGFR positive vs. 14.5 months [95% CI 9.5–17.4 mo] for nEGFR negative; HR = 1.89 [95% CI 1.15–3.10]; $p = 0.011$), and shorter OS (median OS 14.1 months [95% CI 10.3–22.7 mo] for nEGFR positive vs. 23.4 months [95% CI 20.1–29.4 mo] for nEGFR negative; HR = 1.83 [95% CI 1.12–2.99]; $p = 0.014$).

3.3. Nuclear EGFR protein expression and prognosis

According to Fisher's exact test, nEGFR protein positivity was associated with squamous cell histology, compared to adenocarcinoma (nEGFR positive in 41.7% of patients' samples with squamous cell vs. 17.1% in adenocarcinoma specimens, $p = 0.028$), and with higher disease stage (nEGFR positive in 45.5% of stage II vs. 14.5% of stage I, $p = 0.023$). Nuclear EGFR protein expression was not associated with patient's sex, or T or N status.

According to Cox proportional hazard models, of the baseline clinical characteristics (sex, disease stage, histology, T, N, and age), only age was at least marginally associated with PFS ($p = 0.073$), but was not associated with OS. Also nEGFR protein positivity in patients' specimens was associated with shorter PFS, after controlling for age, with an HR of 1.68 (95% CI 1.01–2.81, $p = 0.046$), and with shorter OS with an HR of 1.83 (95% CI 1.12–2.99, $p = 0.016$).

4. Discussion

Nuclear EGFR was first observed in hepatocytes during liver regeneration. Translocation from the cell membrane to the nucleus has been reported with numerous receptor tyrosine kinases (RTKs), including all HER family receptors, MET, and VEGFR2 [3,4]. Protein expression of nEGFR has correlated with shortened survival in cancers of the breast, ovary, and oropharyngeal and esophageal squamous cells. Approximately 25–50% of the tumor cells expressed nEGFR [5–8].

Nuclear translocation of full length EGFR can be initiated by ligand binding, irradiation, cetuximab, and cisplatin [4,9,10]. Early events for movement of EGFR from the plasma membrane to the nucleus include phosphorylation of the dimerized receptor by SRC family kinases and AKT [10,11]. These stimuli induce internalization to endocytic vesicles. EGFR then undergoes retrograde translocation through the Golgi apparatus to the endoplasmic reticulum, whereupon it moves from the outer nuclear membrane to the inner nuclear membrane via interaction between importin β and the nuclear pore complex. In the inner nuclear membrane, EGFR can interact with Sec61 for removal from the membrane and release into the nucleus [4,12].

Within the nucleus three functions have been identified for the EGFR. First, EGFR associates with STAT3, STAT5 and E2F1 to act as a transcriptional co-activator, independent of its kinase activity, to increase the expression of target genes that worsen

the malignant phenotype (cyclin D1, iNOS, B-myb, c-Myc, Aurora kinase A, Breast Cancer Resistance Protein, and COX-2) [3,4,13]. Second, nEGFR phosphorylates proliferating cell nuclear antigen, promoting DNA replication [14]. Third, it activates DNA-dependent protein kinase within the nucleus, stimulating DNA repair following exposure to irradiation and cisplatin [15].

This study demonstrates that a distinct nucleolar pattern of EGFR protein was associated with significantly shorter PFS and OS, higher stage and squamous histology in patients with early stage NSCLC. These correlations were not confounded by exposure to additional anti-cancer therapies. A limitation of our study is our shorter than expected overall survival; this is most certainly related to the fact that all samples were selected from patients who had expired by the time of our analyses. Within our patient cohort, however, nEGFR protein expression was detected in just over a quarter of our samples and was statistically associated with higher stage and squamous histology. These results are consistent with findings from other disease sites [5–8].

Our group, and others, have shown in experimental models that nEGFR contributes to treatment resistance with cetuximab, gefitinib, erlotinib, and irradiation [10,11,15]. For example, we demonstrated that NSCLC cells that developed acquired resistance to cetuximab expressed increased levels of nEGFR, and that forced expression of nEGFR rendered cetuximab-sensitive cells resistant to cetuximab, both in vitro and in vivo [3,10]. Similarly, Liccardi et al. showed that cells expressing EGFR with mutations that impair nuclear transport demonstrated reduced repair of DNA strand breaks following ionizing radiation and reduced repair of inter-strand cross-links following exposure to cisplatin, as compared to cells capable of directing EGFR to the nucleus [15]. Conversely, sensitivity in cetuximab-resistant NSCLC cells was re-established after blocking nuclear translocation of EGFR by co-exposing cells to either dasatinib, a SRC family kinase inhibitor, or MK2206, an AKT inhibitor [10,11].

Investigating the functions of nuclear RTKs in untreated cancer cells also serves as a focus of research [16]. Using sequential immunoprecipitation and immunoelectron microscopy assays, Li and colleagues demonstrated that ErbB2 co-localizes with β-actin and RNA polymerase-I (RNA Pol I) to the nucleoli in multiple breast cancer cell lines. Activation of this complex enhanced binding of RNA Pol I to rDNA, expediting rRNA synthesis and protein translation. These authors proposed that localization of ErbB2 to the nucleus and nucleoli contributed to tumorigenesis by increasing rRNA synthesis and protein translation. Nuclear EGFR has been identified in multiple tumor types in patients who did not undergo prior EGFR inhibiting therapy [5–8], as was the case with our population. Biological mechanisms that signal localization of EGFR to the nucleolus in untreated patients, as well as the potential role of such localization in tumor development, are under study in our laboratory.

5. Conclusion

We have identified nEGFR as a predictor of shortened survival in patients with early stage NSCLC. Preclinical data highlights the kinase dependent and independent processes by which nEGFR stimulates tumor cell growth, progression, and survival [3,4,10,11]. This raises the question of whether or not nEGFR represents not only a useful prognostic factor in NSCLC, but also a potential therapeutic target. The biological functions of nEGFR, and strategies to improve the efficacy of cetuximab, cisplatin and radiation by disrupting nuclear translocation of EGFR, remain the subjects of our translational research efforts.

Conflict of interest

No author of this article had any financial or personal relationships with other people or organizations that could inappropriately influence or bias this article.

Acknowledgements

This work was supported in part by the University of Wisconsin Carbone Cancer Center 2P30 CA014520-34, the University of Wisconsin Foundation Creating Hope Campaign for Lung Cancer Research, the Gundersen Lutheran Medical Foundation, the Clinical and Translational Science Award program, previously through the National Center for Research Resources grant 1UL1RR025011, and now through the National Center for Advancing Translational Sciences grant 9U54TR000021, grant RSG-10-193-01-TBG from the American Cancer Society (DLW), and by NIH grant T32 GM08.1061-01A2 from the Graduate Training in Cellular and Molecular Pathogenesis of Human Diseases (TMB). This manuscript was written solely by the authors; the funding sources for this project did not assist in the writing or reviewing of this submission and did not pay the authors for the conduct or writing of this work. The funding sources exerted no role in the design of this project, nor in the data collection, analyses, or interpretation.

References

[1] Hirsch FR, Varella-Garcia M, Bunn Jr PA, Di Maria MV, Veve R, Bremmes RM, et al. Epidermal growth factor receptor in non-small-cell lung carcinomas: correlation between gene copy number and protein expression and impact on prognosis. J Clin Oncol 2003;21:3798–807.
[2] Khambata-Ford S, Harbison CT, Hart LL, Awad M, Xu L-A, Horak CE, et al. Analysis of potential predictive markers of cetuximab benefit in BMS099, a phase III study of cetuximab and first-line taxane/carboplatin in advanced non-small-cell lung cancer. J Clin Oncol 2010;28:918–27.
[3] Han W, Lo H-W. Landscape of EGFR signaling network in human cancers: biology and therapeutic response in relation to receptor subcellular locations. Cancer Lett 2012;318:124–34.
[4] Brand TM, Iida M, Li C, Wheeler DL. The nuclear epidermal growth factor receptor signaling network and its role in cancer. Discov Med 2011;12:419–32.
[5] Lo H-W, Xia W, Wei Y, Ali-Seyed M, Huang S-F, Hung M-C. Novel prognostic value of nuclear epidermal growth factor receptor in breast cancer. Cancer Res 2005;65:338–48.
[6] Psyrri A, Yu Z, Weinberger PM, Sasaki C, Haffty B, Camp R, et al. Quantitative determination of nuclear and cytoplasmic epidermal growth factor receptor expression in oropharyngeal squamous cell cancer by using automated quantitative analysis. Clin Cancer Res 2005;11:5856–62.
[7] Hishino M, Fukui H, Ono Y, Sekikawa, Ichikawa K, Tomita S, et al. Nuclear expression of phosphorylated EGFR is associated with poor prognosis in patients with esophageal squamous cell carcinoma. Pathobiology 2007;74:15–21.
[8] Xia W, Wei Y, Du Y, Liu J, Chang B, Yu Y-L, et al. Nuclear expression of epidermal growth factor receptor is a novel prognostic value in patients with ovarian cancer. Mol Carcinog 2009;48:610–7.
[9] Dittmann K, Mayer C, Fehrenbacher B, Schaller M, Raju U, Milas L, et al. Radiation-induced epidermal growth factor receptor nuclear import is linked to activation of DNA-dependent protein kinase. J Biol Chem 2005;280:31182–9.
[10] Li C, Iida M, Dunn EF, Ghia AJ, Wheeler DL. Nuclear EGFR contributes to acquired resistance to cetuximab. Oncogene 2009;28:3801–13.
[11] Huang W-C, Chen Y-J, Li L-Y, Wei Y-L, Hsu S-C, Tsai S-L, et al. Nuclear translocation of epidermal growth factor receptor by Akt-dependent phosphorylation enhances breast cancer-resistant protein expression in gefintib-resistant cells. J Biol Chem 2011;286:20558–68.
[12] Wang Y-N, Yamaguchi H, Huo L, Du Y, Lee H-J, Lee H-H, et al. The translocon Sec61β localized in the inner nuclear membrane transports membrane-embedded EGF receptor to the nucleus. J Biol Chem 2010;285:38720–9.
[13] Hanada N, Lo H-W, Day C-P, Pan Y, Nakajima Y, Hung M-C. Co-regulation of B-myb expression by E2F1 and EGF receptor. Mol Carcinog 2006;45:10–7.
[14] Wang S-C, Nakajima Y, Yu YL, Xia W, Chen C-T, Yang C-C, et al. Tyrosine phosphorylation controls PCNA function through protein stability. Nat Cell Biol 2006;8:1359–68.
[15] Liccardi G, Hartley JA, Hochhauser D. EGFR nuclear translocation modulates DNA repair following cisplatin and ionizing radiation. Cancer Res 2011;71:1103–14.
[16] Li L-Y, Chen H, Hsieh Y-H, Wang Y-N, Chu H-J, Chen Y-H, et al. Nuclear erbB2 enhances translation and cell growth by activating transcription of ribosomal RNA genes. Cancer Res 2011;71:4269–79.

NEOPLASIA
www.neoplasia.com

Volume 15 Number 10 October 2013 pp. 1196–1206 1196

Sym004, a Novel EGFR Antibody Mixture, Can Overcome Acquired Resistance to Cetuximab[1]

Mari Iida*, Toni M. Brand*, Megan M. Starr*, Chunrong Li*, Evan J. Huppert*, Neha Luthar*, Mikkel W. Pedersen†, Ivan D. Horak†, Michael Kragh† and Deric L. Wheeler*

*Department of Human Oncology, University of Wisconsin School of Medicine and Public Health, Wisconsin Institutes for Medical Research, Madison, WI; †Symphogen A/S, Lyngby, Denmark

Abstract

The epidermal growth factor receptor (EGFR) is a central regulator of tumor progression in a variety of human cancers. Cetuximab is an anti-EGFR monoclonal antibody that has been approved for head and neck and colorectal cancer treatment, but many patients treated with cetuximab don't respond or eventually acquire resistance. To determine how tumor cells acquire resistance to cetuximab, we previously developed a model of acquired resistance using the non–small cell lung cancer line NCI-H226. These cetuximab-resistant (Ctx^R) cells exhibit increased steady-state EGFR expression secondary to alterations in EGFR trafficking and degradation and, further, retained dependence on EGFR signaling for enhanced growth potential. Here, we examined Sym004, a novel mixture of antibodies directed against distinct epitopes on the extracellular domain of EGFR, as an alternative therapy for Ctx^R tumor cells. Sym004 treatment of Ctx^R clones resulted in rapid EGFR degradation, followed by robust inhibition of cell proliferation and down-regulation of several mitogen-activated protein kinase pathways. To determine whether Sym004 could have therapeutic benefit *in vivo*, we established *de novo* Ctx^R NCI-H226 mouse xenografts and subsequently treated Ctx^R tumors with Sym004. Sym004 treatment of mice harboring Ctx^R tumors resulted in growth delay compared to mice continued on cetuximab. Levels of total and phospho-EGFR were robustly decreased in Ctx^R tumors treated with Sym004. Immunohistochemical analysis of these Sym004-treated xenograft tumors further demonstrated decreased expression of Ki67, and phospho-rpS6, as well as a modest increase in cleaved caspase-3. These results indicate that Sym004 may be an effective targeted therapy for Ctx^R tumors.

Neoplasia (2013) 15, 1196–1206

Abbreviations: Ctx^R, cetuximab-resistant; Ctx^S, cetuximab-sensitive; EGFR, epidermal growth factor receptor; ERK1/2, extracellular signal–regulated kinases 1 and 2; HP, parental NCI-H226 cells; HNSCC, head and neck squamous cell carcinoma; i.p., intraperitoneal; MAPK, mitogen-activated protein kinase; mAb, monoclonal antibody; mCRC, metastatic colorectal cancer; NSCLC, non–small cell lung cancer; siRNA, small interfering RNA

Address all correspondence to: Deric L. Wheeler, PhD, Department of Human Oncology, University of Wisconsin Comprehensive Cancer Center, 1111 Highland Avenue, WIMR 3159, Madison, WI 53705. E-mail: dlwheeler@wisc.edu

[1]The project described was supported, in part, by grant UL1TR000427 from the Clinical and Translational Science Award program, through the National Institutes of Health (NIH) National Center for Advancing Translational Sciences, grant RSG-10-193-01-TBG from the American Cancer Society (D.L.W.), grant 888157 from Symphogen A/S (D.L.W.), and NIH grant T32 GM08.1061-01A2 from Graduate Training in Cellular and Molecular Pathogenesis of Human Diseases (T.M.B.). The content is solely the responsibility of the authors and does not necessarily represent the official views of the NIH. Conflict of interest: D.L.W. holds a laboratory research agreement with Symphogen A/S. M.W.P., I.D.H., and M.K. are employed by Symphogen A/S. No potential conflicts of interest were disclosed by other authors.
Received 5 September 2013; Revised 25 September 2013; Accepted 25 September 2013

DOI 10.1593/neo.131584

Introduction

The epidermal growth factor receptor (EGFR) is a member of the human epidermal growth factor receptor (HER) family of receptor tyrosine kinases that consists of four members: EGFR (ErbB1/HER1), HER2/neu (ErbB2), HER3 (ErbB3), and HER4 (ErbB4). Stimulation of EGFR through ligand binding promotes receptor homodimerization or heterodimerization with other HER family receptors, leading to activation of its intrinsic tyrosine kinase [1,2]. Activation of EGFR initiates various signaling cascades, one of which is the mitogen-activated protein kinase (MAPK) network. MAPKs belong to a group of intracellular serine/threonine protein kinases that consist of various members, including the extracellular signal–regulated kinases 1 and 2 (ERK1/2) and p38 MAPKs (alpha, beta, gamma, delta). Upon activation of EGFR, the MAPK pathway is initiated through the promotion of Ras binding to guanosine triphosphate (GTP), which in turn activates RAF kinases MAPK/extracellular signal-regulated kinases (MEK), and MAPKs. MAPKs can subsequently activate numerous transcription factors such as c-Fos, c-Myc, and Elk-1 and numerous protein kinases such as ribosomal S6 kinase 1 (RSK1) [3]. Collectively, the stimulation of the MAPK pathway by EGFR has been shown to greatly enhance cell proliferation, angiogenesis, invasion, and metastasis in cancer cells.

Aberrant expression or activity of EGFR has been identified in many human epithelial cancers, including non–small cell lung cancer (NSCLC). Therefore, targeting EGFR has been intensely pursued over the last three decades as a cancer treatment strategy. One approach to inhibit the activation of EGFR is through the use of monoclonal antibodies (mAbs) that bind the extracellular domain of EGFR to block natural ligand binding. Cetuximab (IMC-225, Erbitux) is a human/murine chimeric mAb that was developed to bind to the extracellular domain III of EGFR. This interaction partially blocks the ligand-binding domain and sterically hinders the correct extended conformation of the dimerization arm on domain II [4]. The Food and Drug Administration has approved cetuximab treatment for patients with metastatic colorectal cancer (mCRC) and head and neck squamous cell carcinoma (HNSCC). However, while cetuximab has shown beneficial antitumor effects in these cancers, the majority of patients who initially respond eventually acquire resistance [1,5,6].

Numerous efforts have been undertaken to define the molecular mechanisms of acquired resistance to cetuximab [7–14]. Our laboratory has established panels of cetuximab-resistant (Ctx^R) clones from the NSCLC cell line NCI-H226 by exposing these cells *in vitro* to increasing concentrations of cetuximab. Using this model, we have shown that impaired EGFR internalization and degradation lead to increased EGFR surface level expression, increased EGFR kinase activity, and dependence on EGFR induced signaling pathways [7]. These data suggest that EGFR remains a molecular target in this setting and that new therapeutics that can initiate the rapid internalization and robust degradation of EGFR may be a potent anticancer strategy.

Sym004 is a novel 1:1 mixture of a pair of mAbs (992 and 1024) directed against nonoverlapping epitopes on EGFR [15,16]. Sym004 inhibits cancer cell growth and survival by blocking ligand binding, receptor activation, and downstream signaling. Unlike cetuximab, Sym004 induces rapid and efficient removal of the receptor from the cell surface by triggering EGFR internalization and degradation. Additionally, Sym004 has been shown to elicit antibody-dependent cellular cytotoxicity and complement-dependent cytotoxicity *in vivo* [16], while cetuximab has been shown to elicit antibody-dependent cellular cytotoxicity only [16–19].

In this study, we hypothesized that cells with acquired resistance to cetuximab retain growth dependency on the EGFR and would therefore benefit from therapeutic agents that promote EGFR degradation. We found that Sym004 treatment delays the emergence of acquired resistance to cetuximab in NCI-H226 cells both *in vitro* and *in vivo*. Down-regulation of several MAPK pathways was also observed in response to Sym004 treatment. The results presented herein suggest that tumors with acquired resistance to cetuximab can thus be successfully targeted with the novel anti-EGFR therapeutic Sym004.

Materials and Methods

Cell Lines

The human NSCLC cell line NCI-H226 was provided by Drs J. Minna and A. Gazdar (University of Texas Southwestern Medical School, Dallas, TX). The cells were maintained in 10% FBS in RPMI-1640 (Mediatech, Inc, Manassas, VA) with 1% penicillin and streptomycin. The development of Ctx^R cells has been described previously [10].

Small Interfering RNA and Transfection

For small interfering RNAs (siRNAs), Ctx^R cells (HC1, HC4, and HC8) were transiently transfected with siEGFR (ON-TARGETplus, SMART pool #L-003114-00; Dharmacon, Lafayette, CO) using Lipofectamine RNAiMAX according to the manufacturer's instructions (Invitrogen, Carlsbad, CA). The nontargeting siRNA (ON-TARGETplus Non-targeting Pool, #D-001810-10) was obtained from Dharmacon as a control. Cells were then lysed for analysis of protein knockdown by immunoblot analysis after siRNA transfection.

Materials

Cetuximab (IMC-225, Erbitux) was purchased from the University of Wisconsin Pharmacy. Sym004 was generously provided by Symphogen A/S (Lyngby, Denmark).

Antibodies

All antibodies were purchased from commercial sources as indicated below: EGFR, pEGFR (Y1173), and HRP-conjugated goat anti-rabbit IgG and goat anti-mouse IgG were obtained from Santa Cruz Biotechnology, Inc (Dallas, TX). pEGFR (Y1045), pEGFR (Y1068), pERK1/2 (T202/Y204), p44/42 ERK1/2, p-rpS6 (S235/236), rpS6, p-c-RAF (S289/296/301), c-RAF, pRSK1 (S380), RSK1, p-p38 (T180/Y182), and p38 were obtained from Cell Signaling Technology (Danvers, MA). pERK1/2 (T202/Y204/T185/Y187) was purchased from Abcam (Cambridge, MA). α-Tubulin was purchased from Calbiochem (Billerica, MA).

Cell Proliferation Assay

This was performed as previously described [10]. Cells were seeded in six-well plates. Following treatment, monolayers were analyzed by crystal violet assay. All treatments were performed in triplicate. Cells were seeded at 2000 cells per well in 100 μl of media on a 96-well plate, grown for 24 hours, and then treated with drug for 72 hours before analysis using the Cell Counting Kit 8 (Dojindo Molecular Technologies, Rockville, MD) according to the manufacturer's instructions. All treatments were performed in quadruplicate.

Cell Growth Assay In Vivo

Athymic nude mice (4- to 6-week-old males) were obtained from Harlan Laboratories (Indianapolis, IN). All animal procedures and maintenance were conducted in accordance with the institutional guidelines of the University of Wisconsin. Mice were randomized into treatment or control groups. Parental NCI-H226 (HP), HC1, or HC4 cells were injected in the dorsal flank of the mouse at respective day 0 (1×10^6 cells). Once tumors reached 250 mm^3, mice were started on 0.5 mg of cetuximab treatments twice a week by intraperitoneal (i.p.) injection. Tumor volume measurements were evaluated by digital calipers and calculated by the formula (p)/6 × (large diameter) × (small diameter)^2.

Immunoblot Analysis

Whole-cell protein lysate was obtained using Tween-20 lysis buffer (50 mM Hepes, pH 7.4, 150 mM NaCl, 0.1% Tween-20, 10% glycerol, 2.5 mM EGTA, 1 mM EDTA, 1 mM DTT, 1 mM Na_3VO_4, 1 mM PMSF, 1 mM beta-glycerophosphate (BGP), and 10 μg/ml leupeptin and aprotinin). Immunoblot analysis was conducted as previously described [20].

Bromodeoxyuridine Cell Cycle Distribution Analysis

Cells were plated at a density of 800,000 per 100 mm^2 plate and allowed to adhere overnight. The cells were treated with vehicle, 20 μg/ml cetuximab, or 20 μg/ml Sym004 for 24 hours. On the following day, the cells were pulsed with 10 μM bromodeoxyuridine for 1 hour. The cells were harvested by trypsinization, washed with cold phosphate-buffered saline (PBS), and fixed with 70% ethanol for 20 minutes. The cells were then labeled with a fluorescein isothiocyanate–conjugated mouse anti-bromodeoxyuridine antibody and processed according to the manufacturer's recommendations (BD Pharmingen, San Jose, CA). The cells were analyzed by flow cytometry (BD FACScan). ModFit Software (Verity Software House, Topsham, ME) was used to analyze the data.

Phospho-MAPK Array

Cell lines were analyzed in the panel of phosphorylation profiles of MAPK and other serine/threonine kinases after treatment with Sym004 (Human Phospho-MAPK, ARY002B; R&D Systems, Minneapolis, MN). This array specifically screens for relative levels of phosphorylation of 26 individual proteins including 9 MAPKs and other intracellular proteins involved in cellular proliferation. After treatment with or without Sym004 (50 μg/ml), cell lysates were incubated with the membrane. Thereafter, a cocktail of biotinylated detection antibodies, streptavidin-HRP, and chemiluminescent detection reagents was used to detect the phosphorylated protein. The relative expression of specific phosphorylated protein was determined following quantification of scanned images by ImageJ compared with Sym004 and vehicle.

Mouse Xenograft Model

Athymic nude mice (4- to 6-week-old males) were obtained from Harlan Laboratories. All animal procedures and maintenance were conducted in accordance with the institutional guidelines of the University of Wisconsin. Mice were randomized into treatment or control groups. Mice were injected in the dorsal flank of the mouse at respective day 0 (2×10^6 cells). Once tumors reached 200 mm^3, mice were started on their respective treatments (IgG, cetuximab, Sym004). The dose of cetuximab and Sym004 for the experiment was 1, 5, 20, and 50 mg/kg and twice a week by i.p. injection. Tumor volume measurements were evaluated by digital calipers and calculated by the formula (p)/6 × (large diameter) × (small diameter)^2.

Mouse Ctx^R Human Tumor Xenografts

Mice were injected with NCI-H226 (2×10^6 cells), and tumors were allowed to grow to 100 mm^3. All mice were randomized to treatment or control groups and treated with 1 mg/mouse (40 mg/kg) of either cetuximab or IgG i.p. twice weekly. Tumors were monitored for cetuximab resistance that was defined as marked tumor growth in the presence of continued cetuximab therapy. Once Ctx^R tumors reached a volume of ~1000 mm^3, mice were grouped according to similar time points of resistance. At this point, each mouse was treated with either cetuximab (1 mg) or Sym004 (20 mg/kg) i.p. twice weekly. Tumor volume measurements were evaluated by digital calipers and calculated by the formula (p)/6 × (large diameter) × (small diameter)^2.

Mouse Tumor Collection and Protein Isolation

Tumors were collected 3 hours after the last cetuximab or Sym004 treatment. Mice were sedated using isoflurane mixed with oxygen until unconscious. Mice were killed by cervical dislocation, and tumors were promptly collected, washed in PBS, and frozen with isopentane on dry ice. Whole-cell protein lysates from tumor samples were obtained with NP-40 lysis buffer (50 mM Hepes, pH 7.4, 150 mM NaCl, 1% NP-40, 0.5% deoxycholic acid, 10% glycerol, 2.5 mM EGTA, 1 mM EDTA, 1 mM DTT, 1 mM PMSF, and 10 μg/ml leupeptin and aprotinin), homogenized by 10 strokes in a tightly fitting Dounce homogenizer, and quantified. Protein quantitation and immunoblot analysis were performed as stated above.

Immunohistochemistry

Tumor tissue samples were collected from xenograft tumors. Tumor samples were fixed in 4% formaldehyde/PBS paraffin-embedded and section. Sections were heated in 10 mM citrate buffer (pH 6.0) for EGFR, Ki67, and phospho-rpS6 or in boric acid buffer (pH 8.0) for cleaved caspase-3 by Decloaking Chamber. Samples were incubated with rabbit anti-EGFR (Abcam; ab52894, 1:200), rabbit anti-Ki67 (Abcam; ab66155, 1:1000), rabbit cleaved caspase-3 (Biocare, Concord, CA; CP229b, 1:100), and rabbit phospho-rpS6 (S235/236; Cell Signaling Technology; 1:400). Sections were stained by BrightVision rabbit/HRP (Immunologic, Duiven, The Netherlands; DPVR110HRP) or LSAB kit/HRP (Dako, Carpinteria, CA). Antibody binding was revealed by addition of 3,3′-diaminobenzidine substrate. Tissues were counterstained with Mayer's hematoxylin (Thermo Fisher Scientific, Waltham, MA) and were examined using an Olympus BX51 microscope. The immunohistochemical staining was judged as follows; Ki67: staining was analyzed with a PC-based image analysis system (Leica Q500, Cambridge, United Kingdom). With this equipment the positively stained DAB reaction was measured and expressed as percentage of positive stained area in relation to total analyzed viable tumor area. Cleaved Caspase-3: no positive cells, low numbers of positive cells (1+) or moderate numbers of positive cells (2+).

Results

Ctx^R Clones Have Increased EGFR Activity

We have previously reported that three Ctx^R clones (HC1, HC4, and HC8) display a robust Ctx^R phenotype when challenged with

increasing doses of cetuximab as compared to HP parental control cells at 72 hours [10]. To examine the stability of the resistant phenotype *in vivo*, we inoculated 1×10^6 cells of both HP and Ctx^R clones HC1 and HC4 into the dorsal flank of athymic nude mice. Tumors were allowed to grow to 250 mm^3 and then treated with 0.5 mg of cetuximab/mouse i.p. twice weekly for the time indicated. As shown in Figure 1*A*, Ctx^R clones established in culture maintained their resistant phenotype in the xenograft model system. Ctx^R clones displayed increased steady-state expression of EGFR and EGFR phosphorylation (Y1173, Y1068, and Y1045). Increased phosphorylation levels of downstream signaling molecules, including ERK1/2 (T202/Y204/T185/Y187), p38 (T180/Y182), RSK1 (S380), c-RAF (S289/296/301), and rpS6 (S235/236), were detected by immunoblot analysis in the Ctx^R clones (HC1, HC4, HC8) relative to HP control cells (Figure 1*B*). Taken together, these results confirm the establishment of stable Ctx^R clones that exhibit robust activation of the EGFR signaling cascade.

Ctx^R Clones Are Dependent on EGFR for Proliferative Potential

To determine if Ctx^R clones remained dependent on EGFR for enhanced growth potential, we performed proliferation assays using siRNAs targeting EGFR. All three Ctx^R clones displayed proliferation inhibitory effects at 30 nM siEGFR (Figure 2*A*). Loss of EGFR expression resulted in loss of activated c-RAF (S289/296/301) and ERK1/2 (T202/Y204) kinases, demonstrating that MAPK pathway activation is dependent on EGFR activity. Next, we treated Ctx^R clones with 20 μg/ml cetuximab or increasing doses of Sym004 for 72 hours. All Ctx^R clones demonstrated statistically significant, dose-dependent inhibition of proliferation in response to Sym004 treatment compared to cetuximab or vehicle treatment (Figure 2*B*).

Sym004 Effectively Degrades EGFR in Ctx^R Clones, whereas Cetuximab Has No Effect on Total and Phosphorylated EGFR Levels

To investigate if inhibition of cell proliferation by Sym004 is due to EGFR degradation, we examined the expression levels of EGFR in Ctx^R clones treated with 20 μg/ml cetuximab or Sym004 (0.1, 1, 20, 50 μg/ml) for 24 hours (Figure 3*A*). Since our previous study showed that small molecule tyrosine kinase inhibitors (TKIs) decreased EGFR phosphorylation at tyrosine 1173 (Y1173), we chose this site for evaluation of Sym004 [10]. Both activated and total levels of EGFR were decreased at all doses of Sym004 examined in Ctx^R clones tested;

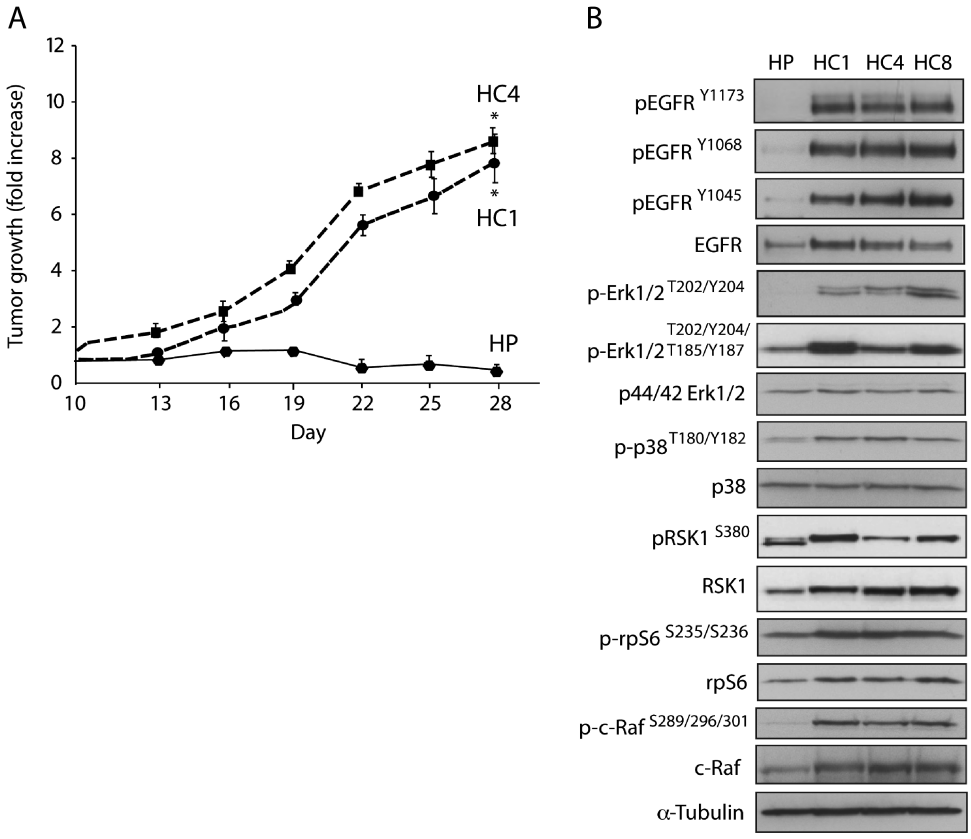

Figure 1. Ctx^R clones have increased EGFR activity. (A) Ctx^R clones are resistant to cetuximab *in vivo*. Male athymic nude mice were injected subcutaneously with 1×10^6 Ctx^S HP or Ctx^R cells (HC1 or HC4) into the dorsal flank. Once tumors reached a volume of 250 mm^3, mice were treated with 0.5 mg of cetuximab twice weekly. Tumor diameters were measured serially with calipers. Tumor volumes were calculated and graphed as fold change in tumor volume + S.E. for each cell line. (B) Ctx^R cells have increased EGFR activity and phosphorylation levels of downstream signaling molecules. HP and Ctx^R clones (HC1, HC4, HC8) were harvested, and protein lysates were fractionated on sodium dodecyl sulfate–polyacrylamide gel electrophoresis (SDS-PAGE), followed by immunoblot analysis for the indicated proteins. α-Tubulin was examined as a loading control for each immunoblot analysis.

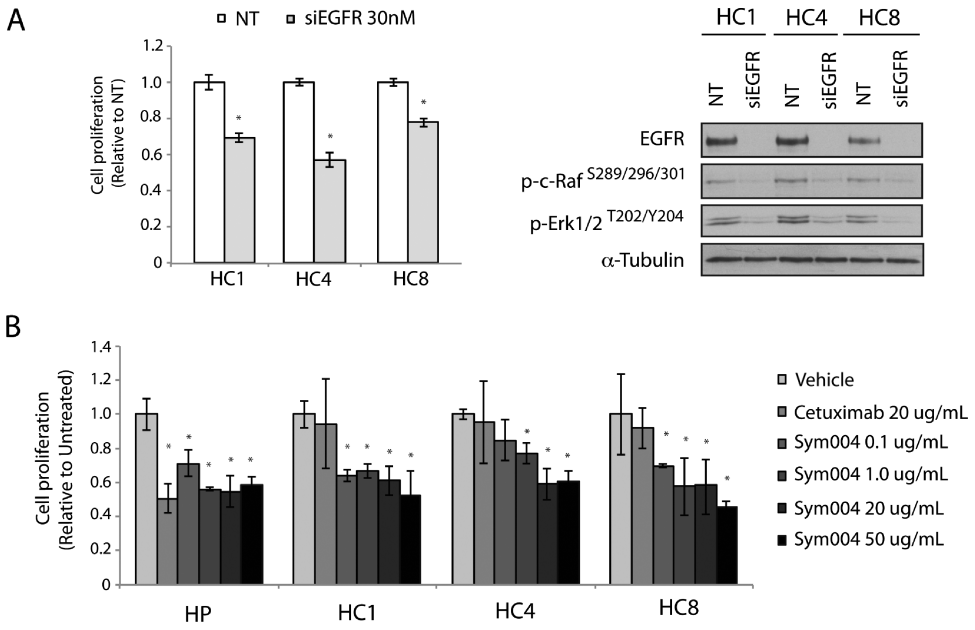

Figure 2. Ctx^R clones are dependent on EGFR for proliferative potential. (A) siEGFR inhibits the proliferation of Ctx^R clones. Ctx^R clones were plated and treated with 30 nM of EGFR siRNA or 30 nM nontargeting (NT) siRNA. Proliferation was measured at 72 hours after treatment using the cell counting kit-8 (CCK-8) proliferation assay described in the experimental procedures. Data points are represented as means ± SEM ($n = 4$). *$P \leq .05$. Ctx^R clones (HC1, HC4, HC8) were harvested, and protein lysates were fractionated on SDS-PAGE, followed by immunoblot analysis for the indicated proteins. α-Tubulin was used as a loading control. (B) Sym004 inhibits the proliferation of Ctx^R clones. HP and Ctx^R cell lines (HC1, HC4, HC8) were plated and allowed to adhere for 24 hours before vehicle, cetuximab (20 μg/ml), or Sym004 treatment: 0.1, 1, 20, or 50 μg/ml. Proliferation was measured at 72 hours after drug treatment using the crystal violet assay and plotted as a percentage of growth relative to untreated control cells. Data points are represented as means ± SEM ($n = 3$).

increasing dosing of Sym004 led to more potent decreases in EGFR levels. In contrast, cetuximab had no impact on total EGFR levels. In a time course experiment, Ctx^R clones were treated with a single dose of 20 μg/ml Sym004 or cetuximab for 24, 48, or 72 hours (Figure 3*B*). The total and phosphorylated EGFR levels were inhibited by Sym004 at all three time points, whereas cetuximab had no effect on total EGFR and slightly activated EGFR in HC1 and HC4 clones at 24 hours post treatment. These results demonstrate that Sym004 can effectively

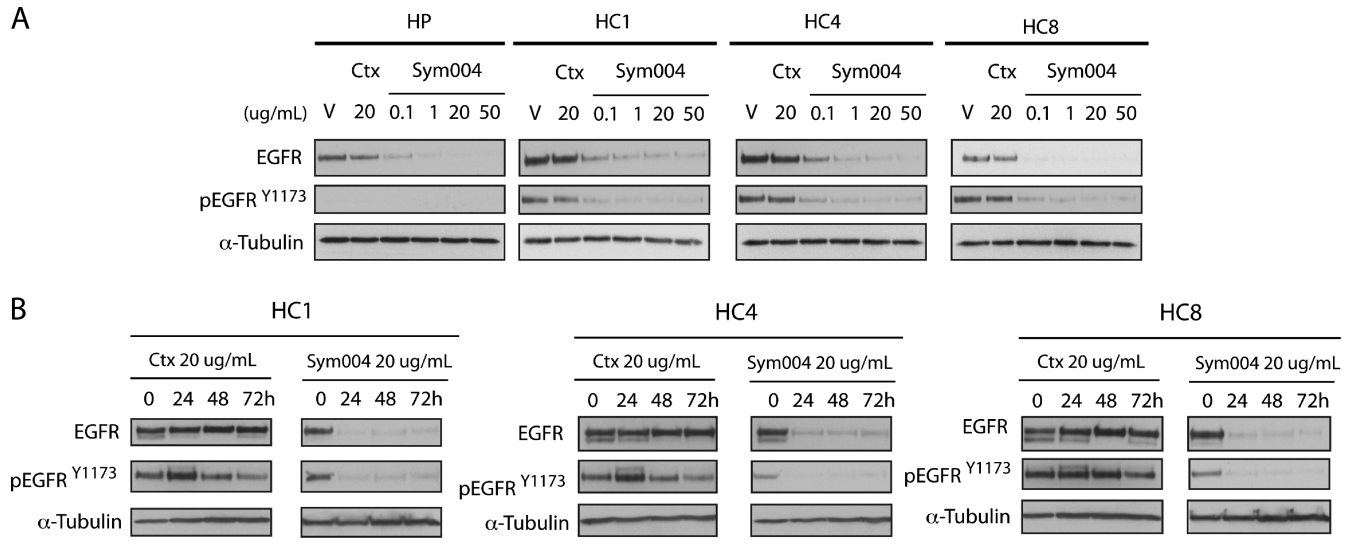

Figure 3. Sym004 effectively degrades EGFR in Ctx^R clones, whereas cetuximab has no effect on total and phosphorylated EGFR levels. (A) Sym004 downregulates total and phosphorylated EGFR in Ctx^R clones. Ctx^R clones (HC1, HC4, HC8) were treated with vehicle, cetuximab (20 μg/ml), or Sym004 (0.1, 1, 20, or 50 μg/ml) for 24 hours. Whole-cell protein lysates were fractionated on SDS-PAGE followed by immunoblot analysis for the indicated proteins. α-Tubulin was used as a loading control. (B) Total and phosphorylated forms of EGFR remain downregulated 72 hours post Sym004 treatment in Ctx^R clones. Cells were treated with a single dose of 20 μg/ml cetuximab or 20 μg/ml Sym004 for 24, 48, or 72 hours. Cell lysates were prepared, and EGFR and phospho-EGFR were determined by immunoblot analysis.

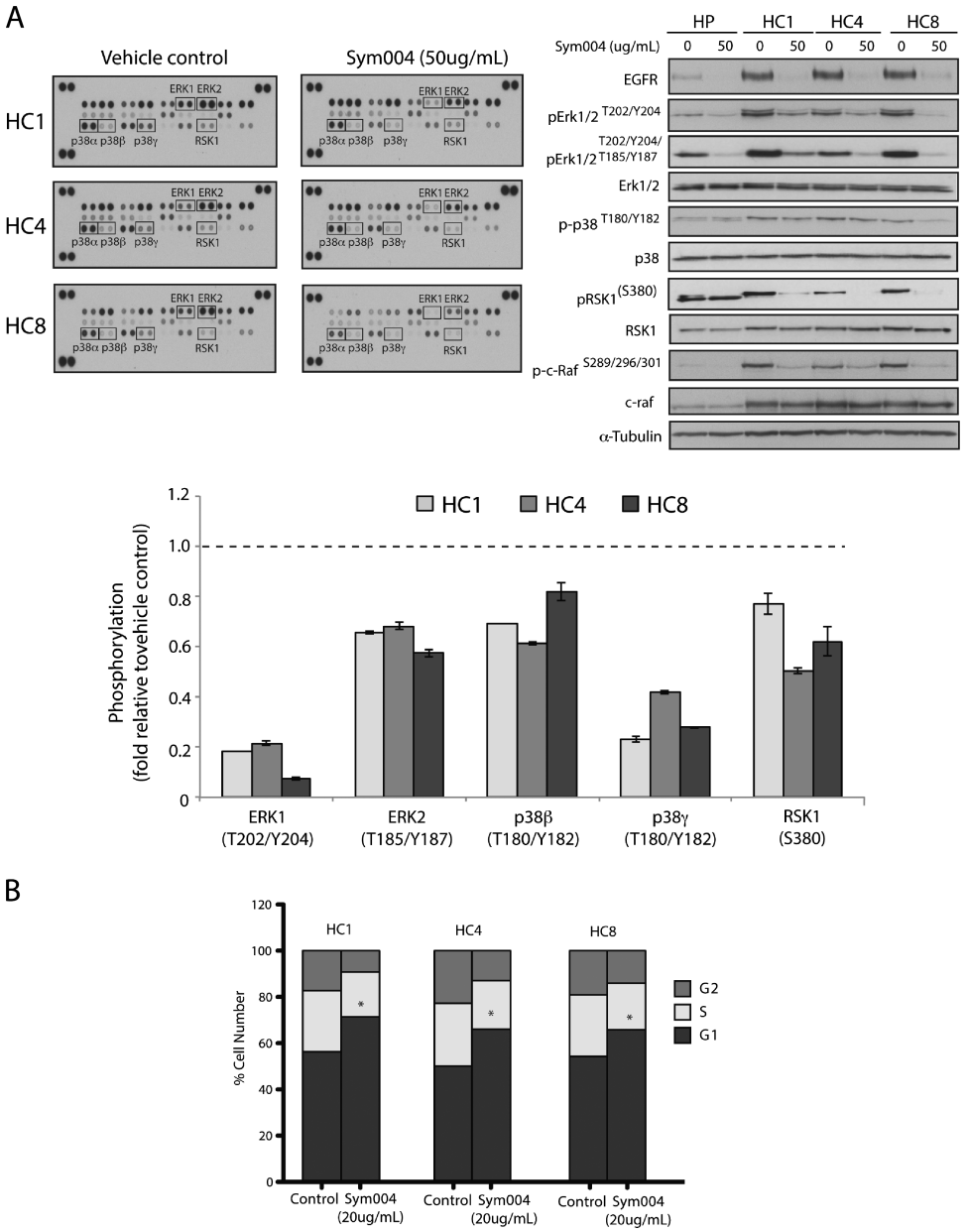

Figure 4. Multiple MAPK effector molecules are inhibited in Ctx^R clones by Sym004 treatment. (A) Sym004 inhibited multiple downstream MAPK effector molecules detected through phospho-kinase array. After treatment with Sym004 (50 μg/ml), cells were collected and cell extracts were incubated with membranes containing antibodies to 26 individual proteins. The membranes were washed and incubated with a cocktail of biotinylated detection antibodies, streptavidin-HRP, and chemiluminescent detection reagents to measure the levels of phosphorylated protein. Quantitation of phosphorylated proteins was completed using scanned images from ImageJ software. Data points are represented as the mean of duplicate spots. Cell extracts were also fractionated on SDS-PAGE, followed by immunoblot analysis for the indicated proteins. α-Tubulin was examined as a loading control for each immunoblot analysis. (B) Sym004 can induce a G_1-phase cell cycle arrest in Ctx^R clones. Cells were treated with 20 μg/ml Sym004 for 24 hours, and cell cycle phase distribution was analyzed as described in the Materials and Methods section. Data points are represented as means ± SEM ($n = 3$). *$P < .05$.

downregulate EGFR in all Ctx^R clones for prolonged periods of time post treatment.

Multiple MAPK Pathway Proteins Are Inhibited in Ctx^R Cells by Sym004 Treatment

Ctx^R cells exhibited an increase in EGFR expression and activation, as well as activated MAPK pathway proteins (Figure 1*B*). To investigate potential mechanisms by which Sym004 elicits antiproliferative effects in Ctx^R clones, we analyzed the effect of Sym004 treatment on MAPK signaling in each clone using a Human Phospho-MAPK Array. Ctx^R clones were treated with vehicle or Sym004 (50 μg/ml) for 24 hours. This Human Phospho-MAPK array includes 26 kinases, 9 of these are MAPKs. As illustrated in Figure 4*A*, Sym004 decreased phosphorylation in three Ctx^R clones by averages of 80% for ERK1, 70% for p38γ, 40% for ERK2, 40% for RSK1, and 30% for P38β, compared with the vehicle control. Consistent with the array results, Western blot analysis indicated that phosphorylation of c-RAF (S289/296/301), ERK1/2 (T202/Y204/T185/Y187),

p38 (T180/Y182), and RSK1 (Ser380) were robustly inhibited after Sym004 treatment in all Ctx^R cells.

Next, cell cycle phase distribution of Ctx^R clones was analyzed post Sym004 treatment. Flow cytometric analysis demonstrated that Sym004 induced a strong G_1 arrest in Ctx^R cell lines (Figure 4*B*). Taken together, these data demonstrate that Sym004 can inhibit EGFR signaling through the MAPK pathway, ultimately impacting cell cycle progression in Ctx^R clones.

Both Cetuximab and Sym004 Delay Tumor Growth in Cetuximab-Sensitive H226 Cells

To investigate the effects of Sym004 *in vivo*, mice bearing established NCI-H226 [cetuximab-sensitive (Ctx^S) parental cell line] xenografts were treated with vehicle control, cetuximab, or Sym004. Mice were injected in the dorsal flank on day 0 (2×10^6 NCI-H226 cells), and once tumors reached an average volume of 200 mm^3 (~18 days), mice were randomly grouped. Cetuximab or Sym004 was administered through i.p. injection at a dose of 1, 5, 20, or 50 mg/kg twice weekly for four consecutive weeks. Mouse weight was measured weekly, and no discernible toxicity was observed in either the cetuximab or Sym004 treatment group. Treatment with either cetuximab or Sym004 showed clear dose-dependent antitumor activity, and both agents significantly delay tumor growth of Ctx^S H226 xenografts at doses of 5 mg/kg or higher compared to the IgG control group (Figure 5).

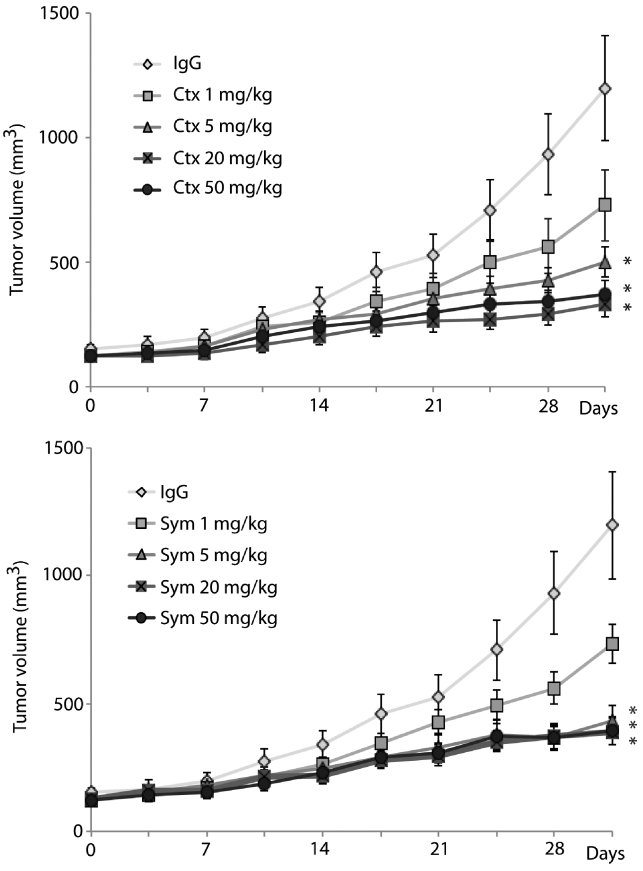

Figure 5. Both cetuximab and Sym004 can effectively control the growth of Ctx^S mouse xenograft tumors. NCI-H226 cells were injected into mice, and tumors were allowed to grow to 200 mm^3. All mice were randomized to treatment or control groups and treated with cetuximab (1, 5, 20, or 50 mg/kg), Sym004 (1, 5, 20, or 50 mg/kg), or IgG (50 mg/kg) i.p. twice weekly.

Sym004 Treatment of Ctx^R Tumors Leads to Tumor Growth Delay In Vivo

Next, we performed a series of mouse xenograft studies of a previously developed model of *de novo* acquired resistance to cetuximab [7]. To develop acquired resistance to cetuximab *in vivo*, we inoculated 40 mice with the NSCLC NCI-H226 cell line unilaterally with 2×10^6 tumor cells in the dorsal flank. Tumors were allowed to grow to 100 mm^3, at which time 30 mice were treated with cetuximab (1 mg/mouse) and 10 mice were treated with IgG control (1 mg/mouse) twice weekly by i.p. injection. IgG-treated tumors grew rapidly uninhibited, whereas cetuximab-treated animals demonstrated tumor control and delayed growth. Tumors were monitored for the development of cetuximab resistance, defined as marked tumor growth in the presence of continued cetuximab therapy. Once Ctx^R tumors reached a volume of ~1000 mm^3, mice were grouped according to similar size at the time of resistance detection. Ctx^R was observed in 21 of 30 tumor xenografts (70%) treated with cetuximab, similar to previous studies from our laboratory [7]. Thus, a total of nine Ctx^R mouse xenograft groups was selected for further study (21 mice in total). Upon establishment of Ctx^R mouse groups, one mouse was maintained on cetuximab (1 mg) therapy, while the other mouse (or mice) in the group was removed from cetuximab and started on 20 mg/kg Sym004 (i.p. twice weekly). The average tumor volume of mice treated with IgG alone is included in all groups for comparison purposes. Eight of 12 (67%) Ctx^R tumors treated with Sym004 demonstrated a tumor response compared to the cetuximab-treated mouse in each group, while four (33%) tumors failed to respond. In Figure 6*A*, we illustrate six of the nine groups where Sym004 delayed tumor growth more than 30 days. The black arrow designates the starting time point of Sym004 treatment.

To further investigate the ability of Sym004 to effectively target EGFR in large tumors *in vivo*, we examined total and phospho-EGFR levels in individual tumors by immunoblot analysis (Figure 6*B*). Sym004-treated Ctx^R tumors had essentially undetectable levels of EGFR, whereas cetuximab-treated Ctx^R tumors retained significant levels of EGFR. These findings were very similar to the results presented in Figure 3*A*. Next, we verified these findings in tissue sections of the tumors by immunohistochemical analysis of EGFR, as well as markers for cell proliferation (Ki67) and apoptosis (cleaved caspase-3; Figure 6*C*). Strong membrane and intracellular EGFR staining were observed in IgG- and cetuximab-treated Ctx^R tumors. Sym004-treated Ctx^R tumors showed moderate intracellular EGFR staining, and no or very limited membrane staining was seen in the majority of tumors examined. The highest numbers of Ki67-positive cells (18%) are seen in IgG followed by cetuximab-treated group (7%), and the lowest numbers are seen in Sym004-treated group (2%). Cleaved caspase-3 staining (black arrows) revealed that the most extensive expression was seen in samples treated with Sym004 followed by cetuximab-treated samples, and the most restricted expression was seen in IgG-treated samples. As a survival marker, phospho-rpS6 (S235/S236) was also stained in these Ctx^R tumors. Ctx^R tumors treated with Sym004 demonstrated prominent inhibition of p-rpS6 compared to IgG or cetuximab-treated Ctx^R tumors (Figure 6*C*). These xenograft studies suggest that Sym004 can effectively inhibit the growth of large Ctx^R tumors, providing strong evidence for the use of Sym004 in the setting of acquired resistance to cetuximab.

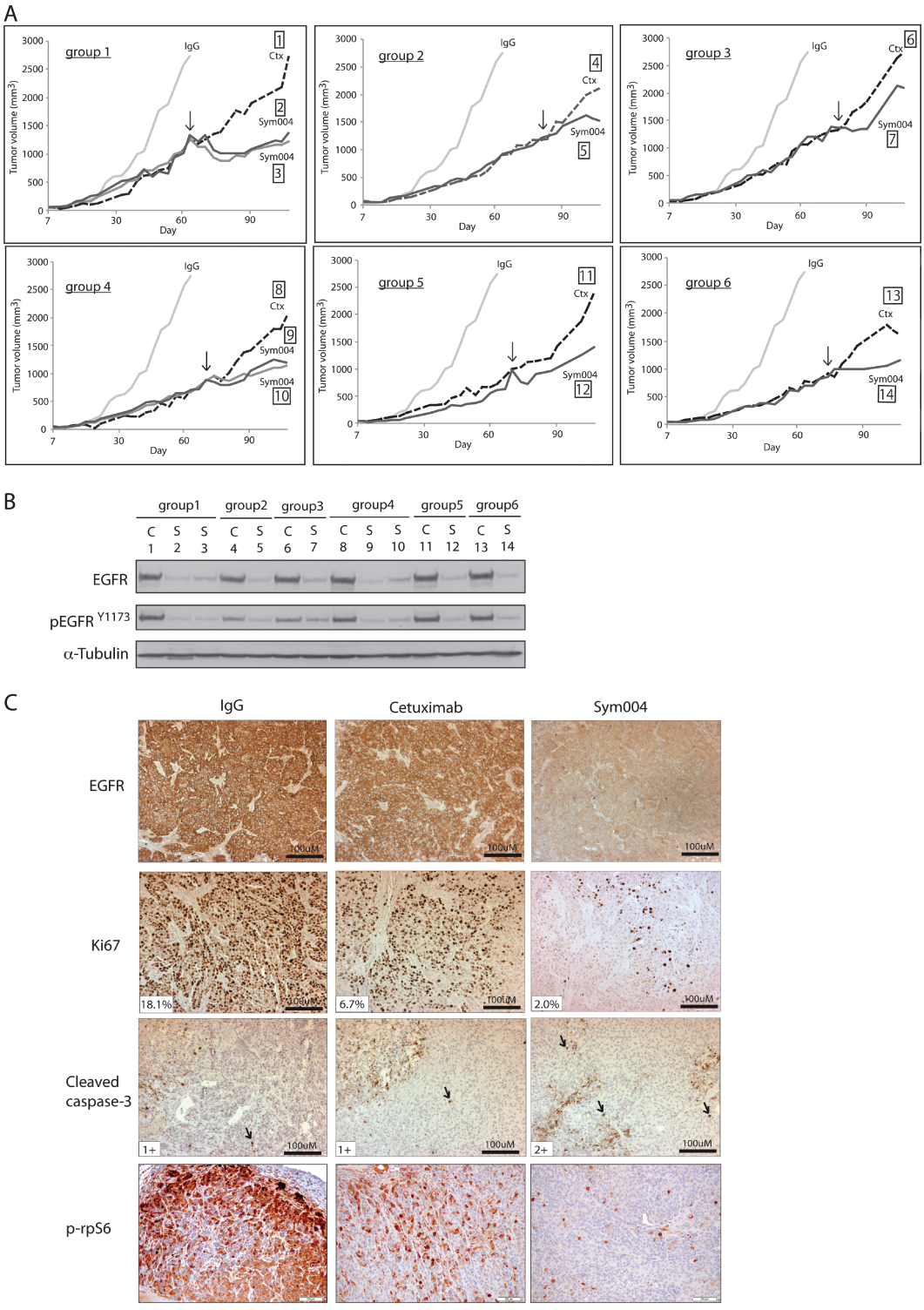

Figure 6. Sym004 treatment delays the growth of Ctx^R xenograft tumors. (A) Growth-inhibitory effects of Sym004 in Ctx^R tumors *in vivo*. Mice were injected with NCI-H226, and tumors were allowed grow to 100 mm^3. All mice were randomized to treatment or control groups and treated with either 1 mg/mouse (40 mg/kg) of cetuximab or IgG i.p. twice weekly. Tumors were monitored for cetuximab resistance, defined as marked tumor growth in the presence of continued cetuximab therapy. Once Ctx^R tumors reached a volume > 1000 mm^3, mice were grouped according to similar time points of resistance. At this point, each mouse was treated with either cetuximab or Sym004 i.p. twice weekly. The black arrow designates the starting time point of Sym004 treatment. The average tumor volume of mice treated with IgG is included in all groups for comparison purposes. (B) Sym004-induced EGFR degradation *in vivo*. Immunoblot analysis of total and activated EGFR in Ctx^R xenograft tumors after cetuximab or Sym004 treatment. C, cetuximab; S, Sym004. (C) The degradation of EGFR in Ctx^R tumors corresponds with loss of proliferation and enhancement of apoptosis. Ctx^R tumor samples after cetuximab or Sym004 treatment *in vivo* were prepared and analyzed for EGFR, proliferation (Ki67), apoptosis (cleaved caspase-3), and phospho-rpS6 immunohistochemistry. Black arrows denote cells positive for cleaved caspase-3. The percentage of Ki67-positive cells and the number of positive cells for cleaved caspase-3 expression are shown.

Discussion

EGFR is one of the most highly targeted receptors in oncology due to its frequent overexpression and aberrant activation in numerous cancers. The anti-EGFR mAb therapy cetuximab is a Food and Drug Administration–approved treatment for mCRC [21] and HNSCC [22] and has shown efficacy in other tumor types such as NSCLC [23,24]. While cetuximab has demonstrated clinical success, both intrinsic and acquired resistance is commonly observed. To characterize the mechanisms of resistance to cetuximab in NSCLC, the cell line NCI-H226 was treated with increasing doses of cetuximab until resistant cell clones developed. In this model, we found that Ctx^R clones had increased EGFR expression and dependency on EGFR for enhanced proliferative potential [10,11]. Therefore, we hypothesized that Sym004, a novel anti-EGFR mAb mixture that leads to rapid internalization and degradation of the EGFR [15], may overcome resistance to cetuximab. The present study demonstrates that Sym004 can elicit potent antiproliferative effects in Ctx^R clones, which corresponded to the degradation of total EGFR. The loss of EGFR inhibited the activity of multiple MAPK signaling proteins corresponding to G_1 phase cell cycle arrest. *De novo* xenograft models of NSCLC (NCI-H226) acquired Ctx^R further indicated that Sym004 could significantly delay the growth of large Ctx^R tumors. Collectively, these data suggest that Sym004 may be an invaluable treatment for EGFR-overexpressing Ctx^R tumors.

Cetuximab is a human/murine chimeric mAb that binds to the extracellular ligand-binding domain III of EGFR [4,25]. Cetuximab prevents EGFR ligand binding and sterically hinders dimerization with other HER receptors; thus, cetuximab has been shown to inhibit signaling cascades emanating from activated EGFR [4,26]. Sym004 is a mixture of two EGFR-directed antibodies that bind to two distinct epitopes on domain III [15,16]. Sym004 can inhibit EGFR activation and downstream signaling pathways but in contrast to cetuximab, it can induce robust EGFR cross-links on the cell surface leading to effective internalization and degradation of the receptor [15,16]. In the present study, increased doses of Sym004 induced potent antiproliferative effects in Ctx^R cell lines (Figure 2*B*), which corresponded to more dramatic losses in total EGFR levels (Figure 3*A*); this finding suggests that loss of EGFR is a central mechanism by which proliferation is inhibited. Treatment of Ctx^R cells with cetuximab had no effect on EGFR levels and slightly enhanced EGFR activity (Figure 3*B*). Mandic et al. reported a similar phenomenon in a variety of different HNSCC cell lines treated with cetuximab [27], indicating that cetuximab may function as a weak ligand in some cases. While the current Ctx^R model has increased dependency on the EGFR, other models of Ctx^R have undergone oncogenic shift to other receptor tyrosine kinases (RTKs) [28] or constitutive activation of EGFR downstream effector molecules [29]; thus, Sym004 may not be an effective treatment option for all Ctx^R tumors. Overall, EGFR-dependent Ctx^R clones can be effectively targeted with Sym004 through the robust degradation of EGFR and loss of downstream signaling emanating from this receptor.

Previous studies in our laboratory have indicated that the Ctx^R clones used in this study have increased expression of EGFR ligands [8]. Further experimentation demonstrated that addition of EGFR ligands to the heparin binding (HP) Ctx^S cell line could enhance resistance to cetuximab. This phenomenon was observed by Hatakeyama et al., where increased expression of HB-EGF was detected in intrinsic Ctx^R HNSCC cell lines and in tumor samples from patients with recurrent disease [30]. Pedersen et al. supported these findings by reporting that EGF could enhance resistance to cetuximab in numerous cancer cell lines; interestingly, researchers further showed that Sym004 treatment of the same cell lines yielded less ligand-induced resistance [15]. Therefore, it seems plausible that Sym004-directed degradation of EGFR in the current Ctx^R model might overcome compensatory up-regulation of ligand.

Another mechanism by which Sym004-directed degradation of EGFR may overcome Ctx^R is through the inhibition of EGFR nuclear translocation. Numerous studies have demonstrated that nuclear EGFR can enhance resistance to cetuximab [8], gefitinib [31], radiation [32,33], and chemotherapy [34,35]. Previous research with the current model demonstrated that inhibition of nuclear EGFR could resensitize resistant clones to cetuximab [8]. Sym004-directed degradation of EGFR appears to deplete both the cell membrane component of EGFR, as well as nuclear EGFR, leading to effective knockdown of the EGFR signaling network. Thus, Sym004 may play a vital role in overcoming resistance to gefitinib, radiation, and chemotherapy as well.

The MAPK signaling pathway is one of the main pathways emanating from activated EGFR, and thus, Ctx^R clones express activated forms of MAPK pathway proteins (Figure 1*B*). Sym004 treatment inhibited two of the four major groups of conventional MAPKs, including ERK1/2 and p38 MAPK, in addition to RSK1 and c-RAF (Figure 4*A*). RSK1 has specifically been shown to play an important role in promoting cell cycle progression past the G_1 checkpoint through the phosphorylation of $p27^{Kip1}$ and serum response factor, ultimately enhancing cyclin D expression [36]. Therefore, inhibition of RSK1 may play a role in the G_1 phase cell cycle arrest observed upon Sym004 treatment (Figure 4*B*). While the status of MAPK signaling proteins were analyzed in this study, the functions of other proteins were likely modulated as well, and therefore, the antiproliferative effects of Sym004 observed here may not be solely due to MAPK inhibition. Additionally, while Sym004 yielded potent antiproliferative effects *in vitro*, apoptosis was only minimally increased (data not shown).

The antiproliferative effects observed *in vitro* were also observed in *de novo* models of acquired resistance to cetuximab *in vitro*. *De novo* acquired resistant models were chosen for study because they more accurately portray the cellular events that result in cetuximab resistance in the clinic. In this model, Ctx^R xenograft tumors were significantly growth delayed upon treatment with Sym004 (Figure 6*A*) compared to Ctx^R tumors that were continued on cetuximab therapy. The fact that 67% of Ctx^R tumors put on Sym004 yielded tumor growth delay demonstrates a unique property of Sym004 inhibition rather than just spontaneous reduction in tumor size. While tumor shrinkage was observed in some mice upon Sym004 treatment, most experienced a delay in growth; growth delay in tumors of this size (>1000 mm^3) demonstrates that Sym004 can robustly inhibit proliferation, which may translate into potent antitumor effects in human patients. Additionally, Sym004 treatment led to robust losses of EGFR and Ki67 staining, while there were minimal changes in cleaved caspase-3 levels (Figure 6*C*). Collectively, the antitumor effects of Sym004 observed in this model of Ctx^R may be exerted through modulations in proliferation pathways rather than apoptosis pathways.

Determining why patients with cancer become resistant to anti-EGFR therapeutics is a major clinical challenge. Data from the present study suggest that Ctx^R tumors may still be addicted to EGFR signaling, and therefore, using Sym004 may be of great clinical promise. Degradation of the EGFR, rather than inactivation, is a powerful anticancer strategy because both kinase-dependent and

independent functions of EGFR will be abolished. This therapeutic may also have antitumor effects in the setting of EGFR-activating mutations (such as L858R and subsequent gatekeeper mutations such as T790M), EGFR S492R mutations (found in patients with mCRC yielding resistance to cetuximab [37]), wild-type and mutant KRAS colorectal tumors (where some KRAS mutant mCRCs may still contain sensitivity to cetuximab [38,39]), and in the case of EGFR-overexpressing breast cancers. Sym004 has now undergone phase I clinical trials in patients with advanced solid tumors, in which patients treated with multiple doses of Sym004 had manageable adverse effects [40]. Sym004 is currently undergoing phase II testing in CRC and HNSCC (http://clinicaltrials.gov). Overall, Sym004 is a promising new molecular targeting agent that may provide more beneficial antitumor effects compared to cetuximab in EGFR-overexpressing cancers.

References

[1] Wheeler DL, Dunn EF, and Harari PM (2010). Understanding resistance to EGFR inhibitors—impact on future treatment strategies. *Nat Rev Clin Oncol* **7**, 493–507.

[2] Yarden Y and Pines G (2012). The ERBB network: at last, cancer therapy meets systems biology. *Nat Rev Cancer* **12**, 553–563.

[3] Sebolt-Leopold JS and Herrera R (2004). Targeting the mitogen-activated protein kinase cascade to treat cancer. *Nat Rev Cancer* **4**, 937–947.

[4] Li S, Schmitz KR, Jeffrey PD, Wiltzius JJ, Kussie P, and Ferguson KM (2005). Structural basis for inhibition of the epidermal growth factor receptor by cetuximab. *Cancer Cell* **7**, 301–311.

[5] Martinelli E, De Palma R, Orditura M, De Vita F, and Ciardiello F (2009). Anti-epidermal growth factor receptor monoclonal antibodies in cancer therapy. *Clin Exp Immunol* **158**, 1–9.

[6] Brand TM, Iida M, and Wheeler DL (2011). Molecular mechanisms of resistance to the EGFR monoclonal antibody cetuximab. *Cancer Biol Ther* **11**, 777–792.

[7] Brand TM, Dunn EF, Iida M, Myers RA, Kostopoulos KT, Li C, Peet CR, and Wheeler DL (2011). Erlotinib is a viable treatment for tumors with acquired resistance to cetuximab. *Cancer Biol Ther* **12**, 436–446.

[8] Li C, Iida M, Dunn EF, Ghia AJ, and Wheeler DL (2009). Nuclear EGFR contributes to acquired resistance to cetuximab. *Oncogene* **28**, 3801–3813.

[9] Li C, Iida M, Dunn EF, and Wheeler DL (2010). Dasatinib blocks cetuximab- and radiation-induced nuclear translocation of the epidermal growth factor receptor in head and neck squamous cell carcinoma. *Radiother Oncol* **97**, 330–337.

[10] Wheeler DL, Huang S, Kruser TJ, Nechrebecki MM, Armstrong EA, Benavente S, Gondi V, Hsu KT, and Harari PM (2008). Mechanisms of acquired resistance to cetuximab: role of HER (ErbB) family members. *Oncogene* **27**, 3944–3956.

[11] Wheeler DL, Iida M, Kruser TJ, Nechrebecki MM, Dunn EF, Armstrong EA, Huang S, and Harari PM (2009). Epidermal growth factor receptor cooperates with Src family kinases in acquired resistance to cetuximab. *Cancer Biol Ther* **8**, 696–703.

[12] van der Veeken J, Oliveira S, Schiffelers RM, Storm G, van Bergen En Henegouwen PM, and Roovers RC (2009). Crosstalk between epidermal growth factor receptor- and insulin-like growth factor-1 receptor signaling: implications for cancer therapy. *Curr Cancer Drug Targets* **9**, 748–760.

[13] Desbois-Mouthon C, Baron A, Blivet-Van Eggelpoël MJ, Fartoux L, Venot C, Bladt F, Housset C, and Rosmorduc O (2009). Insulin-like growth factor-1 receptor inhibition induces a resistance mechanism via the epidermal growth factor receptor/HER3/AKT signaling pathway: rational basis for cotargeting insulin-like growth factor-1 receptor and epidermal growth factor receptor in hepatocellular carcinoma. *Clin Cancer Res* **15**, 5445–5456.

[14] Benavente S, Huang S, Armstrong EA, Chi A, Hsu KT, Wheeler DL, and Harari PM (2009). Establishment and characterization of a model of acquired resistance to epidermal growth factor receptor targeting agents in human cancer cells. *Clin Cancer Res* **15**, 1585–1592.

[15] Pedersen MW, Jacobsen HJ, Koefoed K, Hey A, Pyke C, Haurum JS, and Kragh M (2010). Sym004: a novel synergistic anti-epidermal growth factor receptor antibody mixture with superior anticancer efficacy. *Cancer Res* **70**, 588–597.

[16] Koefoed K, Steinaa L, Søderberg JN, Kjær I, Jacobsen HJ, Meijer PJ, Haurum JS, Jensen A, Kragh M, Andersen PS, et al. (2011). Rational identification of an optimal antibody mixture for targeting the epidermal growth factor receptor. *mAbs* **3**, 584–595.

[17] Kurai J, Chikumi H, Hashimoto K, Yamaguchi K, Yamasaki A, Sako T, Touge H, Makino H, Takata M, Miyata M, et al. (2007). Antibody-dependent cellular cytotoxicity mediated by cetuximab against lung cancer cell lines. *Clin Cancer Res* **13**, 1552–1561.

[18] Derer S, Berger S, Schlaeth M, Schneider-Merck T, Klausz K, Lohse S, Overdijk MB, Dechant M, Kellner C, Nagelmeier I, et al. (2012). Oncogenic KRAS impairs EGFR antibodies' efficiency by C/EBPβ-dependent suppression of EGFR expression. *Neoplasia* **14**, 190–205.

[19] Larbouret C, Gaborit N, Chardès T, Coelho M, Campigna E, Bascoul-Mollevi C, Mach JP, Azria D, Robert B, and Pèlegrin A (2012). In pancreatic carcinoma, dual EGFR/HER2 targeting with cetuximab/trastuzumab is more effective than treatment with trastuzumab/erlotinib or lapatinib alone: implication of receptors' down-regulation and dimers' disruption. *Neoplasia* **14**, 121–130.

[20] Iida M, Brand TM, Campbell DA, Li C, and Wheeler DL (2013). Yes and Lyn play a role in nuclear translocation of the epidermal growth factor receptor. *Oncogene* **32**, 759–767.

[21] Jonker DJ, O'Callaghan CJ, Karapetis CS, Zalcberg JR, Tu D, Au HJ, Berry SR, Krahn M, Price T, Simes RJ, et al. (2007). Cetuximab for the treatment of colorectal cancer. *N Engl J Med* **357**, 2040–2048.

[22] Vermorken JB, Trigo J, Hitt R, Koralewski P, Diaz-Rubio E, Rolland F, Knecht R, Amellal N, Schueler A, and Baselga J (2007). Open-label, uncontrolled, multicenter phase II study to evaluate the efficacy and toxicity of cetuximab as a single agent in patients with recurrent and/or metastatic squamous cell carcinoma of the head and neck who failed to respond to platinum-based therapy. *J Clin Oncol* **25**, 2171–2177.

[23] Pirker R, Pereira JR, Szczesna A, von Pawel J, Krzakowski M, Ramlau R, Vynnychenko I, Park K, Yu CT, Ganul V, et al. (2009). Cetuximab plus chemotherapy in patients with advanced non-small-cell lung cancer (FLEX): an open-label randomised phase III trial. *Lancet* **373**, 1525–1531.

[24] Carillio G, Montanino A, Costanzo R, Sandomenico C, Piccirillo MC, Di Maio M, Daniele G, Giordano P, Bryce J, Normanno N, et al. (2012). Cetuximab in non-small-cell lung cancer. *Expert Rev Anticancer Ther* **12**, 163–175.

[25] Voigt M, Braig F, Göthel M, Schulte A, Lamszus K, Bokemeyer C, and Binder M (2012). Functional dissection of the epidermal growth factor receptor epitopes targeted by panitumumab and cetuximab. *Neoplasia* **14**, 1023–1031.

[26] Graham J, Muhsin M, and Kirkpatrick P (2004). Cetuximab. *Nat Rev Drug Discov* **3**, 549–550.

[27] Mandic R, Rodgarkia-Dara CJ, Zhu L, Folz BJ, Bette M, Weihe E, Neubauer A, and Werner JA (2006). Treatment of HNSCC cell lines with the EGFR-specific inhibitor cetuximab (Erbitux) results in paradox phosphorylation of tyrosine 1173 in the receptor. *FEBS Lett* **580**, 4793–4800.

[28] Bianco R, Rosa R, Damiano V, Daniele G, Gelardi T, Garofalo S, Tarallo V, De Falco S, Melisi D, Benelli R, et al. (2008). Vascular endothelial growth factor receptor-1 contributes to resistance to anti-epidermal growth factor receptor drugs in human cancer cells. *Clin Cancer Res* **14**, 5069–5080.

[29] Kim SM, Kim JS, Kim JH, Yun CO, Kim EM, Kim HK, Solca F, Choi SY, and Cho BC (2010). Acquired resistance to cetuximab is mediated by increased PTEN instability and leads cross-resistance to gefitinib in HCC827 NSCLC cells. *Cancer Lett* **296**, 150–159.

[30] Hatakeyama H, Cheng H, Wirth P, Counsell A, Marcrom SR, Wood CB, Pohlmann PR, Gilbert J, Murphy B, Yarbrough WG, et al. (2010). Regulation of heparin-binding EGF-like growth factor by miR-212 and acquired cetuximab-resistance in head and neck squamous cell carcinoma. *PLoS One* **5**, e12702.

[31] Huang WC, Chen YJ, Li LY, Wei YL, Hsu SC, Tsai SL, Chiu PC, Huang WP, Wang YN, Chen CH, et al. (2011). Nuclear translocation of epidermal growth factor receptor by Akt-dependent phosphorylation enhances breast cancer-resistant protein expression in gefitinib-resistant cells. *J Biol Chem* **286**, 20558–20568.

[32] Dittmann K, Mayer C, Fehrenbacher B, Schaller M, Raju U, Milas L, Chen DJ, Kehlbach R, and Rodemann HP (2005). Radiation-induced epidermal growth factor receptor nuclear import is linked to activation of DNA-dependent protein kinase. *J Biol Chem* **280**, 31182–31189.

[33] Steinle M, Palme D, Misovic M, Rudner J, Dittmann K, Lukowski R, Ruth P, and Huber SM (2011). Ionizing radiation induces migration of glioblastoma cells by activating BK K^+ channels. *Radiother Oncol* **101**, 122–126.

[34] Hsu SC, Miller SA, Wang Y, and Hung MC (2009). Nuclear EGFR is required for cisplatin resistance and DNA repair. *Am J Transl Res* **1**, 249–258.

[35] Liccardi G, Hartley JA, and Hochhauser D (2011). EGFR nuclear translocation modulates DNA repair following cisplatin and ionizing radiation treatment. *Cancer Res* **71**, 1103–1114.

[36] Anjum R and Blenis J (2008). The RSK family of kinases: emerging roles in cellular signalling. *Nat Rev Mol Cell Biol* **9**, 747–758.

[37] Montagut C, Dalmases A, Bellosillo B, Crespo M, Pairet S, Iglesias M, Salido M, Gallen M, Marsters S, Tsai SP, et al. (2012). Identification of a mutation in the extracellular domain of the epidermal growth factor receptor conferring cetuximab resistance in colorectal cancer. *Nat Med* **18**, 221–223.

[38] Dunn EF, Iida M, Myers RA, Campbell DA, Hintz KA, Armstrong EA, Li C, and Wheeler DL (2011). Dasatinib sensitizes KRAS mutant colorectal tumors to cetuximab. *Oncogene* **30**, 561–574.

[39] De Roock W, Jonker DJ, Di Nicolantonio F, Sartore-Bianchi A, Tu D, Siena S, Lamba S, Arena S, Frattini M, Piessevaux H, et al. (2010). Association of KRAS p.G13D mutation with outcome in patients with chemotherapy-refractory metastatic colorectal cancer treated with cetuximab. *JAMA* **304**, 1812–1820.

[40] Dienstmann R (2011). Phase I trial of the first-in-class EGFR mAb mixture, Sym004, in patients with refractory advanced solid tumors. In *JCO, 2011 ASCO Annual Meeting Proceedings (Post-Meeting Edition)*. **29**(15 suppl.), 3089.

RESEARCH PAPER

Cancer Biology & Therapy 14:6, 1–11; June 2013; © 2013 Landes Bioscience

Targeting AKT with the allosteric AKT inhibitor MK-2206 in non-small cell lung cancer cells with acquired resistance to cetuximab

Mari Iida,[1] Toni M. Brand,[1] David A. Campbell,[1] Megan M. Starr,[1] Neha Luthar,[1] Anne M. Traynor[2] and Deric L. Wheeler[1,*]

[1]Department of Human Oncology; University of Wisconsin School of Medicine and Public Health; Wisconsin Institute for Medical Research; Madison, WI USA; [2]Department of Medicine; University of Wisconsin School of Medicine and Public Health; Wisconsin Institute for Medical Research; Madison, WI USA

Keywords: AKT, EGFR, MK-2206, cetuximab, acquired cetuximab-resistance, non-small cell lung cancer, MAPK

Abbreviations: BAD, BCL-2 associated agonist of cell death; BIM, BCL-2-interacting mediator of cell death; Ctx^R, cetuximab-resistant; Ctx^S, cetuximab-sensitive; DNA-PK, DNA-dependent protein kinase; EGFR, epidermal growth factor receptor; eIF4E, eukaryotic translation initiation factor 4E; FoxO, forkhead box O transcription factors; GSK3, glycogen synthase kinase 3; HNSCC, head and neck squamous cell carcinoma; MAPK, mitogen-activated protein kinase; mCRC, metastatic colorectal carcinoma; mTORC2, mammalian target of rapamycin complex 2; NLS, nuclear localization signal; NSCLC, non-small cell lung cancer; PDK1, phosphoinositide-dependent kinase-1; PH, pleckstrin homology; PI3K, phosphatidylinositol 3-kinase; PTEN, phosphatase and tensin homolog; SH2, Src Homology 2; rpS6, ribosomal protein S6; TKD, tyrosine kinase domain

The epidermal growth factor receptor (EGFR) is a central regulator of tumor progression in human cancers. Cetuximab is an anti-EGFR monoclonal antibody that has been approved for use in oncology. Despite clinical success the majority of patients do not respond to cetuximab and those who initially respond frequently acquire resistance. To understand how tumor cells acquire resistance to cetuximab we developed a model of resistance using the non-small cell lung cancer line NCI-H226. We found that cetuximab-resistant (Ctx^R) clones manifested strong activation of EGFR, PI3K/AKT and MAPK. To investigate the role of AKT signaling in cetuximab resistance we analyzed the activation of the AKT pathway effector molecules using a human AKT phospho-antibody array. Strong activation was observed in Ctx^R clones for several key AKT substrates including c-jun, GSK3β, eIF4E, rpS6, IKKα, IRS-1 and Raf1. Inhibition of AKT signaling by siAKT1/2 or by the allosteric AKT inhibitor MK-2206 resulted in robust inhibition of cell proliferation in all Ctx^R clones. Moreover, the combinational treatment of cetuximab and MK-2206 resulted in further decreases in proliferation than either drug alone. This combinatorial treatment resulted in decreased activity of both AKT and MAPK thus highlighting the importance of simultaneous pathway inhibition to maximally affect the growth of Ctx^R cells. Collectively, our findings demonstrate that AKT activation is an important pathway in acquired resistance to cetuximab and suggests that combinatorial therapy directed at both the AKT and EGFR/MAPK pathways may be beneficial in this setting.

Introduction

The epidermal growth factor receptor (EGFR) is a member of the HER family of receptor tyrosine kinases (RTKs), which consists of the EGFR (ErbB1/HER1), HER2/neu (ErbB2), HER3 (ErbB3) and HER4 (ErbB4). All family members contain an extracellular ligand-binding domain (domains I, II, III and IV), a single membrane-spanning region, a juxtamembrane nuclear localization signal (NLS) and a cytoplasmic tyrosine kinase domain (TKD). EGFR activation stimulates many complex intracellular signaling pathways that are tightly regulated by the presence and identity of ligand, the heterodimer composition and the availability of phosphotyrosine-binding proteins. The two primary signaling pathways activated by EGFR include the RAS/RAF/MEK/ERK and the PI3K/AKT axis; however, SRC tyrosine kinases, PLCγ, PKC and STAT activation and downstream signaling have also been well documented.[1] Tumor cell proliferation, survival, invasion and angiogenesis can ultimately be promoted through activation of these pathways. Aberrant expression or activity of the EGFR has been identified as an important biological factor in many human epithelial cancers including head and neck squamous cell carcinoma (HNSCC), non-small cell lung cancer (NSCLC), colorectal cancer (CRC), breast cancer, pancreatic cancer and brain cancer.

Cetuximab (ICM-225, Erbitux) is a human/murine chimeric monoclonal antibody that works by binding to extracellular domain III of EGFR. This interaction partially blocks the ligand-binding domain and sterically hinders the correct extended conformation of the dimerization arm on domain II.[2] Thus, cetuximab inhibits both ligand binding and the proper

*Correspondence to: Deric L. Wheeler; Email: dlwheeler@wisc.edu
Submitted: 07/16/12; Revised: 02/21/13; Accepted: 03/18/13
http://dx.doi.org/10.4161/cbt.24342

positioning of the EGFR dimerization domain, preventing dimerization with other HER family members. Cetuximab has exhibited promising antitumor activity in clinical trials as a monotherapy or use in combination with chemotherapy and/or radiation, particularly in the settings of metastatic CRC (mCRC)[3-8] and HNSCC.[9-13] However, EGFR inhibition by either monoclonal antibodies or small molecule tyrosine kinase inhibitors only demonstrate anti-tumor activity in ~10–20% of cancer patients as reported in several pivotal clinical studies involving different solid tumor types.[14] Over the past several years researchers have observed high levels of intrinsic and acquired resistance to EGFR monoclonal antibody therapy, stimulating a new field of EGFR research.[15]

The serine-threonine kinase AKT was initially identified as the proto-oncogene of the v-AKT oncogenic murine thymoma virus.[16] AKT has three isoforms: AKT1, AKT2 and AKT3. AKT1 and AKT2 are expressed in most tissue types while AKT3 expression is generally restricted to neuronal tissue and the testes.[17] The three isoforms share over 80% homology and are characterized by three conserved functional domains: an N-terminal pleckstrin homology (PH) domain that regulates intracellular trafficking of the protein, a central catalytic domain and a C-terminal regulatory domain. Activation of all three AKT isoforms is dependent on the activity of phosphatidylinositol 3-kinase (PI3K).[18] PI3K is stimulated by a variety of signals, including growth factor and G protein-coupled receptors localized on the cell surface. Activation of PI3K results in the generation of 3'-phosphorylated phosphatidylinositols in the cell membrane, which recruit AKT and other PH domain-containing proteins to the cell membrane. Localization of AKT on the inner leaflet of the cell membrane brings it into close proximity to the serine-threonine kinase phosphoinositide-dependent kinase-1 (PDK1), which phosphorylates AKT at the Thr308 residue of its catalytic domain. The activated conformation of AKT is further stabilized by phosphorylation at the Ser473 residue, either by the mammalian target of rapamycin complex 2 (mTORC2) in response to growth factor stimulation or by DNA-dependent protein kinase (DNA-PK) after DNA damage.[19,20] Additionally, various PI3K independent activators of AKT have also been discovered.[21] In turn, AKT phosphorylates several cellular proteins, including glycogen synthase kinase 3α (GSK3α), GSK3β, forkhead box O transcription factors (FoxO), MDM2, BCL-2-interacting mediator of cell death (BIM) and BCL-2 associated agonist of cell death (BAD) to facilitate cell survival and cell cycle entry (For a review see ref. 22).[22] AKT activity is negatively regulated primarily by phosphatases that dephosphorylate phosphatidylinositols at the cell membrane including phosphatase and tensin homolog (PTEN) and SHP2.

More than 50 substrates of AKT have been identified.[18,23-25] Through these and other effectors, AKT regulates a variety of cellular processes, including proliferation, survival, motility, angiogenesis, differentiation and metabolism/glucose homeostasis. Thus, inhibition of AKT activity is an attractive target for cancer therapies. Currently, several AKT inhibitors are in clinical development for treating cancers. MK-2206 is an orally active allosteric AKT inhibitor that is under development for the treatment of solid tumors. While MK-2206 is equally potent toward purified recombinant human AKT1 (IC_{50}, 5 nmol/L) and AKT2 proteins (IC_{50}, 12 nmol/L), it is approximately 5-fold less potent against human AKT3 (IC_{50}, 65 nmol/L).[26]

Previously we established cetuximab resistant (Ctx^R) clones from the NSCLC cell line NCI-H226 by exposing these cells to increasing concentrations of cetuximab over a 6-mo time course.[27] Total protein levels and activation of EGFR in Ctx^R clones were upregulated, as well as the phosphorylation of MAPK and AKT compared with cetuximab-sensitive (Ctx^S) parental control cells.[27] In this report we investigated if Ctx^R clones acquired a dependency on AKT signaling and whether they would be sensitive to the AKT inhibitor MK-2206 alone or in combination with cetuximab. Individual clones with acquired resistance to cetuximab were treated with MK-2206 resulting in decreased activation of AKT, and its downstream signaling molecules in the AKT pathway. This led to decreased proliferation and increased apoptosis in all Ctx^R clones tested. Moreover, statistically significant decreases in proliferation were noted in combined treatment with cetuximab and MK-2206. The combination of cetuximab and MK-2206 led to the growth inhibition of Ctx^R clones due to reduced signaling by both the MAPK and AKT signaling pathways, suggesting a role for both of these kinases in cetuximab resistance. Taken together, these results suggest that the activation of EGFR and downstream MAPK signaling as well as AKT play a role in cetuximab resistance and that dual targeting of the EGFR and AKT with cetuximab and MK-2206 may provide a strategy to overcome acquired resistance.

Results

NSCLC cell lines with acquired resistance to cetuximab have increased activity of MAPK, AKT and downstream AKT signaling pathways. We previously reported that Ctx^R clones (HC1, HC4 and HC8) exhibited increased activity of EGFR, MAPK and AKT relative to the Ctx^S parental control (HP).[27] To determine if Ctx^R clones exhibited a dependency on AKT signaling we performed proliferation assays using two different non-overlapping small interfering RNAs (siRNA) targeting AKT1/2 (**Fig. 1A**). All three cetuximab-resistant lines displayed growth inhibitory effects at 50 nM with both siAKT1/2(a) and siAKT1/2(b). These data suggest that cells with acquired resistance to cetuximab depend on AKT signaling. Since both siAKT1/2 worked equally well, we chose to work with siAKT1/2(a) from Cell Signaling for remaining studies.

To investigate global activation of AKT signaling pathways in Ctx^R clones we utilized an AKT specific phosphoprotein antibody array to identify phosphorylated proteins that were upregulated in the Ctx^R clone HC4 as compared to parental control HP cells. This antibody array includes 137 well-characterized phospho-specific antibodies for proteins in the AKT pathway, each with six replicates. The paired antibodies for total protein levels for each target are also included in the array to allow determination of the relative levels of phosphorylation for each AKT substrate. Results from this array platform indicated several AKT substrates including c-Jun, eIF4E, GSK3β, IKKα, IRS-1, Raf-1 and S6 ribosomal protein (rpS6) were upregulated in the HC4 Ctx^R clone (**Fig. 1B**).

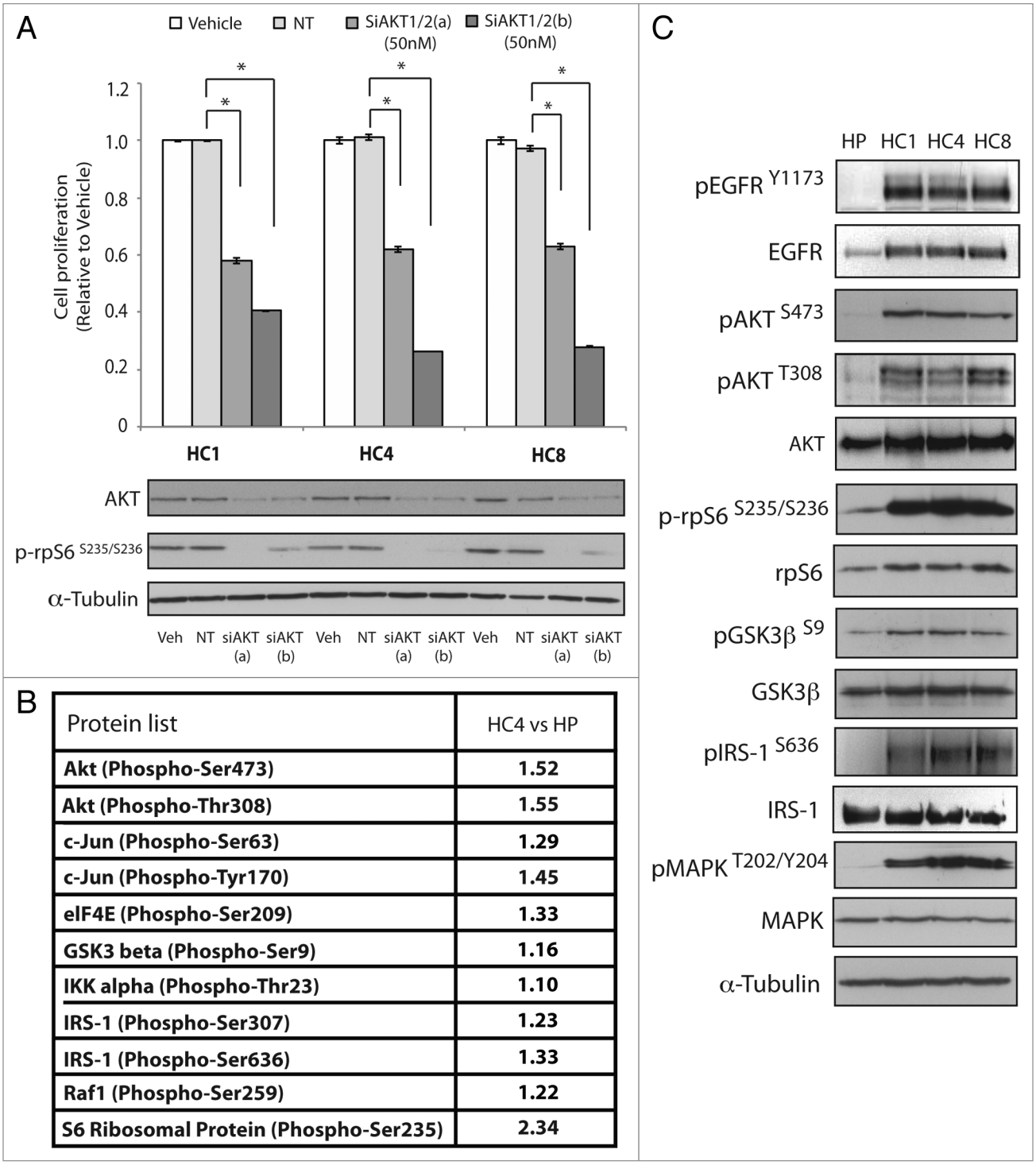

B

Protein list	HC4 vs HP
Akt (Phospho-Ser473)	**1.52**
Akt (Phospho-Thr308)	**1.55**
c-Jun (Phospho-Ser63)	**1.29**
c-Jun (Phospho-Tyr170)	**1.45**
eIF4E (Phospho-Ser209)	**1.33**
GSK3 beta (Phospho-Ser9)	**1.16**
IKK alpha (Phospho-Thr23)	**1.10**
IRS-1 (Phospho-Ser307)	**1.23**
IRS-1 (Phospho-Ser636)	**1.33**
Raf1 (Phospho-Ser259)	**1.22**
S6 Ribosomal Protein (Phospho-Ser235)	**2.34**

Figure 1. Ctx^R clones have increased AKT signaling pathway 5. (**A**) Ctx^R clones are dependent on AKT. Ctx^R clones were plated and treated with 50 nM of AKT1/2(a) siRNA, 50 nM of AKT1/2(b) siRNA or 50 nM non-targeting siRNA. Cell proliferation was measured at 96 h after treatment using the proliferation assay described in materials and methods. Data points are represented as mean ± SEM (n = 4). *p ≤ 0.05. Protein was collected at 96 h after treatment and fractioned by SDS-PAGE and immunoblotted for AKT and phopho-rpS6. α-Tubulin was used as a loading control. (**B**) Fold increase in expression of phosphorylated proteins in Ctx^R HC4 cells compared with parental control HP cells by phosphoprotein arrays. Ctx^S parental cells (HP) and Ctx^R clones (HC4) were harvested and lysed with the extraction buffer provided as described according to manufacturer's instructions for phosphoprotein arrays. (**C**) Ctx^R overexpress EGFR and have increased AKT signaling pathway 5. Ctx^S parental cells (HP) and Ctx^R clones (HC1, HC4 and HC8) were harvested and protein lysates were fractionated on SDS-PAGE followed by immunoblotting for the indicated proteins. α-Tubulin was used as a loading control.

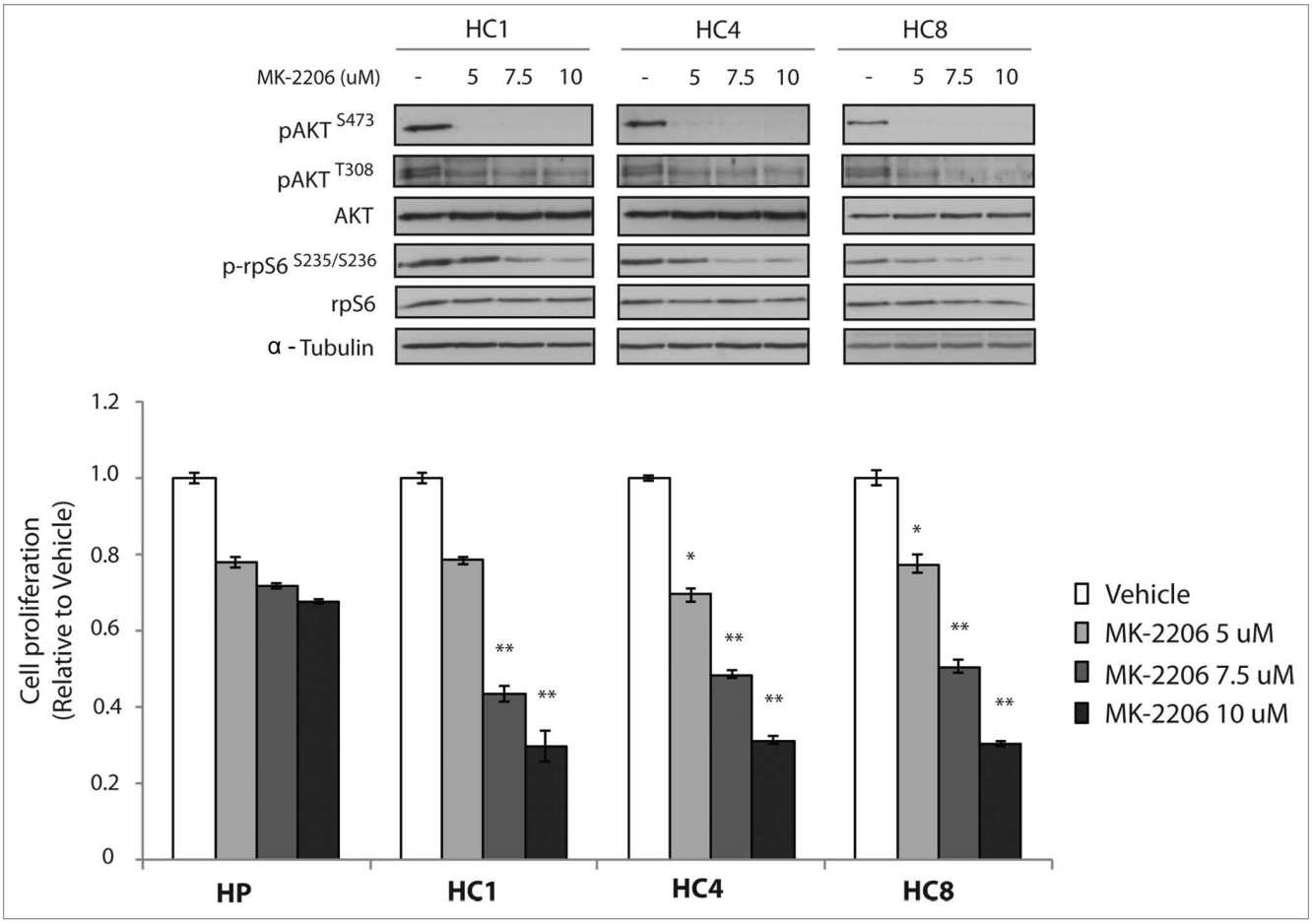

Figure 2. MK-2206, an AKT inhibitor, decreases cell proliferation of Ctx^R clones. MK-2206 significantly inhibits the proliferation of Ctx^R clones. Ctx^R clones (HC1, HC4 and HC8) and Ctx^S parental control (HP) were plated and allowed to adhere for 24 h prior to vehicle (DMSO) or MK-2206 treatment: 5 uM, 7.5 uM or 10 uM. Cell growth was measured at 72 h after drug treatment using the growth proliferation assay described in experimental methods. Data points are represented as mean ± SEM (n = 4). *p ≤ 0.05, **p ≤ 0.001. Whole cell protein lysates were collected after 24 h treatment and fractionated on SDS-PAGE followed by immunoblotting for the indicated proteins. α-Tubulin was used as a loading control.

To confirm the AKT specific phosphoprotein array results we analyzed the activity of various AKT effector molecules via western blot analysis in the three Ctx^R clones HC1, HC4 and HC8 (**Fig. 1C**). We confirmed that the AKT pathway effector molecules rpS6 (serine 235/236), GSK3β (serine 9) and IRS-1 (serine 636) were indeed highly active in all three Ctx^R clones. In addition to activation of MAPK, these results suggest that Ctx^R clones have enhanced activation of AKT signaling pathways and further, they exhibit dependence on these pathways for enhanced growth potential. Phosphorylation levels of AKT substrate proteins in HC4 cells compared with HP cells are summarized in **Table S1**.

Ctx^R cells have increased sensitivity to the allosteric AKT inhibitor MK-2206. We hypothesized that Ctx^R clones may be susceptible to AKT inhibitory therapies since these cells remained dependent on the AKT signaling pathway for sustained growth and survival. To test this hypothesis we challenged Ctx^R clones with the AKT inhibitor MK-2206 (5, 7.5 and 10 μM) for 24 h (**Fig. 2**). MK-2206 is a highly selective and potent non-ATP competitive allosteric AKT inhibitor that is currently undergoing clinical investigation for use in several types of solid tumors. We demonstrate that MK-2206 inhibits the activity of AKT by decreasing the phosphorylation of serine 473 (S473) and threonine 308 (T308), as well as phospho-rpS6 (serine 235/serine 236) (**Fig. 2**). While phospho-AKT S473 is inhibited with 5 μM of MK-2206 there is a dose dependent decrease in phosphorylation of AKT T308 and rpS6. Additionally, MK-2206 treatment demonstrated growth inhibitory effects of all Ctx^R clones with robust, dose dependent responses. This may be due to the enhanced inhibitory effects of AKT T308 and downstream targets at higher concentrations. Treatment with 7.5 μM MK-2206 reduced Ctx^R cell proliferation rates to approximately 50% compared with vehicle control treatment. MK-2206 treatment had minimal effect on the Ctx^S parental cells that have very low levels of AKT activation (**Fig. 1C**). Taken together these results suggest that Ctx^R cells are dependent on AKT activity for proliferation and MK-2206 is an effective treatment for cells with acquired resistance to cetuximab.

MK-2206 blocks AKT downstream signaling pathway in Ctx^R cells. We further explored the mechanisms of cell

growth inhibition in Ctx^R clones by MK-2206. To determine if MK-2206 effects the phosphorylation of other AKT targets in Ctx^R cells, we probed the same AKT specific phosphoprotein array with protein lysate harvested from the Ctx^R clone HC4 treated with 2.5 μM MK-2206 for 24 h. Results from this antibody array showed that 2.5 μM of MK-2206 treatment could mildly inhibit multiple downstream AKT targets including c-jun, eIF4E, GSK3β, IKKα, IRS-1, Raf1 and rpS6 (**Fig. 3A**). Since this is a multiplex array platform the fold changes detected on the array may actually be smaller than the true value. Thus we next validated in all three Ctx^R clones that the activation of AKT, rpS6 and GSK3β were indeed decreased upon treatment with 2.5 and 7.5 μM of MK-2206 for 24 h (**Fig. 3B**). Treatment with 7.5 μM MK-2206 showed significant decreases in the levels of phosphorylated AKT, rpS6 (50–90%) and GSK3β (60–80%), while total levels of AKT, rpS6 and GSK3β were not affected by MK-2206 treatment (**Fig. 3B**). These results indicate MK-2206 is able to abrogate the activation of AKT as well as its downstream signaling effector molecules, which may suggest why MK-2206 can be effective treatment in cetuximab resistant cell lines. Phosphorylation levels of AKT substrate proteins in HC4 cells with 2.5 μM MK-2206 treatment compared with vehicle control are summarized in **Table S1**.

MK-2206 plus cetuximab has greater therapeutic effect than either agent alone. We showed that Ctx^R cells are dependent on AKT activity for proliferation and MK-2206 is an effective treatment for cells with acquired resistance to cetuximab (**Fig. 1 and 2**). To determine if loss of AKT is important in acquired resistant to cetuximab, we treated Ctx^R clones with siAKT1/2(a) and cetuximab for 72 h. The combination treatments resulted in significant cell growth inhibition in Ctx^R clones (**Fig. 4**). Next, we examined if MK-2206 could have therapeutic benefit in Ctx^R cells with cetuximab treatment. We performed cell proliferation analysis using vehicle, cetuximab (0.1, 1, 10, 100 and 1,000 nM), MK-2206 (0.1, 1, 5 and 10 μM) or 100 nM cetuximab plus MK-2206 (0.1, 1, 5 and 10 μM) in HP, HC1, HC4 and HC8. Despite complete resistance up to 1,000 nM of cetuximab, addition of 100 nM of cetuximab led to a marked statistically significant increase of MK-2206 inhibitory potency over a wide range of MK-2206 doses (**Fig. 5A**). To see if the augmentation of growth inhibition of MK-2206 with cetuximab correlated with increased apoptosis, we performed Annexin-V analysis after treatment with vehicle, 100 nM cetuximab, 5 μM MK-2206 or the combination for 24 h (**Fig. 5B**). MK-2206 treatments resulted in a statistically significant increase in apoptosis of Ctx^R clones compared with vehicle control. Furthermore, combinatorial treatment (MK-2206 plus cetuximab) in two out of three cell lines induced a mild enhancement of apoptosis as compared with MK-2206 alone. We further investigated which pathways were inhibited by MK-2206 and cetuximab combination treatment. Ctx^R clones were treated with vehicle, 100 nM cetuximab, 5 uM MK-2206 or combinatorial treatment for 24 h. MAPK phosphorylation level was decreased by cetuximab treatment, while phosphorylation of AKT was inhibited by MK-2206 treatment (**Fig. 6**). Combination of cetuximab with MK-2206 resulted in an inhibition of both phospho-MAPK and phospho-AKT as

A

Protein list	HC4 2.5 uM MK2206 vs Untreated
Akt (Phospho-Ser473)	0.80
Akt (Phospho-Thr308)	0.88
c-Jun (Phospho-Ser63)	0.66
c-Jun (Phospho-Tyr170)	0.88
eIF4E (Phospho-Ser209)	0.82
GSK3 beta (Phospho-Ser9)	0.95
IKK alpha (Phospho-Thr23)	0.95
IRS-1 (Phospho-Ser307)	0.87
IRS-1 (Phospho-Ser636)	0.70
Raf1 (Phospho-Ser259)	0.89
S6 Ribosomal Protein (Phospho-Ser235)	0.70

B

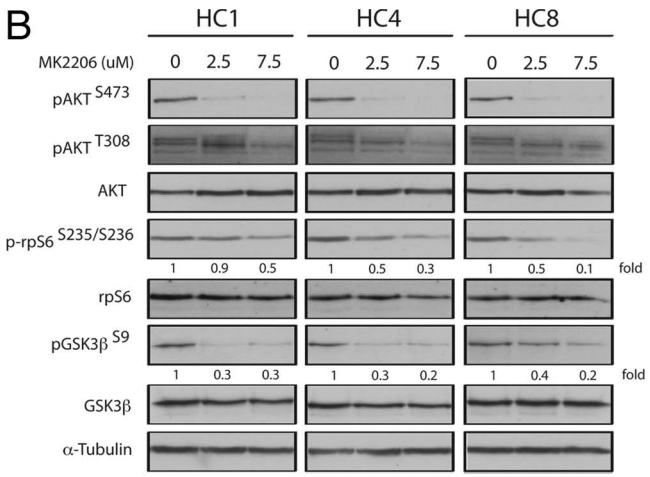

Figure 3. AKT downstream signaling molecules are effectively inhibited with MK-2206 treatment in Ctx^R clones. (**A**) Fold decrease in expression of phosphorylated proteins treated by MK-2206 in cetuximab-resistant HC4 Ctx^R cells compared with vehicle control HC4 cells by phosphoprotein arrays. Ctx^R clone (HC4) was harvested after treatment with 2.5 μM of MK-2206 and lysed with the extraction buffer provided as described according to manufacturer's instructions for phosphoprotein arrays. (**B**) Ctx^R clones (HC1, HC4 and HC8) were treated with vehicle (DMSO) or MK-2206 (2.5 or 7.5 μM) for 24 h. Whole cell protein lysates were fractionated on SDS-PAGE followed by immunoblotting for the indicated proteins. α-Tubulin was used as a loading control.

well as the downstream effector molecule phospho-rpS6 in all Ctx^R clones (**Fig. 6**). Interestingly, treatment with cetuximab or MK-2206 led to modest increases in steady-state expression of phospho-AKT or phospho-MAPK in Ctx^R clones. Overall, these data suggest that MK-2206 and cetuximab combinatorial treatment impact proliferation by the dual targeting of AKT and MAPK, resulting in the downregulation of two prominent signaling pathways.

Discussion

Cetuximab has exhibited promising antitumor activity in clinical trials particularly in the settings of mCRC and HNSCC either as monotherapy or in combination with chemotherapy and/or radiation.[15] However, acquired resistance to cetuximab remains a major obstacle for the successful use of this promising molecular

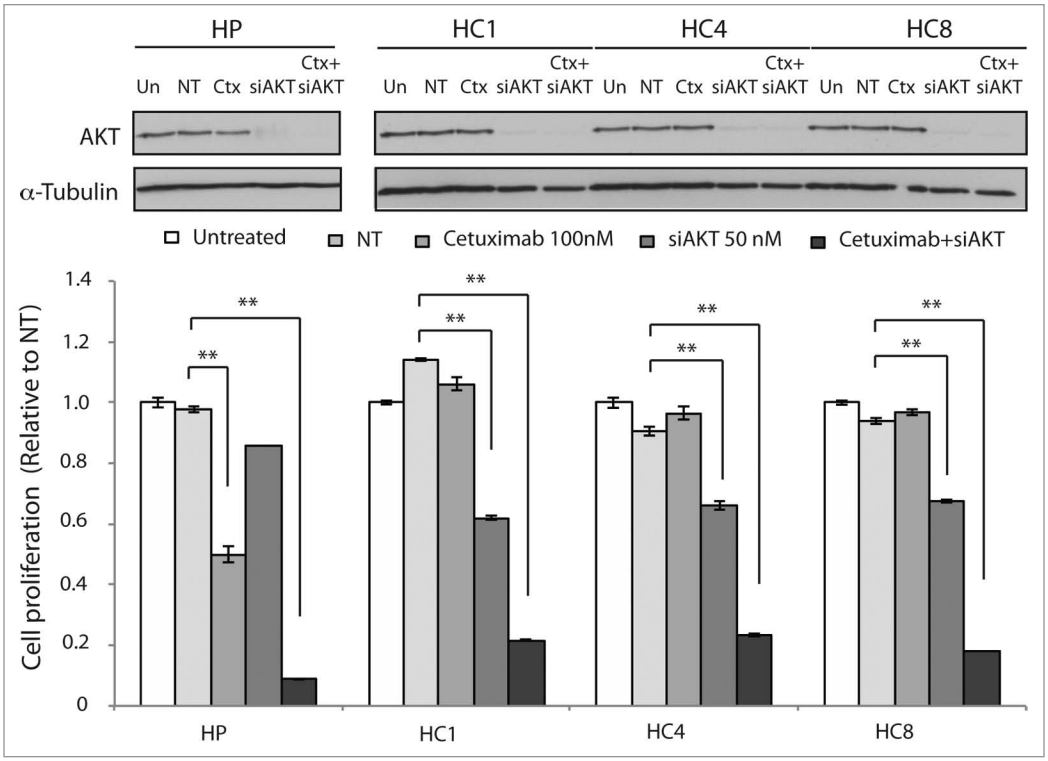

Figure 4. Combination treatment of siAKT and cetuximab Inhibit cell proliferation in Ctx^R clones. Ctx^R clones (HC1, HC4 and HC8) and parental controls (HP) were plated and treated with 50 nM of AKT1/2 siRNA(a) or 50 nM non-targeting siRNA. The next day, cells were treated with DMSO or 100 nM cetuximab for 72 h. Growth was measured at 72 h after drug treatment using the proliferation assay as described in the experimental procedures. Data points are represented as mean ± SEM (n = 4). **p ≤ 0.001. Protein was collected at 72 h after treatment and fractioned by SDS-PAGE and immunoblotted for AKT. α-Tubulin was used as a loading control.

targeting agent.[28,29] Previously, we developed a model of acquired resistance to cetuximab using the NSCLC NCI-H226.[27] Results from these studies indicated that Ctx^R cell lines had increased expression and activation of the EGFR, MAPK and AKT.[27]

In this study we investigated (1) if Ctx^R clones exhibited a dependency on AKT signaling pathways and (2) whether the allosteric AKT inhibitor MK-2206 could be advantageous in the setting of acquired resistance to cetuximab. Gene-silencing studies using siAKT indicated that all Ctx^R NCI-H226 clones remained addicted to AKT signaling pathways (**Fig. 1A**). Various other researchers have noted the upregulation of AKT signaling pathways in defined subsets of human NSCLC, supporting our current study, which demonstrates the overexpression of AKT signaling pathways in numerous Ctx^R clones.[30-32] We also found that Ctx^R cells exhibit increased steady-state activity of the EGFR (**Fig. 1B and C**). Studies by Kim et al. further support our findings by reporting that Ctx^R HCC827 clones also had increased AKT activation and marked decreased protein levels of PTEN.[33] Further, Chen et al. established a pair of cell lines from Huh7 hepatocellular carcinoma cells that are resistant to several tyrosine kinases and Raf kinase inhibitor sorafenib.[34] They found that sorafenib resistant cells exhibited upregulation of AKT signaling compared with the sorafenib sensitive parental Huh7 cells. These results indicate that acquired resistance to molecular targeting agents such as cetuximab and sorafenib may share a common mechanism of resistance through the activation of AKT and its downstream signaling pathways. Overall, the data presented in the current study demonstrate that the activation of AKT plays a role in cetuximab resistance and provides a rational strategy through which cetuximab-based treatment may be improved.

To evaluate this concept, we treated our Ctx^R clones with MK-2206, an AKT-specific inhibitor, and assayed growth inhibition. MK-2206 treatment yielded statistically significant cell growth inhibition of all Ctx^R clones (**Fig. 2**). AKT antibody array and immunoblot analyses revealed AKT substrates such as phospho-rpS6 and phospho-GSK3β were blocked by MK-2206 treatment (**Fig. 3**). We demonstrate that higher concentrations of MK-2206 may be necessary to completely inhibit the activation of AKT (T308) and its downstream targets, which may explain why Ctx^R cells are more sensitive to MK-2206 at higher doses. Hirai et al. determined similar findings in non-small-cell lung cancer cells (NSCLC), with an IC_{50} ranging between 3.4 and 28.6 μM, while AKT inhibition was detected at much lower concentrations.[35] These results suggested that AKT signaling pathways are essential for cell survival in Ctx^R clones and MK-2206 may be a valuable drug for inhibiting this pathway in a variety of cancers. Sangai et al. also revealed that MK-2206 had a dose-dependent effect on cell signaling and tumor growth. Although AKT phosphorylation was inhibited with clinically relevant doses, dose escalation had a greater effect on downstream effectors.[36] Our data indicated that increased amounts of MK-2206 lead to more potent decreases in AKT T308 and rpS6 as well as GSK3β activation (**Fig. 3B**).

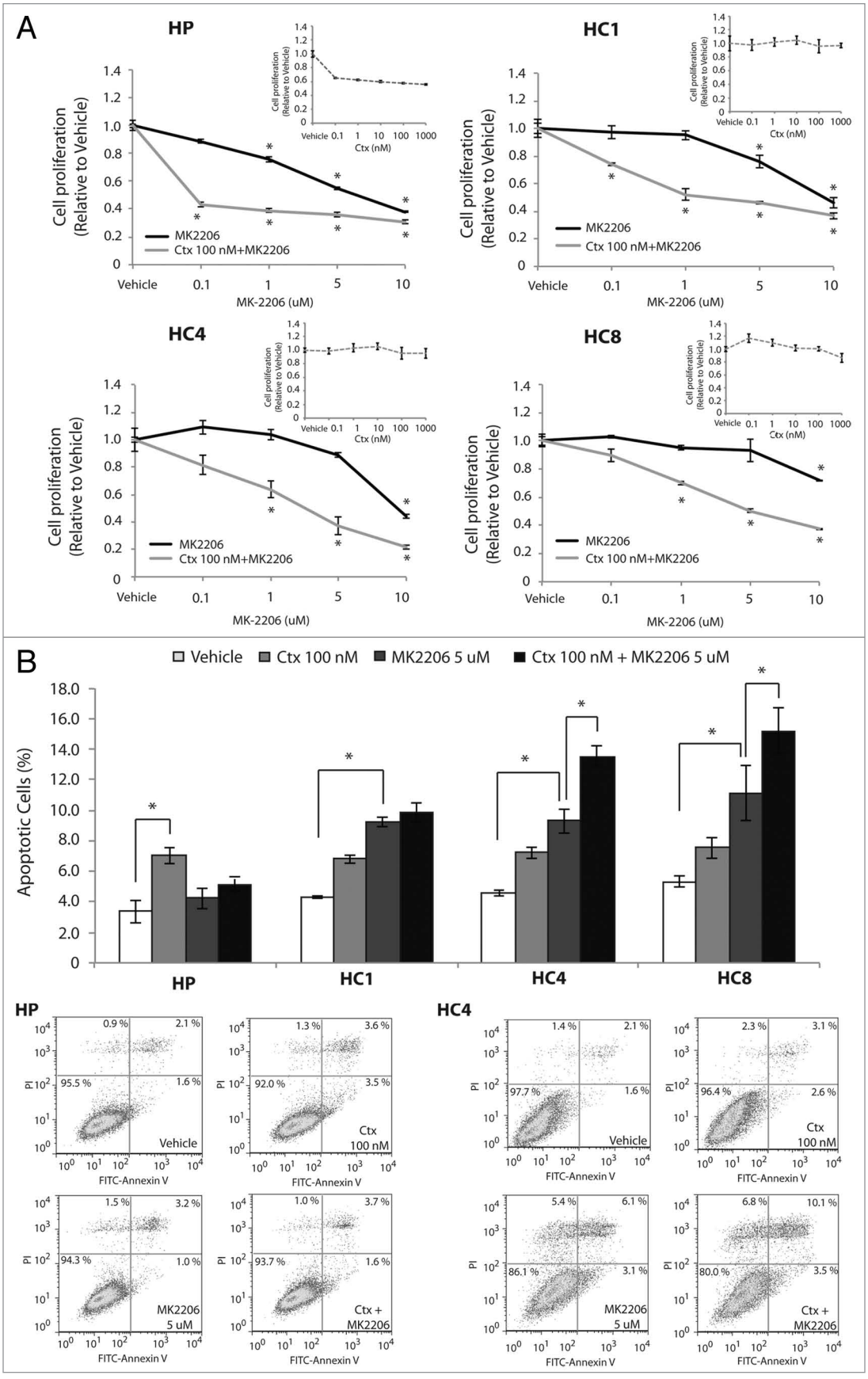

Figure 5. For figure legend, see page 8.

Figure 5 (See previous page). MK-2206 treatment enhanced the susceptibility of Ctx^R cells to cetuximab by inducing apoptosis. (**A**) MK-2206 treatment enhanced the susceptibility of Ctx^R cells to cetuximab. Ctx^R cells (HC1, HC4, HC8) and parental controls (HP) were treated with DMSO, Ctx (0.1–1,000 nM), MK-2206 (0.1–10 μM) or the combination of Ctx 100 nM+ MK-2206 (0.1–10 μM), for 72 h. Growth was measured 72 h after drug treatment using the proliferation assay described in the experimental procedures. Data points are represented as mean ± SEM (n = 4). *p ≤ 0.05. (**B**) MK-2206 plus Cetuximab induced modest apoptosis in Ctx^R clones. Ctx^S parental cell line (HP) or Ctx^R cell lines (HC1, HC4, HC8) were plated and allowed to adhere for 24 h prior to treatment with vehicle (DMSO), cetuximab (100 nM), MK-2206 (5 μM) or the combination (cetuximab + MK-2206) for 24 h prior to Annexin-V analysis via flow cytometry. Annexin-V analysis was described in the materials and methods. Data points are represented as mean ± SEM (n = 3). *p ≤ 0.05. Flow cytometry profile represents Annexin-V-FITC staining in x axis and PI in y axis. The number represents the percentage of cells in each condition.

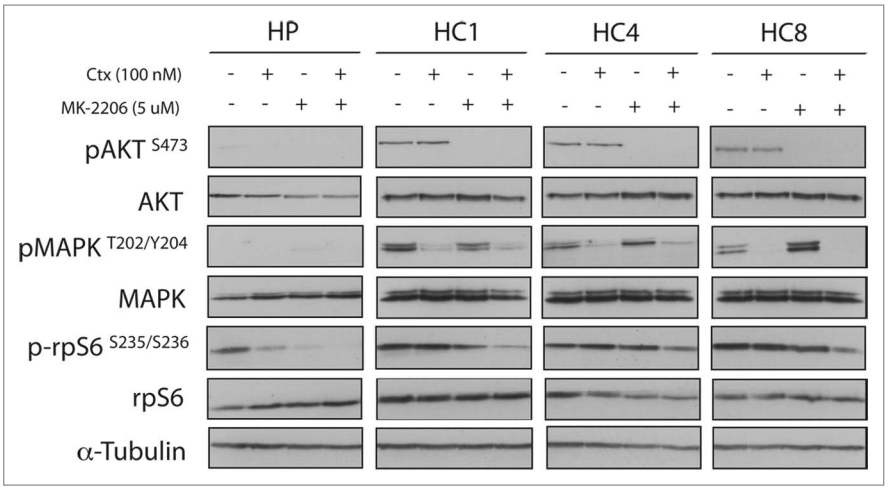

Figure 6. Dual blockade of AKT and EGFR have beneficial effects on AKT and MAPK activity. Ctx^R cells (HC1, HC4 and HC8) were plated and treated with the DMSO (vehicle), 100 nM cetuximab, 5 μM MK-2206 or the combination (cetuximab + MK-2206) for 24 h. Cells were harvested and protein was collected, fractionated by SDS-PAGE and immunoblotted for the indicated proteins. α-Tubulin was used as a loading control.

Treatment of Ctx^R clones with AKT siRNA alone and in addition to cetuximab also significantly inhibited cell proliferation (**Fig. 4**). Further, we analyzed if combinatorial MK-2206 and cetuximab therapy would result in greater anti-proliferative activity than either agent alone (**Fig. 5A**). Addition of 100 nM of cetuximab led to a marked increase of MK-2206 inhibitory potency over a wide range of MK-2206 doses. Various mechanisms have been proposed for the anti-proliferative effects observed with MK-2206 treatment, including the induction of apoptosis, autophagy and promotion of cell cycle arrest.[35,37-40] Cheng et al. reported that the EGFR inhibitor gefitinib could induce approximately 10–17% of glioblastoma cells to undergo apoptosis and MK-2206 treatment enhanced these levels by approximately 10%.[40] In the current study, we observed that MK-2206 treatment alone could induce mild levels of apoptosis (approximately 10% in two cetuximab resistant cell lines), while the addition of cetuximab could enhance levels by approximately 5% (**Fig. 5B**). Thus, the anti-proliferative effects observed with MK-2206 treatment alone and in combination with cetuximab in the current study may be due to alternative mechanisms other than apoptosis.

In the current study, MK-2206 and cetuximab treatment demonstrated greater growth inhibitory effects than MK-2206 alone in all Ctx^R clones. The treatment of Ctx^R clones with cetuximab had no effect on proliferation but did, however, inhibit the activation of MAPK (**Fig. 6**). This finding demonstrates that Ctx^R cells have developed dependency on other growth promoting pathways. When cells were challenged with MK-2206 we observed a growth inhibitory effect that was greatly enhanced with the addition of cetuximab (**Fig. 5**). We speculate that MK-2206 can augment cetuximab response because this combination inhibits both AKT and MAPK activation (**Fig. 6**) and thereby downregulates two critical pathways of cellular proliferation. This finding highlights the importance of simultaneously inhibiting both AKT and MAPK activation to achieve maximal growth inhibitory potential and suggests that either pathway can compensate for the loss of the other to maintain growth-promoting signals. In the current model of cetuximab resistance, Ctx^R cells have become dependent on AKT activity to maintain their growth potential, which is effectively targeted with MK-2206, and enhanced through the inhibition of MAPK with cetuximab. This point is further supported by the modest compensatory increased activation of either AKT by cetuximab or MAPK by MK-2206 (**Fig. 6**). Previous studies have also described similar compensatory activation of AKT upon inhibition of either the MAPK or mTOR1 pathways.[41-46] Overall, the concurrent blockade of AKT and MAPK seems to be crucial for the maximal growth inhibition of Ctx^R clones, a strategy that may be a useful in overcoming cetuximab resistance.

Currently, MK-2206 is undergoing clinical trials in the numerous tumor settings. Yap et al. reported that 33 patients with advanced solid tumors such as colon/rectum, breast, pancreatic and lung received MK-2206 on alternate days. The MK-2206 was well tolerated at biologically active doses that inhibit AKT signaling in this phase I clinical trial.[26] Pal et al. also summarized several ongoing phase I studies with advanced solid tumors using MK-2206 or combinations of both cytotoxic agents and targeted therapies with MK-2206 (for a review see ref. 47).[47] In the current study we demonstrate that AKT and EGFR, through MAPK, cooperate in acquired resistance to cetuximab, suggesting that combinatorial treatment with both cetuximab and MK-2206 or potentially MAPK inhibitors may be an effective strategy for future translational research in the setting of acquired resistance.

Materials and Methods

Cell lines. The human NSCLC line NCI-H226 was purchased from ATCC. The cells were maintained in 10% fetal bovine serum in RPMI-1640 (Mediatech Inc.) with 1% penicillin and streptomycin. The development of cells with acquired resistance to cetuximab has been previously described.[27]

siRNA and transfection. For siRNAs, Ctx^R cells (HC1, HC4 and HC8) were transiently transfected with siRNAs siAKT1/2(a) (#6211S, Cell Signaling Technology) or siAKT1/2(b) (sc-43609, Santa Cruz biotechnology, Inc.) using Lipofectamine RNAiMAX according to the manufacturer's instructions (Invitrogen). The non-targeting siRNA (ON-TARGETplus Non-targeting Pool, #D-001810-10) was obtained from Dharmacon as a control. Cells were then lysed for analysis of protein knockdown by immunoblotting after siRNA transfection.

Compounds. Cetuximab (ICM225, Erbitux) was generously provided by ImClone Systems Inc. MK-2206 was generously provided by Merck Research Laboratories.

All antibodies were purchased from commercial sources as indicated below: EGFR, pEGFR (Y1173), AKT and HRP-conjugated goat-anti-rabbit IgG and goat-anti-mouse IgG were obtained from Santa Cruz Biotechnology Inc. pAKT (S473), pAKT (T308), prpS6 (S235/S236), rpS6, pGSK3β (S9), GSK3β, IRS-1, p-MAPK (T202/Y204) and MAPK were obtained from Cell Signaling Technology. pIRS-1 (S636) was purchased by Thermo Scientific. α-Tubulin was purchased from Calbiochem.

Cell proliferation assay. Cells were seeded at 2,000 cells per well in 100 µl of media on a 96 well plate, grown for 24 h and then treated with drug for 72 h prior to analysis using the Cell Counting Kit 8 (Dojindo Molecular Technologies). Ten microliters of CCK-8 solution was added to each well and incubated for one hour prior to absorbance analysis (A450 nm with plate reader). The percentage of cell growth was calculated by comparison of the A450 reading from treated vs. vehicle control wells. All treatments were performed in quadruplicate.

Immunoblotting analysis. Whole cell protein lysate was obtained by tween-20 lysis buffer (50 mM HEPES, pH 7.4, 150 mM NaCl, 0.1% Tween-20, 10% glycerol, 2.5 mM EGTA, 1 mM EDTA, 1 mM DTT, 1 mM Na_3VO_4, 1 mM PMSF, 1 mM BGP and 10 µg/ml of leupeptin and aprotinin). Samples were sonicated and then centrifuged at 15,000 g for 10 min at 4°C. Protein concentrations were determined by Bradford assay (Bio-Rad Laboratories). Equal amounts of protein were fractionated by SDS-PAGE, transferred to a PVDF membrane (Millipore) and analyzed by incubation with the appropriate primary antibody. Proteins were detected via incubation with HRP-conjugated secondary antibodies and ECL Western Blotting Substrate (Promega Cooperation), SuperSignal* West Dura Extended Duration Chemiluminescent Substrate or SuperSignal* West Femto Maximum Sensitivity Chemiluminescent Substrate (Thermo Fisher Scientific).

Annexin-V apoptosis assay. An amount of 800,000 cells were plated in 100 mm plates and after 24 h of incubation treated with either vehicle, 100 nM cetuximab, 5 uM MK-2206 and the combination for 24 h and harvested after trypsinization. Next, cells were washed with PBS, resuspended in binding buffer (BD Biosciences) and stained with FITC Annexin-V (FITC Annexin-V apoptosis detection kit, BD Biosciences). The cells were analyzed by flow cytometry (BD FACScan). FlowJo Software (Tree Star, Inc.) was used to analyze the data. All experimental arms were done in triplicate and displayed as averages with standard error bars.

Phosphoprotein antibody array. Phosphoprotein arrays were obtained from FullMoon Biosystems, Inc. Cells were seeded in three 150 mm culture dishes and treated 24 h: (1) HP with vehicle, (2) HC4 with vehicle and (3) HC4 with 2.5 µM of MK-2206. Cells were lysed with the extraction buffer provided as described according to manufacturer's instructions. Antibody array analysis was performed by FullMoon Biosystems.

Disclosure of Potential Conflicts of Interest

No potential conflict of interest was disclosed.

Acknowledgments

This project was supported, in part, by grant P30CA014520 from the National Cancer Institute, by grant RSG-10-193-01-TBG from the American Cancer Society (D.L.W.) and by NIH grant T32 GM08.1061-01A2 from Graduate Training in Cellular and Molecular Pathogenesis of Human Diseases (T.M.B.) and the Clinical and Translational Science Award (CTSA) program, previously through the National Center for Research Resources (NCRR) grant 1UL1RR025011 and now by the National Center for Advancing Translational Sciences (NCATS), grant 9U54TR000021 (D.L.W.). The content is solely the responsibility of the authors and does not necessarily represent the official views of the NIH.

Supplemental Materials

Supplemental materials may be found here:
www.landesbioscience.com/journals/cbt/article/24342

References

1. Citri A, Yarden Y. EGF-ERBB signalling: towards the systems level. Nat Rev Mol Cell Biol 2006; 7:505-16; PMID:16829981; http://dx.doi.org/10.1038/nrm1962.
2. Li S, Schmitz KR, Jeffrey PD, Wiltzius JJ, Kussie P, Ferguson KM. Structural basis for inhibition of the epidermal growth factor receptor by cetuximab. Cancer Cell 2005; 7:301-11; PMID:15837620; http://dx.doi.org/10.1016/j.ccr.2005.03.003.
3. Jonker DJ, O'Callaghan CJ, Karapetis CS, Zalcberg JR, Tu D, Au HJ, et al. Cetuximab for the treatment of colorectal cancer. N Engl J Med 2007; 357:2040-8; PMID:18003960; http://dx.doi.org/10.1056/NEJMoa071834.
4. Chung KY, Shia J, Kemeny NE, Shah M, Schwartz GK, Tse A, et al. Cetuximab shows activity in colorectal cancer patients with tumors that do not express the epidermal growth factor receptor by immunohistochemistry. J Clin Oncol 2005; 23:1803-10; PMID:15677699; http://dx.doi.org/10.1200/JCO.2005.08.037.
5. Sobrero AF, Maurel J, Fehrenbacher L, Scheithauer W, Abubakr YA, Lutz MP, et al. EPIC: phase III trial of cetuximab plus irinotecan after fluoropyrimidine and oxaliplatin failure in patients with metastatic colorectal cancer. J Clin Oncol 2008; 26:2311-9; PMID:18390971; http://dx.doi.org/10.1200/JCO.2007.13.1193.

6. Borner M, Koeberle D, Von Moos R, Saletti P, Rauch D, Hess V, et al.; Swiss Group for Clinical Cancer Research (SAKK), Bern, Switzerland. Adding cetuximab to capecitabine plus oxaliplatin (XELOX) in first-line treatment of metastatic colorectal cancer: a randomized phase II trial of the Swiss Group for Clinical Cancer Research SAKK. Ann Oncol 2008; 19:1288-92; PMID:18349029; http://dx.doi.org/10.1093/annonc/mdn058.
7. Bokemeyer C, Bondarenko I, Makhson A, Hartmann JT, Aparicio J, de Braud F, et al. Fluorouracil, leucovorin, and oxaliplatin with and without cetuximab in the first-line treatment of metastatic colorectal cancer. J Clin Oncol 2009; 27:663-71; PMID:19114683; http://dx.doi.org/10.1200/JCO.2008.20.8397.
8. Van Cutsem E, Köhne CH, Hitre E, Zaluski J, Chang Chien CR, Makhson A, et al. Cetuximab and chemotherapy as initial treatment for metastatic colorectal cancer. N Engl J Med 2009; 360:1408-17; PMID:19339720; http://dx.doi.org/10.1056/NEJMoa0805019.
9. Vermorken JB, Mesia R, Rivera F, Remenar E, Kawecki A, Rottey S, et al. Platinum-based chemotherapy plus cetuximab in head and neck cancer. N Engl J Med 2008; 359:1116-27; PMID:18784101; http://dx.doi.org/10.1056/NEJMoa0802656.
10. Bonner JA, Harari PM, Giralt J, Azarnia N, Shin DM, Cohen RB, et al. Radiotherapy plus cetuximab for squamous-cell carcinoma of the head and neck. N Engl J Med 2006; 354:567-78; PMID:16467544; http://dx.doi.org/10.1056/NEJMoa053422.
11. Herbst RS, Arquette M, Shin DM, Dicke K, Vokes EE, Azarnia N, et al. Phase II multicenter study of the epidermal growth factor receptor antibody cetuximab and cisplatin for recurrent and refractory squamous cell carcinoma of the head and neck. J Clin Oncol 2005; 23:5578-87; PMID:16009949; http://dx.doi.org/10.1200/JCO.2005.07.120.
12. Baselga J, Trigo JM, Bourhis J, Tortochaux J, Cortés-Funes H, Hitt R, et al. Phase II multicenter study of the antiepidermal growth factor receptor monoclonal antibody cetuximab in combination with platinum-based chemotherapy in patients with platinum-refractory metastatic and/or recurrent squamous cell carcinoma of the head and neck. J Clin Oncol 2005; 23:5568-77; PMID:16009950; http://dx.doi.org/10.1200/JCO.2005.07.119.
13. Burtness B, Goldwasser MA, Flood W, Mattar B, Forastiere AA; Eastern Cooperative Oncology Group. Phase III randomized trial of cisplatin plus placebo compared with cisplatin plus cetuximab in metastatic/recurrent head and neck cancer: an Eastern Cooperative Oncology Group study. J Clin Oncol 2005; 23:8646-54; PMID:16314626; http://dx.doi.org/10.1200/JCO.2005.02.4646.
14. Pao W, Miller VA, Politi KA, Riely GJ, Somwar R, Zakowski MF, et al. Acquired resistance of lung adenocarcinomas to gefitinib or erlotinib is associated with a second mutation in the EGFR kinase domain. PLoS Med 2005; 2:e73; PMID:15737014; http://dx.doi.org/10.1371/journal.pmed.0020073.
15. Brand TM, Iida M, Wheeler DL. Molecular mechanisms of resistance to the EGFR monoclonal antibody cetuximab. Cancer Biol Ther 2011; 11:777-92; PMID:21293176; http://dx.doi.org/10.4161/cbt.11.9.15050.
16. Staal SP, Hartley JW, Rowe WP. Isolation of transforming murine leukemia viruses from mice with a high incidence of spontaneous lymphoma. Proc Natl Acad Sci U S A 1977; 74:3065-7; PMID:197531; http://dx.doi.org/10.1073/pnas.74.7.3065.
17. Bellacosa A, Testa JR, Moore R, Larue L. A portrait of AKT kinases: human cancer and animal models depict a family with strong individualities. Cancer Biol Ther 2004; 3:268-75; PMID:15034304; http://dx.doi.org/10.4161/cbt.3.3.703.
18. Cantley LC. The phosphoinositide 3-kinase pathway. Science 2002; 296:1655-7; PMID:12040186; http://dx.doi.org/10.1126/science.296.5573.1655.
19. Sarbassov DD, Guertin DA, Ali SM, Sabatini DM. Phosphorylation and regulation of Akt/PKB by the rictor-mTOR complex. Science 2005; 307:1098-101; PMID:15718470; http://dx.doi.org/10.1126/science.1106148.
20. Bozulic L, Surucu B, Hynx D, Hemmings BA. PKBalpha/Akt1 acts downstream of DNA-PK in the DNA double-strand break response and promotes survival. Mol Cell 2008; 30:203-13; PMID:18439899; http://dx.doi.org/10.1016/j.molcel.2008.02.024.
21. Mahajan K, Mahajan NP. PI3K-independent AKT activation in cancers: a treasure trove for novel therapeutics. J Cell Physiol 2012; 227:3178-84; PMID:22307544; http://dx.doi.org/10.1002/jcp.24065.
22. Engelman JA. Targeting PI3K signalling in cancer: opportunities, challenges and limitations. Nat Rev Cancer 2009; 9:550-62; PMID:19629070; http://dx.doi.org/10.1038/nrc2664.
23. Courtney KD, Corcoran RB, Engelman JA. The PI3K pathway as drug target in human cancer. J Clin Oncol 2010; 28:1075-83; PMID:20085938; http://dx.doi.org/10.1200/JCO.2009.25.3641.
24. Fayard E, Xue G, Parcellier A, Bozulic L, Hemmings BA. Protein kinase B (PKB/Akt), a key mediator of the PI3K signaling pathway. Curr Top Microbiol Immunol 2010; 346:31-56; PMID:20517722; http://dx.doi.org/10.1007/82_2010_58.
25. Vasudevan KM, Garraway LA. AKT signaling in physiology and disease. Curr Top Microbiol Immunol 2010; 347:105-33; PMID:20549472; http://dx.doi.org/10.1007/82_2010_66.
26. Yap TA, Yan L, Patnaik A, Fearen I, Olmos D, Papadopoulos K, et al. First-in-man clinical trial of the oral pan-AKT inhibitor MK-2206 in patients with advanced solid tumors. J Clin Oncol 2011; 29:4688-95; PMID:22025163; http://dx.doi.org/10.1200/JCO.2011.35.5263.
27. Wheeler DL, Huang S, Kruser TJ, Nechrebecki MM, Armstrong EA, Benavente S, et al. Mechanisms of acquired resistance to cetuximab: role of HER (ErbB) family members. Oncogene 2008; 27:3944-56; PMID:18297114; http://dx.doi.org/10.1038/onc.2008.19.
28. Wheeler DL, Dunn EF, Harari PM. Understanding resistance to EGFR inhibitors-impact on future treatment strategies. Nat Rev Clin Oncol 2010; 7:493-507; PMID:20551942; http://dx.doi.org/10.1038/nrclinonc.2010.97.
29. Vincenzi B, Zoccoli A, Pantano F, Venditti O, Galluzzo S. Cetuximab: from bench to bedside. Curr Cancer Drug Targets 2010; 10:80-95; PMID:20088790; http://dx.doi.org/10.2174/156800910790980241.
30. Dobashi Y, Suzuki S, Kimura M, Matsubara H, Tsubochi H, Imoto I, et al. Paradigm of kinase-driven pathway downstream of epidermal growth factor receptor/Akt in human lung carcinomas. Hum Pathol 2011; 42:214-26; PMID:21040950; http://dx.doi.org/10.1016/j.humpath.2010.05.025.
31. David O, Jett J, LeBeau H, Dy G, Hughes J, Friedman M, et al. Phospho-Akt overexpression in non-small cell lung cancer confers significant stage-independent survival disadvantage. Clin Cancer Res 2004; 10:6865-71; PMID:15501963; http://dx.doi.org/10.1158/1078-0432.CCR-04-0174.
32. Suzuki S, Igarashi S, Hanawa M, Matsubara H, Ooi A, Dobashi Y. Diversity of epidermal growth factor receptor-mediated activation of downstream molecules in human lung carcinomas. Mod Pathol 2006; 19:986-98; PMID:16648865; http://dx.doi.org/10.1038/modpathol.3800619.
33. Kim SM, Kim JS, Kim JH, Yun CO, Kim EM, Kim HK, et al. Acquired resistance to cetuximab is mediated by increased PTEN instability and leads cross-resistance to gefitinib in HCC827 NSCLC cells. Cancer Lett 2010; 296:150-9; PMID:20444542; http://dx.doi.org/10.1016/j.canlet.2010.04.006.
34. Chen KF, Chen HL, Tai WT, Feng WC, Hsu CH, Chen PJ, et al. Activation of phosphatidylinositol 3-kinase/Akt signaling pathway mediates acquired resistance to sorafenib in hepatocellular carcinoma cells. J Pharmacol Exp Ther 2011; 337:155-61; PMID:21205925; http://dx.doi.org/10.1124/jpet.110.175786.
35. Hirai H, Sootome H, Nakatsuru Y, Miyama K, Taguchi S, Tsujioka K, et al. MK-2206, an allosteric Akt inhibitor, enhances antitumor efficacy by standard chemotherapeutic agents or molecular targeted drugs in vitro and in vivo. Mol Cancer Ther 2010; 9:1956-67; PMID:20571069; http://dx.doi.org/10.1158/1535-7163.MCT-09-1012.
36. Sangai T, Akcakanat A, Chen H, Tarco E, Wu Y, Do KA, et al. Biomarkers of response to Akt inhibitor MK-2206 in breast cancer. Clin Cancer Res 2012; 18:5816-28; PMID:22932669; http://dx.doi.org/10.1158/1078-0432.CCR-12-1141.
37. Balasis ME, Forinash KD, Chen YA, Fulp WJ, Coppola D, Hamilton AD, et al. Combination of farnesyltransferase and Akt inhibitors is synergistic in breast cancer cells and causes significant breast tumor regression in ErbB2 transgenic mice. Clin Cancer Res 2011; 17:2852-62; PMID:21536547; http://dx.doi.org/10.1158/1078-0432.CCR-10-2544.
38. Li Z, Yan S, Attayan N, Ramalingam S, Thiele CJ. Combination of an allosteric Akt Inhibitor MK-2206 with etoposide or rapamycin enhances the antitumor growth effect in neuroblastoma. Clin Cancer Res 2012; 18:3603-15; PMID:22550167; http://dx.doi.org/10.1158/1078-0432.CCR-11-3321.
39. Pant A, Lee II, Lu Z, Rueda BR, Schink J, Kim JJ. Inhibition of AKT with the orally active allosteric AKT inhibitor, MK-2206, sensitizes endometrial cancer cells to progestin. PLoS One 2012; 7:e41593; PMID:22911820; http://dx.doi.org/10.1371/journal.pone.0041593.
40. Cheng Y, Zhang Y, Zhang L, Ren X, Huber-Keener KJ, Liu X, et al. MK-2206, a novel allosteric inhibitor of Akt, synergizes with gefitinib against malignant glioma via modulating both autophagy and apoptosis. Mol Cancer Ther 2012; 11:154-64; PMID:22057914; http://dx.doi.org/10.1158/1535-7163.MCT-11-0606.
41. Mirzoeva OK, Das D, Heiser LM, Bhattacharya S, Siwak D, Gendelman R, et al. Basal subtype and MAPK/ERK kinase (MEK)-phosphoinositide 3-kinase feedback signaling determine susceptibility of breast cancer cells to MEK inhibition. Cancer Res 2009; 69:565-72; PMID:19147570; http://dx.doi.org/10.1158/0008-5472.CAN-08-3389.
42. Gopal YN, Deng W, Woodman SE, Komurov K, Ram P, Smith PD, et al. Basal and treatment-induced activation of AKT mediates resistance to cell death by AZD6244 (ARRY-142886) in Braf-mutant human cutaneous melanoma cells. Cancer Res 2010; 70:8736-47; PMID:20959481; http://dx.doi.org/10.1158/0008-5472.CAN-10-0902.
43. Villanueva J, Vultur A, Lee JT, Somasundaram R, Fukunaga-Kalabis M, Cipolla AK, et al. Acquired resistance to BRAF inhibitors mediated by a RAF kinase switch in melanoma can be overcome by cotargeting MEK and IGF-1R/PI3K. Cancer Cell 2010; 18:683-95; PMID:21156289; http://dx.doi.org/10.1016/j.ccr.2010.11.023.
44. O'Reilly KE, Rojo F, She QB, Solit D, Mills GB, Smith D, et al. mTOR inhibition induces upstream receptor tyrosine kinase signaling and activates Akt. Cancer Res 2006; 66:1500-8; PMID:16452206; http://dx.doi.org/10.1158/0008-5472.CAN-05-2925.
45. Tabernero J, Rojo F, Calvo E, Burris H, Judson I, Hazell K, et al. Dose- and schedule-dependent inhibition of the mammalian target of rapamycin pathway with everolimus: a phase I tumor pharmacodynamic study in patients with advanced solid tumors. J Clin Oncol 2008; 26:1603-10; PMID:18332469; http://dx.doi.org/10.1200/JCO.2007.14.5482.

46. Lu Y, Muller M, Smith D, Dutta B, Komurov K, Iadevaia S, et al. Kinome siRNA-phosphoproteomic screen identifies networks regulating AKT signaling. Oncogene 2011; 30:4567-77; PMID:21666717; http://dx.doi.org/10.1038/onc.2011.164.
47. Pal SK, Reckamp K, Yu H, Figlin RA. Akt inhibitors in clinical development for the treatment of cancer. Expert Opin Investig Drugs 2010; 19:1355-66; PMID:20846000; http://dx.doi.org/10.1517/13543784.2010.520701.

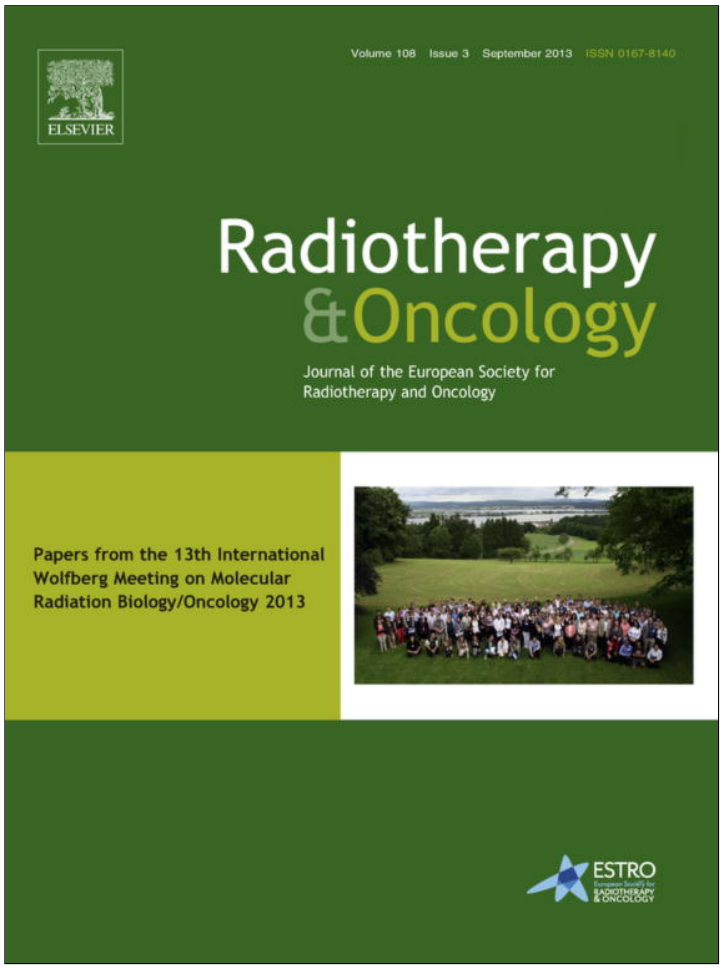

Radiotherapy and Oncology 108 (2013) 370–377

Contents lists available at SciVerse ScienceDirect

Radiotherapy and Oncology

journal homepage: www.thegreenjournal.com

Review

Nuclear EGFR as a molecular target in cancer

Toni M. Brand, Mari Iida, Neha Luthar, Megan M. Starr, Evan J. Huppert, Deric L. Wheeler *

Department of Human Oncology, University of Wisconsin School of Medicine and Public Health, Wisconsin Institute for Medical Research, Madison, USA

ARTICLE INFO

Article history:
Received 25 April 2013
Received in revised form 4 June 2013
Accepted 10 June 2013
Available online 3 July 2013

Keywords:
Nuclear EGFR
Cancer
Resistance

ABSTRACT

The epidermal growth factor receptor (EGFR) has been one of the most targeted receptors in the field of oncology. While anti-EGFR inhibitors have demonstrated clinical success in specific cancers, most patients demonstrate either intrinsic or acquired resistance within one year of treatment. Many mechanisms of resistance to EGFR inhibitors have been identified, one of these being attributed to alternatively localized EGFR from the cell membrane into the cell's nucleus. Inside the nucleus, EGFR functions as a co-transcription factor for several genes involved in cell proliferation and angiogenesis, and as a tyrosine kinase to activate and stabilize proliferating cell nuclear antigen and DNA dependent protein kinase. Nuclear localized EGFR is highly associated with disease progression, worse overall survival in numerous cancers, and enhanced resistance to radiation, chemotherapy, and the anti-EGFR therapies gefitinib and cetuximab. In this review the current knowledge of how nuclear EGFR enhances resistance to cancer therapeutics is discussed, in addition to highlighting ways to target nuclear EGFR as an anti-cancer strategy in the future.

The epidermal growth factor receptor (EGFR) is one of four members of the HER family of receptor tyrosine kinases [1,2]. EGFR contains an extracellular ligand-binding domain, a single membrane-spanning region, a juxtamembrane nuclear localization signal (NLS), a tyrosine kinase domain, and a tyrosine-rich C-terminal tail. Ligand binding causes a conformational change in the receptor that allows for both homo- and hetero-dimerization with other activated HER family members [3]. Dimerization activates the intrinsic tyrosine kinase of each receptor, leading to the phosphorylation of tyrosine residues on each receptor's C-terminal tails. This process serves to activate various growth-promoting signaling cascades such as the RAS/MAPK, PI(3)K/Akt, PLCγ/PKC, and Jak/STAT pathways.

Several early reports describe the overexpression of EGFR in a variety of epithelial tumors. These findings support the hypothesis that deregulated EGFR expression and signaling may play a critical role in the etiology of several human cancers, including lung, head and neck squamous cell carcinoma (HNSCC), colon, pancreatic, brain and breast [4–8]. Discovery of EGFR overexpression in cancer has led to substantial efforts over the last four decades to target the EGFR as a cancer treatment strategy. One approach uses monoclonal antibodies to target the extracellular domain of the EGFR to block natural ligand binding [9,10]. Cetuximab (IMC-C225, Erbitux) prevents receptor activation and dimerization, ultimately inducing receptor internalization and down regulation [11]. Cetuximab, either as monotherapy or in combination with chemotherapy and/or radiation, exhibits promising antitumor activity in HNSCC and metastatic colorectal cancer. A second approach utilizes small molecule tyrosine kinase inhibitors (TKIs) that bind to the ATP-binding site in the tyrosine kinase domain of the EGFR. Three anti-EGFR TKIs, erlotinib (OSI-774, Tarceva), gefitinib (ZD1839, Iressa) and lapatinib (GW572016, Tykerb), have been approved by the FDA for use in oncology. Despite intense clinical and preclinical efforts to develop EGFR inhibitors, collectively they have had modest success in curing patients of tumors that express the EGFR. The underwhelming success of these EGFR inhibitors suggests that a more comprehensive understanding of EGFR biology is needed.

Although plasma membrane EGFR signaling has been intensely researched over the last thirty years, new functions of the EGFR are now beginning to unravel. One new prominent mode of EGFR signaling has been found in the cell's nucleus [12–14]. Research over the last decade has deciphered a distinct series of steps for nuclear EGFR transport [15–18]. Activation of the EGFR results in its endocytosis and interaction with importin β1 via its tripartite nuclear localization sequence (NLS) [19]. EGFR is described to undergo

Abbreviations: EGFR, epidermal growth factor receptor; NLS, nuclear localization signal; DNA-PK, DNA protein kinase; PCNA, proliferating cell nuclear antigen; NPC, nuclear pore complex; ONM, outer nuclear membrane; INM, inner nuclear membrane; iNOS, nitric oxide synthase; COX-2, cyclooxygenase-2; BCRP, breast cancer resistant protein; HNSCC, head and neck squamous cell carcinoma; NLS, nuclear localization sequence; NSLC, non-small cell lung cancer; TKI, tyrosine kinase inhibitor; PNPase, polynucleotide phosphorylase; TNBC, triple negative breast cancer; MUC1, mucin-1; RHA, RNA helicase A; TIP3, TAT interacting protein; LMP1, latent membrane protein 1; TIF2, transcriptional intermediary factor 2.

* Corresponding author. Address: Department of Human Oncology, University of Wisconsin Comprehensive Cancer Center, 1111 Highland Avenue, WIMR 3159, Madison, WI 53705, USA.

E-mail address: dlwheeler@wisc.edu (D.L. Wheeler).

0167-8140/$ - see front matter © 2013 Elsevier Ireland Ltd. All rights reserved.
http://dx.doi.org/10.1016/j.radonc.2013.06.010

COPI-mediated retrograde trafficking from the Golgi to the ER [16]. Once embedded into the ER membrane, EGFR and importin β1 interface with nucleoporins in the nuclear pore complex (NPC) to shuttle EGFR from the outer nuclear membrane (ONM) to the inner nuclear membrane (INM). INM embedded EGFR can be released into the nucleoplasm via association with the Sec61β translocon. This process has been termed the Integral Trafficking from the ER to the Nuclear Envelope Transport model [20].

Upon entry into the nucleus, the EGFR can function in ways distinct from its plasma membrane bound counterpart. Three major functions of nuclear EGFR have been identified (Fig. 1). First, nuclear EGFR can function as a co-transcription factor. Although it was shown in 1994 that a kinase dead EGFR could enhance transcriptional expression of the c-fos gene [21], it was not until 2001 that a landmark paper provided direct evidence that EGFR could regulate the cyclin D1 promoter [22]. Since these initial findings, nuclear EGFR has been shown to co-regulate inducible nitric oxide synthase (iNOS), B-Myb, cyclooxygenase-2 (COX-2), aurora kinase A, c-Myc, breast cancer resistant protein (BCRP), and Stat1 [23–28]. Second, nuclear EGFR has been shown to phosphorylate proliferating cell nuclear antigen (PCNA) on Y211, thereby increasing PCNA stability and ultimately enhancing cellular proliferation. Lastly, EGFR has been shown to enter the nucleus upon radiation treatment and interact with DNA-dependent protein kinase (DNA-PK) leading to repair of radiation-induced DNA double strand breaks [29,30]. Importantly, these nuclear functions have been inversely correlated with overall patient survival in breast, ovarian, oropharyngeal, gallbladder, and lung cancer providing a strong rationale for the molecular targeting of this nuclear receptor [31–36].

The role of nuclear EGFR in resistance to cancer therapeutics

Intrinsic and acquired tumor cell resistance to both conventional and targeted cancer therapies remains one of the largest obstacles to overcome clinically. While nuclear EGFR is observed in cells of high proliferative origin, numerous reports describe increased nuclear localization of EGFR in models of cancer resistance to different therapeutic regimes [28,29,37–39]. These studies identified that nuclear EGFR could enhance resistance by influencing DNA damage repair, DNA replication, and transcription of oncogenes [28,29,37–39]. Thus, nuclear EGFR is now emerging as a potent biomarker for response to numerous cancer therapies. In the following paragraphs, we will discuss the role of nuclear EGFR in resistance to radiation, chemotherapy and the anti-EGFR targeted therapies gefitinib and cetuximab.

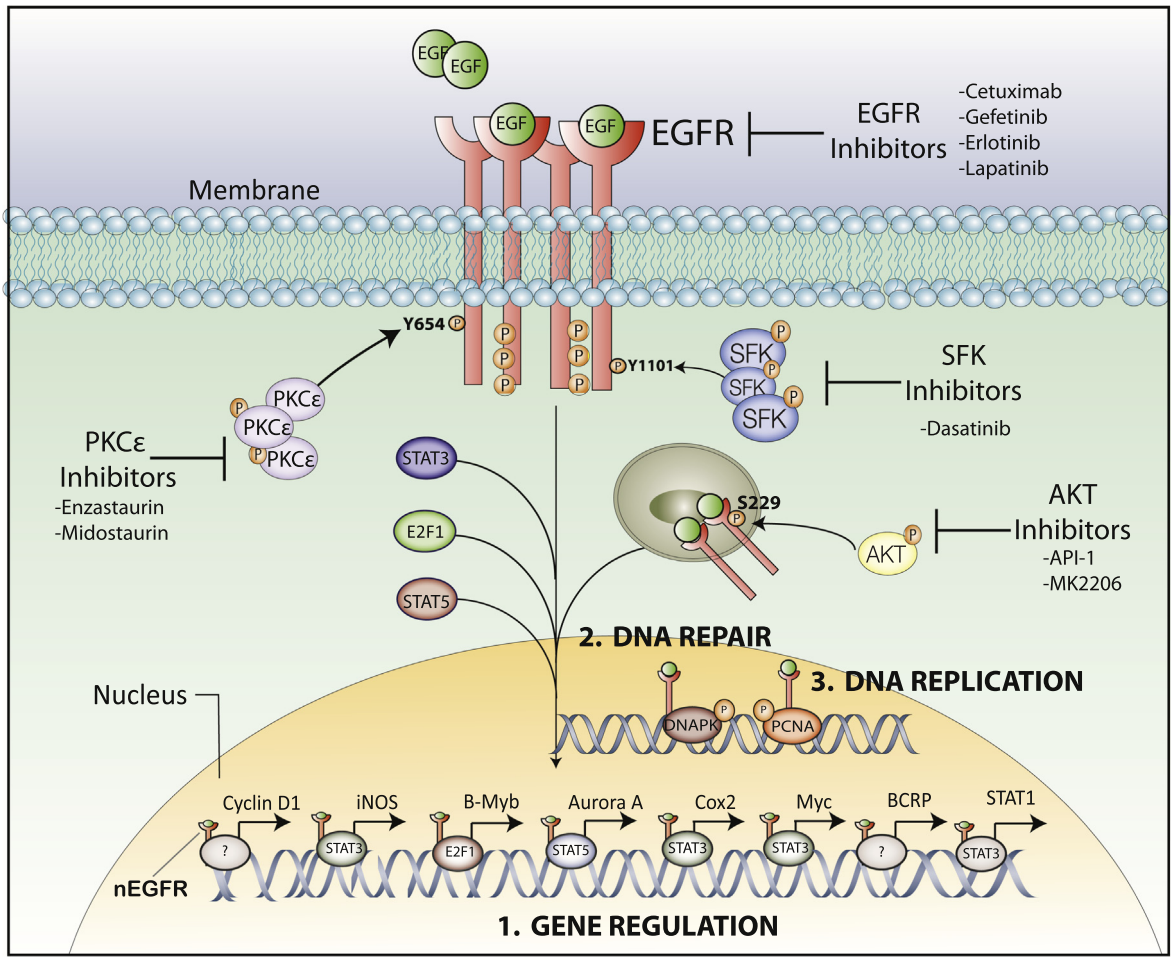

Fig. 1. Nuclear EGFR translocation and function. The nuclear translocation of EGFR has been shown to be dependent on specific phosphorylation events by various intracellular kinases. EGFR phosphorylation at Tyrosine 1101 by SFKs, Serine 229 by AKT, and Threonine 654 by PKCε, have all been shown to stimulate nuclear EGFR translocation. In the nucleus, EGFR has been shown to function as a co-transcription factor alongside STAT3, E2F1, and STAT5 to enhance the transcription of eight gene targets. Nuclear EGFR can also activate and stabilize DNA-PK and PCNA to enhance DNA repair and replication. Collectively, these functions may be inhibited through drugs that target the intracellular kinases identified to influence nuclear EGFR translocation, and thereby sensitize cancer cells to radiation, chemotherapy, and anti-EGFR therapies such as cetuximab and gefitinib.

Nuclear EGFR and radiation resistance

Radiation therapy is one of the most common anti-cancer treatments used due to its ability to induce widespread DNA damage in tumor cells. Enhanced tumor cell DNA damage repair can lead to radiation resistance, a process that is mediated by DNA-PK [40]. In 1997, Schmidt-Ullrich and colleagues observed that radiation treatment of tumor cells led to EGFR activation and internalization similar to growth factor stimulation of the EGFR [41]. Further research demonstrated that tumor cells could be radiosensitized upon inhibition of EGFR activation with cetuximab [42,43], suggesting that EGFR plays a role in promoting DNA damage repair pathways. Pioneering studies by Dittmann et al. demonstrated that EGFR and DNA-PK form a complex in the nucleus upon radiation treatment, and that this interaction enhanced DNA-PK activity and DNA repair [30,44]. Importantly, inhibition of nuclear EGFR localization led to the inactivation of DNA-PK, resulting in less DNA damage repair and increased radiation response [29,30].

To further understand the molecular requirements of nuclear EGFR transport, Dittmann et al. demonstrated that the phosphorylation of EGFR at Tyrosine 654 was necessary for radiation induced nuclear transport and DNA damage repair [45,46]. Additional studies showed that nuclear EGFR participates in chromatin relaxation, a necessary step for recruitment of repair proteins to DNA double strand breaks [47]. A recent study by Liccardi et al. elaborated on these findings by demonstrating that EGFR mutants lacking nuclear localization (constitutively active EGFR L858R and EGFR lacking its NLS) had decreased repair of radiation induced DNA double strand breaks [37]. Collectively, this body of work supports the important role of nuclear EGFR in enhancing DNA-PK induced DNA damage repair upon treatment with radiation therapy.

Interestingly, reports have identified two radioprotectors that enhance the nuclear transport of EGFR in tissues with wild-type p53. *O*-phospho-tyrosine and Bowman–Birk proteinase inhibitor were shown to induce nuclear EGFR localization and activation of DNA-PK in p53 wild-type cells, deeming these cells more resistant to radiation [46,48]. These two radioprotectors may protect normal tissues that have wild-type p53 from the deleterious effects of radiation therapy. PKCε was also shown to play a role in the nuclear translocation of EGFR and *O*-phospho-tyrosine radioprotection, both of which were lost upon PKCε knockdown [49]. Overall, these studies support the role of nuclear EGFR in resistance to radiation therapy.

Most recently, a study identified that nuclear EGFR plays a key role in regulating the activity of an exoribonuclease termed polynucleotide phosphorylase (PNPase), which can function to degrade c-Myc mRNA in the cytoplasm [50]. Researchers show that radiation treatment of breast cancer cells promotes the nuclear association of EGFR and PNPase, and that this association was linked via DNA-PK phosphorylation of PNPase at Serine 776. The phosphorylation of PNPase at Serine 776 abolished its ribonuclease activity and led to the upregulation of c-Myc expression, thereby enhancing radioresistance. Upon inhibition of EGFR or DNA-PK activity, PNPase was no longer activated and c-Myc levels were downregulated, increasing radiosensitivity [50]. Overall, this study highlights a novel role of nuclear EGFR in the regulation of PNPase and augmentation of radiation response.

Nuclear EGFR and cisplatin resistance

Cisplatin is a mainstay chemotherapy used to treat a variety of cancers. Cisplatin elicits DNA damage through crosslinking DNA, preventing replication and cell division and thereby triggering apoptosis [51]. Treatment of tumor cells with cisplatin has also been shown to induce nuclear EGFR translocation much like radiation treatment. In 2009, Hsu et al. demonstrated that wild-type EGFR stable cells were resistant to cisplatin and had enhanced DNA repair upon treatment, while EGFR deleted of its NLS exhibited hindered DNA repair capabilities and sensitivity to cisplatin [39]. Liccardi et al. further supported these findings by showing that stable cell lines deficient in nuclear EGFR lacked DNA crosslinking repair mechanisms and association/activation of DNA-PK [37].

Nuclear EGFR and anti-EGFR therapy resistance

Similar to radiation and chemotherapy, *in-vitro* models studying cancer cell resistance to both gefitinib and cetuximab have demonstrated that resistant cells often retain dependency on the EGFR for enhanced growth potential and contain high levels of nuclear EGFR [28,38,52]. In the case of gefitinib resistance, nuclear EGFR was shown to function as a co-transcriptional activator for breast cancer resistant protein (BCRP/ABCG2), a plasma-membrane bound ATP dependent transporter that can extrude anti-cancer drugs from cells and thereby diminish their effects [28]. Authors hypothesize that this ATP dependent transporter may function to remove gefitinib from cells and thereby enhance resistance [28].

Cetuximab resistance has also been attributed to nuclear EGFR. Various researchers have demonstrated that cetuximab treatment can enhance the nuclear localization of EGFR [38,53,54], and that cell lines with intrinsic resistance to cetuximab contain high levels of nuclear EGFR [38]. In the setting of acquired resistance to cetuximab, Li et al. demonstrated that resistant cells have enhanced nuclear EGFR levels, which was attributed to increased Src Family Kinase (SFK) activity [38,52,55]. Inhibition of SFKs with the small molecule inhibitor dasatinib decreased nuclear EGFR and enhanced plasma membrane bound EGFR levels [38]. Importantly, treatment of resistant cells with dasatinib resensitized them to cetuximab. These findings were further validated via the use of a nuclear localization sequence-tagged EGFR, which enhanced cetuximab resistance in sensitive parental cells [38]. Collectively, this body of work demonstrates that nuclear EGFR plays a role in resistance to both gefitinib and cetuximab therapies.

Targeting nuclear EGFR in cancer: where are we now?

The current body of work focused on the roles of nuclear EGFR in cancer provides a strong rationale for learning how to target this subcellular receptor. Targeting nuclear EGFR may also enhance a cancer cell's dependency on classical membrane-bound functions of EGFR (such as activation of traditional signaling pathways) and thereby sensitize these cells to established targeting agents. Over the past decade numerous studies have focused on the specific proteins and post-translational modifications of EGFR necessary for its nuclear translocation and function. In the following paragraphs we will discuss these molecular determinants and how they have been used to target nuclear EGFR in cancer cells.

Targeting nuclear EGFR with anti-EGFR therapies

Current anti-EGFR therapies inhibit the activation of the EGFR via prevention of ligand binding, receptor dimerization, and through association with the ATP binding pocket of the kinase domain [56,57]. In 2009, Kim et al. demonstrated that the small molecule EGFR inhibitor lapatinib could inhibit EGF induced nuclear EGFR translocation in two breast cancer cell lines; however endogenous levels of nuclear EGFR were not changed [58]. While this study provided evidence that anti-EGFR inhibitors may prevent nuclear EGFR translocation, the majority of current research suggests that these therapies enhance EGFR endocytosis and

nuclear translocation, especially in the setting of acquired resistance [28,38,53,59,60]. In Fig. 2 a panel of HNSCC and breast cancer cell lines were treated with the anti-EGFR inhibitors erlotinib and lapatinib for 24 h and then harvested for whole cell, non-nuclear, and nuclear proteins. While both inhibitors prevented the activation of EGFR at Tyrosine 1173 (Fig. 2A), they did not effect, and in some cases enhanced, nuclear EGFR levels (Fig. 2B). In the HNSCC cell lines in particular, there is an enhancement of non-nuclear EGFR levels as well. This observation may be due to increased EGFR internalization upon TKI treatment, a phenomenon observed in cells treated with cetuximab and gefintib [28,38,53]. Induction of nuclear EGFR translocation may be a rescue mechanism by which a cell becomes more reliant on internal kinase-independent functions of EGFR. Additionally, Weihua et al. further showed that a kinase-dead EGFR is capable of inhibiting autophagic cell death in cancer cell lines, demonstrating that EGFR induced tumorigenesis maybe independent of its kinase activity [61]. Researchers have further demonstrated that a kinase-dead EGFR can undergo endocytosis [62], and work from our lab has indicated that kinase-dead EGFR can effectively translocate to the nucleus (Fig. 3). Collectively, these data suggest that (1) nuclear EGFR is not accurately targeted by kinase inhibiting anti-EGFR therapeutics, and (2) nuclear EGFR translocation and function may be independent of kinase activity, a mechanism by which a cancer cell can sustain enhanced growth and survival.

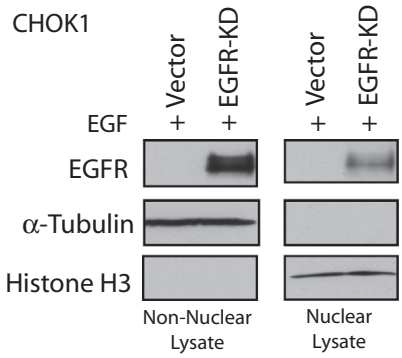

Fig. 3. Kinase dead EGFR can effectively translocate to the nucleus. CHOK1 cells were transfected with vector control or EGFR-kinase dead (KD) for 48 h prior to harvesting non-nuclear and nuclear protein. Lysates were fractionated on SDS–PAGE followed by immunoblotting for EGFR. α-Tubulin and histone H3 were used as loading and purity controls for the non-nuclear and nuclear fractions, respectively.

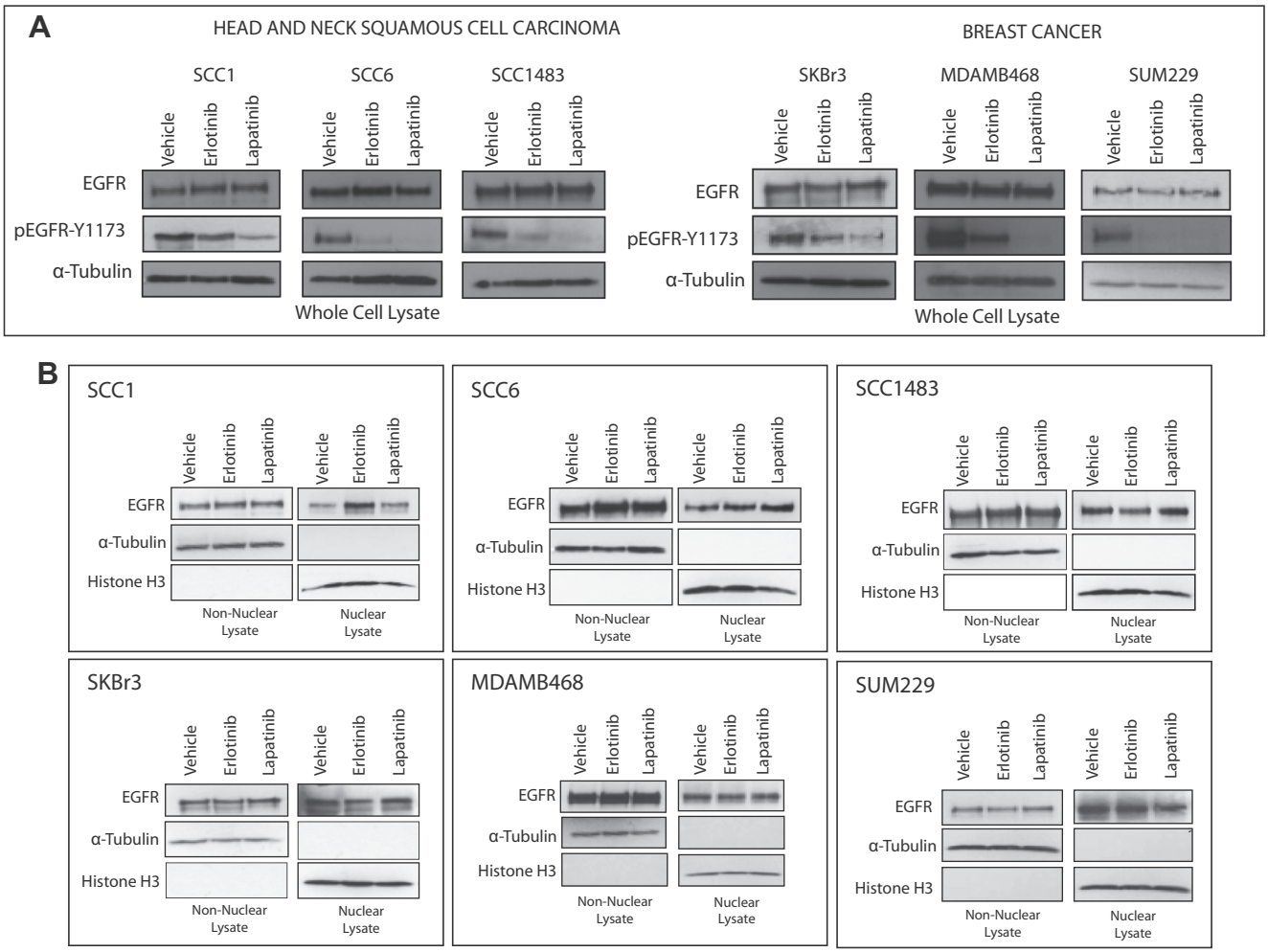

Fig. 2. Current anti-EGFR therapies do not inhibit nuclear EGFR localization. (A) Whole cell lysate was harvested from the HNSCC cell lines SCC1, SCC6, and SCC1483, and from the breast cancer cell lines SKBr3, MDAMB468, and SUM229 24 h post treatment with 100 nM erlotinib or lapatinib therapies. Lysates were fractionated on SDS–PAGE followed by immunoblotting for EGFR, pEGFR-Y1173, and α-tubulin as a loading control. (B) Non-nuclear and nuclear proteins were harvested from the same cell lines 24 h post treatment with 100 nM erlotinib or lapatinib therapies. Lysates were fractionated on SDS–PAGE followed by immunoblotting for EGFR. α-tubulin and Histone H3 were used as loading and purity controls for the non-nuclear and nuclear fractions, respectively.

Targeting nuclear EGFR via AKT inhibition

The initial studies aimed at targeting nuclear EGFR were focused in cell lines that demonstrated resistance to both cetuximab and gefitinib therapies [28,38]. These cell lines were established by treating cells *in-vitro* with increasing concentrations of drug over a several month time period until resistance was observed. Cell lines in both models of resistance demonstrated enhanced nuclear localization of the EGFR as compared to sensitive parental lines [28,38]. In the gefitinib resistant setting, Huang et al. demonstrated that the activity of AKT was enhanced, and that EGFR was specifically phosphorylated by AKT on Serine 229 to promote EGFR nuclear translocation [28]. Importantly, the overexpression of EGFR mutated at Serine 229 or the use of an AKT inhibitor rendered resistant cells more sensitive to gefitinib. Collectively, these data suggest that AKT inhibition may successfully inhibit nuclear EGFR transport and thereby sensitize cells to anti-EGFR therapies such as gefitinib [28].

Targeting nuclear EGFR via Src family kinase inhibition

In the setting of cetuximab resistance, work from our laboratory has shown that resistant cells have both enhanced nuclear EGFR and SFK activity [38,55]. Initial studies demonstrated that SFK inhibition could prevent nuclear EGFR translocation and enhance sensitivity to cetuximab therapy [38]. Further research identified that the SFK family members Yes and Lyn were overexpressed in cetuximab resistant clones and that these SFKs directly phosphorylated EGFR at Tyrosine 1101 to initiate EGFR nuclear translocation [63]. These data demonstrated that nuclear EGFR may be accurately targeted via SFK inhibition of phospho-Tyrosine 1101. Interestingly, current anti-EGFR therapies do not inhibit the activation of EGFR at Tyrosine 1101 (Fig. 4), which may further explain why these agents do not accurately target nuclear EGFR. Collectively, the inhibition of EGFR at Tyrosine 1101 and Serine 229 activity (Fig. 5) with both SFK and AKT inhibitors may lead to the complete inhibition of nuclear EGFR translocation, and sensitization of cells to current anti-EGFR agents [28,38,63].

Targeting nuclear EGFR via the selective COX-2 inhibitor celecoxib

The COX-2 inhibitor celecoxib has demonstrated radiosensitizing effects in various tumors [64,65]. Interestingly, anti-tumor effects of celecoxib treatment have been observed in cell lines that did not express COX-2 to a high degree [66,67]. To elucidate the mechanism of celecoxib radiosensitization, Dittmann et al. demonstrated that celecoxib could inhibit both basal and radiation-induced nuclear EGFR translocation in various cancer cell lines [68]. Celecoxib also inhibited radiation-induced phosphorylation of DNA-PK at Threonine 2609 in cell lines that were radiosensitized with this drug. Overall, this study highlights a COX-2 independent mechanism of celecoxib radiosensitization through the direct inhibition of nuclear EGFR translocation [68]. Thus, this inhibitor may prove to be useful for treatment of nuclear EGFR expressing tumors, even for tumors lacking COX-2 expression.

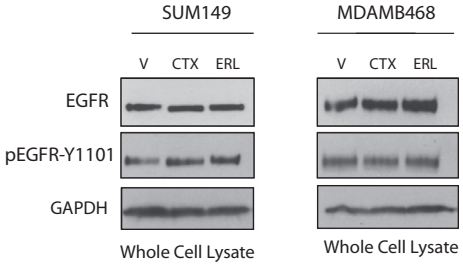

Fig. 4. Current anti-EGFR targeted therapies do not inhibit the phosphorylation of EGFR at Tyrosine 1101. SUM149 and MDAMB468 cells were treated with 100 nM cetuximab or erlotinib for 24 h. Whole cell lysate was fractionated on SDS–PAGE followed by immunotblotting for EGFR and phospho-EGFR Y1101. GAPDH was used as a loading control. V; vector control, CTX; cetuximab, ERL; erlotinib.

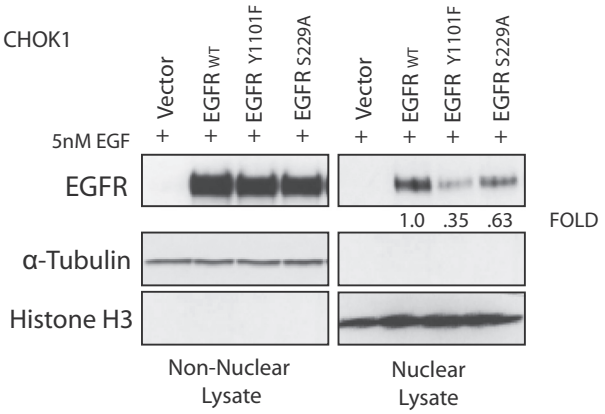

Fig. 5. Phosphorylation of Tyrosine 1101 and Serine 229 influence nuclear EGFR translocation. CHOK1 cells were transfected with vector control, EGFR-WT, EGFR-Y1101F, or EGFR-S229A for 48 h prior to harvesting non-nuclear and nuclear protein. Lysates were fractionated on SDS–PAGE followed by immunoblotting for EGFR. α-Tubulin and Histone H3 were used as loading and purity controls for the non-nuclear and nuclear fractions, respectively.

Targeting nuclear EGFR via PCNA inhibition

Another method of targeting nuclear EGFR is to directly inhibit the activity of its effector molecules. One main effector molecule of nuclear EGFR is PCNA. Nuclear EGFR was initially shown to associate and phosphorylate PCNA at tyrosine 211, which resulted in PCNA stabilization on chromatin and decreased proteosomal degradation, ultimately enhancing DNA replication and repair [69]. In a recent study by Yu et al. researchers demonstrate that treatment of triple negative breast cancer (TNBC) cells with an anti-PCNA peptide (targeting Tyrosine 211) can inhibit the growth of cells *in-vitro* and *in-vivo* mouse models [59]. Additionally, researchers established both geftinib and erlotinib resistant cell lines, both of which contained enhanced nuclear EGFR and activated PCNA levels. Treatment of these resistant cell lines with the anti-PCNA peptide sensitized all cell lines to their respective therapies. These studies suggest that the inhibition of the nuclear EGFR effector molecule PCNA may enhance the dependency of cells on classical EGFR signaling pathways and thereby re-sensitize them to EGFR inhibitors.

Prospective targets of nuclear EGFR translocation and/or function

Over the past five years various studies have identified key proteins that play a role in the regulation of nuclear EGFR translocation and function. The transmembrane protein mucin-1 (MUC1) [70] and RNA helicase A (RHA) [71] have been shown to be instrumental for EGFR association with target gene promoters in the nucleus. Additionally, the transcriptional co-factor Tat interacting protein (TIP3) has been shown to suppress nuclear EGFR translocation, while conversely its loss enhances nuclear EGFR translocation and function [72]. Finally, the latent membrane protein 1 (LMP1) has been shown to promote the interaction of nuclear EGFR with transcriptional intermediary factor 2 (TIF2) to upregulate cyclin D1 expression [73]. Finally, Wanner et al. demonstrated that PKCε could phosphorylate EGFR at Threonine 654 to induce EGFR's nuclear translocation in response to radiation therapy [49]. PKCε

inhibitors such as midostaurin (PKC412) and enzastaurin (LY317615) have been available since the early 2000s and have shown radiosensitizing capabilities, however, their ability to target nuclear EGFR has yet to be examined [74]. Collectively, the proteins MUC1, RHA, TIP2, LMP1, and PKCε may be potential future targets for the inhibition of both nuclear EGFR translocation and function.

Future prospective of the nuclear RTK field

From the identification of nuclear localized EGFR in highly proliferative tissues to the uncovering of its vibrant roles in enhancing tumorigenic processes, the field of nuclear HER family receptors has blossomed over the past ten years. Even with the exposé of over 50 articles citing the presence and/or functions of nuclear EGFR in cancer, this field is still in its infancy. Studies have yet to show that nuclear EGFR functions as a true oncogene separate from its membrane-localized counterpart. The answer to this question lies in the ability to isolate nuclear EGFR and demonstrate that it can lead to the formation and/or progression of cancer on its own. This feat is extremely hard to combat in the laboratory, since membrane, cytoplasmic, and nuclear localized EGFR function simultaneously to elicit downstream oncogenic effects. With the knowledge that nuclear EGFR plays a role in resistance to various cancer therapeutics, and that it is correlated with worse overall survival in numerous cancers, there is an over-arching need to target this nuclear receptor and potentially use it as a biomarker to predict therapeutic outcome in the future.

Materials and methods

Cell lines

The human HNSCC cell lines SCC1, SCC6, and SCC1483 were kindly supplied by Dr. T. Carey (University of Michigan, MI, USA) [75]. The human breast cancer cell lines SKBr3, MDAMB468, and SUM229 were kindly supplied by Dr. J. Boerner (Wayne State University School of Medicine, Karmanos Cancer Institute, MI, USA) [76]. The human MCF-7 and hamster CHOK1 cells were purchased from ATCC (Manassas, VA, USA). All cell lines were maintained in their respective media with 10% fetal bovine serum and 1% penicillin and streptomycin; SCC1, SCC6, SCC1483, SKBR3, and SUM229 cells were maintained in Dulbecco's modified Eagle's medium (Mediatech Inc., Manassas, VA, USA); MDAMB468 and MCF-7 cells were maintained in DMEM/F12K medium (Mediatech Inc.); and CHOK1 cells were maintained in F12K medium (Mediatech Inc.).

Antibodies and compounds

All antibodies were obtained from the following sources: EGFR (SC-03), Histone H3, and HRP-conjugated goat-anti-rabbit IgG, goat-anti mouse IgG and donkey-anti-goat IgG were obtained from Santa Cruz Biotechnology Inc. (Santa Cruz, CA, USA). pEGFR-Y1101 was obtained from Abcam (Cambridge, MA, USA). GAPDH was purchased from Cell Signaling Technology (Danvers, MA, USA). α-tubulin was purchased from Calbiochem (San Diego, CA, USA). Cetuximab (C225, Erbitux) was generously provided by ImClone Systems Inc (New York, NY, USA), erlotinib (OSI-774, Tarceva) was kindly provided by OSI Pharmaceuticals (Farmingdale, NY, USA) and lapatinib (GW572016, Tykerb) was purchased from LC Laboratories (Woburn, MA, USA). EGF was purchased from R&D systems (Minneapolis, MN, USA).

Cellular fractionation and immunoblotting analysis

To obtain nuclear proteins, cells were plated in 15 cm dishes. At ~80–90% confluency, cells were scraped in PBS and swelled in cytoplasmic lysis buffer (20 mM HEPES, pH 7.0, 10 mM KCl, 2 mM $MgCl_2$, 0.5% NP40, 1 mM Na_3VO_4, 1 mM PMSF, 1 mM beta-glycerophosphate (BGP), 10 μg/ml of leupeptin and aprotinin) for 15 min on ice. Cells were then homogenized by 30–40 strokes in a tightly fitting Dounce homogenizer and checked under microscope for intact nuclei. The homogenate was centrifuged at 1500*g* for 5 min at 4 °C to sediment the nuclei. The nuclear pellet was washed 5 times in cytoplasmic lysis buffer to ensure complete removal of cytosolic membranes. After washes, the nuclear pellet was lysed in the same buffer with the addition of 0.5 M NaCl. Nuclear pellets were sonicated for 10 s, and vortexed for 30 s 3 times. The extracted nuclear lysate was centrifuged at 15,000*g* for 10 min at 4 °C, and the supernatants were collected as nuclear lysate. Whole cell protein lysate was obtained through lysis with RIPA buffer (50 mM HEPES, pH 7.4, 150 mM NaCl, .1% Tween-20, 10% glycerol, 2.5 mM EGTA, 1 mM EDTA, 1 mM DTT, 1 mM Na_3VO_4, 1 mM PMSF, 1 mM BGP, and 10 μg/ml of leupeptin and aprotinin). Samples were sonicated for 10 s, and then centrifuged at 15,000*g* for 10 min at 4 °C. All protein lysates were quantified via by Bradford assay (Bio-Rad Laboratories, Hercules, CA, USA). Equal amounts of protein were fractionated by SDA-PAGE, transferred to a PVDF membrane (Millipore, Billerica, MA, USA), and analyzed by incubation with the appropriate primary antibody overnight at 4 °C. Membranes were then subjected to incubation with HRP-conjugated secondary antibodies for 1 h at room temperature. ECL chemiluminescence detection system was used to visual proteins with ECL Western Blotting Substrate (Promega Cooperation, Madison, WI, USA).

Plasmid construction and transfection

pcDNA3-Wild-Type EGFR was kindly provided by Dr. J. Boerner (Wayne State University School of Medicine, Karmanos Cancer Institute, MI, USA). Kinase-dead EGFR K721A, EGFR-Y1101F, and EGFR-S229A were created via QuikChange II XL Site-Directed Mutagenesis Kit (Stratagene, La Jolla, CA, USA) following the manufacturer's instructions. All mutations were verified for correct orientation and integrity via sequencing. All plasmid transfections were performed using Lipofectamine LTX and Opti-MEM I (Invitrogen) according to the manufacturer's instructions. Cells were analyzed 48 h post transfection for expression and nuclear localization of EGFR.

Competing of interests

The authors declare no competing interests.

Authors' contributions

TMB and DLW performed the literature search and drafted the manuscript. TMB and MI performed all experimentation depicted in this manuscript. All authors provided critical review of the manuscript and approved the final draft.

References

[1] Yarden Y, Sliwkowski MX. Untangling the ErbB signalling network. Nat Rev Mol Cell Biol 2001;2:127–37.
[2] The scent of Nobel Prize success. Funct Neurol 2004;19:217–8.
[3] Marmor MD, Skaria KB, Yarden Y. Signal transduction and oncogenesis by ErbB/HER receptors. Int J Radiat Oncol Biol Phys 2004;58:903–13.
[4] Libermann TA, Nusbaum HR, Razon N, Kris R, Lax I, Soreq H, et al. Amplification and overexpression of the EGF receptor gene in primary human glioblastomas. J Cell Sci Suppl 1985;3:161–72.
[5] Libermann TA, Nusbaum HR, Razon N, Kris R, Lax I, Soreq H, et al. Amplification, enhanced expression and possible rearrangement of EGF receptor gene in primary human brain tumours of glial origin. Nature 1985;313:144–7.

[6] Libermann TA, Razon N, Bartal AD, Yarden Y, Schlessinger J, Soreq H. Expression of epidermal growth factor receptors in human brain tumors. Cancer Res 1984;44:753–60.

[7] Veale D, Ashcroft T, Marsh C, Gibson GJ, Harris AL. Epidermal growth factor receptors in non-small cell lung cancer. Br J Cancer 1987;55:513–6.

[8] Weichselbaum RR, Dunphy EJ, Beckett MA, Tybor AG, Moran WJ, Goldman ME, et al. Epidermal growth factor receptor gene amplification and expression in head and neck cancer cell lines. Head Neck 1989;11:437–42.

[9] Sato JD, Kawamoto T, Le AD, Mendelsohn J, Polikoff J, Sato GH. Biological effects in vitro of monoclonal antibodies to human epidermal growth factor receptors. Mol Biol Med 1983;1:511–29.

[10] Kawamoto T, Sato JD, Le A, Polikoff J, Sato GH, Mendelsohn J. Growth stimulation of A431 cells by epidermal growth factor: identification of high-affinity receptors for epidermal growth factor by an anti-receptor monoclonal antibody. Proc Natl Acad Sci USA 1983;80:1337–41.

[11] Sunada H, Magun BE, Mendelsohn J, MacLeod CL. Monoclonal antibody against epidermal growth factor receptor is internalized without stimulating receptor phosphorylation. Proc Natl Acad Sci USA 1986;83:3825–9.

[12] Brand TM, Iida M, Li C, Wheeler DL. The nuclear epidermal growth factor receptor signaling network and its role in cancer. Discov Med 2011;12:419–32.

[13] Wang YN, Yamaguchi H, Hsu JM, Hung MC. Nuclear trafficking of the epidermal growth factor receptor family membrane proteins. Oncogene 2010;29:3997–4006.

[14] Han W, Lo HW. Landscape of EGFR signaling network in human cancers: biology and therapeutic response in relation to receptor subcellular locations. Cancer Lett 2012;318:124–34.

[15] Wang YN, Yamaguchi H, Huo L, Du Y, Lee HJ, Lee HH, et al. The translocon Sec61beta localized in the inner nuclear membrane transports membrane-embedded EGF receptor to the nucleus. J Biol Chem 2010;285:38720–9.

[16] Wang YN, Wang H, Yamaguchi H, Lee HJ, Lee HH, Hung MC. COPI-mediated retrograde trafficking from the Golgi to the ER regulates EGFR nuclear transport. Biochem Biophys Res Commun 2010;399:498–504.

[17] Lo HW, Ali-Seyed M, Wu Y, Bartholomeusz G, Hsu SC, Hung MC. Nuclear-cytoplasmic transport of EGFR involves receptor endocytosis, importin beta1 and CRM1. J Cell Biochem 2006;98:1570–83.

[18] Liao HJ, Carpenter G. Role of the Sec61 translocon in EGF receptor trafficking to the nucleus and gene expression. Mol Biol Cell 2007;18:1064–72.

[19] Hsu SC, Hung MC. Characterization of a novel tripartite nuclear localization sequence in the EGFR family. J Biol Chem 2007;282:10432–40.

[20] Wang YN, Lee HH, Lee HJ, Du Y, Yamaguchi H, Hung MC. Membrane-bound trafficking regulates nuclear transport of integral epidermal growth factor receptor (EGFR) and ErbB-2. J Biol Chem 2012;287:16869–79.

[21] Eldredge ER, Korf GM, Christensen TA, Connolly DC, Getz MJ, Maihle NJ. Activation of c-fos gene expression by a kinase-deficient epidermal growth factor receptor. Mol Cell Biol 1994;14:7527–34.

[22] Lin SY, Makino K, Xia W, Matin A, Wen Y, Kwong KY, et al. Nuclear localization of EGF receptor and its potential new role as a transcription factor. Nat Cell Biol 2001;3:802–8.

[23] Lo HW, Hsu SC, Ali-Seyed M, Gunduz M, Xia W, Wei Y, et al. Nuclear interaction of EGFR and STAT3 in the activation of the iNOS/NO pathway. Cancer Cell 2005;7:575–89.

[24] Hanada N, Lo HW, Day CP, Pan Y, Nakajima Y, Hung MC. Co-regulation of B-Myb expression by E2F1 and EGF receptor. Mol Carcinog 2006;45:10–7.

[25] Lo HW, Cao X, Zhu H, Ali-Osman F. Cyclooxygenase-2 is a novel transcriptional target of the nuclear EGFR–STAT3 and EGFRvIII–STAT3 signaling axes. Mol Cancer Res 2010;8:232–45.

[26] Hung LY, Tseng JT, Lee YC, Xia W, Wang YN, Wu ML, et al. Nuclear epidermal growth factor receptor (EGFR) interacts with signal transducer and activator of transcription 5 (STAT5) in activating Aurora-A gene expression. Nucleic Acids Res 2008;36:4337–51.

[27] Jaganathan S, Yue P, Paladino DC, Bogdanovic J, Huo Q, Turkson J. A functional nuclear epidermal growth factor receptor, SRC and stat3 heteromeric complex in pancreatic cancer cells. Plos One 2011;6:e19605.

[28] Huang WC, Chen YJ, Li LY, Wei YL, Hsu SC, Tsai SL, et al. Nuclear translocation of epidermal growth factor receptor by Akt-dependent phosphorylation enhances breast cancer-resistant protein expression in gefitinib-resistant cells. J Biol Chem 2011;286:20558–68.

[29] Dittmann K, Mayer C, Rodemann HP. Inhibition of radiation-induced EGFR nuclear import by C225 (Cetuximab) suppresses DNA-PK activity. Radiother Oncol 2005;76:157–61.

[30] Dittmann K, Mayer C, Fehrenbacher B, Schaller M, Raju U, Milas L, et al. Radiation-induced epidermal growth factor receptor nuclear import is linked to activation of DNA-dependent protein kinase. J Biol Chem 2005;280:31182–9.

[31] Psyrri A, Yu Z, Weinberger PM, Sasaki C, Haffty B, Camp R, et al. Quantitative determination of nuclear and cytoplasmic epidermal growth factor receptor expression in oropharyngeal squamous cell cancer by using automated quantitative analysis. Clin Cancer Res 2005;11:5856–62.

[32] Lo HW, Xia W, Wei Y, Ali-Seyed M, Huang SF, Hung MC. Novel prognostic value of nuclear epidermal growth factor receptor in breast cancer. Cancer Res 2005;65:338–48.

[33] Xia W, Wei Y, Du Y, Liu J, Chang B, Yu YL, et al. Nuclear expression of epidermal growth factor receptor is a novel prognostic value in patients with ovarian cancer. Mol Carcinog 2009;48:610–7.

[34] Hoshino M, Fukui H, Ono Y, Sekikawa A, Ichikawa K, Tomita S, et al. Nuclear expression of phosphorylated EGFR is associated with poor prognosis of patients with esophageal squamous cell carcinoma. Pathobiology 2007;74:15–21.

[35] Li CF, Fang FM, Wang JM, Tzeng CC, Tai HC, Wei YC, et al. EGFR nuclear import in gallbladder carcinoma: nuclear phosphorylated EGFR upregulates iNOS expression and confers independent prognostic impact. Ann Surg Oncol 2011.

[36] Traynor AM, Weigel TM, Oettel KR, Yang DT, Zhang C, Kim K, et al. Nuclear EGFR expression predicts poor survival in resected non-small cell lung cancer. J Thorac Oncol 2012.

[37] Liccardi G, Hartley JA, Hochhauser D. EGFR nuclear translocation modulates DNA repair following cisplatin and ionizing radiation treatment. Cancer Res 2011;71:1103–14.

[38] Li C, Iida M, Dunn EF, Ghia AJ, Wheeler DL. Nuclear EGFR contributes to acquired resistance to cetuximab. Oncogene 2009;28:3801–13.

[39] Hsu SC, Miller SA, Wang Y, Hung MC. Nuclear EGFR is required for cisplatin resistance and DNA repair. Am J Transl Res 2009;1:249–58.

[40] Curtin NJ. DNA repair dysregulation from cancer driver to therapeutic target. Nat Rev Cancer 2012;12:801–17.

[41] SchmidtUllrich RK, Mikkelsen RB, Dent P, Todd DG, Valerie K, Kavanagh BD, et al. Radiation-induced proliferation of the human A431 squamous carcinoma cells is dependent on EGFR tyrosine phosphorylation. Oncogene 1997;15:1191–7.

[42] Huang SM, Bock JM, Harari PM. Epidermal growth factor receptor blockade with C225 modulates proliferation, apoptosis, and radiosensitivity in squamous cell carcinomas of the head and neck. Cancer Res 1999;59:1935–40.

[43] Huang SM, Li J, Harari PM. Monoclonal antibody blockade of the epidermal growth factor receptor in cancer therapy. Cancer Chemother Biol Response Modif 2001;19:339–52.

[44] Dittmann K, Mayer C, Kehlbach R, Rodemann HP. Radiation-induced caveolin-1 associated EGFR internalization is linked with nuclear EGFR transport and activation of DNA-PK. Mol Cancer 2008;7:69.

[45] Dittmann K, Mayer C, Fehrenbacher B, Schaller M, Kehlbach R, Rodemann HP. Nuclear EGFR shuttling induced by ionizing radiation is regulated by phosphorylation at residue Thr654. FEBS Lett 2010;584:3878–84.

[46] Dittmann K, Mayer C, Wanner G, Kehlbach R, Rodemann HP. The radioprotector *O*-phospho-tyrosine stimulates DNA-repair via epidermal growth factor receptor- and DNA-dependent kinase phosphorylation. Radiother Oncol 2007;84:328–34.

[47] Dittmann K, Mayer C, Fehrenbacher B, Schaller M, Kehlbach R, Rodemann HP. Nuclear epidermal growth factor receptor modulates cellular radio-sensitivity by regulation of chromatin access. Radiother Oncol 2011;99:317–22.

[48] Dittmann K, Mayer C, Kehlbach R, Rodemann HP. The radioprotector Bowman–Birk proteinase inhibitor stimulates DNA repair via epidermal growth factor receptor phosphorylation and nuclear transport. Radiother Oncol 2008;86:375–82.

[49] Wanner G, Mayer C, Kehlbach R, Rodemann HP, Dittmann K. Activation of protein kinase C epsilon stimulates DNA-repair via epidermal growth factor receptor nuclear accumulation. Radiother Oncol 2008;86:383–90.

[50] Yu YL, Chou RH, Wu CH, Wang YN, Chang WJ, Tseng YJ, et al. Nuclear EGFR suppresses ribonuclease activity of polynucleotide phosphorylase through DNAPK-mediated phosphorylation at serine 776. J Biol Chem 2012;287:31015–26.

[51] Wang D, Lippard SJ. Cellular processing of platinum anticancer drugs. Nat Rev Drug Discov 2005;4:307–20.

[52] Wheeler DL, Huang S, Kruser TJ, Nechrebecki MM, Armstrong EA, Benavente S, et al. Mechanisms of acquired resistance to cetuximab: role of HER (ErbB) family members. Oncogene 2008;27:3944–56.

[53] Liao HJ, Carpenter G. Cetuximab/C225-induced intracellular trafficking of epidermal growth factor receptor. Cancer Res 2009;69:6179–83.

[54] Li C, Iida M, Dunn EF, Wheeler DL. Dasatinib blocks cetuximab- and radiation-induced nuclear translocation of the epidermal growth factor receptor in head and neck squamous cell carcinoma. Radiother Oncol 2010;97:330–7.

[55] Wheeler DL, Iida M, Kruser TJ, Nechrebecki MM, Dunn EF, Armstrong EA, et al. Epidermal growth factor receptor cooperates with Src family kinases in acquired resistance to cetuximab. Cancer Biol Ther 2009;8:696–703.

[56] Wheeler DL, Dunn EF, Harari PM. Understanding resistance to EGFR inhibitors-impact on future treatment strategies. Nat Rev Clin Oncol 2010;7:493–507.

[57] Brand TM, Iida M, Wheeler DL. Molecular mechanisms of resistance to the EGFR monoclonal antibody cetuximab. Cancer Biol Ther 2011;11.

[58] Kim HP, Yoon YK, Kim JW, Han SW, Hur HS, Park J, et al. Lapatinib, a dual EGFR and HER2 tyrosine kinase inhibitor, downregulates thymidylate synthase by inhibiting the nuclear translocation of EGFR and HER2. Plos One 2009;4.

[59] Yu YL, Chou RH, Liang JH, Chang WJ, Su KJ, Tseng YJ, et al. Targeting the EGFR/PCNA signaling suppresses tumor growth of triple-negative breast cancer cells with cell-penetrating PCNA peptides. Plos One 2013;8.

[60] Oliveras-Ferraros C, Vazquez-Martin A, Lopez-Bonet E, Martin-Castillo B, Del Barco S, Brunet J, et al. Growth and molecular interactions of the anti-EGFR antibody cetuximab and the DNA cross-linking agent cisplatin in gefitinib-resistant MDA-MB-468 cells: new prospects in the treatment of triple-negative/basal-like breast cancer. Int J Oncol 2008;33:1165–76.

[61] Weihua Z, Tsan R, Huang WC, Wu Q, Chiu CH, Fidler IJ, et al. Survival of cancer cells is maintained by EGFR independent of its kinase activity. Cancer Cell 2008;13:385–93.

[62] Wang Q, Villeneuve G, Wang Z. Control of epidermal growth factor receptor endocytosis by receptor dimerization, rather than receptor kinase activation. EMBO Rep 2005;6:942–8.
[63] Iida M, Brand TM, Campbell DA, Li C, Wheeler DL. Yes and Lyn play a role in nuclear translocation of the epidermal growth factor receptor. Oncogene 2012.
[64] Milas L. Cyclooxygenase-2 (COX-2) enzyme inhibitors as potential enhancers of tumor radioresponse. Semin Radiat Oncol 2001;11:290–9.
[65] Choy H, Milas L. Enhancing radiotherapy with cyclooxygenase-2 enzyme inhibitors: a rational advance? J Natl Cancer Inst 2003;95:1440–52.
[66] Maier TJ, Schilling K, Schmidt R, Geisslinger G, Grosch S. Cyclooxygenase-2 (COX-2)-dependent and -independent anticarcinogenic effects of celecoxib in human colon carcinoma cells. Biochem Pharmacol 2004;67:1469–78.
[67] Patel MI, Subbaramaiah K, Du BH, Chang M, Yang PY, Newman RA, et al. Celecoxib inhibits prostate cancer growth: evidence of a cyclooxygenase-2-independent mechanism. Clin Cancer Res 2005;11:1999–2007.
[68] Dittmann KH, Mayer C, Ohneseit PA, Raju U, Andratschke NH, Milas L, et al. Celecoxib induced tumor cell radiosensitization by inhibiting radiation induced nuclear EGFR transport and DNA-repair: a COX-2 independent mechanism. Int J Radiat Oncol Biol Phys 2008;70:203–12.
[69] Wang SC, Nakajima Y, Yu YL, Xia W, Chen CT, Yang CC, et al. Tyrosine phosphorylation controls PCNA function through protein stability. Nat Cell Biol 2006;8:1359–68.
[70] Bitler BG, Goverdhan A, Schroeder JA. MUC1 regulates nuclear localization and function of the epidermal growth factor receptor. J Cell Sci 2010;123:1716–23.
[71] Huo LF, Wang YN, Xia WY, Hsu SC, Lai CC, Li LY, et al. RNA helicase A is a DNA-binding partner for EGFR-mediated transcriptional activation in the nucleus. Proc Natl Acad Sci USA 2010;107:16125–30.
[72] Li A, Zhang C, Gao S, Chen F, Yang C, Luo R, et al. TIP30 loss enhances cytoplasmic and nuclear EGFR signaling and promotes lung adenocarcinogenesis in mice. Oncogene 2013;32:2273–81.
[73] Shi Y, Tao Y, Jiang Y, Xu Y, Yan B, Chen X, et al. Nuclear epidermal growth factor receptor interacts with transcriptional intermediary factor 2 to activate cyclin D1 gene expression triggered by the oncoprotein latent membrane protein 1. Carcinogenesis 2012;33:1468–78.
[74] Mackay HJ, Twelves CJ. Targeting the protein kinase C family: are we there yet? Nat Rev Cancer 2008;8. 255-255.
[75] Brenner JC, Graham MP, Kumar B, Saunders LM, Kupfer R, Lyons RH, et al. Genotyping of 73 Um-Scc head and neck squamous cell carcinoma cell lines. Head Neck J Sci Spec 2010;32:417–26.
[76] Irwin ME, Mueller KL, Bohin N, Ge YB, Boerner JL. Lipid raft localization of EGFR alters the response of cancer cells to the EGFR tyrosine kinase inhibitor gefitinib. J Cell Physiol 2011;226:2316–28.

Oncogene (2012) 1 – 9

www.nature.com/onc

ORIGINAL ARTICLE

Yes and Lyn play a role in nuclear translocation of the epidermal growth factor receptor

M Iida[1,2], TM Brand[1,2], DA Campbell[1], C Li[1] and DL Wheeler[1]

The epidermal growth factor receptor (EGFR) is a central regulator of tumor progression in human cancers. Cetuximab is an anti-EGFR antibody that has been approved for use in oncology. Previously we investigated mechanisms of resistance to cetuximab using a model derived from the non-small cell lung cancer line NCI-H226. We demonstrated that cetuximab-resistant clones (Ctx^R) had increased nuclear localization of the EGFR. This process was mediated by Src family kinases (SFKs), and nuclear EGFR had a role in resistance to cetuximab. To better understand SFK-mediated nuclear translocation of EGFR, we investigated which SFK member(s) controlled this process as well as the EGFR tyrosine residues that are involved. Analyses of mRNA and protein expression indicated upregulation of the SFK members Yes (v-Yes-1 yamaguchi sarcoma viral oncogene) and Lyn (v-yes-1 Yamaguchi sarcoma viral-related oncogene homolog) in all Ctx^R clones. Further, immunoprecipitation analysis revealed that EGFR interacts with Yes and Lyn in Ctx^R clones, but not in cetuximab-sensitive (Ctx^S) parental cells. Using RNAi interference, we found that knockdown of either Yes or Lyn led to loss of EGFR translocation to the nucleus. Conversely, overexpression of Yes or Lyn in low nuclear EGFR-expressing Ctx^S parental cells led to increased nuclear EGFR. Chromatin immunoprecipitation (ChIP) assays confirmed nuclear EGFR complexes associated with the promoter of the known EGFR target genes B-Myb and iNOS. Further, all Ctx^R clones exhibited upregulation of B-Myb and iNOS at the mRNA and protein levels. siRNAs directed at Yes or Lyn led to decreased binding of EGFR complexes to the B-Myb and iNOS promoters based on ChIP analyses. SFKs have been shown to phosphorylate EGFR on tyrosines 845 and 1101 (Y845 and Y1101), and mutation of Y1101, but not Y845, impaired nuclear entry of the EGFR. Taken together, our findings demonstrate that Yes and Lyn phosphorylate EGFR at Y1101, which influences EGFR nuclear translocation in this model of cetuximab resistance.

Oncogene advance online publication, 19 March 2012; doi:10.1038/onc.2012.90

Keywords: nuclear EGFR; SFK; Yes; Lyn

INTRODUCTION

Activation of the epidermal growth factor receptor (EGFR), a receptor tyrosine kinase (RTK), provides cells with potent growth and survival signals that enable tumors to manifest.[1–3] Aberrant expression or activity of the EGFR is identified as a major etiological factor in many human epithelial cancers including colorectal cancer, head and neck squamous cell carcinoma (HNSCC), non-small cell lung cancer (NSCLC), breast and brain cancers.[2,4,5] In the classical EGFR signaling pathway, ligand binding to the EGFR allows for receptor homo- or hetero-dimerization at the plasma membrane. This interaction activates each receptor's tyrosine kinase domain and induces autophosphorylation of each dimer's cytoplasmic tail. The phosphorylated cytoplasmic tail of the EGFR serves as docking sites for numerous proteins that initiate key oncogenic pathways including the RAS/RAF/MEK/ERK and phosphatidylinositol 3-kinase-Akt pathways; however, the activation of src family tyrosine kinases (SFKs), phospholipase C-gamma, protein kinase C and signal transducers and activators of transcription (STAT) proteins have also been documented.[1,6]

In addition to the classical signaling pathways initiated by the EGFR at the cell surface, there is now an emerging novel signaling pathway influenced by EGFR located in the nucleus. The full-length EGFR can be shuttled from the plasma membrane to the nucleus in a series of well-defined steps.[7–9] These events include receptor internalization to the early endosome and interaction with importin β1 via its tripartite nuclear localization sequence, followed by COPI-mediated retrograde trafficking to the golgi apparatus and the endoplasmic reticulum.[10,11] Once in the endoplasmic reticulum the EGFR-importin β1 complex moves to the outer nuclear membrane where importin β1 interacts with nucleoporin 62 lining the nuclear pore channel to shuttle the EGFR-importin β1 complex to the inner nuclear membrane. Here, the complex interacts with the Sec61 β translocon to be released from the membrane into the nucleus.[12,13]

Within the nucleus, EGFR serves as a transcriptional co-activator for a series of tumor-promoting genes including cyclin D1, inducible nitric oxide synthase (iNOS), aurora kinase A, B-Myb, COX2, c-Myc, breast cancer-resistant protein (BCRP) and GRP78.[14–21] Additionally, nuclear EGFR can phosphorylate and stabilize the proliferating cell nuclear antigen at the replication fork of the dividing cell,[22] and activate DNA-PK to enhance DNA repair.[23]

High levels of nuclear EGFR correlate with poor clinical outcome in breast cancer, oropharyngeal squamous cell cancer, ovarian cancer, and gallbladder cancer.[24–28] Nuclear EGFR also contributes to cancer cells resistance to cetuximab,[29] gefitinib,[20] cisplatin and radiation therapy.[30–33] Taken together, these pieces of evidence suggest that nuclear EGFR has a role in the promotion of cancer and provides a rationale for studying the mechanisms of EGFR nuclear translocation in order to target the nuclear functions of the EGFR.

[1]Department of Human Oncology, University of Wisconsin School of Medicine and Public Health, Madison, WI, USA. [2]These authors contributed equally to this work. Correspondence: Professor DL Wheeler, Department of Human Oncology, University of Wisconsin Comprehensive Cancer Center, 1111 Highland Avenue, WIMR 3159, Madison, WI 53705, USA. E-mail: dlwheeler@wisc.edu
Received 13 August 2011; revised 26 January 2012; accepted 12 February 2012

It is well established that SFKs are necessary for full activation of the EGFR.[34,35] Src kinase is the prototypical member of this family of non-RTKs that include Yes (v-Yes-1 yamaguchi sarcoma viral oncogene), Fyn, Lyn (v-yes-1 Yamaguchi sarcoma viral-related oncogene homolog), Lck, Hck Fgr, Blk and Yrk.[36,37] These SFKs mediate mitogenic signals from a variety of RTKs.[38,39] It has been observed that SFKs can phosphorylate EGFR at both tyrosine 845 (Y845) and tyrosine 1101 (Y1101). EGFR Y845 is located in the activation loop of the kinase domain that is highly conserved among other RTKs. Phosphorylation of EGFR Y845 appears to be critical for EGFR-mediated mitogenesis, and is critical for the phosphorylation and activation of the STAT5b transcription factor.[34,40,41] The second known Src-mediated phosphorylation site is Y1101, which lies within the carboxyl-terminal region of the EGFR; however, the function of Y1101 has not been fully elucidated.[34] Oncogenic cooperation between Src and EGFR has been well established in breast cancer,[34,42] glioblastoma,[43] HNSCC and NSCLC.[44-47]

We established six clonal Ctx^R variants of the NCI-H226 NSCLC line.[29,48,49] In previous reports, we found that Ctx^R clones had a dramatic increase in nuclear EGFR localization, in addition to having increased SFK activity.[29,44] Further, we reported that the SFK inhibitor dasatinib (BMS-354825, Sprycel) could (1) block SFK activation, (2) decrease nuclear EGFR translocation, (3) increase plasma membrane levels of the EGFR, and (4) re-sensitize Ctx^R cell lines to cetuximab. Collectively, these findings suggest that SFKs have a crucial role in nuclear translocation of the EGFR in this model of cetuximab-resistance. However, the specific SFKs involved in the mediation of EGFR nuclear translocation and how they mediate this process are unknown.

In the current study, we demonstrate that Ctx^R clones had increased expression of the SFKs Yes and Lyn. Both Yes and Lyn were strongly associated with EGFR in Ctx^R clones as compared to the Ctx^S parental cell line. Depletion of either Yes or Lyn kinase decreased EGFR nuclear translocation, and reduced phosphorylation at Y845 and Y1101 of the EGFR. Reciprocally, overexpression of Yes or Lyn increased EGFR nuclear translocation in the Ctx^S parental cell line. Furthermore, mutation of Y1101 of the EGFR impaired its nuclear translocation. Collectively, these data suggest that Yes, Lyn and Y1101 of the EGFR are involved in EGFR nuclear translocation in this model of acquired resistance to cetuximab.

RESULTS

The SFK inhibitor Dasatinib blocks nuclear translocation of the EGFR

We have previously reported that Ctx^R clones have increased nuclear EGFR and activation of SFKs (Figures 1a and b).[29,48] Using this model, we determined the effects of the SFK inhibitor dasatinib on the phosphorylation status of the EGFR in three Ctx^R clones (HC1, HC4 and HC8) and the Ctx^S parental clone (HP) after treatment with 100 nM of dasatinib for 24 h. Dasatinib inhibited the full activation of SFKs as indicated by the loss of phospho-Y419 and decreased the phosphorylation of EGFR at the known SFK phosphorylation sites Y845 and Y1101 (Figure 1b). Also, treatment with dasatinib led to modest increases in steady-state expression of total SFKs in all Ctx^R clones.

To determine the effects of dasatinib treatment on nuclear translocation of EGFR, we treated the Ctx^R clones and the Ctx^S parental clone with 100 nM of dasatinib for 24 h followed by nuclear fractionation. As illustrated in Figure 1c, dasatinib treatment reduced EGFR nuclear translocation in Ctx^R clones. The Ctx^S parental clone has very low levels of nuclear EGFR and dasatinib treatment had no effect. Thus, the inhibition of SFK activity decreased the phosphorylation of EGFR at Y845 and Y1101 as well as impaired nuclear entry of the EGFR. These results suggested that SFK phosphorylation of EGFR may have a role in inducing its nuclear translocation.

Yes and Lyn are overexpressed and associate with the EGFR in Ctx^R clones

On the basis of our previous findings with clonal Ctx^R variants of the NCI-H226 NSCLC line, we hypothesized that SFK member(s) may regulate EGFR nuclear translocation. To identify the specific SFKs that are necessary for EGFR nuclear translocation, we performed microarray analysis comparing Ctx^S HP parental cells to the three Ctx^R clones (HC1, HC4 and HC8). Microarray analysis demonstrated an $\sim$4-fold upregulation of Yes and Lyn kinases and $\sim$3-fold downregulation of Src kinase in all of the three Ctx^R cells compared with sensitive parental line (HP) (data not shown). Other SFK family members did not exhibit significant expression level changes in the three Ctx^R clones (HC1, HC4 and HC8).

To validate the microarray findings we performed quantitative PCR (qPCR) analysis. These results confirmed the microarray data indicating upregulation of Lyn ($\sim$3-fold) and Yes ($\sim$1.5-fold), and downregulation of Src kinase ($\sim$2-fold) in all three Ctx^R clones (Figure 2a). Next, we examined whether these increased mRNA levels reflected total protein levels in Ctx^R when compared with Ctx^S cells. We found that total protein levels of Yes and Lyn were increased 1.3- to 2.1-fold in Ctx^R clones compared with parental cells (Figure 2b). Finally, we investigated whether EGFR associated with Yes and Lyn. Immunoprecipitation analysis of EGFR-binding partners indicated that EGFR displayed increased association to Yes and Lyn in all three Ctx^R clones as compared with the Ctx^S HP cell line (Figure 2c). Collectively, these results indicate that Yes and Lyn are upregulated in Ctx^R clones and have increased association with the EGFR.

Yes and Lyn are necessary for nuclear translocation of EGFR in Ctx^R cells

To further investigate if Yes and/or Lyn expression altered EGFR activation and nuclear translocation, we performed gene-silencing experiments using siRNA directed against Yes or Lyn in Ctx^R clones (HC1, HC4 and HC8). Ctx^S cells were not included in these siRNA studies because the cells have negligible levels of nuclear EGFR. After treatment with siYES or siLYN in Ctx^R clones for 72 h we observed decreased phosphorylation of EGFR Y845 (70–99%) and EGFR Y1101 (40–85%) relative to control non-targeting siRNA (NT) (Figure 3a). Moreover, siYES and siLYN decreased the nuclear localization of EGFR in Ctx^R clones (Figure 3b).

Knockdown studies of Yes or Lyn in cells with high nuclear EGFR expression led to decreased nuclear EGFR levels. Therefore, we hypothesized that the overexpression of Yes or Lyn could increase the level of nuclear EGFR in a cell line with low levels of EGFR in the nucleus. To test this hypothesis, we overexpressed Yes or Lyn in Ctx^S cells, which express low levels of nuclear EGFR. First, Yes and Lyn were cloned into mammalian expression vectors, expressed in Chinese hamster ovary K1 (CHO-K1) cells and characterized for increased total Yes and Lyn protein expression and activity (Figure 4a). Comparable increases in Yes and Lyn expression and activation were observed in Ctx^S cells after transfection compared with vector only (Figure 4b). Consistent with siRNA observations, transient transfection of Yes or Lyn into Ctx^S cells significantly increased (3–3.5-fold) nuclear EGFR translocation (Figure 4c). Interestingly, Yes and Lyn were also detected in nucleus of HP cells after transfection. To determine if Ctx^R cells with increased nuclear EGFR also express more Yes and Lyn in the nucleus compared with Ctx^S cells, we determined nuclear Yes and Lyn levels in Ctx^R clones and Ctx^S cells. As seen with EGFR, increased levels of both Yes and Lyn were found in the nucleus of Ctx^R clones compared with Ctx^S cells (Figure 4d). These siRNA and overexpression results suggest that Yes and Lyn have a role in EGFR nuclear translocation.

Depletion of Yes or Lyn decreases binding of nuclear EGFR complexes to the B-Myb and iNOS promoter regions

Nuclear EGFR and various transcription factor complexes have been shown to bind promoter regions and regulate the

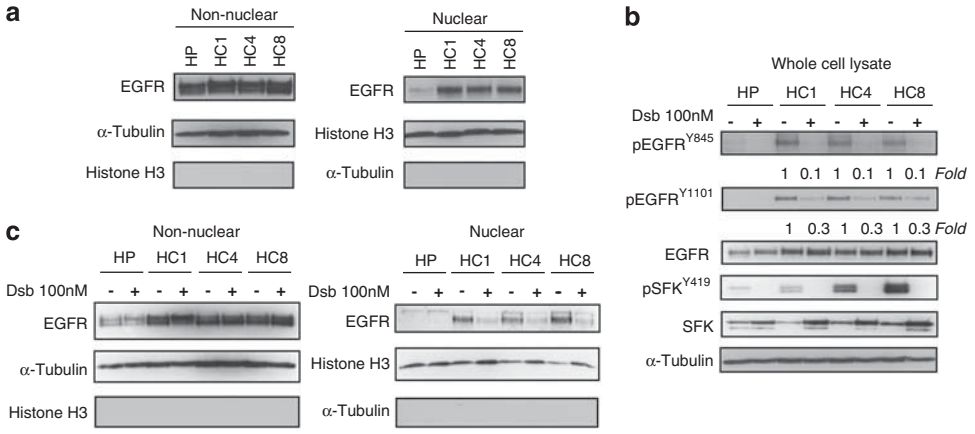

Figure 1. SFKs are essential for EGFR translocation to the nucleus. (**a**) Ctx^R clones (HC1, HC4 and HC8) have increased nuclear EGFR localization as compared with Ctx^S cell line (HP). Cells were harvested for non-nuclear and nuclear protein, and fractionated on SDS–PAGE followed by immunoblotting for indicated proteins. Histone H3 and α-tubulin were used as loading and purity controls for the nuclear and non-nuclear fractions, respectively. (**b**) Dasatinib decreased EGFR activity in Ctx^R cells. Ctx^R clones (HC1, HC4 and HC8) and Ctx^S HP cell line were treated with 100 nM dasatinib for 24 h. Cells were harvested and protein lysates were fractionated on SDS–PAGE followed by immunoblotting for the indicated proteins. α-tubulin was used as a loading control. Expression was quantitated using ImageJ software. (**c**) Dasatinib can inhibit EGFR nuclear translocation in Ctx^R clones. Ctx^R clones (HC1, HC4, and HC8) and Ctx^S cell line (HP) were treated with 100 nM dasatinib for 24 h. Cells were harvested for non-nuclear and nuclear protein, and fractionated on SDS–PAGE followed by immunoblotting for indicated proteins. Histone H3 and α-tubulin were used as loading and purity controls for the nuclear and non-nuclear fractions, respectively.

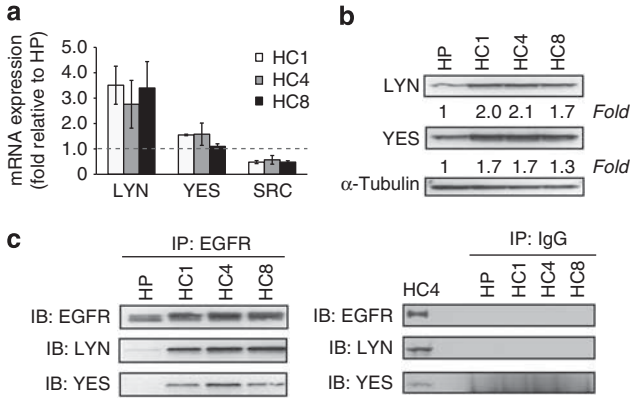

Figure 2. Yes and Lyn SFK family members are overexpressed in Ctx^R cells. (**a**) Yes and Lyn mRNA is upregulated in Ctx^R clones (HC1, HC4, and HC8). Lyn (3.6–4.5-fold), Yes (~1.5-fold) and Src (−2.3 to −3.5-fold) mRNA expression levels were compared with that of the Ctx^S cell line (HP) by qPCR. (**b**) Total protein levels of Yes and Lyn were increased (1.3–2.1-fold) in Ctx^R clones (HC1, HC4, and HC8) as compared with the Ctx^S cell line (HP). Cells were harvested and protein lysates were fractionated on SDS–PAGE followed by immunoblotting for the indicated proteins. α-tubulin was used as a loading control. Protein expression was quantitated using ImageJ software. (**c**) Analysis of EGFR binding partners in Ctx^R cells using immunoprecipitation assay indicated that EGFR displayed increased binding with Yes and Lyn as compared with the Ctx^S parental cell line. Cells were harvested and EGFR or IgG were immunoprecipitated with anti-mouse EGFR antibody or normal mouse IgG. The immunoprecipitate complexes were fractionated on SDS–PAGE followed by immunoblotting for indicated proteins.

transcription of multiple genes including cyclin D1, iNOS, B-Myb, Aurora Kinase A, COX2, c-Myc, BCRP and GRP78.[14–21] To confirm that nuclear EGFR complexes in Ctx^R clones bound to known EGFR target gene promoters, we performed chromatin immunoprecipitation-qPCR (ChIP-qPCR) analysis of the B-Myb and iNOS promoters. We demonstrated that Ctx^R clones have increased EGFR association with the B-Myb (3–9-fold increase in EGFR binding) and iNOS (6–12-fold increase in EGFR binding) promoter regions as compared with Ctx^S parental cell line (Figure 5a). These results indicate that nuclear EGFR complexes bind known EGFR target promoters in Ctx^R clones more strongly than in Ctx^S HP cells.

Given the high binding of nuclear EGFR complexes to the B-Myb and iNOS promoters, we performed qPCR to determine whether this binding resulted in increased expression of *B-Myb* and *iNOS* genes as previously reported.[15,16] Results in Figure 5b indicated that B-Myb mRNA expression was increased approximately 4-fold in all Ctx^R clones as compared with Ctx^S parental cells, whereas iNOS mRNA expression was increased 4–11-fold in Ctx^R clones when compared with Ctx^S parental cells. Furthermore, B-Myb protein expression was upregulated approximately 3-fold and iNOS protein expression was upregulated 2–14-fold in Ctx^R clones (Figure 5c). Using the Ctx^R HC4 clone we demonstrate that silencing of Yes or Lyn using siRNA reduced nuclear EGFR complex formation with the B-Myb and iNOS promoters as detected by ChIP-qPCR (Figure 5d). Additionally, the protein expression of both B-Myb and iNOS were decreased (60–70%) after siYES or siLYN transfection compared with control NT in HC4 (Figure 5d). Collectively, these data demonstrate that Ctx^R clones with high levels of nuclear EGFR associate more strongly with known EGFR-regulated promoter regions, and that these association (demonstrated with B-Myb and iNOS) can be prevented upon depletion of Yes or Lyn.

EGFR Y1101 is involved in nuclear translocation

Analysis of known SFK phosphorylation sites on the EGFR showed increased phosphorylation of Y845 and Y1101 in Ctx^R clones (Figure 1b). However, the relevance of these two tyrosine sites for EGFR nuclear translocation is unknown. To determine whether phosphorylation of one or both of these tyrosine residues is involved in EGFR nuclear translocation, MCF-7 breast cancer cells (which express very low EGFR levels) were transiently transfected with cDNAs encoding wild-type (WT) EGFR or the following EGFR mutants: EGFR-Y845F or EGFR-Y1101F. Immunoprecipitation of WT and mutant EGFR followed by immunoblotting with antibodies directed against pEGFR^{Y845} or pEGFR^{Y1101} showed reduced phosphorylation of Y845 and Y1101. (Figure 6a). To induce

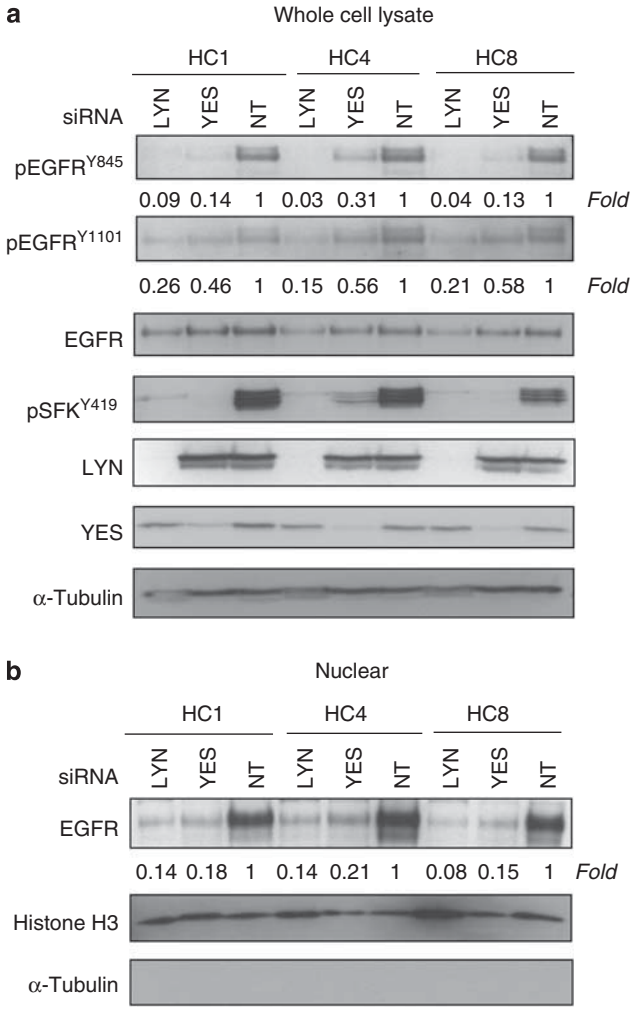

Figure 3. siYES and siLYN can reduce the nuclear localization of the EGFR. (**a**) siYES and siLYN decreased phosphorylation of EGFR tyrosine 845 (Y845), tyrosine 1101 (Y1101) and SFK tyrosine 419 (Y419). Cells were harvested 72 h after treatment with either siYES or siLYN, and protein lysates were fractionated on SDS–PAGE followed by immunoblotting for the indicated proteins. The NT was used as a control. α-tubulin was used as a loading control. Protein expression was quantitated using ImageJ software. (**b**) siYES and siLYN can reduce the nuclear localization of the EGFR. Cells were harvested for non-nuclear and nuclear protein, and fractionated on SDS–PAGE followed by immunoblotting for indicated proteins after 72 h treatment with either siYES or siLYN. The NT was used as a control. Histone H3 and α-tubulin were used as loading and purity controls for the nuclear and non-nuclear fractions, respectively. Protein expression was quantitated using ImageJ software.

nuclear translocation of the EGFR we treated the transfected cells with epidermal growth factor (EGF) for 45 min before cell lysis and nuclear fractionation. The results of this experiment indicated that EGF was able to induce nuclear translocation of EGFR in both EGFR-WT and EGFR-Y845F mutant cells (Figure 6b). However, EGF-induced EGFR nuclear translocation was diminished ~70% in EGFR-Y1101F mutant cells as compared with EGFR-WT-expressing cells (Figure 6b). Furthermore, qPCR analysis revealed that B-Myb and iNOS mRNA expression were downregulated in cells transfected with EGFR-Y1101F mutant compared with EGFR-WT-transfected cells (Figure 6c). Collectively, these data suggest that the phosphorylation of Y1101 is important for the nuclear translocation of EGFR, whereas the phosphorylation of Y845 does not appear to be essential for this process.

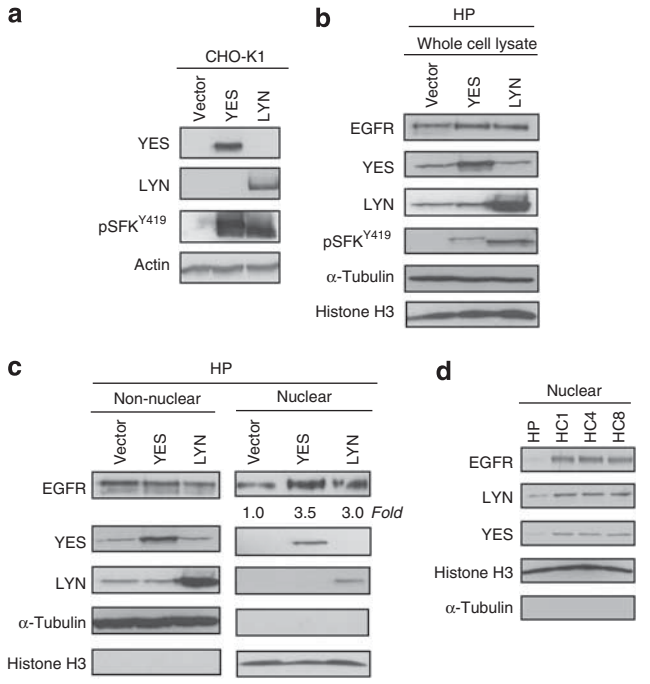

Figure 4. YES and LYN can induce the nuclear localization of the EGFR. (**a**) Increased levels of total protein expression of Yes and Lyn were detected in Chinese hamster ovary (CHO-K1) cells 48 h after transfection with either a Yes or Lyn mammalian expression vector. (**b**) Increased Yes and Lyn expression as well as increased levels of pSFK Y419 were observed in Ctx^{S} cells after 48 h transfection compared with vector only. (**c**) Nuclear EGFR translocation was increased by overexpression of Yes and Lyn. Cells were transfected with a Yes or Lyn mammalian expression vector and harvested for non-nuclear and nuclear protein. Each protein was fractionated on SDS–PAGE followed by immunoblotting. Histone H3 and α-tubulin were used as loading and purity controls for the nuclear and non-nuclear fractions, respectively. (**d**) Ctx^{R} clones (HC1, HC4 and HC8) have increased nuclear Yes and Lyn localization as compared with Ctx^{s} cell line (HP). Cells were harvested for non-nuclear and nuclear protein, and fractionated on SDS–PAGE followed by immunoblotting for indicated proteins. Histone H3 and α-tubulin were used as loading and purity controls for the nuclear and non-nuclear fractions, respectively.

DISCUSSION

The nuclear localization of RTKs have been observed for over 20 years; however, only in the past 10 years has research begun to focus on how they translocate from the cell surface to the nucleus and what functions they perform there. All four HER family members have been identified in the nucleus of various types of human cancer cells and tumor specimens.[9,50–53] Currently, eight target genes of nuclear EGFR have been identified,[14–21] and nuclear EGFR has been correlated with resistance to cetuximab, radiation, cisplatin and gefitinib therapies.[20,23,29–33] Collectively, these results suggest an emerging role of the nuclear EGFR signaling network in cancer progression and response to therapeutic modalities.

Several studies have examined how EGFR moves from the plasma membrane to the nucleus of the cell. It has been shown that the full-length EGFR can be shuttled from the plasma membrane to the nucleus through associations with importin β1, the nuclear pore complex, and the Sec61 β translocon.[7,10,13] Despite this mechanism of EGFR nuclear translocation, the early events at the plasma membrane that may serve as critical initiating signals for the movement of the EGFR to the nucleus have yet to be defined and form the basis of the current study.

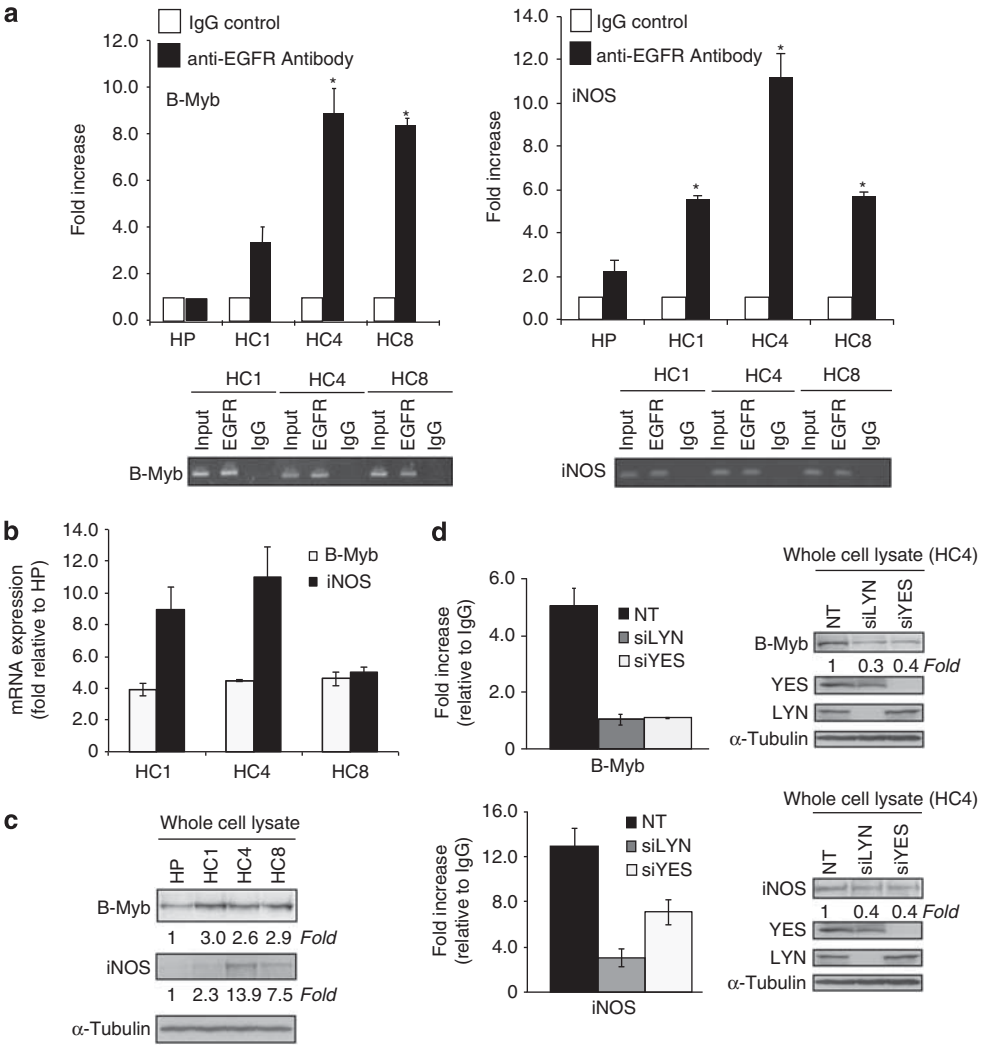

Figure 5. Yes and Lyn influence the binding of EGFR complexes to the B-Myb and iNOS promoter regions. (**a**) EGFR-regulated gene promoter regions are more strongly associated with EGFR in Ctx^R clones (HC1, HC4, and HC8) as compared with Ctx^S cells (HP). EGFR-ChIP and subsequent qPCR from the ChIP sample for the presence of B-Myb and iNOS promoter sequences. Data points are represented as mean ± s.e.m. ($n = 3$). *$P < 0.05$. qPCR specificity for the B-Myb and iNOS promoter regions was also confirmed by agarose gel electrophoresis of semi-qPCR products. (**b**) B-Myb and iNOS mRNA levels were significantly upregulated in Ctx^R cells (HC1, HC4, and HC8) as compared with the Ctx^S cell line (HP) by qPCR. The mRNA expression of B-Myb and iNOS in HP, HC1, HC4 and HC8 were determined by qPCR. Data points are represented as mean ± s.e.m. ($n = 3$). (**c**) B-Myb and iNOS protein levels were increased in Ctx^R cells (HC1, HC4, and HC8) as compared with the Ctx^S cell line (HP) by immunoblot analysis. Cells were harvested and protein lysates were fractionated on SDS–PAGE followed by immunoblotting for the indicated proteins. α-tubulin was used as a loading control. (**d**) Loss of Yes or Lyn prevents EGFR association with B-Myb and iNOS promoters, and corresponds with a decrease in protein expression. EGFR-ChIP and subsequent qPCR from the ChIP sample for the presence of B-Myb and iNOS promoter sequences. The NT was used as a control. B-Myb and iNOS protein levels were decreased in HC4 after siYES or siLYN treatment by immunoblot analysis. Cells were harvested after treatment with siLYN or siYES for 72 h and protein lysates were fractionated on SDS–PAGE followed by immunoblotting for the indicated proteins. α-tubulin was used as a loading control.

To further elucidate the molecular requirements for EGFR nuclear transport we utilized a previously established model of acquired resistance to cetuximab in the NCI-H226 NSCLC cell line.[48] In this model, Ctx^R cells were observed to have increased levels of nuclear EGFR as compared with their Ctx^S parental cells, making it an ideal model for investigating events involved in nuclear translocation of the EGFR.[29] Additionally, Ctx^R cell lines were shown to have increased expression and activity of SFKs.[44] Further investigation using dasatinib, an inhibitor of SFKs, demonstrated that SFK activity was necessary for the nuclear transport of EGFR in this model of cetuximab-resistance.[29] In the current study, we identified Yes and Lyn to have increased expression and association with the EGFR (Figure 2). This result is consistent with other reports identifying Yes and Lyn interaction and activation of the EGFR.[54–57] In addition, loss of Yes and Lyn expression using siRNA technology led to reduced phosphorylation of Y845 and Y1101 of the EGFR and more importantly impaired nuclear EGFR accumulation (Figure 3). Consistent with this observation, overexpression of Yes and Lyn in Ctx^S cells that express low levels of nuclear EGFR significantly increased (3 ~ 3.5 fold) nuclear EGFR translocation (Figure 4b). ChIP assays demonstrated that nuclear EGFR complexes bind to B-Myb and iNOS promoter regions and siYES and siLYN decreased binding to these promoters (Figure 5). Mutagenesis studies of Y845 and Y1101 indicated that Y1101, not Y845, might be necessary for nuclear translocation of the EGFR from the membrane to the nucleus (Figure 6). Recently, Jaganathan *et al.*[19] reported that Src and EGFR associate in the nucleus with the transcription factor STAT3 to

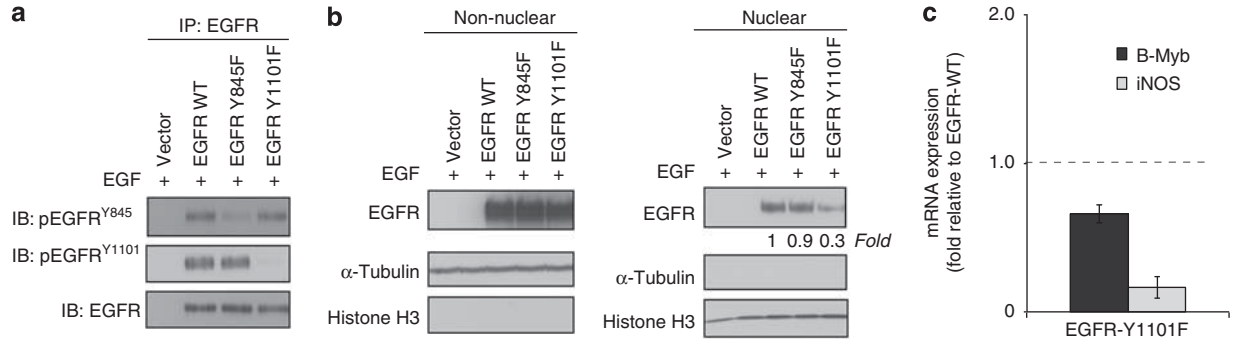

Figure 6. Phosphorylation of EGFR at Y1101 is involved in the nuclear localization of EGFR. (**a**) Immunoprecipitation of total EGFR followed by immunoblotting with anti-pEGFR Y845, anti-pEGFR Y1101 or pan-EGFR antibodies. MCF7 Cells overexpressing EGFR-WT, EGFR-Y845F or EGFR-Y1101F were harvested after stimulation with 100 ng/ml of EGF for 45 min. A total of 500 ug of cell lysate was immunoprecipitated with pan-EGFR antibody. The immunoprecipitates were fractionated on SDS–PAGE followed by immunoblotting for the indicated proteins. (**b**) Mutation of Y1101, but not Y845, reduces the nuclear localization of EGFR in MCF-7 breast cancer cells. Cells were transiently transfected with plasmids encoding the EGFR WT, EGFR-Y845F, EGFR-Y1101F or vector only. Forty-eight h after transfection the cells were incubated with EGF (100 ng/ml) for 45 min, harvested for whole-cell lysate, non-nuclear, and nuclear protein, and fractionated on SDS–PAGE followed by immunoblotting for indicated proteins. Histone H3 and α-tubulin were used as loading and purity controls for the nuclear and non-nuclear fractions, respectively. (**c**) B-Myb and iNOS mRNA levels were downregulated in HC4 cells transfected with EGFR-Y1101F mutant compared with EGFR-WT-transfected cells by qPCR. Cells were transiently transfected with plasmids encoding the EGFR-WT or EGFR-Y1101F. Twenty-fourth post transfection the cells were treated with EGF (100 ng/ml) for 45 min, and harvested for RNA. The mRNA expression of B-Myb and iNOS was determined by qPCR.

regulate the expression of the c-Myc gene in pancreatic cancer. Consistent with this report, we found that Yes or Lyn not only increased the levels of nuclear EGFR but also had increased nuclear localization themselves, suggesting that they may have been imported into the nucleus with the EGFR. Collectively, these studies provide evidence for the role of SFKs in mediating nuclear translocation of the EGFR. However, it remains to be investigated whether Yes or Lyn are solely responsible for this nuclear translocation, or if SFKs exhibit a functional redundancy where the overexpression of one or more SFKs may result in the induction of nuclear EGFR in various cancers.

Y845 and Y1101 of the EGFR are phosphorylated by SFKs.[34] Biscardi *et al*.[34] utilized a GST-bound SH2 domain of the c-Src protein to demonstrate its specific binding to the EGFR via affinity chromatography. Subsequently, these investigators identified and validated that EGFR was indeed phosphorylated by c-Src at Y845 and Y1101. Breast cancer cell lines with high levels of Src activity also had increased levels of phospho Y845 and Y1101 of the EGFR. Researchers further showed that phospho-Y845 was necessary for full EGFR activation and EGF-induced DNA synthesis.[34] This study represented a landmark finding by identifying novel Src phosphorylation sites on the EGFR and the role of tyrosine 845 in the complete activation of the EGFR. Further studies looking at the function of EGFR Y845 demonstrated that Y845 mediated EGFR binding to the mitochondrial protein cytochrome c oxidase subunit II at the mitochondria; however, EGFR Y845 was not necessary for its movement to the mitochondria.[58] These findings support our data that EGFR Y845 may not be required for the intracellular trafficking of the EGFR.

In the current study, we corroborate findings of Biscardi *et al*. by showing that Y845 and Y1101 are Src-specific phosphorylation sites through the use of the SFK inhibitor dasatinib (Figure 1b). In addition, siRNA directed towards Yes and Lyn decreased the phosphorylation of EGFR Y845 and Y1101 (Figure 3a). Our data further suggests that Y1101, not Y845, may be a critical molecular determinant in the localization of nuclear EGFR as indicated by site-directed mutagenesis (Figure 6b). It should be noted, however, that mutation of Y1101 did not completely block translocation of the EGFR to the nucleus, suggesting that other post-translational modifications of the EGFR may be necessary. Recent evidence has identified another key phosphorylation site on the EGFR, serine 229 (S229), as being necessary for EGFR translocation to the nucleus.[20] It was reported that the serine/threonine kinase AKT can influence the nuclear translocation of the EGFR by phosphorylating S229 on the EGFR in a model of gefitinib resistance. In this model, gefitinib-resistant A431 cells have both increased AKT activity and increased nuclear EGFR as compared with gefitinib-sensitive A431 cells. Using an antibody that recognizes the phosphorylated consensus motif of AKT substrates and subsequent mass spectrometry, Huang *et al*. revealed that EGFR was phosphorylated by AKT at S229.[20] Inhibition of AKT kinase activity prevented this phosphorylation event, and decreased the nuclear transport of EGFR, providing evidence for the role of alternative kinases and post-translational modifications of the EGFR that indeed affect its nuclear translocation. Collectively, these findings suggest that the phosphorylation of the EGFR on Y1101 by Yes and Lyn together with AKT phosphorylation of S229 may be critical molecular determinants that influence the nuclear localization of the EGFR.

EGFR is tightly linked to the etiology of HNSCC, NSCLC, colorectal cancer, breast and brain cancers. Accordingly, five EGFR inhibitors, three tyrosine kinase inhibitors and two monoclonal antibodies, have been developed for clinical use to inhibit EGFR activation and downstream signaling. Despite the successes of these agents, many tumors do not respond to EGFR inhibition, or eventually become resistant to this therapeutic strategy. Accumulating evidence suggests that nuclear EGFR has a role in resistance to radiation, cetuximab, cisplatin and gefitinib therapies.[20,23,29–33] The mechanisms for how nuclear EGFR leads to this resistance are not clear. However, work from our laboratory suggests that nuclear translocation can protect EGFR from the inhibitory effects of cetuximab causing resistance to this therapy.[29] The results presented in this study provide a potential mechanism for the key molecules involved in nuclear localization of the EGFR providing rational targets to prevent nuclear translocation and thus nuclear function of the EGFR.

In summary, the data presented in the current study has identified the SFKs Yes and Lyn to have a crucial role in nuclear translocation of the EGFR in a model of cetuximab-resistance. In addition, the SFK phosphorylation site Y1101 of the EGFR appears to be involved in translocation of the EGFR from the plasma membrane to the nucleus. These findings are of instrumental value in understanding the molecular requirements for nuclear

EGFR transport, and for potentially targeting nuclear EGFR in the future.

MATERIALS AND METHODS

Cell lines

The human NSCLC line NCI-H226, the human breast cancer line MCF-7 and CHO-K1 cells were purchased from ATCC (Manassas, VA, USA). The cells were maintained in 10% fetal bovine serum in RPMI-1640 for H226, DMEM/F12K for MCF-7 and F12K for CHO-K1 (Mediatech Inc., Manassas, VA, USA) with 1% penicillin and streptomycin. The development of cells with acquired resistance to cetuximab has been previously described.[48]

Plasmid constructs and transfection

EGFR WT, Y845F and Y1101F mutants, were kindly provided from Dr Julie Boerner (Wayne State University School of Medicine, Karmanos Cancer Institute, MI, USA). The presence of 845F and 1101F mutations were confirmed by DNA sequencing. For transient transfections, MCF-7 cells were transfected with plasmid DNA for each construct or pcDNA3.1 vector using Lipofectamine LTX and Opti-MEM I (Invitrogen, Carlsbad, CA, USA) according to the manufacturer's recommendations. Either 24 h (for RNA) or 48 h (for protein) after transfection, EGF (100 ng/ml; Millipore, Billerica, MA, USA) was added to the plates for 45 min. Cells were collected, isolated RNA or fractionated and screened for their EGFR expression levels by qPCR or immunoblotting as described below. For siRNAs, Ctx^R cells (HC1, HC4 and HC8) were transiently transfected with siYES (ON-TARGETplus SMARTpool YES1: L-003184-00, Dharmacon, Lafayette, CO, USA) or siLYN (ON-TARGETplus SMARTpool LYN: L-003153-00) using Lipofectamine RNAiMAX according to the manufacture's instructions (Invitrogen). The NT (ON-TARGETplus Non-targeting Pool, D-001810-10) was obtained from Dharmacon as a control. Cells were then lysed for analysis of protein knockdown by immunoblotting 72 h after siRNA transfection. WT human YES (source ID: 5260751) and LYN (source ID: 8992174) cDNAs were purchased from Open Biosystems (Lafayette, CO, USA) and cloned into the *NOTI*/*PAC*I restriction sites of the pQCXIP expression vector (Clontech, Mountain View, CA, USA). YES-PQCXIP, LYN-PQCXIP, or PQXCIP vector were transiently transfected into CHO-K1 cells by using Lipofectamine 2000 (Invitrogen) according to the manufacturer's recommendations. Forty-eight hours after transfection, cells were collected and lysed. HP parental cells were transiently transfected with the same constructs using Lipofectamine LTX (Invitrogen) according to the manufacturer's recommendations. Forty-eight hours after transfection, cells were collected and fractionated for nuclear protein. Nuclear EGFR expression levels were then detected via immunoblot analysis.

Compounds

Dasatinib (BMS-354825, Sprycel) was generously provided by Bristol-Myers Squibb (New York, NY, USA).

Antibodies

All antibodies were purchased from commercial sources as indicated below: EGFR, B-Myb, Actin, Histone H3, HRP-conjugated goat-anti-rabbit IgG, goat-anti-mouse IgG and donkey-anti-goat IgG were obtained from Santa Cruz Biotechnology Inc. (Santa Cruz, CA, USA). SFK, YES, LYN, pSFK (Y419) and normal mouse IgG were obtained from Cell Signaling Technology (Beverly, MA, USA). pEGFR (Y1101) was purchased from Abcam (Cambridge, MA, USA). Anti-mouse EGFR and pEGFR (Y845) were purchased from Invitrogen. Polyclonal iNOS was obtained from BD Biosciences (San Jose, CA, USA). α-tubulin was purchased from Calbiochem (San Diego, CA, USA).

Cellular fractionation and immunoblotting analysis

Cells were swelled in cytoplasmic lysis buffer (20 mM hydroxyethyl piperazineethanesulfonic acid (HEPES), pH 7.0, 10 mM KCl, 2 mM $MgCl_2$, 0.5% NP40, 1 mM Na_3VO_4, 1 mM phenylmethanesulfonylfluoride (PMSF), 1 mM beta-glycerophosphate (BGP), 10 μg/ml of leupeptin and aprotinin) for 10 min on ice and homogenized by 20–30 strokes in a tightly fitting Dounce homogenizer. The homogenate was centrifuged at 1500 *g* for 5 min at 4 °C to sediment the nuclei. The supernatant was then centrifuged at 15 000 *g* for 10 min at 4 °C, and the resulting supernatant formed the non-nuclear fraction. The nuclear pellet was washed three times in cytoplasmic lysis buffer and re-suspended in the same buffer containing 0.5 M NaCl to extract nuclear proteins. After sonication and vortex, the extracted sample was centrifuged at 15 000 *g* for 10 min at 4 °C. Whole cell protein lysate was obtained by tween-20 lysis buffer (50 mM HEPES, pH 7.4, 150 mM NaCl, 0.1% Tween-20, 10% glycerol, 2.5 mM ethylene glycol tetraacetic acid, 1 mM EDTA, 1 mM dithiothreitol (DTT), 1 mM Na_3VO_4, 1 mM PMSF, 1 mM BGP and 10 μg/ml of leupeptin and aprotinin). Samples were sonicated and then centrifuged at 15 000 *g* for 10 min at 4 °C. Protein concentrations were determined by Bradford assay (Bio-Rad Laboratories, Hercules, CA, USA). Equal amounts of protein were fractionated by SDS–PAGE, transferred to a polyvinylidene fluoride membrane (Millipore), and analyzed by incubation with the appropriate primary antibody. Proteins were detected via incubation with HRP-conjugated secondary antibodies and ECL chemiluminescence detection system (GE Healthcare Life Sciences, Piscataway, NJ, USA), ECL Western Blotting Substrate (Promega Cooperation, Madison, WI, USA), SuperSignal* West Dura Extended Duration Chemiluminescent Substrate or SuperSignal* West Femto Maximum Sensitivity Chemiluminescent Substrate (Thermo Fisher Scientific, Waltham, MA, USA).

Immunoprecipitation

Cells were lysed with NP-40 lysis buffer (50 mM HEPES, pH 7.4, 150 mM NaCl, 1% NP-40, 0.5% Deoxycholic acid, 10% glycerol, 2.5 mM ethylene glycol tetraacetic acid, 1 mM EDTA, 1 mM DTT, 1 mM PMSF, 1 mM BGP and 10 μg/ml of leupeptin and aprotinin). Cell lysates containing 0.5 mg of protein were incubated overnight at 4 °C with 1 μg of anti-mouse EGFR antibody (Invitrogen) or normal mouse IgG (Cell Signaling Technology). After adding 25 μl of protein A/G agarose beads (Santa Cruz), cell lysates were incubated for another 2 h at 4 °C. The immunoprecipitates were pelleted by centrifugation and washed several times with NP-40 lysis buffer. The captured immunocomplexes were then eluted by boiling the beads in 2 × SDS sample buffer for 5 min and subjected to immunoblot analysis as described above.

Microarray analysis

Total RNAs extracted from HP, HC1, HC4 and HC8 using an RNeasy kit (Qiagen Inc., Valencia, CA, USA). Gene expression profiling using the HT-HG-U133 Human Genome Array (Affymetrix, Santa Clara, CA, USA) containing over 22 000 well-characterized genes. After Robust Multichip Average (RMA) normalization, data were analyzed using Partek Discovery Suite (St Louis, MO, USA) and signature genes were the genes that increased or decreased >2-fold expression levels in three Ctx^R clones (HC1, HC4 and HC8) compared with sensitive parental line (HP) with P-value <0.05.

cDNA synthesis and qPCR

cDNA from total RNA of HP, HC1, HC4 and HC8 were synthesized using SuperScript III First-Strand Synthesis System (Invitrogen). qPCR analysis was performed using a Bio-Rad iQ5 Real-Time PCR Detection System (Bio-Rad Laboratories) using the iQ Supermix as recommended by manufacturer. All reactions were performed in triplicate. The sequences of primer sets used for this analysis are as follows: Lyn-F: 5′-GGCTCCAGA AGCAATCAACT-3′, Lyn-R: 5′-TCACGTCGGCATTAGTTCTC-3′; Yes-F: 5′-CTAGTAACA AAGGGCC GAGTG-3′, Yes-R: 5′-ATCCTGTATCCTCGCTCCAC-3′; Src-F: 5′-GAGGAG CCC ATTTACATCGT-3′, Src-R: 5′-TGAGAAAGTCCAGCAAACTCC-3′, B-Myb-F: 5′-ATG TCCAGTGCCTGGAAGAC-3′, B-Myb-R: 5′-AGATGAGGGTCCGAGATG TG-3′. iNOS-F: 5′-CCATAAGGCCAAAGGGATTT-3′, iNOS-R: 5′-ATCTGGA GGGGTAGGCTTGT-3′. Fold increases or decreases in gene expression were determined by quantitation of cDNA from target samples (HC1, HC4 and HC8) relative to a calibrator sample (HP). Human β-actin gene (F: 5′-CAGCCATGTACGTTGCTATCCAGG-3′, R: 5′-AGGTCCAGA CGCAGGATGGC ATG-3′) was used as the endogenous control for normalization of initial RNA

levels. To determine this normalized value, $2^{-\Delta\Delta CT}$ values were compared between target and calibrator samples, where the change in crossing threshold $(\Delta Ct) = Ct_{target\ gene} - Ct_{b\text{-}actin}$ and $\Delta\Delta Ct = \Delta Ct_{HC1,\ HC4\ or\ HC8} - \Delta Ct_{HP}$.

ChIP assay

Cells were fixed with formaldehyde at a final concentration of 1% for 15 min at room temperature, stopped fixation by 1.25 M glycine for 5 min. Subsequently, cells were washed with ice-cold PBS and collected in the tube and centrifuge at 4 °C for 5 min. The cell pellets were lysed in cell lysis buffer (5 mM HEPES, pH 8.0, 85 mM KCl, 0.5% NP-40 and 10 mM sodium pyrophosphate) by a Dounce homogenizer. After centrifuge, supernatant was removed, and the nuclei pellets were lysed in nuclei lysis buffer (Tris-HCl 50 mM, pH 8.1, 10 mM EDTA, 1% SDS and 10 mM sodium pyrophosphate). The lysate was sonicated on ice to shear DNA, and the supernatant was pre-cleared with protein A/G agarose beads (Santa Cruz) in dilution buffer (16.7 mM Tris-HCl, pH 8.1, 1.2 mM EDTA, 167 mM NaCl, 1.1% Triton X-100, 0.01% SDS and 10 mM sodium pyrophosphate) for 1 h at 4 °C. The pre-cleared lysates were immunoprecipitated by incubating with protein A/G beads containing 1 ug of anti-EGFR antibody or IgG and rotated at 4 °C for overnight. The beads were washed with wash buffer I (25 mM Tris-HCl, pH 8.0, 2 mM EDTA, 150 mM NaCl, 1% Triton X-100, 0.1% SDS and 10 mM sodium pyrophosphate), wash buffer II (25 mM Tris-HCl, pH 8.0, 2 mM EDTA, 500 mM NaCl, 1% Triton X-100, 0.1% SDS and 10 mM sodium pyrophosphate), wash buffer III (10 mM Tris-HCl, pH 8.0, 1 mM EDTA, 250 mM LiCl, 1% NP-40, 1% deoxycholic acid and 10 mM sodium pyrophosphate) and TE buffer (10 mM Tris-HCl, pH8.0, 1 mM EDTA, 10 mM sodium pyrophosphate). The bound protein was eluted twice with elute buffer (100 mM $NaHCO_3$ and 1% SDS). Then, 5 M NaCl was added to the pooled eluent and incubated at 68 °C overnight. The DNA was recovered and purified using DNA purification kit (Qiagen). The purified chromatin-immunoprecipitated DNA was used as a template for the qPCR of the promoter regions using the following primer pairs: B-Myb-F: 5′-CTGGTCTTAGCTACCCGTGAG TTGA-3′ and B-Myb-R: 5′-CAGGAGTATCCCACATAGCGAACAC-3′,[15] iNOS-F: 5′-TGATGAA CTGCCACCTTGGAC-3′ and iNOS-R: 5′-TTCACCCAACCC ACCTCTTTC-3′.[16] The qPCR program was: 95 °C for 3 min, followed by 40 cycles of 95 °C for 15 s and 60 °C for 30 s for B-Myb or 55 °C for 30 s for iNOS. The qPCR was performed using the iQ5 Real-time PCR Detection system (Bio-Rad).

ABBREVIATIONS

BCRP, breast cancer-resistance protein; CRC, colorectal cancer; Ctx^R, cetuximab-resistant; Ctx^S, cetuximab-sensitive; DMSO, dimethyl sulfoxide; EGF, epidermal growth factor; EGFR, epidermal growth factor receptor; ER, endoplasmic reticulum; FBS, fetal bovine serum; FGFR, fibroblast growth factor receptor; HNSCC, head and neck squamous cell carcinoma; iNOS, inducible nitric oxide synthase; Lyn, v-yes-1 Yamaguchi sarcoma viral-related oncogene homolog; mAb, monoclonal antibody; NSCLC, non-small cell lung cancer; PGFR, platelet-derived growth factor; PI3K, phosphatidylinositol 3-kinase; PKC, protein kinase C; PLCγ, phospholipase C-gamma; qPCR, quantitative PCR; RTK, receptor tyrosine kinase; SFK, Src-family kinases; STAT, signal transducers and activators of transcription; Yes, v-Yes-1 yamaguchi sarcoma viral oncogene.

CONFLICT OF INTEREST

The authors declare no conflict of interest.

ACKNOWLEDGEMENTS

This project was supported, in part, by grant P30CA014520 from the National Cancer Institute, grant 1UL1RR025011 from the Clinical and Translational Science Award program of the National Center for Research Resources and the National Institutes of Health (DLW) by grant RSG-10-193-01-TBG from the American Cancer Society (DLW), and by NIH grant T32 GM08.1061-01A2 from Graduate Training in Cellular and Molecular Pathogenesis of Human Diseases (TMB).

REFERENCES

1 Yarden Y, Sliwkowski MX. Untangling the ErbB signalling network. *Nat Rev Mol Cell Biol* 2001; **2**: 127 - 137.
2 Wheeler DL, Dunn EF, Harari PM. Understanding resistance to EGFR inhibitors-impact on future treatment strategies. *Nat Rev Clin Oncol* 2010; **7**: 493 - 507.
3 Brand TM, Iida M, Wheeler DL. Molecular mechanisms of resistance to the EGFR monoclonal antibody cetuximab. *Cancer Biol Ther* 2011; **11**: 777 - 792.
4 Pao W, Chmielecki J. Rational, biologically based treatment of EGFR-mutant non-small-cell lung cancer. *Nat Rev Cancer* 2010; **10**: 760 - 774.
5 Gschwind A, Fischer OM, Ullrich A. The discovery of receptor tyrosine kinases: targets for cancer therapy. *Nat Rev Cancer* 2004; **4**: 361 - 370.
6 Marmor MD, Skaria KB, Yarden Y. Signal transduction and oncogenesis by ErbB/HER receptors. *Int J Radiat Oncol Biol Phys* 2004; **58**: 903 - 913.
7 Wang YN, Yamaguchi H, Hsu JM, Hung MC. Nuclear trafficking of the epidermal growth factor receptor family membrane proteins. *Oncogene* 2010; **29**: 3997 - 4006.
8 Brand TM, Iida M, Li C, Wheeler DL. The nuclear epidermal growth factor receptor signaling network and its role in cancer. *Discov Med* 2011; **12**: 419 - 432.
9 Carpenter G, Liao HJ. Trafficking of receptor tyrosine kinases to the nucleus. *Exp Cell Res* 2009; **315**: 1556 - 1566.
10 Lo HW, Ali-Seyed M, Wu Y, Bartholomeusz G, Hsu SC, Hung MC. Nuclear-cytoplasmic transport of EGFR involves receptor endocytosis, importin beta1 and CRM1. *J Cell Biochem* 2006; **98**: 1570 - 1583.
11 Hsu SC, Hung MC. Characterization of a novel tripartite nuclear localization sequence in the EGFR family. *J Biol Chem* 2007; **282**: 10432 - 10440.
12 Wang YN, Yamaguchi H, Huo L, Du Y, Lee HJ, Lee HH *et al.* The translocon Sec61beta localized in the inner nuclear membrane transports membrane-embedded EGF receptor to the nucleus. *J Biol Chem* 2010; **285**: 38720 - 38729.
13 Liao HJ, Carpenter G. Role of the Sec61 translocon in EGF receptor trafficking to the nucleus and gene expression. *Mol Biol Cell* 2007; **18**: 1064 - 1072.
14 Lin SY, Makino K, Xia W, Matin A, Wen Y, Kwong KY *et al.* Nuclear localization of EGF receptor and its potential new role as a transcription factor. *Nat Cell Biol* 2001; **3**: 802 - 808.
15 Hanada N, Lo HW, Day CP, Pan Y, Nakajima Y, Hung MC. Co-regulation of B-Myb expression by E2F1 and EGF receptor. *Mol Carcinog* 2006; **45**: 10 - 17.
16 Lo HW, Hsu SC, Ali-Seyed M, Gunduz M, Xia W, Wei Y *et al.* Nuclear interaction of EGFR and STAT3 in the activation of the iNOS/NO pathway. *Cancer Cell* 2005; **7**: 575 - 589.
17 Hung LY, Tseng JT, Lee YC, Xia W, Wang YN, Wu ML *et al.* Nuclear epidermal growth factor receptor (EGFR) interacts with signal transducer and activator of transcription 5 (STAT5) in activating Aurora-A gene expression. *Nucleic Acids Res* 2008; **36**: 4337 - 4351.
18 Lo HW, Cao X, Zhu H, Ali-Osman F. Cyclooxygenase-2 is a novel transcriptional target of the nuclear EGFR-STAT3 and EGFRvIII-STAT3 signaling axes. *Mol Cancer Res* 2010; **8**: 232 - 245.
19 Jaganathan S, Yue P, Paladino DC, Bogdanovic J, Huo Q, Turkson J. A functional nuclear epidermal growth factor receptor, SRC and Stat3 heteromeric complex in pancreatic cancer cells. *PLoS One* 2011; **6**: e19605.
20 Huang WC, Chen YJ, Li LY, Wei YL, Hsu SC, Tsai SL *et al.* Nuclear translocation of epidermal growth factor receptor by Akt-dependent phosphorylation enhances breast cancer-resistant protein expression in gefitinib-resistant cells. *J Biol Chem* 2011; **286**: 20558 - 20568.
21 Piccione EC, Lieu TJ, Gentile CF, Williams TR, Connolly AJ, Godwin AK *et al.* A novel epidermal growth factor receptor variant lacking multiple domains directly activates transcription and is overexpressed in tumors. *Oncogene* (e-pub ahead of print 10 October 2011; doi:10.1038/onc.2011.465).
22 Wang SC, Nakajima Y, Yu YL, Xia W, Chen CT, Yang CC *et al.* Tyrosine phosphorylation controls PCNA function through protein stability. *Nat Cell Biol* 2006; **8**: 1359 - 1368.
23 Dittmann K, Mayer C, Fehrenbacher B, Schaller M, Raju U, Milas L *et al.* Radiation-induced epidermal growth factor receptor nuclear import is linked to activation of DNA-dependent protein kinase. *J Biol Chem* 2005; **280**: 31182 - 31189.
24 Lo HW, Xia W, Wei Y, Ali-Seyed M, Huang SF, Hung MC. Novel prognostic value of nuclear epidermal growth factor receptor in breast cancer. *Cancer Res* 2005; **65**: 338 - 348.
25 Hadzisejdic I, Mustac E, Jonjic N, Petkovic M, Grahovac B. Nuclear EGFR in ductal invasive breast cancer: correlation with cyclin-D1 and prognosis. *Mod Pathol* 2010; **23**: 392 - 403.
26 Xia W, Wei Y, Du Y, Liu J, Chang B, Yu YL *et al.* Nuclear expression of epidermal growth factor receptor is a novel prognostic value in patients with ovarian cancer. *Mol Carcinog* 2009; **48**: 610 - 617.
27 Psyrri A, Yu Z, Weinberger PM, Sasaki C, Haffty B, Camp R *et al.* Quantitative determination of nuclear and cytoplasmic epidermal growth factor receptor expression in oropharyngeal squamous cell cancer by using automated quantitative analysis. *Clin Cancer Res* 2005; **11**: 5856 - 5862.

28 Li CF, Fang FM, Wang JM, Tzeng CC, Tai HC, Wei YC *et al.* EGFR nuclear import in gallbladder carcinoma: nuclear phosphorylated EGFR upregulates iNOS expression and confers independent prognostic impact. *Ann Surg Oncol* 2012; **19**: 443 - 454.
29 Li C, Iida M, Dunn EF, Ghia AJ, Wheeler DL. Nuclear EGFR contributes to acquired resistance to cetuximab. *Oncogene* 2009; **28**: 3801 - 3813.
30 Li C, Iida M, Dunn EF, Wheeler DL. Dasatinib blocks cetuximab- and radiation-induced nuclear translocation of the epidermal growth factor receptor in head and neck squamous cell carcinoma. *Radiother Oncol* 2010; **97**: 330 - 337.
31 Hsu SC, Miller SA, Wang Y, Hung MC. Nuclear EGFR is required for cisplatin resistance and DNA repair. *Am J Transl Res* 2009; **1**: 249 - 258.
32 Liccardi G, Hartley JA, Hochhauser D. EGFR nuclear translocation modulates DNA repair following cisplatin and ionizing radiation treatment. *Cancer Res* 2011; **71**: 1103 - 1114.
33 Dittmann K, Mayer C, Kehlbach R, Rodemann HP. Radiation-induced caveolin-1 associated EGFR internalization is linked with nuclear EGFR transport and activation of DNA-PK. *Mol Cancer* 2008; **7**: 69.
34 Biscardi JS, Maa MC, Tice DA, Cox ME, Leu TH, Parsons SJ. c-Src-mediated phosphorylation of the epidermal growth factor receptor on Tyr845 and Tyr1101 is associated with modulation of receptor function. *J Biol Chem* 1999; **274**: 8335 - 8343.
35 Maa MC, Leu TH, McCarley DJ, Schatzman RC, Parsons SJ. Potentiation of epidermal growth factor receptor-mediated oncogenesis by c-Src: implications for the etiology of multiple human cancers. *Proc Natl Acad Sci USA* 1995; **92**: 6981 - 6985.
36 Wheeler DL, Iida M, Dunn EF. The role of Src in solid tumors. *Oncologist* 2009; **14**: 667 - 678.
37 Kim LC, Song L, Haura EB. Src kinases as therapeutic targets for cancer. *Nat Rev Clin Oncol* 2009; **6**: 587 - 595.
38 Thomas SM, Brugge JS. Cellular functions regulated by Src family kinases. *Annu Rev Cell Dev Biol* 1997; **13**: 513 - 609.
39 Bromann PA, Korkaya H, Courtneidge SA. The interplay between Src family kinases and receptor tyrosine kinases. *Oncogene* 2004; **23**: 7957 - 7968.
40 Tice DA, Biscardi JS, Nickles AL, Parsons SJ. Mechanism of biological synergy between cellular Src and epidermal growth factor receptor. *Proc Natl Acad Sci USA* 1999; **96**: 1415 - 1420.
41 Kloth MT, Laughlin KK, Biscardi JS, Boerner JL, Parsons SJ, Silva CM. STAT5b, a mediator of synergism between c-Src and the epidermal growth factor receptor. *J Biol Chem* 2003; **278**: 1671 - 1679.
42 Ottenhoff-Kalff AE, Rijksen G, van Beurden EA, Hennipman A, Michels AA, Staal GE. Characterization of protein tyrosine kinases from human breast cancer: involvement of the c-src oncogene product. *Cancer Res* 1992; **52**: 4773 - 4778.
43 Lu KV, Zhu S, Cvrljevic A, Huang TT, Sarkaria S, Ahkavan D *et al.* Fyn and SRC are effectors of oncogenic epidermal growth factor receptor signaling in glioblastoma patients. *Cancer Res* 2009; **69**: 6889 - 6898.
44 Wheeler DL, Iida M, Kruser TJ, Nechrebecki MM, Dunn EF, Armstrong EA *et al.* Epidermal growth factor receptor cooperates with Src family kinases in acquired resistance to cetuximab. *Cancer Biol Ther* 2009; **8**: 696 - 703.
45 Zhang J, Kalyankrishna S, Wislez M, Thilaganathan N, Saigal B, Wei W *et al.* SRC-family kinases are activated in non-small cell lung cancer and promote the survival of epidermal growth factor receptor-dependent cell lines. *Am J Pathol* 2007; **170**: 366 - 376.
46 Fu YN, Yeh CL, Cheng HH, Yang CH, Tsai SF, Huang SF *et al.* EGFR mutants found in non-small cell lung cancer show different levels of sensitivity to suppression of Src: implications in targeting therapy. *Oncogene* 2008; **27**: 957 - 965.
47 Koppikar P, Choi SH, Egloff AM, Cai Q, Suzuki S, Freilino M *et al.* Combined inhibition of c-Src and epidermal growth factor receptor abrogates growth and invasion of head and neck squamous cell carcinoma. *Clin Cancer Res* 2008; **14**: 4284 - 4291.
48 Wheeler DL, Huang S, Kruser TJ, Nechrebecki MM, Armstrong EA, Benavente S *et al.* Mechanisms of acquired resistance to cetuximab: role of HER (ErbB) family members. *Oncogene* 2008; **27**: 3944 - 3956.
49 Brand TM, Dunn EF, Iida M, Myers RA, Kostopoulos KT, Li C *et al.* Erlotinib is a viable treatment for tumors with acquired resistance to cetuximab. *Cancer Biol Ther* 2011; **12**: 436 - 446.
50 Massie C, Mills IG. The developing role of receptors and adaptors. *Nat Rev Cancer* 2006; **6**: 403 - 409.
51 Carpenter G. Nuclear localization and possible functions of receptor tyrosine kinases. *Curr Opin Cell Biol* 2003; **15**: 143 - 148.
52 Wang SC, Hung MC. Nuclear translocation of the epidermal growth factor receptor family membrane tyrosine kinase receptors. *Clin Cancer Res* 2009; **15**: 6484 - 6489.
53 Lo HW, Hung MC. Nuclear EGFR signalling network in cancers: linking EGFR pathway to cell cycle progression, nitric oxide pathway and patient survival. *Br J Cancer* 2006; **94**: 184 - 188.
54 Zhao Y, He D, Saatian B, Watkins T, Spannhake EW, Pyne NJ *et al.* Regulation of lysophosphatidic acid-induced epidermal growth factor receptor transactivation and interleukin-8 secretion in human bronchial epithelial cells by protein kinase Cdelta, Lyn kinase, and matrix metalloproteinases. *J Biol Chem* 2006; **281**: 19501 - 19511.
55 Xi S, Zhang Q, Dyer KF, Lerner EC, Smithgall TE, Gooding WE *et al.* Src kinases mediate STAT growth pathways in squamous cell carcinoma of the head and neck. *J Biol Chem* 2003; **278**: 31574 - 31583.
56 Kasai A, Shima T, Okada M. Role of Src family tyrosine kinases in the down-regulation of epidermal growth factor signaling in PC12 cells. *Genes Cells* 2005; **10**: 1175 - 1187.
57 Su T, Bryant DM, Luton F, Verges M, Ulrich SM, Hansen KC *et al.* A kinase cascade leading to Rab11-FIP5 controls transcytosis of the polymeric immunoglobulin receptor. *Nat Cell Biol* 2010; **12**: 1143 - 1153.
58 Boerner JL, Demory ML, Silva C, Parsons SJ. Phosphorylation of Y845 on the epidermal growth factor receptor mediates binding to the mitochondrial protein cytochrome c oxidase subunit II. *Mol Cell Biol* 2004; **24**: 7059 - 7071.

AXL mediates the nuclear translocation of the epidermal growth factor receptor

Toni M. Brand[1], Mari Iida[1], Kelsey L. Corrigan[1],Cara M. Braverman[1], John Coan[1], Bailey Flannigan[1], Andrew P. Stein[1], Ravi Salgia[2], Randall J. Kimple[1], and Deric L. Wheeler[1]

[1]Department of Human Oncology, University of Wisconsin School of Medicine and Public Health, 1111 Highland Ave, Madison, Wisconsin, 53705 USA

[2]Department of Medicine, Division of Hematology/Oncology, University of Chicago, M255, 5841 South Maryland Avenue, Chicago, IL 60637 USA

Running Title: AXL mediates nuclear EGFR translocation

Key Words: AXL, EGFR, cetuximab

To whom requests for reprints should be addressed: Deric L. Wheeler Ph.D., Department of Human Oncology, University of Wisconsin Comprehensive Cancer Center, 1111 Highland Avenue, WIMR 3159, Madison, Wisconsin 53705. Phone: (608) 262-7837; fax: (608) 263-9947; e-mail: dlwheeler@wisc.edu.

Financial Support: The project described was supported by the Clinical and Translational Science Award (CTSA) program, through the NIH National Center for Advancing Translational Sciences (NCATS) grant UL1TR000427 (KL2TR000428), grant RSG-10-193-01-TBG from the American Cancer Society (D.L.Wheeler), and grant W81XWH-12-1-0467 from United States Army Medical Research and Materiel Command (D.L.Wheeler), CA160639 (R.J.Kimple), and the NIH/NCI P30 CA014520 (UW Comprehensive Cancer Center Grant). TLF is supported in part by the University of Wisconsin Science and Medicine Graduate Research Scholars program.

Abstract: 250 words

The epidermal growth factor receptor (EGFR) is an important therapeutic target in several human cancers. Unfortunately, resistance to anti-EGFR therapeutics is a common clinical outcome. Previous studies in our laboratory have identified several mechanisms of resistance to the anti-EGFR monoclonal antibody, cetuximab. First, EGFR was found to drive cetuximab resistance through localization within the cell's nucleus. Second, the receptor tyrosine kinase, AXL, was found to mediate cetuximab resistance through constitutively activating EGFR on the plasma membrane. On the basis of these findings, we hypothesized that AXL may mediate the nuclear translocation of EGFR in cetuximab resistant cells. To examine this question, several cetuximab resistant models were analyzed for EGFR and AXL expression by immunohistochemical analysis. Strikingly, cetuximab resistant cell line xenografts and patient-derived xenografts expressed significantly elevated levels of nuclear EGFR localization and AXL. Using cellular fractionation, super resolution microscopy, and electron microcopy, genetic ablation of AXL blocked nuclear EGFR expression and resulted in its accumulation outside the nuclear envelope and on the cell surface. Building off previous studies in our laboratory indicating that Src Family Kinases (SFKs) and HER family ligands mediate nuclear EGFR translocation, we next examined if AXL regulates nuclear EGFR trafficking through these pathways. Indeed, AXL knockdown downregulated the expression of the SFKs Yes and Lyn, and the cognate ligand for HER3, neuregulin-1. Furthermore, EGFR and HER3 complexes were disassociated upon AXL knockdown, which resulted in a decrease in nuclear HER3 expression as well. Collectively, these data uncover a novel role for AXL in mediating nuclear EGFR translocation, and suggest that these functions may influence cetuximab resistant phenotypes.